2006

MOLECULAR ECOLOGY OF MARINE ALGAL VIRUSES

MARTINEZ, JOAQUIN MARTINEZ

MOLECULAR ECOLOGY OF MARINE ALGAL VIRUSES

By

JOAQUÍN MARTÍNEZ MARTÍNEZ

A thesis submitted to the University of
Plymouth for the degree of

DOCTOR OF PHILOSOPHY

Department of Biological Sciences
University of Plymouth

In collaboration with
The Marine Biological Association (UK)
Plymouth Marine Laboratory (UK)
University of Bergen (Norway)

September 2006

Abstract

In this study phytoplankton viruses were investigated from a point of view of their genotypic richness, ecology and role in controlling two microalgae species: *Emiliania huxleyi* and *Phaeocystis pouchetii*.

Host specificity determined for *Emiliania huxleyi*-virus (EhV) isolates revealed a highly variable host range suggesting a relation between virus specificity and genetic or phenotypic variations within *E. huxleyi* strains and EhVs. Subsequently the dynamics and genetic richness of *Emiliania huxleyi* and EhVs were monitored in mesocosm experiments and during the progression of a natural bloom in the sea. The results confirmed the role of virus infection in regulating the intraspecific succession of *E. huxleyi* in the ocean. Furthermore, they revealed significant differences in genotypic composition and dynamics among blooms. The mesocosm setup appeared to be a very robust experimental system, which allowed reproducibility. The most important factor determining the development of the blooms in the enclosures was the experimental manipulation (i.e. nutrient addition), whereas the effect of filling of the enclosures, delay in nutrient addition and position in the raft were of minor importance.

Further laboratory experiments revealed differences in the genomic content of different EhVs. EhV isolates from the English Channel carry a putative phosphate permease gene (ehv117) while the only available EhV from a Norwegian fjord has replaced ehv117 with a putative endonuclease, suggesting different propagation strategies among closely related EhVs. Culture studies using one of the English Channel isolates and *E. huxleyi* CCMP 1516 showed that the lack of phosphate (P) reduced the growth rate of the host and inhibited the production of viral particles. Furthermore, P availability was shown to have an effect on the level of ehv117 expression.

In addition, other mesocosm studies revealed that specific viruses (PpVs) play a significant role in the termination of induced *Phaeocystis pouchetii* blooms. However, the role of PpVs may be significant only for the flagellated stage of *P. pouchetii*. Phenotypic characteristics of PpVs isolated during these studies indicate that they are probably members of the *Phycodnaviridae* family.

List of contents

Guide to figures

Guide to tables

Page

List of symbols and abbreviations

#	number
AA	acrylic acid
AcMNPV	*Autographa californica* nucleopolyhedrovirus
AFC	analytical flow cytometry
AlHV	*Alcelaphine* herpesvirus
BmNPV	*Bombyx mori* nucleopolyhedrovirus
BoHV	*Bovine* herpesvirus
CbV	*Chrysochromulina brevifilum* virus
CDS	coding sequence
CLEV	*Choristoneura biennis* entomopoxvirus
CPC	cell photosynthetic capacity
C_T	fluorescence threshold value
CTAB	hexadecyltrimethyl ammonium bromide
DAN	day after start of nutrient addition
DCMU	3'-(3,4-dichlorophenyl)-1',1'-dimethylurea
DGGE	denaturing gradient gel electrophoresis
DMS	dimethyl sulfide
DMSP	dimethylsulfoniopropionate
dNTPs	deoxynucleotides
E	efficiency
EC	English Channel
EHV	*Equine* herpesvirus
EhV(s)	*Emiliania huxleyi*-specific virus(es)
ehv117	EhV-86's putative phosphate permease gene
EsV	*Ectocarpus siliculosus* virus

F	forward
F_0	minimum fluorescence
F_M	maximum fluorescence
FsV	*Feldmannia* sp. virus
F_V	$F_0 - F_M$
FWPV	Fowl poxvirus
GTE	glucose/Tris/EDTA buffer
GPA	calcium binding protein gene
HaV	*Heterosigma akashiwo* virus
HzSNPV	*Helicoverpa zea* nucleopolyhedrovirus
IIV	Invertebrate iridescent virus
LdMNPV	*Lymantria dispar* nucleopolyhedrovirus
MCP	major capsid protein gene
MOCV	*Molluscum contagiasum* virus
MpV	*Micromonas pusilla* virus
MWCO	molecular weight cut off
N/A	not applicable
NAC	no amplification control
n.d.	not determined
NTC	no template control
OFL	orange fluorescence
OTU	operational taxonomic unit
PBCV	*Chlorella* NC64A virus
PBS	phosphate buffered saline
PFGE	pulse field gel electrophoresis
P+G	1% paraformaldehyde + 0.05% glutaraldehyde
PgV	*Phaeocystis globosa* virus

pol	polymerase
POS	position of enclosures
PpV	*Phaeocystis pouchetii* virus
R	reverse
RAPD	random amplified polymorfic DNA
RFL	red fluorescence
RN	Raunefjorden
R.U.	relative units
SDS	Sodium Dodecyl Sulphate
sp(p)	specie(s)
SSC	Side Scatter
TAE	Tris/acetate/EDTA buffer
Taq	*Thermus aquaticus*
TBE	Tris/borate/EDTA buffer
TE	Tris/EDTA buffer
TEM	transmission electron microscopy
TFF	tangential flow filtration
TG	nutrient treatment group
VACV	*Vaccinia* virus
VLP(s)	virus-like particle(s)
v/v	volume:volume ratio
w/v	weight:volume ratio
× g	relative centrifugal force
X-GAL	5-bromo-4-chloro-3-indolyl-β-D-galactopyanoside

Acknowledgements

There are many people I would like to thank for their help and support, without which this work would not have been possible at all. Firstly, I would like to thank my supervisor William H. Wilson for trusting me and giving me the opportunity of doing this project. Equally thanks to the rest of my supervisors/advisors Declan C. Schroeder, Gunnar Bratbak, Aud Larsen and Ruth-Anne Saanda. I will always appreciate their highly valuable advice, encouraging supervision and friendship. Thank you also to Graham Bradley for being my link to Plymouth University.

Thanks also to the members of the Vanngruppe at the University of Bergen (Norway) who despite not being supervisors gave very generously with their time. Especially to Evy Skjoldal for helping me finding my way around in the lab, to Mikal Heldal for teaching and helping me with the transmission electron microscopy and to Svein Norland and Frede Thingstad for their great help with the statistical analysis of data. I will also be always grateful to the present and past crew of the Wilson group (Willie, Declan, Vicky, Andrea, Matt, Claire, Mike, Jayme, Bex, Susan and Karen) for making my lab work in Plymouth an enjoyable experience, providing ALWAYS useful advice, nice chatting and friendship. Many thanks to Mike J. Allen who unfortunately for him sat too close to me, both in the office and in the lab, and had to bravely stand my constant 'hey Mike, I have a question...'

I thank all those involved in the Bergen mesocosm studies. Access to the mesocosm facilities at the University of Bergen was funded by U.S. National Science Foundation grant OPP-00-83381 and by the Improving Human Potential Programme from the European Union through contract number HPRI-CT-2001-00181 "Bergen Marine".

I would also like to acknowledge the many friends (too many to mention each one of them), in and out these departments, that made of the years my PhD lasted an unforgettable and personally enriching experience.

Most of all I cannot thank enough my family whose love, support, encouragement and proximity despite the distance make me go forward every day.
Sobre todo quiero dedicar esta tesis a mi familia, a los que nunca podré agradecer lo suficiente su cariño, apoyo, motivación y proximidad, a pesar de la distancia. Ellos son las razones que me permiten seguir adelante cada día.

Author's declaration

At no time during the registration for the degree of Doctor of Philosophy has the author been registered for any other University award without prior agreement of the Graduate Committee.

This study was financed with the aid of studentships from the Marine Biological Association (UK) and Plymouth marine Laboratory (UK) and from the European Community through the *Energy, Environment and Sustainable Development* program, the *Bergen Advanced Training Site for Marine Ecology, Contract # EVK3-CT-2000-57129.*

List of papers and manuscripts derived from this work:

- Schroeder DC, Biggi GF, Hall M, Davy J, **Martínez Martínez J**, Richardson AJ, Malin G, Wilson WH (2005) A genetic marker to separate *Emiliania huxleyi* (Prymnesiophyceae) morphotypes. J. Phycol. 41:874-879
- **Martínez Martínez J**, Norland S, Thingstad F, Schoeder DC, Bratbak G, Wilson WH, Larsen A (2006) Variability in microbial population dynamics between similarly perturbed mesocosms. J. Plankton Res. 28:783-791
- Nejstgaard JC, Frischer ME, Verity P, Anderson JT, Jacobsen A, Zirbel MJ, Larsen A, **Martínez Martínez J,** Sazhin AF, Walters T, Bronk DA, Whipple SJ, Borrett SR, Patten BC, Long JD (2006) Plankton development and trophic transfer in seawater enclosures added nutrients and *Phaeocystis pouchetii*. Mar. Ecol. Prog. Ser. 321:99-121
- **Martínez Martínez J**, Schroeder DC, Larsen A, Bratbak G, Wilson WH (In press) Molecular dynamics of *Emiliania huxleyi* and their co-occurring viruses during two separate mesocosm studies. Appl. Environ. Microbiol.
- **Martínez Martínez J**, Schroeder DC, Wilson WH (Submitted) Dynamics and genotypic composition of *Emiliania huxleyi* and their co-occurring viruses during a coccolithophore bloom in the North Sea. Appl. Environ. Microbiol.
- Allen MJ, **Martínez Martínez J**, Schroeder DC, Somerfield PJ, Wilson WH (In press) Use of microarrays to assess genomic variability in the *Coccolithoviridae*. Environ. Microbiol.

- Whipple SJ, Patten BC, Verity P, Nejstgaard JC, Long JD, Anderson JT, Hay ME, Jacobsen A, Larsen A, **Martínez Martínez J**, Borrett SR (Submitted) Gaining integrated understanding of *Phaeocystis* spp. (In Press) through model-driven laboratory and mesocosm studies. Biogeochemistry
- Jacobsen A, Larsen A, **Martínez Martínez J**, Frischer ME, Verita PG (Submitted.) Are colonies or colonial cells of *Phaeocystis pouchetii* (Haptophyta) susceptible to viral infection? Biogeochemistry

Relevant scientific seminars and conferences attended at which work was presented:

- Host and virus genotypic diversity during a bloom of the marine coccolithophorid *Emiliania huxleyi*. **Poster** at ESF Workshop on Environmental Genomics and Environmental Metagenomics in Granada, Spain. November 2004
- Host and virus genotypic diversity during blooms of the marine coccolithophorid *Emiliania huxleyi*. **Oral presentation** at the 4th VEG workshop in Lemington Spa, UK. February 2005
- Molecular dynamics of EhVs in blooms of the marine coccolithophorid *Emiliania huxleyi*. **Oral presentation** at the 4th Algal Virus Workshop in Amsterdam, The Netherlands. April 2005
- Molecular ecology of coccolithovirus. Giant marine viruses that kill the bloom forming microalgae *Emiliania huxleyi*. **Poster** at GRC Applied and Environmental Microbiology in Connecticut, USA. July 2005

Word count of main body of thesis: 47,696 words

J. Martínez Martínez

Signed

Date 1st September 2006

CHAPTER ONE

Introduction

1. Introduction

The work described in this thesis focuses on investigating the diversity and ecology of marine viruses, and their role in controlling two important planktonic algal species: *Emiliania huxleyi* and *Phaeocystis pouchetii*. In this chapter, attention will be drawn to the need to improve our understanding of the relationships between organisms, food web structure, biodiversity and biogeochemical cycles in the oceanic microbial food web. The importance and current knowledge of phytoplankton and virus activities in the marine pelagic ecosystem will be summarized. Finally the factors affecting viral control of host, host defence mechanisms and the fate of viruses in the water will be reviewed. Special attention will be given to the *E. huxleyi* and *P. pouchetii* host-virus systems.

1.1. Oceanic biogeochemistry

Biogeochemical processes in the ocean control the Earth's climate and absorb the impact of human perturbations on the environment. At the core of biogeochemistry is the carbon cycle and its interconnections with the cycles of other elements involved in life processes, such as nitrogen, oxygen, phosphorus and metals. Carbon cycling is tied to biological productivity in the oceans. Carbon dioxide (CO_2) is sequestered from the atmosphere into the oceans by physical processes, and by the surface ocean biological pump, which draws carbon into organic matter. Therefore, in order to understand the changes in oceanic biogeochemistry we must first understand the behaviour of the marine biotic system and changes in plankton productivity.

The exchange of CO_2 between the oceans and the atmosphere is influenced by the ratio of carbon uptake to calcite production in the surface of the ocean and the subsequent calcite flux by particles sinking out. The particle ratio depends on the composition of the plankton communities and the degree to which these communities are composed of carbonate or

non-carbonate producers. In addition, given that viruses cause a significant amount of marine microbial mortality, viral lysis of cells also plays an important role in marine geochemical cycles. In surface waters viruses accelerate the transformation of particulate organic carbon (POC) into dissolved pools resulting in an increase of community respiration and decrease of carbon transfer efficiency to higher trophic levels (Suttle 2005). Similarly viruses has an effect on availability and cycling of nutrients other than carbon, e.g. nitrogen, phosphorus and iron, which are also released by viral lysis (Gobler et al. 1997). The accumulation of CO_2 in the atmosphere and its potential impact on global warming has generated interest in understanding the global carbon cycle. However, the carbon cycle within the ocean environment is not fully understood, but clearly microorganisms will profoundly influence it (Bratbak et al. 1992, Thingstad et al. 1993, Middelboe & Lyck 2002, Teira et al. 2003). It has been estimated that a marine virus contains about 0.2 fg of carbon, this translates into 200Mt of carbon in marine viruses (Suttle 2005).

1.2. Phytoplankton dynamics

Many of the recent episodes of ecological change in coastal and open-ocean waters are related directly or indirectly to phytoplankton species. These include anoxia and associated mortality of fish and shellfish (Rosenberg et al. 1990, Honjo 1993), the doubling of biomass and community shifts in invertebrates (Beukema 1991), and the accumulation of thick foam on beaches (Pieters et al. 1980, Batje & Michaelis 1986). Therefore, the study of species composition, abundance, and production rate of the phytoplankton is central to understand some important environmental changes in the oceans.

Phytoplankton are defined as free-floating unicells and colonies that grow photoautotrophically in aquatic environments (Vaulot 2001). They are at the base of the pelagic food web and microbial loop in the oceanic ecosystem (Azam et al. 1983, Bratbak

et al. 1994, Wommack & Colwell 2000). All phytoplankton species are capable of photosynthesis, and often phytoplanktonic primary production represents the main source of organic carbon in certain environments (Jassby et al. 1993). The marine phytoplankton comprises some 5000 species (Hallegraeff 1993), including a broad range of cell sizes, morphologies, physiologies and biochemical compositions (Margalef 1978). Population dynamics of the phytoplankton are the result of changes in biomass, composition and spatial distribution. The variables that affect those processes can be physical (e.g. light availability, turbulent mixing in the water column), chemical (e.g. nutrients), and biological (e.g. life cycle) (Cloern 1996). Until recently, grazing by zooplankton and sinking were considered the main cell loss factors. Selective feeding of zooplankton depending on algal size and abundance influences the phytoplankton species succession (Kleppel 1993). On the other hand, although all microalgal species are subject to sinking, the sinking rate varies depending on size, life-cycle, physiological status and motility with a subsequent impact on species succession.

Frequently, the primary productivity is balanced by the phytoplankton losses, resulting in a population growth rate close to zero (Evans & Parslow 1985). Yet, many microalgae species dynamics include episodic rapid population increases known as "blooms". During a bloom the primary productivity temporarily exceeds the losses resulting in exceptionally high biomass (Paerl 1988). Usually, during a bloom episode the species composition of the phytoplankton community changes rapidly. Blooms occur in response to optimum physical and chemical conditions. Their magnitude is determined by the initial nutrient concentrations, currents and water turbulence, grazing pressure and climatic conditions (Paerl 1988).

The fluctuations in phytoplankton populations are closely linked to ocean biogeochemistry and will have subsequent ecological implications in trophic dynamics. Phytoplankton

transform inorganic substrates into organic matter, which becomes available to heterotrophs through direct consumption of live algae or by assimilation of excreted dissolved organic matter (DOM). The connection between microalgal metabolites and bacterial production is now well documented (Riemann et al. 1990, Norrman et al. 1995, Bratbak et al. 1998a, Teira et al. 2003). However, the bacterial response to phytoplankton primary productivity is not always observed due to losses of bacterioplankton by grazing or viral lysis (Bratbak et al. 1990).

Phytoplankton are also grazed by zooplankton. The population growth rate of copepods such as *Calanus pacificus* and *Acartia* sp., not capable of storing big food reserves, is sensitive to fluctuations in phytoplankton biomass. Their rate of egg production is highly determined by the abundance and composition of the phytoplankton (Beckman & Peterson 1986, Shin et al. 2003, Ask 2004). Phytoplankton dynamics are also coupled to higher levels of the marine food web through predation on either zooplankton or directly on phytoplankton (Townsend 1984, Starr et al. 1991, Ruiz et al. 1992, Powell et al. 1995). Phytoplankton also affect the concentrations of dissolved inorganic nutrients (Horrigan et al. 1990), play important roles in the cycling of some trace elements (Sanders & Riedel 1993, Fuhrman 1999) and the release of trace gases to the atmosphere (Dacey & Wakeham 1986, Belviso et al. 1990, Malin & Kirst 1997). An example is dimethyl sulfide (DMS), which is produced by certain phytoplankton species such as *Emiliania huxleyi* and *Phaeocystis* sp. DMS has an effect on global climate as it is believed to be the dominant precursor of cloud condensation nuclei in the marine atmosphere (for reviews see Malin et al. (1994) and Simó (2001)). All these processes occur continuously and are ecologically and biogeochemically significant particularly during blooms, when phytoplankton production and loses are imbalanced.

1.3. Detection and discrimination of phytoplankton groups

Phytoplankton blooms are usually attributable to single species. Therefore, it is necessary to discriminate phytoplankton at the group or species level for the characterization of the blooms. Traditionally, this has been done by light microscopy and additionally, in the case of harmful algal blooms, by analysis for toxins. These techniques are, however, difficult and time consuming. Another issue is that, frequently, phenotypic attributes such as morphology or pigment composition are not enough to distinguish between species.

New molecular tools have proven useful for characterization, phylogeny and diversity studies of several phytoplankton species. These techniques include random amplified polymorphic DNA (RAPD), denaturing gradient gel electrophoresis, fluorescence *in situ* hybridization and sequencing; and the development of genetic markers that target unique DNA or RNA features (see review by de Bruin et al. (2003)). The use of these genetic markers allows quick detection and discrimination of phytoplankton species or even strains. In addition, these molecular tools are normally more accurate than microscopic analysis and allow detection of cells occurring even in low concentration. The utilization of molecular probes for real-time PCR will allow simultaneous identification and quantification of phytoplankton species. In real-time PCR the process of amplification is monitored in real time by using fluorescence techniques (Heid et al. 1996, Nazarenko et al. 1997). The information obtained, as amplification curves, can be used to quantify the initial amount of template molecules with high precision.

1.4. Phytoplankton species studied in the thesis

The *E. huxleyi* and *P. pouchetii* host-virus systems were selected as models in this thesis for a number of reasons. These two species of the class Prymnesiophyceae are ubiquitous, form intense blooms and play an important role in the biogeochemistry of the ocean by significantly influencing the carbon and sulphur cycles, which in turn affect global climate.

1.4.1. *Emiliania huxleyi*

E. huxleyi (Lohmann) Hay and Mohler has existed for the past 270,000 years, since it differentiated from *Gephyrocapsa* Kamptner (Thierstein et al. 1977) and is the most numerous coccolithophore in the ocean today. Its cells have a diameter of 3 to 8 μm and are covered by calcium carbonate plates (coccoliths), built of microcrystals with different forms and sizes.

The coccoliths are produced in an intracellular vesicle with the reticular body supplying constituents, and then they are extruded upon completion (Corstjens et al. 1998). *E. huxleyi* has a complex life cycle with at least four kinds of cell: coccolith forming, naked, scaly and amoeboid (for review see Paasche (2002)). There is considerable intraspecific differentiation among *E. huxleyi* isolates with respect to coccolith morphology, physiological properties and immunological properties of the polysaccharide associated with coccoliths. Based on these differences, *E. huxleyi* is currently separated into four morphotypes, A and B being the most extensively characterised (Paasche 1964, van Bleijswijk et al. 1991, Young & Westbroek 1991). *E. huxleyi* cell morphotypes A and B clearly differ in morphological features and growth parameters. Morphotype A coccoliths have smaller height:width ratio and thicker shield elements than morphotype B coccoliths, and are usually smaller than morphotype B coccoliths. The coccolith's central area elements are curved fluted rods in morphotype A and straight irregular lamellae in B (van Bleijswijk et al. 1991). Within morphotype A there is a more subtle differentiation that separates between Scandinavian and Atlantic A-isolates (Båtvik et al. 1997). Morphotype B cells contain more calcite carbon and more organic carbon than morphotype A cells (van Bleijswijk et al. 1994). There is also ample evidence of genetic diversity, even between clones from the same bloom (Medlin et al. 1996, Iglesias-Rodriguez et al. 2002). Schroeder et al. (2005) showed that a gene encoding a protein with calcium-binding motifs (designated GPA), thought to be involved in regulating coccolith morphology (Corstjens et

al. 1998), could be used as a genetic marker to definitively resolve differences that could be attributed to different *E. huxleyi* genotypes within the A and B morphotypes kept in culture.

An overview by Westbroek et al. (1993) advocated *E. huxleyi* as a global model organism. A factor that also favours study on this species is the facility to grow it in laboratory culture. Much of the interest in *E. huxleyi* is derived from its ability to form vast blooms during spring and summer in offshore, coastal and oceanic waters at mid-latitudes (45 to 55° N) (Ackleson et al. 1988). Indeed, coccolithophore blooms are seasonally predictable in certain areas including the North Sea (Holligan et al. 1983), and Norwegian fjords (Bratbak et al. 1993). These blooms significantly affect the Earth's climate system through: (1) the production of coccoliths which is accompanied by outputs of CO_2 (Holligan et al. 1993), (2) emissions of DMS to the atmosphere (for review see Simó (2001)), and (3) affecting the heat exchange between the ocean and the atmosphere by influencing the optical properties of the water (Holligan et al. 1993, Stramska & Dickey 1993).

E. huxleyi blooms are visible from satellites due to the increase of the sea surface reflectance caused especially when the coccoliths are released from dying cells (Holligan et al. 1983). This property is of great interest to provide real-time information on the position of these blooms to support research vessels that can provide a detailed assessment of physicochemical and biological parameters (Holligan et al. 1983, Holligan et al. 1993, van der Wal et al. 1995).

Since *E. huxleyi* was reported to contain viral particles approximately 200 nm in diameter (Manton & Leadbeater 1974), many researchers have investigated different aspects of this host-virus system (see Section 1.5 onwards).

1.4.2. *Phaeocystis pouchetii*

P. pouchetii (Hariot) Lagerheim has a complex life cycle that involves solitary cells and colonies, usually coexisting during a bloom (Rousseau et al. 1994). Most *Phaeocystis* colonies have a membrane or integument; others consist of mucus aggregates of cells with no true membrane (Zingone et al. 1999). With respect to grazing by zooplankton and benthic filter feeders, single cells and colonies function as different phytoplankton functional groups. For instance, solitary cells are grazed mainly by microzooplankton and colonial morphs by mesozooplankton (Weisse et al. 1994, Hamm 2000), producing major shifts in trophic pathways.

Dense, nearly monospecific blooms of *Phaeocystis* are frequent in nutrient-rich areas. In the last few decades, intense blooms of *Phaeocystis* have increased in North European waters in relation to increased nutrient input in these areas (Lancelot et al. 1994).
P. pouchetii has been shown in mesocosms to be more successful when phosphate concentration is high (Egge & Heimdal 1994). This genus is a predominant component of the phytoplankton in northern Norwegian fjords (Sargent et al. 1985) in addition to many other environments(Garrison et al. 1983, Wassman et al. 1990), where they are thought to play key roles in trophic-dynamic and biogeochemical ecology (Keller et al. 1989, Thingstad & Billen 1994, Weisse et al. 1994, Veldhuis & Wassman 2005).
One characteristic of *Phaeocystis* blooms is significant input of organic matter to the pelagic environment (Thingstad & Billen 1994), mainly due to the production of mucoid colonial material which may represent up to 90 % of total algal biomass (Rousseau et al. 1990). Despite the nutritive value of *Phaeocystis* (Claustre et al. 1990), diverse negative effects of their blooms have been known for a long time: inhibition of bacterial growth (Sieburth 1960), clogging of mussel gills (Pieters et al. 1980), clogging of fishing nets (Hardy 1926), and production of fish toxins (Aanesen et al. 1998).

As with many other phytoplankton from all major classes, *Phaeocystis* have been found to be susceptible to viral infection. Norwegian researchers isolated and characterised a species-specific virus for *P. pouchetii* (Jacobsen et al. 1996), and investigated its relation to host cell growth (Bratbak et al. 1998b). They found evidence that indicates that solitary cells are infected but colonial forms are not, and suggested that the gelatinous matrix of *P. pouchetii* colonies may protect against infection. Another hypothesis is that colony membranes have pores too small to allow viral particles to enter (Whipple et al. 2005). Therefore, life-cycle stages may influence the chances of survival and bloom formation. Also important is the dimethylsulfoniopropionate (DMSP) produced by *Phaeocystis*, among other phytoplankton species. DMSP can be cleaved to form DMS and acrylic acid (AA) (Davidson & Marchant 1992, Liss et al. 1994), thus the importance of *Phaeocystis* in global change research. Experiments have shown a substantial release of DMS and DMSP as a consequence of viral lysis of cultures of *P. pouchetii* (Malin et al. 1998).

1.5. The origins of marine virology

A virus is a non-cellular genetic element surrounded by a protein shell that lacks intrinsic metabolism. Viruses take over the reproductive machinery of a suitable host for their own reproduction, this can happen basically in three ways: (1) Lytic infection: the virus nucleic acid is introduced into the host cell, directing the host to produce progeny viruses, and then these are released by bursting the cell, (2) Chronic infection: the host cell releases the progeny viruses by extrusion; this type of infection is non-lethal, (3) Lysogeny: the viral nucleic acid is incorporated into the host genome, where it reproduces as genetic material in the host cell line. Certain events, such as stress, can induce a switch to lytic infection. Viral particles include a large range of shapes and sizes (Flint et al. 2000), usually between 20 and 200 nm long. A given type of virus usually has a restricted range of hosts. Some infect only a single species or even just a subspecies whilst others may infect more than one related species or a genus.

Knowledge of the existence of marine viruses or 'virioplankton' has existed for some time (Kriss & Rukina 1947). Initially, most studies were focused on bacterioplankton, characterising isolates based on morphology, host range and adaptation to environmental conditions (Spencer 1960, Hidaka 1971, Zachary 1976). Yet, marine virioplankton are composed of both pro- and eukaryotic viruses and, in theory, all cellular organisms are susceptible to infection. However, the concentration of viruses in natural unpolluted waters was in general believed to be low and without significant ecological importance until high viral abundance was shown by direct counts using host-independent methods such as transmission electron microscopy (TEM) (Sieburth et al. 1988, Bergh et al. 1989, Proctor & Fuhrman 1990). Viruses are the most abundant and genetically diverse biological entities in the sea (Bergh et al. 1989, Wommack et al. 1992, Cochlan et al. 1993, Paul et al. 1993, Noble & Fuhrman 1998).

After recognition of microbes' importance in aquatic ecology (Azam et al. 1983), the potential significance of high numbers of active viruses in the ocean, up to 10^7 and 10^8 ml^{-1} (Bergh et al. 1989) became evident and added a new dimension to our understanding of biological oceanographic processes. The biogeochemical and ecological effects of viruses in the ocean are nowadays generally accepted although still many aspects still remain unknown. Virus infection is important in controlling the structure and diversity of microbial and phytoplankton communities through their roles in succession dynamics (Cottrell & Suttle 1991a, Suttle & Chan 1993, Castberg et al. 2001, Larsen et al. 2001, Weinbauer & Rassoulzadegan 2004) and play important roles in nutrients (Wilhelm & Suttle 1999) and biochemical cycling (Fuhrman 1999) (Figure 1.1).

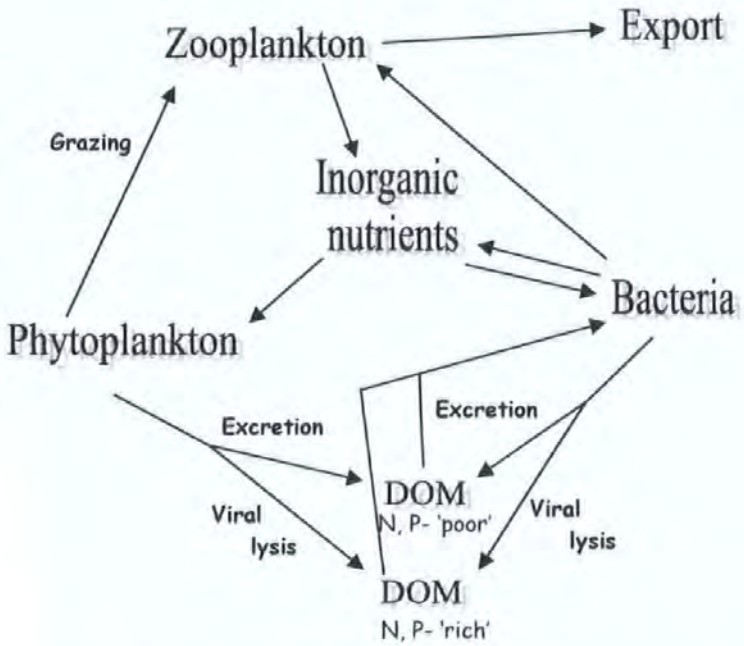

Fig. 1.1. Simplified diagram of the microbial food web. There is a net effect of converting organic matter into dissolved inorganic nutrients. Viruses cause cell lysis and divert the particulate production of their host into N and P rich, dissolved organic matter (DOM) (Adapted from Fuhrman (1999) and Brussaard (2004)).

1.6. Algal viruses

Although most viruses in seawater are associated with heterotrophic bacterioplankton (Wilcox & Fuhrman 1994), a significant proportion infects oceanic primary producers (Suttle et al. 1990, Suttle 1992). Virus-like particles (VLPs) have been observed in several algal classes (Manton & Leadbeater 1974, Pienaar 1976, Dodds 1979, van Etten et al. 1991). Abundant literature indicates that viruses can serve as important mortality agents for phytoplankton (Mayer & Taylor 1979, Bratbak et al. 1993, Bratbak et al. 1996b, Brussaard et al. 1996b, Castberg et al. 2001, Larsen et al. 2001, Wilson et al. 2002a, Wilson et al. 2002b).

The first algal virus was isolated in 1979 against the marine eukaryotic algae species *Micromonas pusilla* (Mayer & Taylor 1979). These researchers noted that *M. pusilla* cells isolated during a study of nanoplankton in British Columbia disappeared rapidly in culture. Addition of filtrates generated from the medium of these cultures produced the lysis of

healthy *M. pusilla* cells. TEM analysis of the lysate revealed polyhedral VLPs of 130-135 nm in diameter. The initial reports on *M. pusilla* viruses were followed by the isolation and characterisation of a number of other marine eukaryotic algae viruses (Table 1.1).
The position of phytoplankton at the base of the pelagic food web and the potential risks for human health (Hallegraeff 1993) and aquaculture (Nagasaki et al. 1999) derived from toxic phytoplankton blooms, placed great interest on understanding processes in algal virus ecology. In most cases, viruses that infect phytoplankton are host specific, infecting just one species or even just a single host strain. On the other hand, more than one type of viral particle may occur in an algal cell (Brussaard et al. 1996b, Baudoux & Brussaard 2005, Lawrence & Suttle 2005). However, little is still known of the biology of these systems. Understanding the factors that determine when and how a particular virus can and cannot infect an algal host under natural conditions is of great interest, due to the different ecological and biogeochemical implications.

The isolation and characterisation of a virus that infects a *Chlorella*-like species led to the formation of the Phycodnaviridae family (Meints et al. 1986, van Etten 1995, van Etten & Meints 1999b). This new, distinct family of viruses are specific to freshwater and marine phytoplankton and macroalgae (van Etten et al. 2002, Wilson et al. 2005b).
Phycodnaviruses are found in nature in a broad range of environments and conditions and have been isolated from distant geographical locations (Meints et al. 1986, Cottrell & Suttle 1991b, Jacobsen et al. 1996, Nagasaki & Yamaguchi 1997, Lawrence et al. 2001, Castberg et al. 2002, Wilson et al. 2002b, Ortmann & Suttle 2005). They are polyhedral, lack an obvious tail, are 100-220 nm in diameter and contain 100 to 560 kbp dsDNA genomes.

Apart from the variability in terms of particle and genome size, the known members within this family also differ in burst size, latent period and infection rate among other

characteristics (Table 1.1). Molecular approaches have proven vital for the study of phylogenetic relationships among *Phycodnaviridae* viruses. Chen & Suttle (1996) showed the great potential of the highly conserved DNA polymerase (*pol*) gene for phylogenetic analysis using specific algal-virus primers to establish evolutionary relationships among this family. Short & Suttle (1999) also used these primers to study diversity in natural virus communities. Analyses based on this and other genes have shown the existence of several clades within the *Phycodnaviridae* depending on the specific host infected (Chen & Suttle 1995, 1996, Schroeder et al. 2002) (Figure 1.2). Despite the proven potential of the DNA *pol* gene, the designed degenerate set of primers gave negative results when used on a dsDNA virus infecting *Pyramimonas orientalis* (Sandaa et al. 2001).

Schroeder et al. (2002) found that viruses isolated from *E. huxleyi*, based on phylogenic analysis of the DNA *pol* genes, belong to a new genus within the *Phycodnaviridae* family. They proposed to name the new genus *Coccolithovirus*. Differences between members of the genus were elucidated by host range analysis and sequence analysis of a gene fragment encoding part of their putative Major Capsid Protein (MCP).

Currently, the *Phycodnaviridae* family consists of six genera: *Coccolithovirus*, *Chlorovirus*, *Prasinovirus*, *Prymnesiovirus*, *Phaeovirus* and *Raphidovirus* (Wilson et al. 2005b) (Figure 1.2).

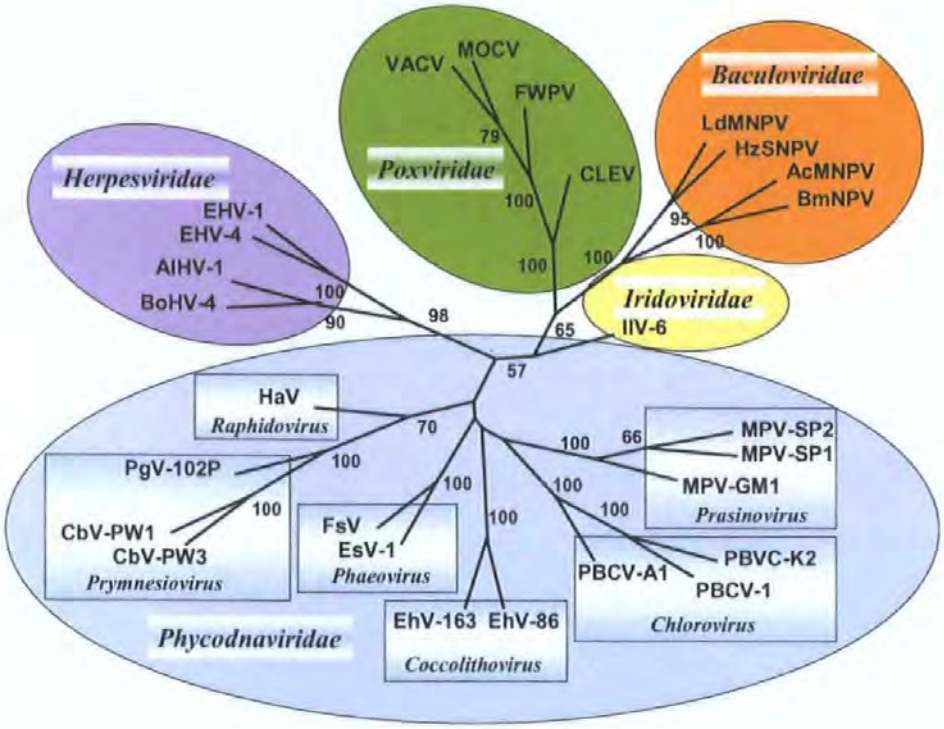

Fig. 1.2. Phylogenetic tree of DNA polymerase gene fragments from members of the family *Phycodnaviridae* and other large dsDNA viruses generated using protein parsimony analysis of the 100 bootstrapped data sets (Phylip). The numbers at the branches are the bootstrap values indicating the relative strengths of those branches. Abbreviations are: *Phycodnaviridae*: HaV, *Heterosigma akashiwo* virus; CbV-xx, viruses that infect *Chrysochromulina brevifilum*; PgV-102P, *Phaeocystis globosa* virus 102 (Plymouth); FsV, *Feldmannia* sp. virus; EsV-1, *Ectocarpus siliculosus* virus 1; EhV-xx, viruses that infect *Emiliania huxleyi*; MpV-xx, viruses that infect *Micromonas pusilla*; PBCV-1 and PBCV-NY2A, viruses that infect *Chlorella* NC64A; *Herpesviridae*: EHV-1, *Equine* herpesvirus *1*; EHV-4, *Equine* herpesvirus *4*; BoHV-4, *Bovine* herpesvirus *4*; AlHV-1, *Alcelaphine* herpesvirus 1; *Poxviridae*: VACV, *Vaccinia* virus; MOCV, *Molluscum contagiasum* virus; FWPV, Fowl poxvirus; CLEV, *Choristoneura biennis* entomopoxvirus; *Baculoviridae*: AcMNPV, *Autographa californica* nucleopolyhedrovirus; BmNPV, *Bombyx mori* nucleopolyhedrovirus; HzSNPV, *Helicoverpa zea* nucleopolyhedrovirus; LdMNPV, *Lymantria dispar* nucleopolyhedrovirus; *Iridoviridae*: IIV-6, Invertebrate iridescent virus 6 (Wilson et al. 2005b).

Some of these viruses are host specific and only infect single isolates or species of algae. For example, chloroviruses only attach to cell walls of certain unicellular, eukaryotic, chlorella-like green algae. Virus attachment is followed by dissolution of the host wall at the point of attachment and entry of the viral DNA and associated proteins (glycoproteins, myristylated proteins and several phosphoproteins) into the cell, leaving an empty capsid

on the host surface. Beginning ~2-4 h post-infection, progeny virions are assembled in the cytoplasm of the host. Infectious virions can be detected inside the cell ~30-40 min prior to virus release; virus release occurs by cell lysis. Coccolithoviruses, prymnesioviruses and raphidoviruses have wider host ranges, where individual viruses can infect a range of host isolates within specific algal species; however they do not cross the species barrier.

Infection of the prasinoviruses occurs when virions adhere to the wall-less host cell surface, followed by fusion of adjacent host and particle surfaces. Empty particles remain on the cell surface following the release of core contents. An eclipse period of approximately 3 h follows the attachment stage. The virus growth cycle is complete after approximately 14 h. During the replication cycle, particles appear in the cytoplasm and are associated with the production of cytoplasmic fibrils (~5-8 nm in diameter) and clusters of membrane bound vesicles that are absent in healthy cells. Particles are released into the medium via localized ruptures in the cell membrane; ruptures often appear at several locations on the same cell.

Less is known about the replication of coccolithoviruses, prymnesioviruses and raphidoviruses. Virus formation is observed in the cytoplasm and the nucleus remains intact and separate from the viroplasm that consists of a fibrillar matrix. Ultimately, viral production results in the disruption of organelles, lysis of the cell and release of the virus particles.

The phaeoviruses infect the wall-less spore or gamete stage of filamentous brown algae. These viruses appear as virus particles in sporangial or gametangial cells of the host. Depending on the virus, viral particles are formed in unilocular and plurilocular sporangia, or gametangia (EsV-1) others only form in unilocular sporangia (*Feldmannia species*

virus). A few of these viruses can infect more than one species of brown algae (for review on the *Phycodnaviridae* family see Wilson et al. 2005b)

Hosts for some of the chloroviruses and coccolithoviruses can easily be grown in the laboratory and the viruses can be plaque-assayed. The hosts for some of the other viruses are either cultured axenically (e.g., prymnesiovirus hosts, *P. globosa*) or non-axenically in uni-alga cultures (e.g. hosts for the prasinoviruses and raphidoviruses). The brown algal viruses, which only appear in mature gametangia or sporangia cells of their hosts, can also be grown in the laboratory.

In addition to the Phycodnaviridae family that has dsDNA genomes, ssRNA viruses have been reported to infect the two toxic harmful algal bloom species *Heterosigma akashiwo* (Raphidophyceae) (Tai et al. 2003) and *Heterocapsa circularisquama* (Dinophyceae) (Nagasaki et al. 2005). The recently completed genomic sequence of the ssRNA *H. akashiwo* virus led to the creation of the Marnaviridae family (Lang et al. 2004). Also, a dsRNA virus of the family Reoviridae (Fields et al. 1996) has been found to infect *M. pusilla* (Prasinophyceae) (Brussaard et al. 2004a) (Table 1.1).

The difficulty to cultivate susceptible hosts to propagate viruses in the laboratory limits our knowledge about marine viral diversity. An additional complication is the lack of a single genetic element shared by all viruses (Rohwer & Edwards 2002). However, all viruses from certain taxonomic groups share conserved genes that can be used to study diversity within those viral groups. For example, some studies of diversity of phages that infect cyanobacteria have been based on sequences of structural proteins (Fuller et al. 1998, Zhong et al. 2002, Mühling et al. 2005, Short & Suttle 2005) and diversity of algal viruses has been mainly studied by sequencing DNA *pol* genes (Chen & Suttle 1995, 1996, Chen

et al. 1996). A few other genetic markers are available, such as those based on the MCP gene of *E. huxleyi*-specific viruses (EhV) (Schroeder et al. 2002).

Sequencing of shotgun libraries from environmental microbial communities, or metagenomics, has emerged as a powerful tool that enables the discovery of completely novel groups of microbes regardless of their ability to be cultured in the laboratory (Rondon et al. 2000). Metagenomics could therefore unlock the massive uncultured microbial diversity present in the environment to provide new molecules for therapeutic and biotechnological applications. Metagenomic data from coastal waters and sediments has revealed incredibly high genetic richness in marine viral communities. In addition, these results suggest that the majority of environmental viruses are still uncharacterized since 75 % of the sequences produced did not match any known genes (Breitbart et al. 2002, Breitbart et al. 2004, Breitbart & Rohwer 2005). Furthermore, metagenomics analyses provide important insights into biogeographical distribution and community structure (i.e. the number of genotypes and relative abundances).

Host class	Prymnesiophyceae	Chrysophyceae	Prasinophyceae	Prymnesiophyceae
Host species	*Phaeocystis pouchetii*	*Aureococcus anophagefferens*	*Pyramimonas orientalis*	*Phaeocystis globosa*
Virus family	*Phycodnaviridae*	*Phycodnaviridae*	*Phycodnaviridae*	*Phycodnaviridae*
Virus genus	n.d.	n.d.	n.d.	Prymnesiovirus
Genome type	dsDNA	dsDNA	dsDNA	dsDNA
Genome size (kbp)	~ 460	n.d.	560	n.d.
Diameter (nm)	130-160	140-160	180-220	100-170
Latent period (h)	12-18	24	14-19	10-16
Burst size (# cell^{-1})	350-600	n.d.	800-1000	n.d.
References	(Jacobsen et al. 1996, Larsen et al. 2004)	(Gastrich et al. 1998)	(Sandaa et al. 2001)	(Brussaard et al. 2004a)
Host class	Prymnesiophyceae	Prymnesiophyceae	Dinophyceae	Dinophyceae
Host species	*Chrysochromulina brevifilum*	*Chrysochromulina ericina*	*Heterocapsa circularisquama*	*Heterocapsa circularisquama*
Virus family	*Phycodnaviridae*	*Phycodnaviridae*	*Phycodnaviridae*	n.d.
Virus genus	Prymnesiovirus	n.d.	n.d.	n.d.
Genome type	dsDNA	dsDNA	dsDNA	ssRNA
Genome size (kbp)	n.d.	510	n.d.	4.4
Diameter (nm)	145-170	160	180-210	30
Latent period (h)	n.d.	14-19	24-48	24-48
Burst size (# cell^{-1})	Several thousand	1800-4100	n.d.	7000-43000
References	(Suttle & Chan 1995)	(Sandaa et al. 2001)	(Tarutani et al. 2001)	Tomaru, unp. data
Host class	Prymnesiophyceae	Chlorophyceae	Prasinophyceae	Prasinophyceae
Host species	*Emiliania huxleyi*	*Chlorella*-like alga	*Micromonas pusilla*	*Micromonas pusilla*
Virus family	*Phycodnaviridae*	*Phycodnaviridae*	*Phycodnaviridae*	*Reoviridae*
Virus genus	Coccolithovirus	Chlorovirus	Prasinovirus	n.d.
Genome type	dsDNA	dsDNA	dsDNA	dsRNA
Genome size (kbp)	~410-415	330-380	77-110	25.5
Diameter (nm)	150-200	190	115-135	65-80
Latent period (h)	12-14	3-4	7-14	36
Burst size (# cell^{-1})	400-1000	200-350	72	460-520
References	(Wilson et al. 2005b)	(Meints et al. 1986)	(Waters & Chan 1982); (Cottrell & Suttle 1991a)	Brussaard, unp. data
Host class	Raphidophyceae	Raphidophyceae		
Host species	*Heterosigma akashiwo*	*Heterosigma akashiwo*		
Virus family	*Phycodnaviridae*	n.d.		
Virus genus	Raphidovirus	n.d.		
Genome type	dsDNA	ssRNA		
Genome size (kbp)	n.d.	9.1		
Diameter (nm)	180-220	25		
Latent period (h)	30-33	24		
Burst size (# cell^{-1})	770	100000		
References	(Nagasaki et al. 1994); (Nagasaki et al. 1999)	(Tai et al. 2003); (Lawrence et al. 2001)		

Table 1.1. Main characteristics of marine eukaryotic phytoplankton viruses in culture (adapted from (Brussaard 2004)). n.d. denotes not determined.

1.7. Role of phytoplankton viruses

Viral abundances in the sea are variable over geographical and temporal scales (Bratbak et al. 1996a). This may be an indication of corresponding host-virus interactions and fast degradation of a large percentage of viruses released into the water (Fuhrman 1999). The importance of phytoplankton viruses as active agents in the ocean has been demonstrated by numerous studies. The infection by lytic virus of unicellular phytoplankton results, inevitably, in cell death, and directly affects population abundance. However, the implications of viral infection are more than mortality alone.

1.7.1. Viral-mediated mortality: impact on abundance, structure and community dynamics.

Addition of a native virus concentrate to a field seawater sample led to reduction of the phytoplankton primary productivity by as much as 78 %, indicating that viruses are a possible regulating factor of phytoplankton community structure (Suttle et al. 1990, Suttle 1992).

Preventative viral control can limit the size of the host populations, maintaining them at non-blooming level (Suttle & Chan 1994, Bratbak et al. 1996a, Suttle 2000b, Larsen et al. 2001). Such stable host-virus coexistence has been observed in the *M. pusilla*-virus system, where viral infection keeps the algal biomass below bloom abundance (Zingone et al. 1999). During a mesocosm experiment, Evans et al. (2003) estimated a virally induced turnover rate of *Micromonas* sp. between 9 and 25 % d^{-1}. Total cell lysis rates of natural phytoplankton populations are highly variable both temporally and spatially (Brussaard et al. 1996a, Brussaard et al. 1996b, Agusti & Duarte 2000, Riegman et al. 2002). The most evident viral activity is the significant contribution to the decline of many phytoplankton blooms.

Mesocosm and field studies of *E. huxleyi* blooms showed that the collapse of these blooms is accompanied by a concurrent increase in the abundance of viral particles identified as *E. huxleyi*-specific viruses. Bratbak et al. (1993) reported that viruses were responsible for up to 100 % of the net mortality of the *E. huxleyi*, while Brussaard et al. (1996b) showed that as many as 50 % of cells were visibly infected during the decay of a bloom. Further observations show a dynamic relationship of viruses infecting *E. huxleyi* with their host, and an intimate link to the rest of the microbial community, possibly acting as a driving force in bloom successions (Castberg et al. 2001, Jacquet et al. 2002, Wilson et al. 2002a).

Several studies have investigated the role of viruses in controlling, among others, the bloom forming species *P. pouchetii* and have found similar results to those described above (Billen & Fontigny 1987, Bratbak et al. 1998a, Bratbak et al. 1998b, Jacobsen 2000, Larsen et al. 2004). Viruses have, as a result, a great influence in regulating interspecies competition and succession. As described by Thingstad (2000) in his 'kill the winner' model, coexistence of competing phytoplankton species is ensured by host-specific viruses that prevent the best competitors from building up a high biomass.

We are also aware of morphological and genetic heterogeneity within a specific geographical population of one phytoplankton species (see review by Medlin et al. (2000)) and within the virus group that infect them (e.g. Cottrell & Suttle 1995b, Chen et al. 1996, Fuller et al. 1998, Schroeder et al. 2002, Schroeder et al. 2003). One can thus expect viruses to affect phytoplankton diversity and structuring also at intraspecies level.

Ultimately, viruses serve as vectors for the transfer of genetic material (transduction) between phytoplankton communities (Jiang & Paul 1998a). Phages often carry in their genomes inserted genes that may come from other phages or hosts (Juhala et al. 2000). The acquisition of ecologically important genes is a way of adaptation to new environments.

For example, genes involved in phosphate metabolism have been found in many marine phages (Rohwer et al. 2000, Chen & Lu 2002). Also, cyanophages that infect *Synechococcus* and *Prochlorococcus* have acquired photosynthetic genes (Mann et al. 2003). This phenomenon may be a beneficial trait to the viruses or their photosynthetic cyanobacterial hosts, or may represent an untapped pool of genes involved in the formation of the photosynthetic apparatus that are prone to lateral gene transfer (Zeidner et al. 2005). Phages carrying such genes between environments contribute to local and global lateral gene transfer (Breitbart & Rohwer 2005). Yet, genetic exchange is probably the most understudied aspect of marine viruses.

1.7.2. Biogeochemical and ecological implications

Suttle et al.(1990) showed that viruses were able to inhibit primary production of phytoplankton. Therefore, the existence of algal viruses in the ocean may explain difficulties in balancing rates of primary production with loss rates for phytoplankton and sinks for organic carbon. Phytoplankton photosynthesis is responsible for the main input of primary production of carbon in the ocean (Ducklow & Carlson 1992). Thus, death of a variety of phytoplankton by viruses affects the flow of organic carbon and energy in the oceanic food web (Wilhelm & Suttle 1999) (Figure 1). Moreover, viral-induced phytoplankton cells lysis means an important release of proteins, carbohydrates, nucleic acids, and organic nitrogen and phosphorus compounds into the environment. This constitutes a significant supply of nutrients to support other photosynthetic and heterotrophic microorganisms (Middelboe et al. 1996, Gobler et al. 1997). Therefore by promoting recycling of organic matter viruses can fuel plankton production.

Bacterial production and respiration are also tightly related to the supply of biodegradable organic matter by phytoplankton lysis (Brussaard et al. 1996a, Bratbak et al. 1998a, Fuhrman 1999, Middelboe & Lyck 2002). The inclusion of viruses into a food web model

demonstrated that lysis due to viruses recycled up to 26 % of the photosynthetically fixed organic carbon back to dissolved organic matter (Wilhelm & Suttle 1999). In turn, this has more implications than just the structuring and functioning of aquatic food webs. Global changes in the carbon budget of the planet affect temperature, and therefore, ocean circulation. The event of El Niño is a clear example of how changes in the circulation of the ocean drastically affect climate (Wilhelm & Suttle 1999).

Many phytoplankton species produce DMSP, including *P. pouchetii*, *E. huxleyi* and *M. pusilla* (Hill et al. 1998, Malin et al. 1998, Wilson et al. 2002b). The discovery of viruses able to infect phytoplankton led Malin et al. (1992) to propose that algal viruses could also be important for global climate due to their effect inducing the release of DMS to the atmosphere. Phytoplankton release DMSP via excretion, autolysis, zooplankton grazing and viral lysis. During these processes DMSP may be cleaved to DMS and acrylic acid (AA) by the algal lyases and/or by the lyases of other organisms, mainly heterotrophic prokaryotes. Whether substantial DMS is fluxed to the atmosphere, or whether it is degraded by microbes depend on complex interactions within the food web. In grazing, a fraction of the algal DMSP is assimilated by the grazer. For instance, it has been suggested that low DMS concentrations are produced when copepods graze natural phytoplanktonic populations, as the DMSP ingested remains stored in various parts of the body of the copepods and is compacted into faecal pellets (Kwint & Kramer 1995, Kwint et al. 1996). In addition, several studies have shown that under most circumstances DMS is a minor product of DMSP metabolism and a large percentage of DMSP is utilized through a second degradation pathway that does not produce DMS (Kiene 1996, van Duyl et al. 1998). In addition to degrading DMSP, certain bacteria may use DMS as a substrate (Kelly & Smith 1990, Visscher & Vangemerden 1991). During incubation experiments conducted in the eastern tropical Pacific it was shown that DMS was removed 3 to 430 times faster by biological activity than by ventilation to the atmosphere (Kiene & Bates 1990). Hence, it

is important to study the processes and interactions between viruses, zooplankton grazers and protists in order to predict the extent of oceanic DMS output to the atmosphere compared to its degradation in the water (for review see Simó (2001)).

1.8. Factors that influence viral infection and replication

In order to fully understand the impact of viruses on phytoplankton populations, it is vital to identify factors which control viral infection and replication. Although abundant in the environment, not all viruses observed are infectious. The number of infectious viruses or titer can be estimated by plaque assay (Cottrell & Suttle 1995a, Bratbak et al. 1996a, Schroeder et al. 2002, Wilson et al. 2002b, Wilson et al. 2005a) or serial endpoint dilution (Flint et al. 2000). Plaque assay experiments require the host to grow on agar plates, this method is not suitable for the majority of pelagic phytoplankton species and so the endpoint dilutions method is more frequently used.

Since the virus reproduction depends on the metabolism of the host cell, it seems evident that healthy phytoplankton will ensure virus success. Hence, environmental variables, such as light, temperature and nutrient availability that affect the host's physiology ultimately affect viral replication. Yet, van Etten et al. (1983) found that viruses that infect *Chlorella* could replicate in the dark since they did not depend on host photosynthesis. *P. pouchetii* and *H. akashiwo* viruses' infectivity and the length of the lytic cycle were not affected by light limitation (Bratbak et al. 1998b, Juneau et al. 2003). However, burst size was reduced in the *Chlorella* and *P. pouchetii* viruses. On the other hand, light was shown to be important for virus production in *Pyramimonas orientalis* (Thyrhaug et al. 2002). These researchers showed that cultures infected at the onset of the light period lysed during the dark phase, possibly avoiding long exposure to light and so loss of infectivity due to UV radiation. The production of viruses was up to 8 times lower when infection was at the beginning of the dark phase.

The effect of temperature on virus infectivity varies among different virus-host systems (van Etten et al. 1991, Cottrell & Suttle 1995a, Suttle 2000a, Nagasaki 2001). For example, *Chlorella* viruses kept infectivity for more than one year if stored at 4°C (van Etten et al. 1991). However, the adsorption rate was 50 % higher at 25 °C than at 4 °C (Meints et al. 1984).

Several studies of eukaryotic phytoplankton have shown the negative effect of nutrient limitation on viral infection processes. For example, *P. pouchetii* and *E. huxleyi* exhibit a reduced burst size under phosphate depleted, as compared to phosphate-replete conditions (Bratbak et al. 1993). Jacquet et al. (2002) reported a delay in *E. huxleyi*-specific virus production in nitrogen-depleted enclosures during a mesocosm experiment designed to monitor an *E. huxleyi* bloom. However, Schroeder et al. (2003) did not find any effect on the succession dynamics of *E. huxleyi*-specific virus genotypes due to nutrient depletion during the same mesocosm study.

1.9. Host resistance to viral infection

Host strain resistance to viral attack has been reported for most eukaryotic viruses in culture (Cottrell & Suttle 1991a, Nagasaki & Yamaguchi 1998, Zingone et al. 1999, Tarutani et al. 2001), and it is an important assumption in models that describe the effect of viruses in regulating diversity in the oceans (Thingstad & Lignell 1997). Theory suggests that resistance has a high physiological cost for the host cells, and it may mean losing competition against susceptible hosts, even when viruses are present (Levin et al. 1977). However, resistance at low or no-cost is also possible (Lenski 1988). Several strategies for how hosts avoid viral attack have been described or suggested.

Viruses travel by passive diffusion, and therefore the encounter rate with a suitable host is random and depends on both host and virus abundance in the environment, as well as on

host cell size and motility (Murray & Jackson 1992). The bigger the host cell, the more likely it is for a virus to reach its surface. But due to the higher concentrations of small particles in the sea, any given virus has more probability of contacting a small particle. Motion of host cells enhances transport rates and so the chance of encounter. Hence, large and non-motile phytoplankton cells might be less susceptible to viral infection than small and mobile ones. In addition, other characteristics of phytoplankton morphotypes may be important adaptations to escape viral infection. For example, during *E. huxleyi* blooms the rate of infection was higher on flagellated scale-bearing cells relative to lithed cells (Bratbak et al. 1995, Brussaard et al. 1996b).

It has recently been suggested that when the host cells are lysed they may release an inhibitor that lessens the infection rate in the phytoplankton population. Thyrhaug et al. (2003) observed that populations of *E. huxleyi*, *P. pouchetii*, *Pyramimonas orientalis*, and *Chrysochromulina ericina* were able to recover from viral infection, which led them to suggest the possibility of a viral resistance mechanism. They incubated cultures of these phytoplankton species with virus-free lysate (obtained by 0.02 μm filtration of stock virus lysate) for 10 min before viral addition. The results showed a reduction of the rate and extent of cell lysis, which was most pronounced in *E. huxleyi*.

Another study on *E. huxleyi* also showed important biological and ecological differences among the studied *E. huxleyi*-virus isolates (EhVs) regarding infectivity. All 10 virus isolates which were the subject of the study only infected *E. huxleyi* strains that had previously been shown to exhibit low DMSP-lyase activity, while the ones with high DMSP-lyase activity were resistant to infection (Schroeder et al. 2002).

Apoptosis or self-destruction in phytoplankton is usually a response to nutrient limitation or other physiological stressors (for review see Bidle and Falkowski (2004)). Recently, it

has also been found that apoptosis may begin in response to biogeochemical alterations upon viral infection in *H. akashiwo* (Lawrence et al. 2001), *P. globosa* (Brussaard and Berges, unpublished data), and *E. huxleyi* (Bidle et al. 2005). This finding points at apoptosis as a possible defence mechanism of phytoplankton populations. Death of infected individuals may stop production of new viral progeny and thus prevent infection of other members of the phytoplankton population (Brussaard 2004). In contrast, the discovery in an EhV of genes involved in the formation of ceramide, an intracellular signal for apoptosis, led to the theory that this EhV 'encodes a mechanism for inducing apoptosis as a strategy for killing the host cell and disseminating progeny virions' (Wilson et al. 2005a).

Finally, lysogeny has been suggested as a strategy to avoid degradation and to ensure virus survival when the host is at low densities or in nutrient limited conditions. In addition, lysogeny may confer benefits to the host, such as immunity against related viruses and the acquisition of new functions encoded by the viral genome (Lenski 1988, Jiang & Paul 1998a). Studies of lysogeny have mainly focused on heterotrophic bacteria (Steward & Levin 1984, Wilcox & Fuhrman 1994, Jiang & Paul 1998b), yet there is evidence of lysogeny in isolates and populations of the marine cyanobacteria *Synechococcus* spp (Wilson et al. 1996, Sode et al. 1997, Wilson & Mann 1997, Wilson et al. 1998). However, there is no conclusive evidence of lysogeny occurring in eukaryotic phytoplankton. A reason for this can be simply the difficulty of working with lysogenic host-virus systems and the lack of known natural lysogeny-inducing agents. Interestingly, lysogeny has been observed for members of the *Phycodnaviridae* family that infect the macroalgae *Ectocarpus siliculosus* Dillwyn. These viruses only infect the free-swimming spores or gametes (zoids) of the algae; vegetative cells are resistant to infection probably due to the lack of suitable receptors for the virus, or the protection given by their cell walls (Muller et al. 2000). Upon infection the viruses remain lysogenic, integrated in the host genome

(Delaroque et al. 1999) and are transmitted to every cell within the host through mitosis as the spore develops. Release of virus particles occurs synchronised with that of zoids from the reproductive cells of the host (Muller 1991).

1.10. Viral decay

The term 'decay' refers to the reduction over time of countable, infectious viral particles. Heldal & Bratbak (1991) pointed out that when measuring decay in whole viral communities, new virus production must be stopped. Several studies revealed a wide range of viral turnover times, from less than one hour up to a few days (Heldal & Bratbak 1991, Suttle & Chen 1992, Noble & Fuhrman 1997). An important consideration when estimating viral decay is the fact that a virus might lose its infectivity, and therefore the ability to kill the host before it cannot be detected by measuring techniques (Wommack et al. 1996).

Many biological and abiological factors, such as sunlight, grazing by protozoa, adsorption to a host cell or other particles, and hydrolytic enzymes, have an effect on viral decay in the sea. Sunlight has been reported as the main single decay factor, as it results in genome damage and the loss of transcription (Suttle & Chen 1992, Wilhelm et al. 1998, Suttle 2000b, 2000a). Sunlight-induced damage is greater at the ocean surface, where the viruses cannot escape solar radiation, than in the deep sea. The susceptibility to damage from light varies among different viruses, and some degree of adaptation has been observed depending on the environmental conditions. For instance, in sunny regions viruses show more resistance to light (Noble & Fuhrman 1997). Although light is responsible for viral decay, it has also been implicated in mechanisms in the host that can repair damaged viral DNA and restore infectivity to high proportions of viruses. Restoration rates of sunlight-damaged viruses are higher in oceanic waters compared to coastal or estuarine environments (Weinbauer et al. 1997, Wilhelm et al. 1998, Weinbauer et al. 1999). Suttle

& Chen (1992) found significant protozoan grazing on viruses and suggested that selective grazing on larger members of the virioplankton may be the major factor controlling the size structure of marine viruses.

Viruses can sink out of the photic zone by adsorption to aggregates and particles. This may have a significant contribution to viral decay in coastal waters with high concentration of colloidal and particulate matter (Proctor & Fuhrman 1991). However, the effect of adsorption can yield mixed results. Irreversible binding to particulate material means loss of viruses, while reversible adsorption to particles such as clay may protect the viruses from other forms of degradation (Proctor & Fuhrman 1991). Kapuscinski & Mitchell (1980) hypothesized that viruses adsorbed to clay sink on low water-mixing days, but are resuspended due to mixing currents, still capable of producing infection. Indeed, sediments have been recorded as reservoirs of algal viruses (Suttle 2000a, Lawrence et al. 2002). The theory of sinking as a defence mechanism of viruses might also be supported by the fact that the viruses themselves stimulate the size of aggregates formed during algal blooms (Peduzzi & Weinbauer 1993).

Although no studies on viral losses have focussed specifically on phytoplankton viruses, it is likely that the response to decay mechanisms will be similar to that of total virus communities or bacteriophages investigated.

1.11. Aims of the project

This thesis is concerned with the study of the molecular ecology of marine algal viruses. During this study host and virus population dynamics during a bloom of *P. pouchetii* was investigated. In addition, viruses were isolated and basic characterisation was conducted. However, the main focus of this project was on the *E. huxleyi*-virus system. Blooms of both phytoplankton species can be induced in marine mesocosms by adding nutrients

(Bratbak et al. 1993, Jacobsen et al. 1995). Furthermore, their periodicity and easy detection by satellite images, in the case of *E. huxleyi*, facilitate their study.

The primary aims were to study the microbial community dynamics during the progression of *E. huxleyi* blooms, and to determine the genotypic diversity of both, *E. huxleyi* and their specific viruses in the sea based on GPA and MCP markers (Schroeder et al. 2002, Schroeder et al. 2003, Schroeder et al. 2005). The bulk of this thesis focused on a series of mesocosm studies in a Norwegian fjord, and data collected during cruises in the North Sea and the English Channel between 1999 and 2003. The field work allowed the study of these processes in the context of semi- and completely natural conditions. Additionally, it provided a unique set of data to check for geographical differences in the genotypic composition of the blooms on a temporal scale. To understand the role played by *E. huxleyi* in the global cycles of carbon and sulphur and in climate regulation it is important to study the biogeography and intraspecific composition of such blooms because they may differ in their physiology and ecology.

Further laboratory experiments were conducted to investigate the role of nutrient availability in virus propagation and gene expression. A broad collection of *E. huxleyi* strains, from several different locations of the northern and southern hemispheres, and virus isolates available (Schroeder et al. 2002, Wilson et al. 2002b), made possible the study of these processes in culture. In addition, host range experiments were carried out by inoculating the host cultures with fresh viral lysates.

CHAPTER TWO

Materials and methods

2. Materials and methods

2.1. Materials

2.1.1. Chemicals, reagents and laboratory consumables

General laboratory chemicals (analytical grade or higher) and consumables were obtained from Fisher-Scientific (Leicester, UK), Promega (Southampton, UK), Invitrogen (Paisley, UK) or Sigma-Aldrich (Poole, UK). All other reagents and consumable suppliers are listed in the text where appropriate. Ultrapure 18 MOhm water was obtained from a Synergy 185 water purification unit (Millipore, Watford, UK).

2.1.2. Commonly used solutions

Solution	Components
SM buffer	0.1 M NaCl; 8 mM $MgSO_4 \cdot 7H_2O$; 50 mM Tris/HCl; 0.005 % (w/v) glycerine
10 × TBE	0.89 M Tris-borate; 20 mM EDTA, pH 8.0
10 × TAE	400 mM Tris-acetate; 10 mM EDTA pH 8.0
GTE buffer	50 mM glucose; 25 mM Tris HCl; 10 mM EDTA pH 8.0
TE 10:1 buffer pH 8.0	10 mM-Tris HCl; 1 mM EDTA pH 8.0
DNA loading buffer	0.05 % (w/v) Bromophenol blue; 50 % (w/v) Sucrose; 10 mM EDTA pH 8.0
1 × PBS pH 7.2	137 mM NaCl; 2.7 mM KCl; 4.3 mM Na_2HPO_4; 1.47 mM KH_2PO_4

Table 2.1. Composition of commonly used solutions

2.1.3. Growth media

Medium	Components
f/2 medium	884 µM $NaNO_3$; 36 µM $NaH_2PO_4 \cdot H_2O$ 11.7 µM Fe EDTA·$6H_2O$; 0.9 µM $MnCl_2 \cdot 4H_2O$; 12 µM $Na_2EDTA \cdot 2H_2O$; 0.04 µM $CuSO_4 \cdot 5H_2O$; 0.03 µM $Na_2MoO_4 \cdot 2H_2O$; 0.08 µM $ZnSO_4 \cdot 7H_2O$; 0.05 µM $CoCl_2 \cdot 6H_2O$; 0.37 nM vitamin B_{12}; 2 nM biotin; 0.3 µM thiamine HCl
Luria-Bertani (LB) broth medium (per litre)	10 g Tryptone; 5 g Yeast extract; 10 g NaCl;
Luria-Bertani (LB) broth-agar medium (per litre)	10 g Tryptone; 5 g Yeast extract; 10 g NaCl; 15 g Agar
SOC medium (per litre)	20 g Tryptone; 5 g Yeast extract; 0.5 g NaCl; 10 ml 1 M $MgCl_2$; 10 ml 1 M $MgSO_4$; 2 ml 20% (w/v) Glucose

Table 2.2 Composition of used growth media

f/2 seawater medium (Guillard 1975) (Table 2.2) was made from 30 kD filtered and autoclaved seawater collected from a coastal station (Sta. L4: 50°15'N, 4°13'W) which lies approximately 10 km off Plymouth in the English Channel or alternatively from Raunefjorden, at the Marine Biological Field Station (Norway). Seawater collected at the latter location was diluted with 20 % volume of distilled water to reduce the salinity.

2.1.4. Virus isolates

Emiliania huxleyi-virus (EhV) strain isolates were obtained from the Plymouth Virus Collection (UK). Viruses were originally isolated from seawater samples collected at different stations and depths during the latter stages of natural *E. huxleyi* blooms in and from an *E. huxleyi*-induced bloom (Schroeder et al. 2002, Wilson et al. 2002b).

P. pouchetii-virus (PpV) strains isolated during induced blooms were obtained from the Virus Collection at the University of Bergen, Department of Biology (www.uib.no) (Jacobsen et al. 1996) (Table 2.3).

Isolate	Date	Area[1]	Latitude/ Longitude	GenBank accession numbers (MCP fragment)[3]
EhV-84	26/7/1999	EC[2]	50°15′N; 4°13′W	AF453849
EhV-86	30/7/1999	EC	50°13.79′N; 4°9.59′W	AF453848*
EhV-88	26/7/1999	EC[2]	50°15′N; 4°13′W	AF453850
EhV-163	20/7/2000	RN	60°16' N; 5°14' E	AF453851
EhV-201	27/7/2001	EC	49°56.21′N; 4°19.97′W	AF453857
EhV-202	27/7/2001	EC	50°00.36′N; 4°18.87′W	AF453856
EhV-203	27/7/2001	EC	50°00.36′N; 4°18.87′W	AF453855
EhV-205	27/7/2001	EC	49°56.21′N; 4°19.97′W	AF453854
EhV-207	01/8/2001	EC[2]	50°15′N; 4°13′W	AF453853
EhV-208	01/8/2001	EC[2]	50°15′N; 4°13′W	AF453852
PpV-AJ96	1996	RN	60°16' N; 5°14' E	N/A
PpV-AL02	2002	RN	60°16' N; 5°14' E	N/A

Table 2.3. Isolation details of EhV and PpV isolates used in this thesis and GenBank references for their sequence data. [1]Western English Channel, off the coast of Plymouth, UK (EC). Raunefjorden, Western Norway during a mesocosm experiment (RN). [2]Station L4. [3]271 bp-284 bp fragments (*716 bp) from a gene encoding the putative major capsid protein in EhV. N/A: not applicable

2.1.5. Phytoplankton strains

Non-axenic clonal strains of *Emiliania huxleyi* (Lohmann) Hay and Mohler were obtained from the Provasoli-Guillard Center for the Cultivation of Marine Phytoplankton (CCMP, Maine, USA; http://ccmp.bigelow.org/) and from the Plymouth Culture Collection (Marine Biological Association, UK; http://www.mba.ac.uk/). The axenic and clonal culture of *E. huxleyi* strain CCMP 1516 was obtained from Michael Steinke (University of East Anglia, UK) (Table 2.4). Cultures of *Phaeocystis pouchetii* strain AJ01, *Micromonas pusilla*, *Chrysochromulina ericina*, *Pyramimonas orientalis*, *Nephroselmis rotunda*, *Isochrysis galvana* and *Synechococcus* spp. were obtained from the Culture Collection at the University of Bergen, Department of Biology (www.uib.no). *P. pouchetii* strain AJ01 was originally isolated from the Norwegian coast (60°16′N, 5° 7′E) by Anita Jacobsen in spring 1994.

Clone designation	Isolation date	Other names	Origin	Cell Type	CMM group	Accession number	Liths	DMSP activity	Reference/Source
92A	1950/57	CCMP 379, UTEX 1016, CCAP920/1A	English Channel	?	I	AY629172	No	High	(Steinke et al. 1998)
92D	1975		English Channel	B	II	AY629177	Some	?	(Young and Westbroek, 1991; Green et al. 1996; Medlin et al. 1996)
92E	1992		English Channel	A	I IV	AY629178 AY750878	Yes	?	PCC
92F	1992		English Channel	?			No	?	
Bloom 215	2002		English Channel	A	I	AY629179	?	?	PCC
Bloom			English Channel	?			?	?	
CCMP 1516	1991		North Pacific	A	III IV	AY629166 AY629167	Yes	Low	(Steinke et al. 1998)
		CCMP 1516 (b)*			IV	AY629167	No	?	PCC
Van 556	1984		North Pacific	?			No	?	
EH2	1990		South Pacific	?			Yes	?	
Ch25/90	1990	Texel B, Ch 25	North Atlantic	B	II	AY629181	Yes	?	(Green et al. 1996; Medlin et al. 1996; van Bleijswijk, 1996)
Ch24/90	1990		North Atlantic	A			Yes	?	(Young and Westbroek, 1991; van Bleijswijk, 1996)
5_90_25b	1990		North Atlantic	?	I	AY629176	Yes	?	PCC
G1779Ga	1989		North Atlantic	?			Yes	?	
DWN61/3/2	1991		North Atlantic	?			Yes	?	

Table continues in next page

Clone designation	Isolation date	Other names	Origin	Cell Type	CMM group	Accession number	Liths	DMSP activity	Reference/Source
BOF92	1990		North Atlantic	?	?		Yes	?	
CCMP 88E	1988		Gulf of Maine	?	?		Yes	?	
CCMP 374	1989	89E, CCMP 1949	Gulf of Maine	?	I IV	AY629170 AY629171		Low	(Steinke et al. 1998)
F61	1970		Oslo fjord	?	?		No	?	
CCMP 370	1959	451 B, F451	Oslo fjord	?	I	AY629168	No	Low	(Steinke et al. 1998)
L	1959/68/80	LN, Lsc, Ln, S	Oslo fjord	A	I III	AY629173 AY629174	No	Low	(Young and Westbroek, 1991; Medlin et al. 1996; van Bleijswijk, 1996)
CCMP 373	1960	BT6, CSIRO-CS-57	Sargasso Sea	A	I	AY629169	No	High	(Medlin et al., 1996; Steinke et al. 1998)
CCMP 1A1	1987	CCMP 372	Sargasso Sea	A	IV	AY629175	Yes	?	PCC
CCMP 12-1	1987	CCMP 371	Sargasso Sea	?	?		Yes	?	
CCMP MCH1	1967	CCMP 375	Sargasso Sea	?	?		Yes	?	
South Africa	1983		Indian Ocean	?	?		Yes	?	
NZ EH	1992	CAWPO 6	New Zealand	?	?		Yes	?	

Table 2.4. *Emiliania huxleyi* isolates used in this study. CCM group: allelic genotype or Coccolith Morphology Motif. Accession number: GenBank number corresponding to a putative calcium binding protein gene sequence fragment. PCC: Plymouth Culture Collection. ? symbol: not known. * symbol: CCMP 1516 (b) is a non-calcifying strain closely related to the calcifying CCMP 1516 strain (a change in calcification state has occurred during culturing since the original isolation of the strain)

2.1.6. Oligonucleotides

Oligomers designed to the calcium-binding protein (GPA) cDNA of *E. huxleyi* strain L and to the Major Capsid Protein (MCP) of EhV-86 were used to assess genetic richness of *E. huxleyi* and EhVs in natural communities. M13 oligomers were used to amplify DNA fragments ligated into pGEM®–T Easy Vectors (Promega, Southampton, UK). Phos-F1 and Phos-R1 oligomers were designed to the putative phosphate permease gene (ehv117) of EhV-86. TaqMan primers and probe for real-time reverse-transcription PCR reactions were also designed to the nucleotide sequence of the ehv117 gene of EhV-86.

Oligomer	Sequence	Reference
GPA-F1	5'-GAG GAG GAG AAG CCG AGC CT-3'	Schroeder et al. (2005)
GPA-F2	5'-CAG GCG CTC TTC GGG CTG GG-3'	This study
GPA-R1	5'-CTT GAA TCC TCT GTG CTG AGC GAG-3'	Schroeder et al. (2005)
MCP-F1	5'-GTC TTC GTA CCA GAA GCA CTC GCT-3'	Schroeder et al. (2002)
MCP-R1	5'-ACG CCT CGG TGT ACG CAC CCT CA-3'	Schroeder et al. (2002)
MCP-F2	5'-CGC CCG GGG CGC GCC CCG GGC GGG GCG GGG GCA CGG GGG GTT CGC GCT CGA GTC GAT C-3'	Schroeder et al. (2003)
MCP-R2	5'-GAC CTT TAG GCC AGG GAG-3'	Schroeder et al. (2003)
M13-F	5'-GTA AAA CGA CGG CCA GT-3'	Hoffmann et al. (2001)
M13-R	5'-CAG GAA ACA GCT ATG AC-3'	Hoffmann et al. (2001)
Phos-F1	5'-TAG TTT ACC AAA CGG AGC -3'	This study
Phos-R1	5'-TTA AGA TGT TTC ATT AAA CA -3'	This study
qPCR-F	5'-ACA CCA AGT CGT GGT GTT TGT ATT-3'	This study
qPCR-R	5'-TGA TAA CGG AAT CCC CAT ATA GCT-3'	This study
qPCR-probe	5'-AGC TTG GTT CCG CGG TTG TAA TTA TCA CC-3'	This study

Table 2.5. Oligonucleotides and their sequences used in this study. F and R denote forward and reverse primer respectively. Sequence underlined in MCP-F2 is the GC-clamp added to the 5' end of the oligonucleotide and necessary for DGGE analysis. The 'q' prefix denotes the primers and probe used for real-time PCR assays (Section 2.14).

2.2. General methods

2.2.1. Concentration and storage of seawater samples and viral lysates

When required, seawater and lysate samples were concentrated 25-100 fold by means of tangential flow filtration (TFF) through a 100,000 molecular weight cut off (MWCO) polyethersulfone membrane (Vivaflow 200, Vivascience) according to the manufacturer's protocol. Typically, samples were pre-filtered through 0.8 µm and then 0.45 µm or 0.2 µm pore size Supor-450 47 mm diameter filters (PALL Corp), prior the concentration step. The concentrates were stored at 4 °C until further processing.

2.2.2. Maintenance of phytoplankton cultures

Cultures were maintained at exponential growth phase by periodically transferring 5-10% (v/v) cultures in fresh f/2 seawater medium (Guillard 1975) (Table 2.2). Light was supplied by fluorescence tubes at 100 µmol photons m^{-2} s^{-1} under a light-dark cycle of 16:8h. *P. pouchetii* cultures were kept at 8 °C; all other phytoplankton species were grown at 15 °C.

2.2.3. Isolation of new viruses

Isolation of viruses from seawater samples was conducted by adding filtered seawater sub-samples to exponentially growing phytoplankton cultures or alternatively by enrichment cultures method. When lysates were produced virus clones were obtained by further plaque assay purification. The experiments were carried out under the culturing conditions described in Section 2.2.2.

2.2.3.1. Inoculation of phytoplankton-host cultures

Aliquots (0.5 ml) of concentrated seawater samples were inoculated into 20 ml of exponentially growing phytoplankton cultures (~ 1-2 × 10^6 cells ml^{-1}). The cultures were inspected daily for lysis. Lysis was determined by colour comparison to 20 ml of uninfected host cultures and by analytical flow cytometry (AFC) (Section 2.2.5).

2.2.3.2. Enrichment cultures

Aliquots of exponentially growing phytoplankton cultures were transferred to f/2 medium (Guillard 1975) (10 % v/v) prepared from natural untreated seawater filtered through a 0.45 μm pore size Supor-450 47 mm diameter filters (PALL Corp). Additionally, aliquots of the same phytoplankton species were transferred to sterile f/2 medium to serve as negative controls. The growth of the cultures in the natural seawater f/2 medium was monitored daily. When cultures lysed AFC was employed to confirm whether or not lysis had been caused by specific viruses.

2.2.3.3. Plaque assay

Virus clones were obtained by plaque assay purification as described by Schroeder et al. (2002). A detailed protocol for this method is given below: bottom 1.5 % (w/v) electophoresis grade agarose plates were prepared by mixing sterile 7.5 % agarose in distilled water to 30 kD filtered autoclaved seawater while both solutions were at about 70 °C. The combined 1.5 % agarose seawater mixture was left to cool to 55 °C, after which the necessary nutrients for f/2 medium were added and the solution was poured and allowed to set at room temperature in Petri dishes.

Exponentially growing phytoplankton cells were harvested by centrifugation at 5,000 g for 5 min at 4 °C and re-suspended in f/2 medium (50 × concentration). The re-suspended cells were then mixed with 100 μl dilution (10^{-2}, 10^{-4}, 10^{-6} and 10^{-8}) of the virus stocks in sterile f/2 medium and incubated, at the appropriate temperature for each phytoplankton species, under constant illumination for 2 h to allow viruses to absorb. The virus-host suspension was mixed with 3 ml of molten 0.4 % (w/v) electrophoresis grade agarose (40 °C), made with f/2 medium, and poured onto the bottom 1.5 % (w/v) agarose plates. The plates were then kept in plastic bags and transferred to the incubator at the appropriate temperature and light conditions (Section 2.2.2). The plates were monitored daily until clear plaques were

visible. Single plaques were lifted from the plate using sterile pipette tips, re-suspended in 0.5 ml f/2 medium and used for subsequent inoculations after overnight incubation at 4 °C.

2.2.4. Host range determination

For host range determination, fresh working solutions of virus lysates were obtained from stock lysates stored at 4 °C. Briefly, 1 ml of each lysate was added to 100 ml of exponentially growing cultures of the host strain originally used for their isolation. Once clearing of the host culture was observed, the lysate was passed through a 0.2 µm syringe filter (Gelman) and the filtrate containing virus was stored at 4 °C. The host range for each virus strain was determined by adding 500 µl of each fresh virus lysate to 20 ml of several exponentially growing phytoplankton cultures. The inoculated cultures were occasionally agitated to encourage virus adsorption. Growth of the host cultures was monitored daily over a 14 day period. Lysis was determined by colour comparison to 20 ml of uninfected cultures and by AFC (see Section 2.2.6). Cultures that were not lysed 14 days after the viral inoculation were considered to be non-susceptible to the virus strain. The experiment was repeated once more in order to verify the results.

2.2.5. Cell photosynthetic capacity (CPC)

CPC was measured using the photosynthetic inhibitor 3'-(3,4-dichlorophenyl)-1',1'-dimethyl urea (DCMU) method. Analysis was performed in triplicate on approximately 3 ml sub-samples of a 10 ml sample. Prior to measurement samples were dark adapted by incubation at 15 °C for 30 min. Fluorescence was measured on a 10-AU Turner Designs fluorometer before and 60 s after the addition of 50 µl of 3 mM DCMU in ethanol. Variable fluorescence expressed as F_V/F_M was calculated according to the following equation: $F_V/F_M = (F_M - F_0)/F_M$. Where F_0 is the minimum fluorescence, obtained after the period of dark adaptation, F_M is the maximum fluorescence, obtained after the addition of

DCMU closing all the reaction centres in the photosystem II and reducing the probability of photochemistry to zero, and F_V is the difference between F_M and F_0.

2.2.6. Analytical flow cytometry (AFC)

AFC analyses were performed with FACSCalibur or FACScan flow cytometers (Becton Dickinson, Franklin Lakes, USA), both equipped with an air-cooled laser providing 15 mW at 488 nm and with standard filter set-up. Typically, algal counts were obtained from fresh samples at high flow rate (average 97µl min^{-1}). Alternatively, 1 ml seawater samples for phytoplankton counts were fixed with P+G (1% paraformaldehyde + 0.05% glutaraldehyde final concentration) for 10 min at room temperature in the dark, then snap frozen in liquid nitrogen and stored at -80 °C until analysed (Marie et al. 1997). The trigger was set on red fluorescence and the samples were run on the cytometer for 300 s for natural samples or 120 s for counts on culture samples. Discrimination of the algal groups in field samples was based on groups observed in scatter plots of side-scatter signal (SSC) and pigment autofluorescence (chlorophyll and phycoerythrin for *Synechococcus* sp. and cryptophyte populations). The most common fluorescing pigments are chlorophyll and phycoerythrin, which give red and orange fluorescence respectively. Some algal groups contain only chlorophyll, while others contain both pigments. Phytoplankton group identification was supported by comparison with pure cultures AFC signatures and previous studies (Castberg et al. 2001, Larsen et al. 2001, Li & Dickie 2001, Jacquet et al. 2002).

Virus and bacteria enumeration was performed on fixed samples. 1ml samples were fixed with 20 µl of 25 % glutaraldehyde (0.5 % final concentration) for 30 min at 4 °C, then frozen in liquid nitrogen and stored at -80 °C until analysed (Marie et al. 1999b). Prior to analysis the samples were thawed at 37 °C, diluted in TE 10:1 buffer (Table 2.1) and stained with SYBR Green I (Molecular Probes Inc., Eugene, USA) in a water-bath at 80 °C

for 10 min (Marie et al. 1999a). Natural samples were typically diluted 50 to 200 times, while culture samples were diluted 100 to 10000 times. The commercial stock solution of SYBR Green I was diluted to a final dilution 1.0×10^{-4}. Virus and bacteria analysis was performed at medium flow rate (average 48 µl min^{-1}). The samples were analysed for 1 min at an event rate between 100 and 1000 s^{-1}. The discrimination of virus and bacteria groups was based on groups observed in scatter plots of SSC signal versus green DNA-dye (SYBR Green) fluorescence. Fluorescence beads (Molecular Probes Inc., Eugene, USA) with a diameter of 0.95 µm were added to each sample analysed as an internal reference. Listmode files were analysed using CYTOWIN (Vaulot 1989, available through http://www.sb-roscoff.fr/Phyto/cyto.html#cytowin, and EcoFlow v1.0.5, available from the authors).

2.2.7 Enumeration of phytoplankton cells and colonies by light microscopy

Phytoplankton cells (live samples) were counted on a Leitz Dialux-20 light microscope with phase contrast at 400× magnification using a Fuchs Rosenthal haematocytometer with a counting error of ±10% (Lund et al. 1958). Phytoplankton colonies were counted in 1 ml samples in a Sedgwick-Rafter chamber.

2.2.8. Transmission Electron Microscopy (TEM)

Aliquots of virus lysates (2 ml) were pipetted into centrifuge tubes with plastic-molded flat bottoms covered by cellulose nitrate filters (Sartorius). Electron microscope nickel grids with carbon-coated Formvar film were then dropped through the water column onto the filters. The viral particles in the samples were collected on the grids by ultracentrifugation in a swing-out rotor as described in (Bratbak & Heldal 1993). The supernatant was discarded and the grids were left to air-dry.

The grids were stained with 2 % uranyl acetate and viewed at 30,000 to 50,000 times magnification in a JEOL 100S transmission electron microscope. When necessary, the lysate was diluted in sterile 30 kD filtered seawater to ensure an even distribution of the viral particles on the grid and facilitate the analysis of the images produced.

2.2.9. Dialysis of virus lysates for removal of excess nutrients

Fragments (12 cm length) of transparent, seamless regenerated cellulose dialysis tubing (33 mm diameter) (Fisher-Scientific, Leicester, UK) were pre-treated to ensure a uniform pore size and removal of heavy metals. The pre-treatment consisted of boiling the tubing for 10 min in a 2 % $NaHCO_3$ and 0.05 % EDTA solution. Then the solution was discarded and the tubing boiled twice for 10 min in distilled water. Once cooled the tubing was stored at 4 °C in a 20 % (v/v) solution. Prior to use, the dialysis tubing was rinsed thoroughly with distilled water. One end of the tubing was sealed, then the virus lysate (approximately 100 ml) was poured inside and the other end of the tubing sealed. The filled tubing was then placed in 2 L of oligotrophic, 30 kD filtered, autoclaved seawater at 4 °C and agitated gently with a magnetic bar and stirrer motor. The dialysis tubing containing the virus lysate was left to reach equilibrium for 3 h. The oligotrophic water was replaced and the process repeated two more times.

2.2.10. Pulse field gel electrophoresis (PFGE)

PFGE analysis was performed according to the optimised protocol described by Larsen et al. (2001). Briefly, concentrated seawater samples and culture lysates (40 ml) were clarified by centrifuging in a swing-out centrifuge (Beckman J2-HS) at 7500 rpm for 30 min at 4 °C. Viruses in the supernatant were subsequently concentrated by ultracentrifugation (Beckman L8-M with SW-28 rotor) for 2 h at 35,000 × g at 10 °C. The viral pellet was re-suspended in 400 µl SM buffer (Wommack et al. 1999) (Table 2.1) and incubated overnight at 4 °C. Equal volumes of viral concentrate and molten 1.5 % InCert

agarose (FMC, Rockland, Maine) were mixed and dispensed into plug moulds. After the gel had solidified the plugs were punched out from the moulds into a small volume of buffer (250 mM EDTA, 1 % SDS) containing 1 mg ml^{-1} Proteinase K. The plugs were incubated in the dark at 30°C overnight. The Proteinase K buffer was decanted and the plugs were washed 3 times, for 30 min each time, in TE 10:1 buffer (Table 2.1). When the virus agarose plugs were not immediately analysed they were stored at 4 °C in TE 20:50. The viral plugs were loaded into the wells of a 1 % SeaKem GTG agarose (FMC, Rockland, Maine) gel in 1 × TBE gel buffer (Table 2.1) alongside plugs containing phage lambda concatamers (BioRad, Richmond, CA) that served as molecular weight markers. The plugs were sealed in the wells with an overlay of molten 1 % agarose. Samples were electrophoresed using a Bio-Rad DR-II CHEF Cell (Bio-Rad, UK) electrophoresis unit operating at 6 V cm^{-1} with pulse ramps from 20 to 45 s at 14 °C for 23 h in 0.5 × TBE tank buffer (Table 2.1). Following electrophoresis, the gels were stained for 30 min in SYBR green I (Molecular Probes Inc., Eugene, USA) according to the manufacturer's instructions and digitally scanned for fluorescence using a laser fluoroimager (Fuji Film, FLA 2000).

2.2.11. Nucleic acid isolation and quantification

2.2.11.1. Hexadecyltrimethyl ammonium bromide (CTAB) method for DNA extraction from virus lysates

Concentration of the virus fraction was a necessary step prior to DNA purification: 58.4 g NaCl were added to 0.5 L lysate and gently dissolved. The solution was let stand at 4 °C for at least 1 h and then centrifuged for 10 min at 5,000 × g in a swing-out centrifuge (Eppendorf 5810R). PEG 6000 (Fisher-Scientific, Leicester, UK) was added to the supernatant (10 % final percentage) and gently dissolved, followed by an overnight incubation at 4 °C. The solution was then centrifuged at 6,000 g for 25 min at 4 °C, the supernatant was carefully discarded and the tubes were left to dry upside down on paper towels for a few minutes at room temperature. For DNA isolation, the virus pellet was re-

suspended in 0.5 ml pre-warmed lysis buffer (0.5 % SDS, 20 μg ml^{-1} proteinase K) by briefly vortexing, followed by 30 min incubation at 55 °C with constant and gentle shaking. Then, 80 μl 5 M NaCl and 100 μl pre-warmed 10 % CTAB solution in 0.7 M NaCl were added and the mixture was incubated at 65 °C for 10 min, after which the DNA was extracted with 500 μl of chloroform:isoamyl alcohol (24:1). Following centrifugation (5 min, 20,000 × g) the top phase was discarded and the DNA was precipitated with addition of 0.6 volumes of isopropanol. DNA was pelleted after 10 min room temperature incubation by centrifugation at 20,000 × g for 10 min. Finally, the pellet was washed in 500 μl cold 70 % ethanol, air dried and re-suspended in 35 μl TE 10:1 buffer (Table 2.1).

2.2.11.2. Phenol/chloroform DNA extraction

Typically environmental samples were collected for DNA extraction by filtering seawater samples onto 0.45 μm pore size Supor-450 47 mm diameter filters (PALL Corp). Total genomic DNA was recovered from the cellular fraction retained on the filters using an adapted protocol of the phenol/chloroform method previously described by Schroeder et al. (2002) with the following modifications: the filter was cut into small (~5-10 mm^2) easily dissolvable pieces and placed into a 2 ml Eppendorf tube with 800 μl GTE buffer (Table 2.1) containing lysozyme (10 mg ml^{-1}) and 100 μl 0.5 M EDTA. The samples were incubated for 1-2 h at room temperature whilst being gently shaken. 200 μl 10 % SDS (w/v) was added to disrupt cellular membranes and the tubes were incubated for another 10 min at room temperature. Phenol (0.8 × volume) was added to the samples to dissolve the filter paper. The aqueous layer was separated from the phenol layer by 10 min centrifugation (this and the successive centrifugation steps were done at 20,000 × g) and the phenol phase was disposed of. After this DNA was extracted with an equal volume of chloroform:isoamyl alcohol (24:1). The mixture was centrifuged (10 min) and the top aqueous layer transferred to a clean 2 ml Eppendorf tube. Then, 0.5 × volume 7.5 M NH_4Ac, pH 7.5 was added and, after 30 min incubation at room temperature, the solution

was centrifuged (20,000 g, 15 min). The supernatant was successively transferred to a clean tube and the DNA was precipitated with the addition of 2.5 × volume ice-cold 100 % ethanol. Samples were incubated overnight at 4 °C to increase the recovery yield. Following a 30 min centrifugation at 20,000 × g, the DNA pellet was washed in 500 µl ice-cold 70 % ethanol, followed by a 5 min centrifugation (20,000 × g). The ethanol was then discarded and the pellet left to air-dry. Finally, DNA was re-suspended in 50 µl TE buffer, quantified via a BioPhotometer spectrophotometer (Eppendorf, Cambridge, UK) and stored at 4 °C or -20 °C until further processing.

The phenol/chloroform method was used on virus lysates with the following modifications: 0.5 ml 50-fold concentrated virus lysate (Section 2.2.1) were place in a 1.5 ml Eppendorf tube and heated at 80-90 °C for 1 min, then transferred to ice for another minute. The process was repeated 3 times. The sample was then treated with proteinase K (final concentration 50 µg/ml) in a lysis buffer containing 20 mM EDTA, pH 8.0 and 0.5 % SDS (w/v) at 65 °C for 1 h. Phenol (0.1 × volume) was added to the samples, and the DNA was extracted and precipitated as described above.

2.2.11.3. Isolation of total RNA from infected and uninfected cells

Cultures (250 ml) were filtered through 0.45 µm pore size Supor-450 47 mm diameter filters (PALL Corp). Cells from each filter were resuspended in 2 ml of 1 x Phosphate buffered saline (PBS) (diethylpyrocarbonate treated (1/1000) for 15 min, then autoclaved) (Table 2.1), centrifuged (20,000 × g, 5 min), resuspended (by vortexing) in 2 ml RNAlater™ RNA Stabilization Reagent (Qiagen) and stored at -20°C until ready for processing (samples were process within 24 h after storing). RNA extraction was performed using an RNeasy Midi Kit (Qiagen). Samples were centrifuged (20,000 × g, 5 min) and the pellet resuspended in 2 ml RLT (+ 20 µl β mercapto-ethanol). Following vigorous vortexing (1 min, in 5 second bursts), the samples were spun (20,000 × g, 5 min)

and the supernatant transferred to a 15 ml Falcon tube containing 2 ml 70 % ethanol. Following vigorous mixing the samples were applied to a Qiagen MidiPrep column, centrifuged (3,200 × g, 5 min) and the flow-through discarded. Columns were washed once with 4 ml RW1 buffer (3,200 × g, 5 min) and twice with 2.5 ml RPE buffer (3,200 × g, 5 min) and transferred to a new Falcon tube. RNase free water (250 µl) was added, the samples incubated (room temperature, 1 min) and the RNA eluted by centrifugation (3,200 × g, 5 min). RNA solutions were precipitated with 0.5 × volumes of 7.5 M NH_4Ac and 2 volumes of 100 % ethanol at -80 °C overnight. Following centrifugation (20,000 × g, 30 min), the pellet was washed twice with 70 % ethanol (20,000 × g, 5 min). The pellet was air-dried, resuspended in 50 µl RNase-free water and stored at -80 °C.

2.2.11.4. DNase treatment of RNA samples

RNA samples were treated with RNase free Turbo DNase™ (Ambion) to remove traces of DNA contamination, according to the manufacturer's recommendations.

2.2.11.5. Nucleic acid quantification

Genomic DNA concentrations were determined by absorbance at 260 nm using a Biophotometer spectrophotometer (Eppendorf, Cambridge, UK). RNA quantity and quality was assessed using RNA 6000 Pico LabChip® kit (Agilent Technologies) on an Agilent Bioanalyzer 2100 system (www.agilent.com).

2.2.12. Amplification of DNA fragments by polymerase chain reaction (PCR)

All PCR reactions were conducted in a PTC-200 Peltier Thermal cycler (MJ Research) in 25 µl final volume reactions. The PCR reactions were set up as follows: 10-100 ng DNA (alternatively 1 µl virus lysate) template was added to a reaction mixture containing 1 U Taq DNA polymerase (Promega), 1 × PCR reaction buffer (Promega), 0.25 mM dNTPs, 2-3 mM $MgCl_2$, 10 pmol of each primer and molecular biology grade water (Sigma-

Aldrich) up to a volume of 25 µl. PCR reactions were performed with an initial denaturing step of 95 °C for 5 min, followed by 35 cycles of denaturing at 95 °C for 60 s, annealing at 50-60 °C (optimised for each pair of primers) for 60 s, and extension at 72 °C for 60 s respectively. The reactions finished with final cycle of denaturing at 95 °C for 30 s, annealing at 60 °C for 300 s, and extension at 72 °C for 300 s. Finally, the reactions were cooled down to 15 °C. PCR products were resolved by electrophoresis of 5 µl aliquots (Section 2.2.13). For increasing amplification specificity nested (two stages) PCR reactions were performed using 2.5 µl of the first stage PCR products as template.

2.2.13. Agarose gel electrophoresis

Ultrapure agarose (SeaKem GTM) at a concentration of 1.2 % (w/v) was dissolved in an appropriate volume of 1 × TAE buffer (Table 2.1) by heating to boiling point in a microwave oven. The solution was cooled down to approximately 60 °C and ethidium bromide was added to a final concentration of 0.5 µg ml^{-1}. The solution was then poured into a gel former and allowed to solidify at room temperature. Samples were loaded in the gel with 1 × bromophenol blue loading buffer (Table 2.1). Electrophoresis was performed in 1 × TAE buffer at 90-120 volts for 30-60 min. The gels were visualized on a UV transilluminator, and photographed with a Gel Doc 2000 system (Bio-Rad). Band sizes were estimated using 100 bp or λ-HindIII size markers (Promega) run alongside the samples.

2.2.14. Denaturing gradient gel electrophoresis (DGGE)

DGGE was conducted in 30 to 50 % linear denaturing gradient 8 % polyacrylamide gels where 100 % denaturant is a mixture of 7 M urea and 40 % deionised formamide. PCR products were treated with Mung Bean nuclease (Promega) according to the manufacturer's instructions to degrade single-stranded DNA ends (5µl PCR product, 2 µl 1:10 diluted enzyme and 3 µl molecular biology grade water (Sigma-Aldrich) were

incubated at 37 °C for 10 min). The resultant 10 µl samples were loaded into wells with 4 µl 6 × gel loading buffer (Table 2.1). Electrophoresis was carried out for 3.5 h in 1 × TAE (Table 2.1) at 200V at a constant temperature of 60 °C using the D-code electrophoresis system (Bio-Rad). Gels were stained in 0.1 × SYBR® Gold (Molecular probes) solution for 30 min and bands visualized and photographed as described previously in Section 2.2.13.

Typically, single bands were excised and incubated in 50 µl of molecular biology grade water (Sigma-Aldrich) at 4 °C overnight. Following incubation at 95 °C for 5 min, 2 µl aliquots were used as template for PCR reaction using the appropriate pair of primers. The products run on a DGGE gel as described previously to check for single band purity.

2.2.15. Automated DNA sequencing

Prior to sequencing of PCR products, unincorporated dNTPs and primers were removed by means of a clean up step with ExoSAP-IT (USB Corporation) following the manufacturer's recommendations. PCR product (2.5 µl) and 1 µl ExoSAP-IT were mixed and incubated at 37 °C for 15 min, and then the ExoSAP-IT was inactivated by heating to 80 °C for 15 min. These steps were done in a thermal cycler.

The sequencing reactions (final volume 20 µl) were prepared using a BigDye Terminator v3.1 cycle sequencing kit (Applied Biosystems, UK) according to the manufacturer's instructions in a PTC-200 Peltier Thermal cycler (MJ Research). Subsequently, the DNA was cleaned up using genCLEAN 96 Well Dye Terminator Removal plates (Genetix, Hampshire, UK) following the manufacturer's recommendations. Alternatively the DNA was recovered by ethanol precipitation as follows: 5 µl 125 mM EDTA and 60 µl 100% ethanol were added to each sample and gently mixed. The mixture was then incubated at room temperature for 15 min in the dark. The tubes were then centrifuged at 3,000 × g for 30 min at 4 °C. The supernatant was discarded and the pellet was washed in 60 µl 70 %

ethanol at 1650 × g for 15 min. Finally, the air dried pellet was re-suspended in 15 µl HiDi formamide (Applied Biosystems, UK). The re-suspended DNA was denatured by heating at 94 °C for 3 min prior to sequencing. Sequencing was carried out on an ABI 3100 capillary sequencer (Applied Biosystems, UK) in accordance with the manufacturer's instructions. The data for each fragment was analysed using DNAStar software (Lasergene) and aligned using ClustalW (http://www.ebi.ac.uk/clustalw/).

2.2.16. Molecular cloning

PCR products were ligated into cloning vectors using the pGEM®–T Easy Vector System (Promega) in accordance with the manufacturer's instructions. The ligation products were then transformed using Subcloning Efficiency™ DH5-α Competent Cells (Invitrogen) according to the manufacturer's recommendations and plated onto LB-agar (Table 2.2) plates containing 100 µg ml^{-1} ampicillin (Sigma-Aldrich). Prior to plating, X-Gal (20 µl of 50 mg ml^{-1}) was spread over the surface of each plate and allowed to absorb for 30 minutes at 37 °C. Plates were then incubated overnight at 37 °C to allow growth of colonies.

2.2.17. Isolation of recombinant plasmid DNA

Selected cloned colonies (Section 2.2.16) were transferred into 3 ml of LB broth medium (Table 2.2) and grown overnight at 37 °C. The next morning, the 3 ml cultures were centrifuged at 20,000 g for approximately 20 s and the supernatant was removed. Plasmids were isolated using the GenElute Plasmid MiniPrep Kit (Sigma-Aldrich) according to the manufacturer's recommendations.

2.2.18. Reverse-transcription reactions

2.2.18.1. Production of RNA transcripts from DNA fragments

RNA transcripts were produced using an AmpliScribe™ T7 Transcription kit (Cambio, UK) according to the manufacturer's recommendations. DNA template was prepared as

follows: PCR reactions (Section 2.2.12) with M13 primers (Table 2.5) were performed using plasmid DNA template (Section 2.2.17). The PCR products were blunt ended with Mung Bean nuclease (Promega) according to the manufacturer's recommendations and then run on an agarose gel (Section 2.2.13). DNA was extracted from the gels using Wizard® SV Gel and PCR Clean-Up System (Promega) as instructed by the manufacturer. Untranscribed DNA template was removed with DNase (Section 2.2.11.4).

2.2.18.2. Synthesis of cDNA from total RNA

Synthesis of cDNA from RNA samples was done using random hexamers and TaqMan Reverse Transcription reagents using MultiScribe™ Reverse Transcriptase (Applied Biosystems, UK) following the manufacturer's guidelines. The reverse transcription thermal cycling consisted of an initial incubation step (25 °C for 10 min) followed by a 30 min cycle at 48 °C, and finally a reverse transcriptase inactivation step at 95 °C for 5 min.

2.2.19. Real-time PCR

Real-time PCR assay on cDNA samples was carried out in optical-grade 96-well plates in an ABI PRISM®7000 Sequence Detection System (Applied Biosystems, UK). The thermal cycling conditions were as follows: an initial cycle of 95 °C for 10 min followed by 40 cycles of 95 °C for 15 s and 60 °C for 1 min.

2.2.19.1. Detection of fluorescence contaminants

To check for the presence of fluorescence contaminants in the heat block of the thermal cycler (that may cause false positives) new background components must be run prior to a real-time PCR assay according to the manufacturer's recommendations. Once confirmed that the block is free of fluorescence contaminants it is necessary to rule out the presence of such contaminants in the sample by including three No Amplification Controls (NACs) and three No Template Controls (NTCs) in the assay. NAC includes all the reverse-

transcriptase PCR reagents except the transcriptase; for NTC, the reverse-transcription PCR does not include the RNA template. No product should be amplified for any of the controls; if a product is amplified, it indicates that one or more of the PCR reagents is contaminated with DNA which may be the amplicon. NACs and NTCs were included in each set of measurements.

2.2.19.2. Primers and probe design and optimisation

TaqMan primers and probe (Table 2.5) for the real-time PCR assay were designed to nucleotide sequences using the Primer Express® software (Applied Biosystems, UK). The probe was labelled at the 5' end with the reported dye 6-carboxyfluorescein (6-FAM) and at the 3' end with the quencher dye 6-carboxytetramethylrodamine (TAMRA) (Applied Biosystems, UK). Prior to any further analysis, the optimum concentrations for primers and probe were determined according to the manufacturer's recommendations.

2.2.19.3. PCR reaction mix

The real-time PCR reactions were set up as follows: 10 µl cDNA template was added to a reaction mixture which contained 25 µl TaqMan® Universal MasterMix (Applied Biosystems, UK), 300 nM of each primer (forward and reverse), 125 nM probe and molecular biology grade water (Sigma-Aldrich) up to a volume of 50 µl. All reactions were prepared in triplicate to control pipetting errors; a standard deviation of C_T (threshold) value > 0.16 indicates inaccurate pipetting (TaqMan® Universal PCR MasterMix Protocol, Applied Biosystems, UK) and therefore the inaccurate replicate should be removed from the analysis.

2.2.19.4. Construction of calibration curve

A calibration curve was employed to enable an accurate quantification of the target gene's expression. To construct the calibration curve, serially diluted RNA standard template (100

pg, 10 pg, 1 pg, 0.1 pg and 0.01 pg) was employed (in triplicate for each concentration) in reverse-transcription and real-time PCR reactions. The RNA template for the calibration curve reaction was obtained as described in Section 2.2.18.1. Synthesis of cDNA from RNA samples was done by reverse-transcription of RNA with random hexamers (Section 2.2.18.2). Samples for the construction of the calibration curve were loaded in the same plate as the RNA samples to be quantified. A new calibration curve was generated for each set of measurements since small shifts in the fluorescence signal occur from experiment to experiment.

The calibration curve was generated automatically by the ABI PRISM® 7000 Sequence Detection System (Applied Biosystems, UK) by plotting the logarithm of each standard concentration against the cycle number at which the fluorescence signal increased above the background or threshold value (C_T). Using the calibration curve, the ABI PRISM® 7000 SDS software calculated the target gene expression from the C_T value obtained for each of the samples with unknown concentration. In this study, gene expression was estimated as initial amount of target gene RNA contained in 1000 pg total RNA template added to the real-time reverse-transcriptase PCR reactions. The slope of the calibration curve was used in the following equation to determine the reaction efficiency (E): $E = 10^{-1/slope} - 1$. According to this, E = 1 means a doubling of the product in each cycle.

2.2.20. Mesocosm experiments

2.2.20.1. Set up

Mesocosm experiments were designed to monitor the progression of phytoplankton-induced blooms. These experiments consisted of transparent polyethylene enclosures (4.5 m deep, 2 m diameter, ca. 11 m^3, 90 % light penetration of the photosynthetic active radiation) purchased from ANI-TEX (Notodden, Norway) mounted on floating frames moored along the south side of a raft (for details see Egge and Aksnes (1992)) in the

middle of the bay in Raunefjorden at the Norwegian National Mesocosm Center, Marine Biological Station, University of Bergen in Western Norway (60°16' N, 05°14' E). Figure 2.1 shows the mesocosm design. Details of the site and facility are at http://www.bio.uib.no/lsf/inst2.html. The enclosures were filled *in situ* with unfiltered fjord water from an adjacent point to the raft at 2 m depth using a submersible centrifugal pump (ITT Flycht A/S, Oslo Norway, model 3085-182), designed to minimize plankton damage, at a flow rate of ca. 1.5 m^3 per minute. Mixing was accomplished by an airlift-system (Figure 2.1B) which re-circulated the entire volume ca. 5 times per day (~ 40 L min^{-1}) for the duration of each experiment (Jacobsen et al. 1995).

A

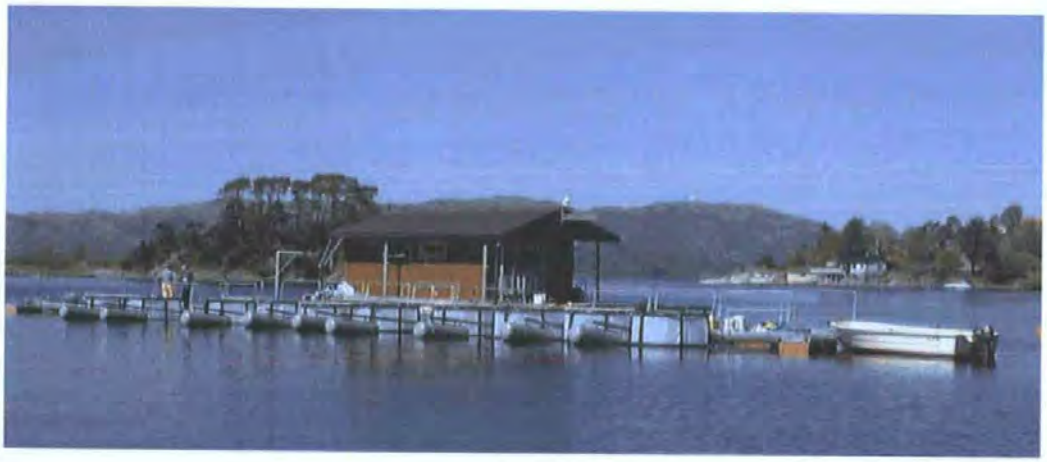

B

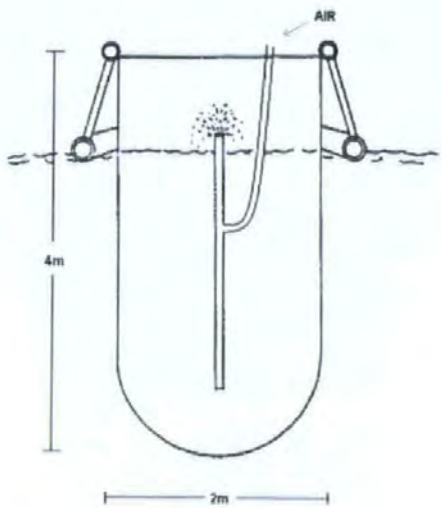

Fig. 2.1. (**A**) The floating raft with the sea enclosures (www.ifm.uib.no/batmare/facilities.html). (**B**) Detail of one of the enclosures showing airlift system. (Diagram adapted from Egge & Aksnes, (1992)).

2.2.20.2. Sampling procedure and analysis of environmental parameters

Surface seawater samples for analysis of physical and biological parameters were collected in 30 L carboys. Because the mescosms were fully mixed, it was not necessary to analyze depth-profiled samples for these parameters.

Nutrient concentrations were measured using standard methods (Strickland & Parsons 1972) adapted to an autoanalyser (Foyn et al. 1981) equipped with autosampling, detection and computing units from SANplus Segmented Flow Analyser (Skalar Analytic).

Chlorophyll *a* analysis was conducted according to the method of Parsons et al. (1984). Seawater samples were filtered onto GF/Fs (Whatman, Maidstone, UK) or alternatively onto 25 mm 0.45 µm cellulose-acetate filters (Sartorius AG, Germany) and extracted in 90% acetone overnight at 4 °C prior to fluorometric analysis using a Turner Designs 10-AU fluorometer.

Temperature, salinity and oxygen concentration profiles in each mesocosm were determined using a multiparameter water quality monitor OTS, Isi Model 85 and a SD204 CTD (SAIV A/S, Bergen Norway) (data not shown). Solar irradiance was measured every 10-15 min using a LI-COR 190 quanta-sensor (LI-COR, Lincoln, NE, USA) and stored using a LI-COR 1400 data logger. Additionally, global radiation data was obtained from the continuous monitoring programme at the Department of Geophysics, University of Bergen, located approximately 20 km from the mesocosm site. *In situ* light profiles from surface to the bottom of the mesocosms were occasionally obtained using a horizontally mounted underwater LI-192 underwater quantum sensor.

CHAPTER THREE

Intraspecies host specificity of *Emiliania huxleyi*-virus isolates

3. Intraspecies host specificity of *Emiliania huxleyi*-virus isolates

3.1. Introduction

In most cases, phytoplankton viruses are host specific and infect just one species or even just a single host strain (Nagasaki & Yamaguchi 1998, Wilson et al. 2005b). For instance, individual coccolithoviruses, i.e. viruses specific to *Emiliania huxleyi* (EhVs), are able to infect several host strain isolates (Schroeder et al. 2002). However, little is still known of the biology of these systems.

It is clear that viral infection plays a role in natural communities' diversity, structuring, competition and succession at interspecies level (Castberg et al. 2001, Larsen et al. 2001). Additionally, morphological and genetic heterogeneity observed within a specific geographical population of one phytoplankton species (Barker et al. 1994, Rynearson & Ambrust 2000, Schroeder et al. 2005), and within the virus group that infect them (Cottrell & Suttle 1995b, Chen et al. 1996, Fuller et al. 1998, Schroeder et al. 2002, Schroeder et al. 2003), suggest that viruses also affect phytoplankton diversity, structuring, competition and succession at intraspecies level (Mühling et al. 2005). However, host strain resistance to viral attack has been reported for most eukaryotic viruses in culture (Cottrell & Suttle 1991a, Nagasaki & Yamaguchi 1998, Zingone et al. 1999, Tarutani et al. 2001), and it is an important assumption in models that describe the effect of viruses in regulating diversity in the oceans (Thingstad & Lignell 1997).

Understanding the factors that determine when and how a particular virus can and cannot infect an algal host under natural conditions is of great interest, due to the different ecological and biogeochemical implications. The difficulty in cultivating susceptible hosts to propagate viruses in the laboratory limits our knowledge about marine viral diversity and specificity. However, that is not the case for *E. huxleyi*, which can easily be grown in the laboratory and their specific viruses can be plaque-assayed.

Bratbak et al. (1996b) first reported the isolation of an *E. huxleyi*-specific virus (EhV) by plaque assay, however they were unable to propagate it further for characterization. Wilson et al. (2002b) went one step further and isolated two viruses from an *E. huxleyi* bloom in the Western English Channel. Basic characterization by these workers revealed they were lytic viruses of approximately 170 nm-190 nm in diameter with an icosahedral symmetry. Schroeder et al. (2002) extended the research conducted by Wilson et al. (2002b) characterising *E. huxleyi* viruses originally isolated from the English Channel and a Norwegian fjord. In addition to the elucidation of the classic phenotypic characteristics of the isolates, i.e. genome type and size, virion shape and size and host range, they also determined the evolutionary relationship of those virus isolates to other members of *Phycodnaviridae*. They concluded that those viruses belong to a new genus they named *Coccolithovirus*. Differences within members of the *Coccolithovirus* were elucidated by host range and sequence analysis of a gene fragment encoding part of their putative major capsid protein.

In this chapter I will present the results from a more extended host range experiment than the one performed by Schroeder et al. (2002). Host specificity of the 10 EhV isolates used by Schroeder et al. (2002) were tested against the same *E. huxleyi* strains used in that study plus 19 extra new *E. huxleyi* strains available in culture. The *E. huxleyi* strains were originally isolated from the same geographical locations as the viruses as well as from other distant areas in different years. The purpose of this experiment was to examine the diversity of both virus and algal strains in terms of infectivity and susceptibility as well as to investigate whether or not susceptibility may be explained by known common features shared by the hosts; such as location, number of liths or DMSP-lyase activity.

A host range study is a simple, yet crucial first step to help set the scene in the analysis of virus/host diversity. Hence, it was decided to make this a short focused chapter.

3.2. Materials and methods

3.2.1. Virus isolates and *E. huxleyi* cultures

The ten clonal EhV strains used in this experiment (Table 2.3) were obtained from the Plymouth Virus Collection. Viruses were originally isolated from seawater samples collected during the latter stages of *E. huxleyi* blooms in Western English Channel, during July 1999 and 2001, and from an *E. huxleyi*-induced bloom in a Western Norwegian fjord in June 2000 (Schroeder et al. 2002, Wilson et al. 2002b). Further information about the virus strains is described in Section 2.1.4.

E. huxleyi strains were obtained from the Provasoli-Guillard Center for the Cultivation of Marine Phytoplankton (http://ccmp.bigelow.org/) and the Plymouth Culture Collection (http://www.mba.ac.uk/). Full details are summarized in Table 2.4.

3.2.2. Host range determination

Host range determination was conducted, as described in Section 2.2.4, on 26 different cultures of *E. huxleyi* strains (Table 2.4, except BOF92) and using 10 different EhV isolates (see Table 2.3).

3.3. Results

Nine of the *E. huxleyi* strains showed no evidence of lysis by any of the EhVs tested (Table 3.1). Four of those strains (92A//CCMP 379, 92D, 92E and Bloom E. hux 215) came from the English Channel; Van 556 was isolated from the North Pacific; NZ EH from the South Pacific; CCMP 373 from the Sargasso Sea; CH 25/90 from the North Sea; and F61 from Oslo Fjord. Three other *E. huxleyi* strains, 92F (English Channel), Bloom E. hux (English Channel) and CCMP 374 (Gulf of Maine) were good hosts for all of the EhVs. The remaining *E.huxleyi* isolates showed variable susceptibility to infection as they were lysed by 1 to 9 of the EhV strains.

No pattern was observed in terms of possession or lack of liths. Four out of seven naked-cell *E. huxleyi* strains were resistant to infection (92A//CCMP 379, Van 556, CCMP 373 and F61). In addition, another naked strain, CCMP 370, was susceptible only to EhV-163 and it lysed at low speed.

The two *E. huxleyi* strains known to have high DMSP-lyase activity (92A//CCMP379 and CCMP 373) were not susceptible to infection, whereas the four previously reported *E. huxleyi* strains with comparatively low DMSP-lyse activity (CCMP 370, CCMP 1516, L and CCMP 374) (Steinke et al. 1998) were lysed by at least one EhV. We lack information regarding DMSP-lyase activity for the rest of the *E. huxleyi* strains tested.
The only two *E. huxleyi* strains with B-morphotype cells, 92D (English Channel) and CH25/90 (North Atlantic) were also non-susceptible to infection.

Looking at the results from the point of view of virus specificity rather than host susceptibility we see that all of the EhVs were infectious to 6-15 of the 26 *E. huxleyi* strains tested. Although all the 10 EhVs were shown to have similar host ranges (Table 3.1), there were some marked differences. Two of the EhV strains (EhV-201 and EhV-207)

that were isolated in 2001 from the English Channel showed identical host range. They lysed cultures of 14 different *E. huxleyi* strains from all the geographical locations. EhV-202 also had the same host range, although showed slow lysis (two weeks for complete lysis) of *E. huxleyi* strain EH2. EhV-208 was able to lyse the same 14 host cultures plus CCMP 88E (Gulf of Maine), hence EhV-208 has the broadest host range. The rest of the EhV strains differ in their host range, each one showing a unique infection profile.

The results presented here confirm the observations described by Schroeder et al. (2002), for the common *E. huxleyi* strains tested, apart from a single difference. While Schroeder et al. (2002) found CCMP 370 to be resistant to infection by all of the tested EhV strains, a positive result (slow lysis) for CCMP 370 when inoculated with EhV-163 was observed in this study (Table 3.1). It is possible that Schroeder et al. (2002) did not observe lysis because their incubation times were shorter (7 days).

Host range observed for CCMP 1516 was as previously described by Schroeder et al. (2002). Additionally, in this study CCMP 1516b was tested, an extra *E. huxleyi* strain that originated from CCMP 1516. Despite the common origin of both cultures they revealed different host ranges. CCMP 1516 was resistant to EhV-203 while CCMP 1516b showed resistance to EhV-163 (Table 3.1).

The addition of viruses to exponentially growing *E. huxleyi* cultures usually resulted in the collapse of the culture 3-4 days post inoculation. However, individual cross reactions between EhVs and *E. huxleyi* strains were highly diverse and some of the EhV isolates took up to 2 weeks to completely lyse some of their hosts (labelled as $+^2$ in Table 3.1). Despite the slow lysis, when compared to the other lysed cultures, proliferation of surviving cells was not observed and the result was complete lysis of the *E. huxleyi* culture.

E.huxleyi↓ EhV isolate →	84	86	88	163	201	202	203	205	207	208
92A//CCMP 379(English Channel)	-	-	-	-	-	-	-	-	-	-
92D (English Channel)	-	-	-	-	-	-	-	-	-	-
92E (English Channel)	-	-	-	-	-	-	-	-	-	-
Bloom E.hux 215 (English Channel)	-	-	-	-	-	-	-	-	-	-
Van 556 (North Pacific)	-	-	-	-	-	-	-	-	-	-
NZ EH (South Pacific)	-	-	-	-	-	-	-	-	-	-
CCMP 373 (Sargasso Sea)	-	-	-	-	-	-	-	-	-	-
CH 25/90 (North Atlantic)	-	-	-	-	-	-	-	-	-	-
F61 (Oslo Fjord)	-	-	-	-	-	-	-	-	-	-
CH 24/90 (North Atlantic)	-	-	-	-	-	-	-	-	-	+
CCMP 88E (Gulf of Maine)	-	-	-	$+^2$	-	-	-	-	-	-
CCMP 370 (Oslo Fjord)	-	-	-	$+^2$	-	-	-	-	-	-
CCMP 12-1//371 (Sargasso Sea)	-	-	$+^2$	$+^2$	$+^2$	$+^2$	-	$+^2$	$+^2$	$+^2$
CCMP MCH1 (Sargasso Sea)	-	-	-	-	+	+	-	+	+	+
EH2 (Australia- South Pacific)	+	+	+	-	+	$+^2$	-	+	+	+
South Africa (Indian Ocean)	$+^2$	$+^2$	$+^2$	-	$+^2$	$+^2$	-	$+^2$	$+^2$	$+^2$
CCMP 1516 (North Pacific)	+	+	+	+	+	+	-	+	+	+
CCMP 1A1//372 (Sargasso Sea)	-	+	+	+	+	+	-	+	+	+
CCMP 1516 b (North Pacific)	+	+	+	-	+	+	$+^2$	+	+	+
5/90/25b (North Atlantic)	+	+		+	+	+	-	+	+	+
G1779Ga (North Atlantic)	+	+		-	+	+	-	+	+	+
DWN61/3/2 (North Atlantic)	+	+		+	+	+	+	+	+	+
L (Oslo Fjord)	$+^2$	+	$+^2$	+	$+^2$	$+^2$	+	-	$+^2$	+
92F (English Channel)	+	+	+	+	$+^2$	$+^2$	$+^2$	$+^2$	$+^2$	$+^2$
Bloom E.hux (English Channel)	+	+	+	$+^2$	+	+	$+^2$	+	+	+
CCMP 374 (Gulf of Maine)	+	+	+	+	+	+	+	+	+	+

Table 3.1. Host range study of the *Emiliania huxleyi* virus (EhV) isolates with *E. huxleyi* host strains kept in culture. + culture lyisis; - no evidence of culture lysis; $+^2$ slow lysis when compared to the other lysed cultures. The white gaps denote information not available.

3.4. Discussion

The results presented in this chapter indicate that EhVs and *E. huxleyi* strains are phenotypically and/or genotypically diverse based on host specificity and susceptibility respectively. Actually, most of the EhV strains tested can be distinguished from each other just based on their unique host ranges. Genotypic diversity was previously reported within EhVs (Schroeder et al. 2002, Schroeder et al. 2003) and *E. huxleyi* strains (Schroeder et al. 2005) based on the nucleotide composition of fragments of the major capsid protein, gene which is involved in infection processes (Girod et al. 2002, Chen & Icenogle 2004) and the calcium-binding protein gene, thought to be involved in regulating coccolith morphology (Corstjens et al. 1998), respectively.

No obvious relationship, in terms of susceptibility, was found between the geographical locations from where both EhVs and *E. huxleyi* strains were originally isolated. Individual viruses are infectious to *E. huxleyi* from very distant oceanic regions. One might think that *E. huxleyi* strains isolated from the same area as the viruses would have been more suitable as a host for those virus isolates than the *E. huxleyi* strains isolated from distant oceanic regions. However, 5 of the *E. huxleyi* strains that showed resistance to all the EhVs tested came originally from the English Channel, as did 9 of the EhVs (EhV-84, EhV-86, EhV-88, EhV-201, EhV-202, EhV-203, EhV-205, EhV-207 and EhV208).

Several studies have shown that phytoplankton cells are highly sensitive to viral infection in the late log growth phase and become less susceptible in the stationary phase. It has also been observed that a reduction in burst size occurs when the host cells are in stationary phase (van Etten et al. 1991, Bratbak et al. 1998b, Nagasaki et al. 2003). These observations suggest that the host susceptibility to viral infection and viral proliferation vary depending on the physiological conditions of the host. Since DNA viruses utilize the biosynthetic function of the host, it is likely that hosts with high biosynthesis activity are

the most suitable for viral replication. In this experiment all the host cultures were inoculated with the EhVs during the log phase, cell concentration and virus to host ratio was also identical in all cases as well as light and temperature conditions. Therefore, it is possible to conclude that the differences observed in host ranges are due to intrinsic biological characteristics of the *E. huxleyi* strains and/or the EhVs. Furthermore, those characteristics may explain the variable lysis speed of individual *E. huxleyi* strains when inoculated with different EhVs.

So, what do EhV specificity and *E. huxleyi* strain susceptibility depend on? The next step in order to try to establish a pattern that determines susceptibility or resistance to viral infection was to look at some of the known biological characteristics of the hosts, such as existence or lack of liths, DMS production or cell morphotype. Previous studies have reported that during *E. huxleyi* blooms the rate of infection was higher on flagellated scale-bearing cells relative to lithed cells (Bratbak et al. 1995, Brussaard et al. 1996b). Because of these results it had been argued that coccoliths had a defensive function against viral infection. However, the results presented in this chapter do not support this idea as most of the naked-celled *E. huxleyi* strains tested were not lysed while most of the lithed strains were susceptible to infection.

The two strains previously reported to exhibit high DMSP-lyase activity (92A//CCMP379 and CCMP373) (Steinke et al. 1998) were resistant to infection, while those with known relatively low DMSP-lyase activity were infected. Based on the same observations Schroeder et al. (2002) suggested that high DMSP-lyase activity in *E. huxleyi* might be linked to some sort of anti-viral mechanism. DMSP-lyase activity per cell in *E. huxleyi* is independent of cell growth stage (Wolfe & Steinke 1996), therefore our results were not biased by the physiological conditions of the cultures. However, with the lack of DMSP-lyase activity measurements for most of the *E. huxleyi* strains used in this experiment it is

impossible to argue positively or negatively for this hypothesis. Further investigation is required in this aspect.

Both *E. huxleyi* B-morphotype strains utilized during this experiment were not susceptible to infection by any of the EhVs tested. However, this is not indicative of resistance to infection determined by the cell morphotype since several of the A-morphotype strains also showed resistance. It is likely that this result is just a consequence of lacking more cultures of B-morphotype strains and EhVs isolates to perform a more extensive host range assay.

Motility of *E. huxleyi* cells has also been reported as a factor that may increase infectivity rates (Bratbak et al. 1995). Viruses travel by passive diffusion and therefore the encounter rate with a suitable host is random and depend on both host and virus abundance in the environment, as well as on host cell size and motility (Murray & Jackson 1992). Motion of host cells enhance transport rates and so the chance of encounter. Hence, non-motile phytoplankton cells might be less susceptible to viral infection than motile ones. This idea can, however, not be examined during small scale laboratory experiments due to the high concentrations of host used, that ensures encounter with the virus particles.

It is interesting to point out the different host range observed for CCMP 1516 and CCMP 1516b. CCMP 1516b is a non-calcifying strain closely related to the calcifying CCMP 1516 strain (a change in calcification state has occurred during culturing since the strain was first isolated in 1991 (http://ccmp.bigelow.org/)) (Table 2.4). It is intriguing to postulate that this host range difference could be a direct, or indirect, effect of the calcification state of the host. Schroeder et al (2005) found that both *E. huxleyi* strains differ, at least, in the allelic composition of their calcium-binding protein (GPA) gene. CCMP 1516b presents a single allele for the GPA gene, identical to one of the two alleles in CCMP 1516. Host range mutations of viruses and of host cells in laboratory culture has

also been observed for *Micromonas pusilla*-specific viruses (Waters & Chan 1982). Considering the high diversity among both host and virus strains, this may be an important factor in sustaining their coexistence in natural environments. These observations raise the following question: does the GPA gene determine, at least in part, susceptibility? It is thought that GPA is involved in nucleating the calcium carbonate crystals during coccolith development or delivery of calcium to the coccolith vesicle (Corstjens et al. 1998). Therefore, the GPA gene may encode significant differences that could be attributed to different *E. huxleyi* strains, which may determine differences in chemical signals or receptors that affect viral specificity.

3.5. Conclusions

Determining host range as part of algal virus characterization is a necessary step towards understanding their ecological role in the marine environment. The highly variable host range shown in this study indicates a complex interaction between EhVs and *E. huxleyi* strains in nature in terms of specificity and susceptibility. Considering the huge diversity among both EhV and *E. huxleyi* strains in the ocean, the genotypical and phenotypical differences that may determine host range specificity could be important factors in sustaining their coexistence in natural environments.

Intraspecies host specificity of EhVs is important in terms of ecological implications in the aquatic environment and for designing screening tests for viruses present in natural systems. Natural blooms of *E. huxleyi* can be formed by a broad diversity of strains and several different EhVs have been detected during the progression of these blooms in the sea (see Chapters 5 and 6). Host range determines which *E. huxleyi* strains survive and therefore it has implications for local ecology, climate and biogeochemistry cycling and production of compounds such as DMS, calcite and carbon dioxide.

The results suggest that specificity is likely to be related to specific genetic or phenotypic variations within *E. huxleyi* strains and the EhVs, which do not depend on adaptations to the abiotic environment, as those observed between *E. huxleyi* strains CCMP 1516 and CCMP 1516b. Further molecular investigations looking at specific genes are required in order to find the genetic features that determine infectivity in this host/virus system.

CHAPTER FOUR

Diversity and succession of microbial populations during *Emiliania huxleyi*-dominated blooms in seawater enclosures

4. Diversity and succession of microbial populations during *Emiliania huxleyi*-dominated blooms in seawater enclosures

4.1. Introduction

Several laboratory, field and mesocosm studies have shown the importance of viral control in the demise of *E. huxleyi* blooms and succession of the associated microbial populations (Bratbak et al. 1993, Bratbak et al. 1996b, Brussaard et al. 1996b, Castberg et al. 2001, Jacquet et al. 2002, Wilson et al. 2002a). It is thus likely that viruses ultimately influence *E. huxleyi*'s production of calcium carbonate coccoliths and its role in CO_2 cycling and dimethylsulphide (DMS), processes that make *E. huxleyi* such an important species for global ecology.

To compensate for the limited realism of laboratory experiments and to avoid the difficulties entailed in field work, large enclosures filled with natural seawater (i.e. mesocosm experiments) have been used in plankton ecology research since early last century when the first landbased systems were developed (Petterson et al. 1939). Mesocosm studies were afterwards improved by the use of transparent enclosures situated in a natural body of water, which have been claimed to have a higher degree of realism than land constructions (Egge 1993). These systems have been employed in marine phytoplankton studies since early 1960's (McAllister et al. 1961, Antia et al. 1963). Irradiance and temperature in such enclosures follow natural fluctuations, and the phytoplankton succession resembles an accelerated version of what is typically found in marine environments (Davis 1982). The controlled water masses in a mesocosm render budget studies (Riemann et al. 1990) and model verifications possible (Andersen et al. 1987, Keller & Riebesell 1989), making the experiments well suited for studying effects of chemical, physical and biological manipulations on natural plankton communities. However, costs and working load when putting up such systems are not insignificant.

Wishes to manipulate several parameters, or investigating gradients of one single parameter, combined with the high degree of repeatability of experiments demonstrated over the years (Egge 1993), therefore often result in a solution where limited number of replicate enclosures are used when the experimental set-ups is designed. One consequence of this is that the reproducibility, and thereby the scientific value of the results produced are frequently questioned. Crucial for both conceptual and numerical modelling of such experiments is whether all or parts of, the pelagic food web can be considered to be in steady state in the natural system upon enclosure, and whether this steady state remains undisturbed by the filling and enclosing operations. Should this not be the case, the observed dynamics will not be a function only of the perturbation applied, but mixed with the transient effects of the unbalances in the particular state of the initial food web, as well as the transient responses to the perturbation exerted by the filling procedures.

A mesocosm experiment carried out in Norway in June 2003 was designed to closely monitor an *E. huxleyi* bloom and its termination by viral infection, as well as the influence of such events on the rest of the microbial community. In order to do so it was an essential part of the study to accurately predict the virus induced crash of the bloom. Therefore, nitrate and phosphate (at a N:P ratio of 15:1) were added at three different starting regimes with a one-day stagger between regimes. The expectation was that the progression of the consequent *E. huxleyi* blooms would result in a similar one-day stagger between each regime. This design also provided us with a unique possibility to investigate the validity of the three main assumptions associated with mesocosm experiments: (1) steady state of the microbial part of the food web, (2) no perturbation due to the filling of the bags and (3) light is not a limiting effect (Thingstad et al. in press). The consequence of these assumptions being valid would be identical dynamic responses in all the enclosures, only delayed by the difference in onset of nutrient addition between the three treatment groups.

To describe the microbial food web dynamics we employed analytical flow cytometry (AFC), allowing us to monitor changes in abundances. This technique, which measures light scattering and fluorescence characteristics from individual particles, has the advantage of large sample throughput and good counting statistics (Vives-Rego et al. 2000), providing data of a quality well suited for the between-treatments comparisons needed in this study.

4.2. Materials and methods

4.2.1. Experimental design

The mesocosm experiment was carried out in Raunefjorden, western Norway, from the 3rd of June until the 15th of June 2003. Ten mesocosm bags were moored along the south side of a raft in the middle of the bay (for details see Section 2.2.20). The bags were numbered #1 to #10 in the east-west direction (Figure 4.1). The enclosures were filled on 2nd June with unfiltered seawater.

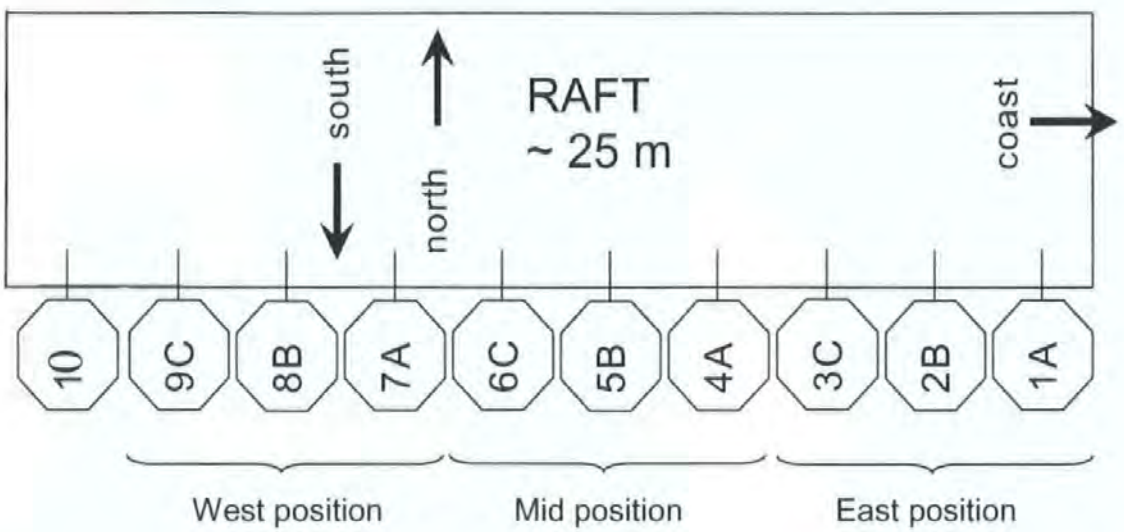

Fig. 4.1. Diagram of the floating raft and the sea enclosures, indicating their number and which Treatment Group (TG) each enclosure represented; A nutrient addition on 3rd June; B nutrient addition on 4th June and C nutrient addition on 5th June (see Section 4.2.2).

4.2.2. Nutrient and copepod treatments

The 10 bags were divided in 4 treatment groups, allowing triplication of 3 of them: Treatment Group A (TGA) (bags #1, #4 and #7), TGB (bags #2, #5, and #8), TGC (bags #3, #6, and #9) and TGD (bag #10) (Figure 4.1A). Inorganic nutrients were added daily at 10:00h in a N:P ratio of 15:1 (1.5 μM $NaNO_3$ and 0.1μM KH_2PO_4) to TGA (starting 3rd June), TGB and TGD (starting 4th June) and TGC (starting 5th June). Additionally, on 5th June copepods concentration was increased in TGD (bag #10) from 0.7 L^{-1} to 4.7 L^{-1}, i.e. approximately 6-fold increase. The added copepods were collected from the fjord at 4.5 m depth using a plankton net 25 cm diameter with a 35 μm mesh.

4.2.3. Analytical flow cytometry (AFC)

For daily flow cytometric counts of microalgae, virus and bacteria population samples were collected at 09:00 h by filling a small plastic bottle from the surface of each enclosure and from the fjord (from a point adjacent to enclosure #10). All AFC analyses were performed with a FACSCalibur flow cytometer (Becton Dickinson, Franklin Lakes, USA) as described in Section 2.2.6. The phytoplankton counts were done from fresh samples whereas virus and bacteria enumeration was performed on glutaraldehyde-fixed samples.

4.2.4. Statistical analysis

A variance partitioning and a discriminant analysis (McLachlan 1992) (Statistica 6.1, StatSoft, Tulsa, USA) of the data set were performed for comparing the biological variation with reproducibility between enclosures and for investigating the validity of the ideal set of assumptions described above (Section 4.1). The abundance of virus population V4 (see Section 4.3.1) was initially undetectable and for these time points we used an estimated detection limit of 1×10^6 virus ml^{-1} (the lowest counted number was 1.2×10^6). The subsequent analysis was not very sensitive to this choice. For the statistical analysis all population abundances were replaced by their logarithms and each variable normalized (i.e. algal populations A1-A6, bacteria B and virus populations V1-V4, see Section 4.3.1) to have zero mean and standard deviation of 1. In addition, each observation vector (the *n*-dimensional vector describing one enclosure at a given time point) was described by three grouping variables: 1) TG: the delay before initial nutrient addition (TGA: no delay, TGB 1 day delay and TGC: 2 days delay). 2) DAN: days after start of nutrient addition (-2 to 12 days) and 3) POS: the position of the enclosure at the raft (East, Mid and West). The differences between the observation vectors were calculated as Mahalanobis distances. Data from bag #10 (TGD) and the fjord were not included in the statistical analysis since they were not done in triplicates. The statistical analysis was performed by Svein Norland.

4.2.5. Light irradiance

Global radiation data was obtained from the continuous monitoring programme at the Department of Geophysics, University of Bergen, located approximately 20 km from the mesocosm site (Section 2.2.20.2).

4.2.6. Virus isolation

One litre water samples collected from bag #1 on 5th, 7th and 9th June were filtered and concentrated (see Section 2.2.1). *E. huxleyi*-specific viruses were isolated from those samples using cultures of *E. huxleyi* strains (Table 2.4) as described in Section 2.2.3.1. When lysates were produced, PCR amplification (Section 2.2.12) of virus MCP gene was conducted in two stages using two pairs of MCP specific oligomers (Table 2.5). DGGE analysis of second-stage nested PCR product was conducted as described in Section 2.2.14 to reveal the number of different virus strains in the lysate. Plaque assays (Section 2.2.3.3) were then performed in order to produce clonal isolates of the different virus strains. DGGE was used to verify whether the new lysates were clonal.

Isolation of other algal viruses was achieved using enrichment cultures method (Section 2.2.3.2). For this purpose, one litre 0.45 μm-filtered seawater sample from bag #1 (collected at the end of the bloom) was divided into 20 ml aliquots and used to prepare f/2 medium for culturing *Phaeocystis pouchetii*, *Micromonas pusilla*, *Chrysochromulina ericina*, *Pyramimonas orientalis*, *Nephroselmis rotunda*, *Isochrysis galvana* and *Synechococcus* sp. AFC signature of the lysates produced were compared with those of the virus groups detected in the enclosures between 3rd and15th June.

4.3. Results

4.3.1. Diversity and succession of the microbial populations

Four major groups of primary producers (*E. huxleyi*, *Synechococcus* sp., picoeukaryotes and nanoeukaryotes) were observed in all the analysed samples from the 10 different enclosures as well as from the samples collected from the fjord daily (Figure 4.2). The AFC images also revealed two minor algal groups (unknown and cryptophytes) found in relatively low numbers.

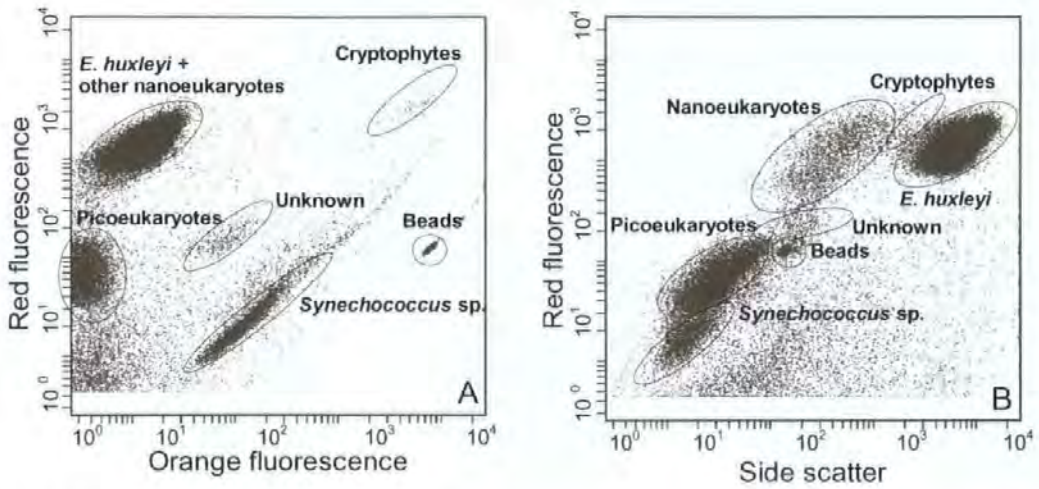

Fig. 4.2. Representative biparametric flow cytometry plots showing populations of taxonomic groups of primary producers. (**A**) *Synechococcus* sp., picoeukaryotes, nanoeukaryotes (including *E. huxleyi*), cryptophytes and an unknown group were discriminated using a combination of red and orange fluorescence signals; (**B**) *E. huxleyi* (with coccoliths) were separated from other nanoeukaryotes and *E. huxleyi* cells without coccoliths using a combination of red fluorescence and side scatter (for simplicity labelled "*E. huxleyi*" and "nanoeukaryotes" in the plot).

Description of each phytoplankton group:

***E. huxleyi*:** this group was characterised by high side scatter (SSC) and red fluorescence (RFL) values and low orange fluorescence (OFL) values- characteristics resembling those of pure cultures of *Emiliania huxleyi*.

***Synechococcus* sp.:** had the lowest RFL and SSC signals but the highest value for OFL out of the four major algal groups. The high OFL signals and low SSC and RFL signals are properties consistent with that of *Synechococcus* sp.

Picoeukaryotes: relatively low RFL and SSC compare to group *E. huxleyi* but higher than those values for group *Synechococcus* sp. The size and pigmentation of the algae in this population indicate that this group consisted of one or more species of picoeukaryotes with size and pigments similar to *M. pusilla* (Castberg et al. 2001, Larsen et al. 2001, Jacquet et al. 2002).

Nanoeukaryotes: similar RFL and OFL values as *E. huxleyi* but lower SSC values. The comparison with the signals of pure cultures of naked *E. huxleyi* (personal observation) might lead to conclude that this cluster includes naked *E. huxleyi*. As the group seemed to consist of more than one population it is preferable to be less specific and according to its characteristics can be referred to as nanoeukaryotes (one or several species).

Unknown: RFL signal slightly lower than RFL of nanoeukaryotes but approximately the same value of SSC, nevertheless the OFL signal is more similar to the OFL signal for *Synechococcus* sp. This group will be referred to as 'Unknown' hereafter since it did not resemble the AFC signature of any of the phytoplankton cultures available for comparison.

Cryptophytes: the high RFL, OFL and SSC values of this group indicate that the population was most likely consisting of cryptophytes -found in previous analogous mesocosm experiments in the same area, always in low numbers (Bratbak et al. 1993). This population has been also detected previously by flow cytometry (Larsen et al. 2001).

Temporal progression of phytoplankton groups:

The comparison of the primary producer populations' temporal progression showed that the replicates in each treatment group of enclosures followed similar patterns, although there were some differences in levels and timing of peaks of cell abundances (Figure 4.3).

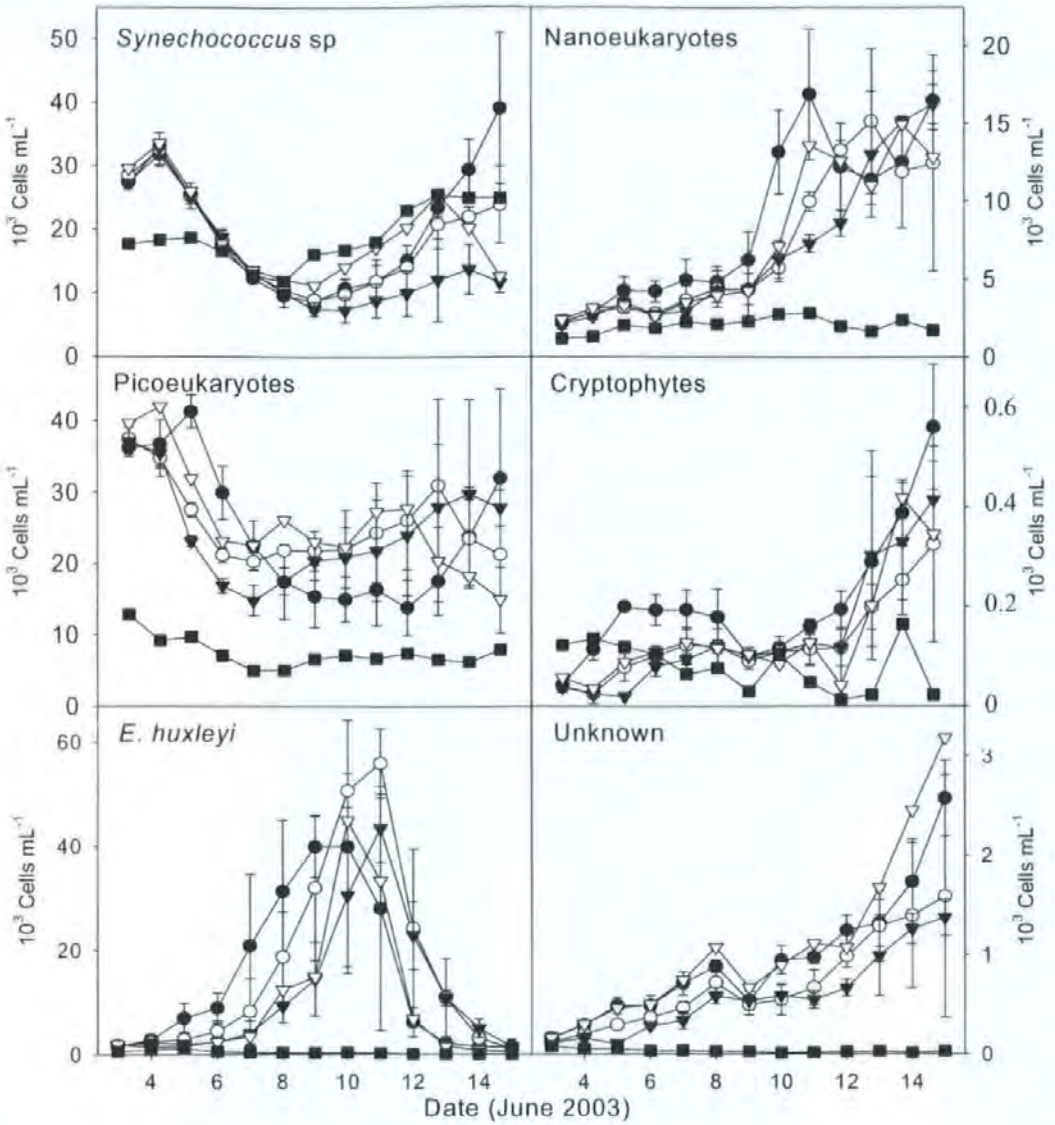

Fig. 4.3. Time series development of the 6 primary producer populations as determined by flow cytometry. (●) TGA, (○) TGB, (▼) TGC, (Δ) Bag 10, (■) fjord. For TGA, TGB and TGC lines indicate mean values for the 3 mesocosm bags in each Treatment Group (TG), and the error bars indicate standard deviation.

Synechococcus sp. and picoeukaryotes numerically dominated the microalgae community in all the enclosures at the start of the study between 3rd-6th June with abundances around 2.7×10^4 cells ml^{-1} for *Synechococcus* sp. and 3.7×10^4 cells ml^{-1} for picoeukaryotes on the first sampling day. *Synechococcus* sp. abundance peaked concurrently in all the enclosures between the 3rd and 4th June followed by a 5-6 days period with steady decrease. *Synechococcus* sp. concentrations increased again following the collapse of the *Emiliania huxleyi* population, again numerically dominating the community together with

picoeukaryotes towards the end of the experimental period. Towards the end of the study *Synechococcus* sp. abundance diverged between the four treatment groups.

For picoeukaryote abundance, a clear difference between TGA, and TGB and TGC was observed at the start of the study (Figure 4.3). In TGA an initial increase in picoeukaryote abundance was observed, prior to a sharp decline from 4.1×10^4 to 1.4×10^4 cells ml^{-1}. In contrast, in TGB and TGC where nutrient addition started one and two days later, respectively, picoeukaryote abundance decreased sharply with no initial increase. In addition, picoeukaryotes in TGB and TGC recovered sooner compared to TGA. On 12th June, picoeukaryotes in TGA eventually recovered with a fast growth rate from 1.4×10^4 to 3.2×10^4 cells ml^{-1} over 3 days. The picoeukaryote development in TGD was similar to TGB and TGC; however it experienced an initial increase in abundance as TGA. Towards the end of the study this group decreased again in TGB, TGC and TGD.

E. huxleyi experienced an increase in all the bags from the first day (3rd June). Growth rate was notably higher from days 4 and 5 with maximal rates between 1.3 and ~ 3 division d^{-1} in all the bags. Maximum *E. huxleyi*–cell abundances were reached on 10th June in TGA and TGD and on 11th June in TGB and TGC. After reaching maximum abundances, *E. huxleyi* concentrations fell rapidly down to approximately the same cell numbers as before initiation of the bloom. *E. huxleyi* accounted for only 2-2.9 % of the phytoplankton community at the beginning of the study period, but clearly dominated it when it reached its highest abundance (values ranged between 46.6 % in bag #5 to 62.2 % in bags #1 and #2). Throughout the entire period of study *E. huxleyi* population was not significant in the fjord.

In the four treatment groups, nanoeukaryote abundances increased slowly during the first half of the mesocosm experiment until the collapse of *E. huxleyi* populations, whereupon

nanoeukaryote growth rates increased rapidly. Maximum nanoeukaryote abundances were reached on 11th June in TGA and TGD, 13th June in TGB and 15th June in TGC. In TGA, TGB and TGD a decline in nanoeukaryote abundance was observed over the last few days of the experiment. The other two algal groups, referred to as cryptophytes and unknown, remained stable at low numbers or had low growth rate until the crash of *E. huxleyi*. Only on the last few days both populations experienced a significant increase. However, compared to the rest of the groups they did not seem to play an important role in terms of abundance in the community (maximum concentrations of 2-3 × 10^3 cells ml^{-1} for the unknown group and 5-6 × 10^2 cells ml^{-1} for the cryptophytes). The 6 phytoplankton groups remained at relatively low abundances in the fjord throughout the entire experiment and not one of them experienced any significant fluctuations in their abundance.

AFC analysis of samples diluted in TE buffer and stained with DNA dye SYBR Green I revealed the presence of heterotrophic bacteria, *Emiliania huxleyi*- specific viruses (EhV, V4) and 3 other different groups of viruses (referred to as V1, V2 and V3) (Figure 4.4).

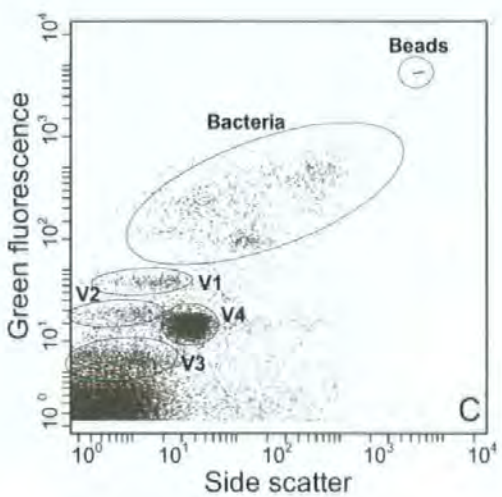

Fig. 4.4. Representative biparametric flow cytometry plot showing populations of viruses and bacteria. Heterotrophic bacteria, *E. huxleyi*-specific viruses (V4) and different groups of viruses (V1, V2 and V3) were discriminated on the basis of the green DNA dye complex fluorescence versus side scatter signal.

Description of each group:

Bacteria: this group was characterised by both high SSC and green fluorescence (GFL) values, which made it easily discernible from the virus populations (with lower SSC and GFL signals). The bacteria in the enclosures were grouped and counted as one big group, though the AFC signature suggests that more than one type of bacterium were present.

V1: had higher GFL values than the other virus populations.

V2: GFL values between those of V1 and V3.

V3: among the four distinct virus groups V3 is the one with the lowest fluorescence values.

V4: had substantially higher SSC values than the other virus groups and GFL values between those for V2 and V3. The increase in V4 numbers was followed by a sudden decrease in the algal group A1 (*E. huxleyi*). This relation together with the characteristic signature of V4 in the flow cytometer (Castberg et al. 2001, Wilson et al. 2002a) indicates that V4 correspond to *E. huxleyi*-specific viruses, and therefore we will refer to it as EhV.

Temporal progression of bacteria and viruses:

Bacterial abundances were stable during the first half of the experiment in all the mesocosm bags and the fjord, remaining at approximately 2×10^6 cells ml^{-1} in the bags and 1×10^6 cells ml^{-1} in the fjord until 9th June (Figure 4.5). Bacterial abundances then increased rapidly, coinciding with the *E. huxleyi* bloom crash, leading to maximum abundances on 12th June in all the bags (maximum concentrations of approximately $7\text{-}10 \times 10^6$ cells ml^{-1}). The peak in abundance was reached one day earlier in the fjord (3.6×10^6 cells ml^{-1}). Afterwards, bacteria slowly declined. A second bacterial increase could be observed in the fjord during the last two days of study.

All four virus groups V1-V4 (EhV) remained in relatively low numbers and with low increase in abundance in the 10 bags during most of the study period. Then, subsequently to the culmination of the *E. huxleyi* bloom they increased more markedly. For V3 and V4 (EhV), rapid increase in abundance started on 8th June, and for V2 it started on 9th June, coinciding with the collapse of the *E.huxleyi* bloom and the increase in bacterial abundances. The period with rapid increase in V1 abundance came after 11th June.

V4 (EhV) was not observed in any of the enclosures during the first half of the mesocosm experiment. If these EhVs were already present in the water, their numbers were very low rendering their signature impossible to dissociate from the background. From 9th June EhV appeared as a clear group in TGA and TGD (first enclosures to receive nutrients) and from 10th June it was observed as a discernible population in TGB and TGC. EhV abundances peaked first on 12th June in TGA, TGB and TGD and then two days later in bags TGC. On 14th June a second minor peak was observed for TGA, TGB and TGD. Different peak levels of abundance were registered for the four treatment groups being TGC<TGB<TGD<TGA (12×10^6, 22×10^6, 24×10^6 and 31×10^6 virus ml^{-1} respectively). Throughout the entire period of study the EhV group was not measurable in samples collected from the fjord.

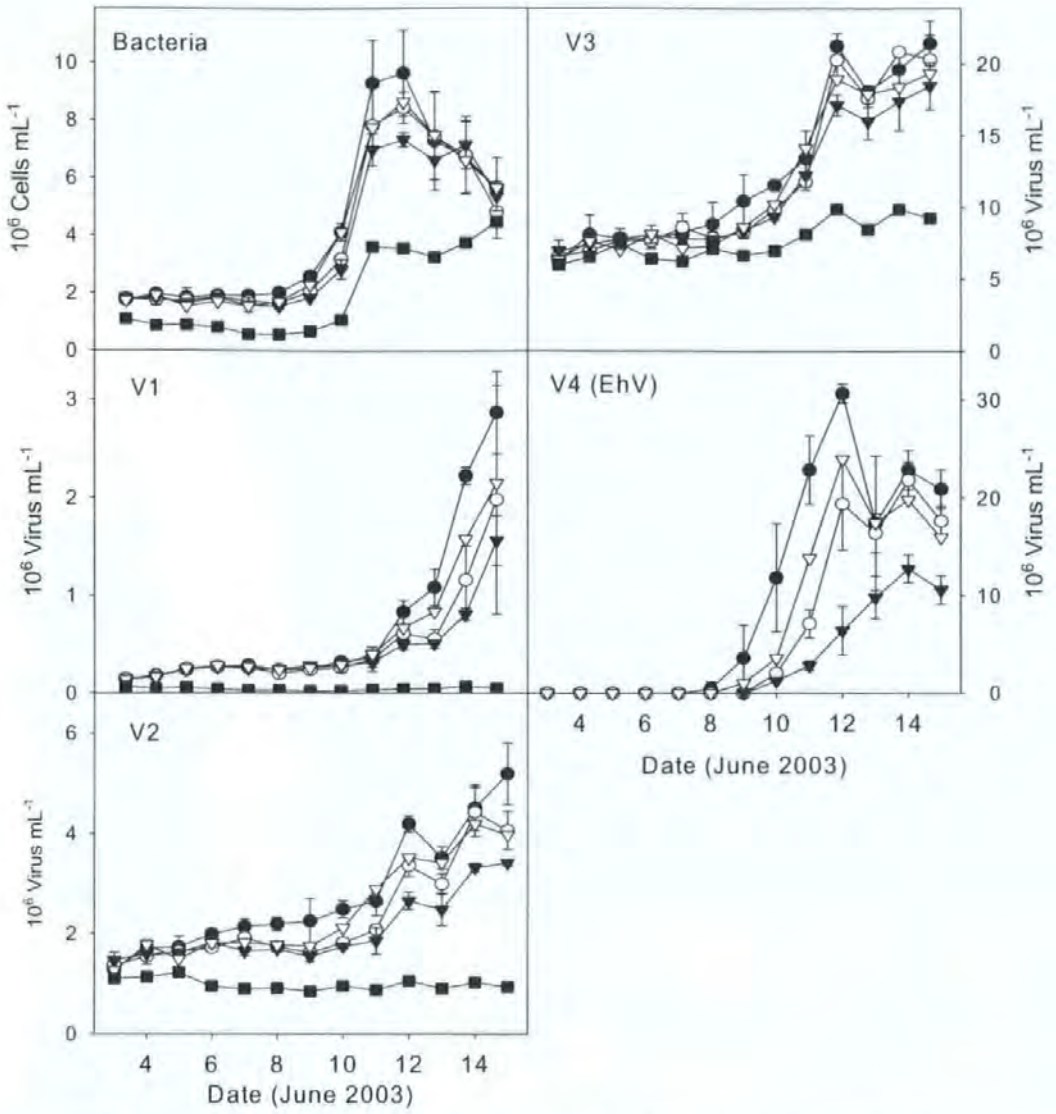

Fig. 4.5. Time series development of virus and bacteria populations as determined by flow cytometry. (●) TGA, (○) TGB, (▼) TGC, (▽) Bag 10, (■) fjord. For TGA, TGB and TGC lines indicate mean values for the 3 mesocosm bags in each Treatment Group, and the error bars indicate standard deviation.

The data above was also plotted relative to days after start of nutrient addition (DAN) to facilitate the subsequent interpretation of the statistical analysis, for which the observation vectors were grouped according to DAN. Figures 4.6 and 4.7 show how most populations responded to nutrient addition with the same time lag, and their graphs largely overlap when the time series are plotted relative to DAN. The *Synechococcus* and the picoeukaryote populations declined 1-3 days after the experiment started and did not respond to the initial nutrient addition, and these graphs are staggered in Figure 4.6. Growth of bacteria is also staggered (Figure 4.7).

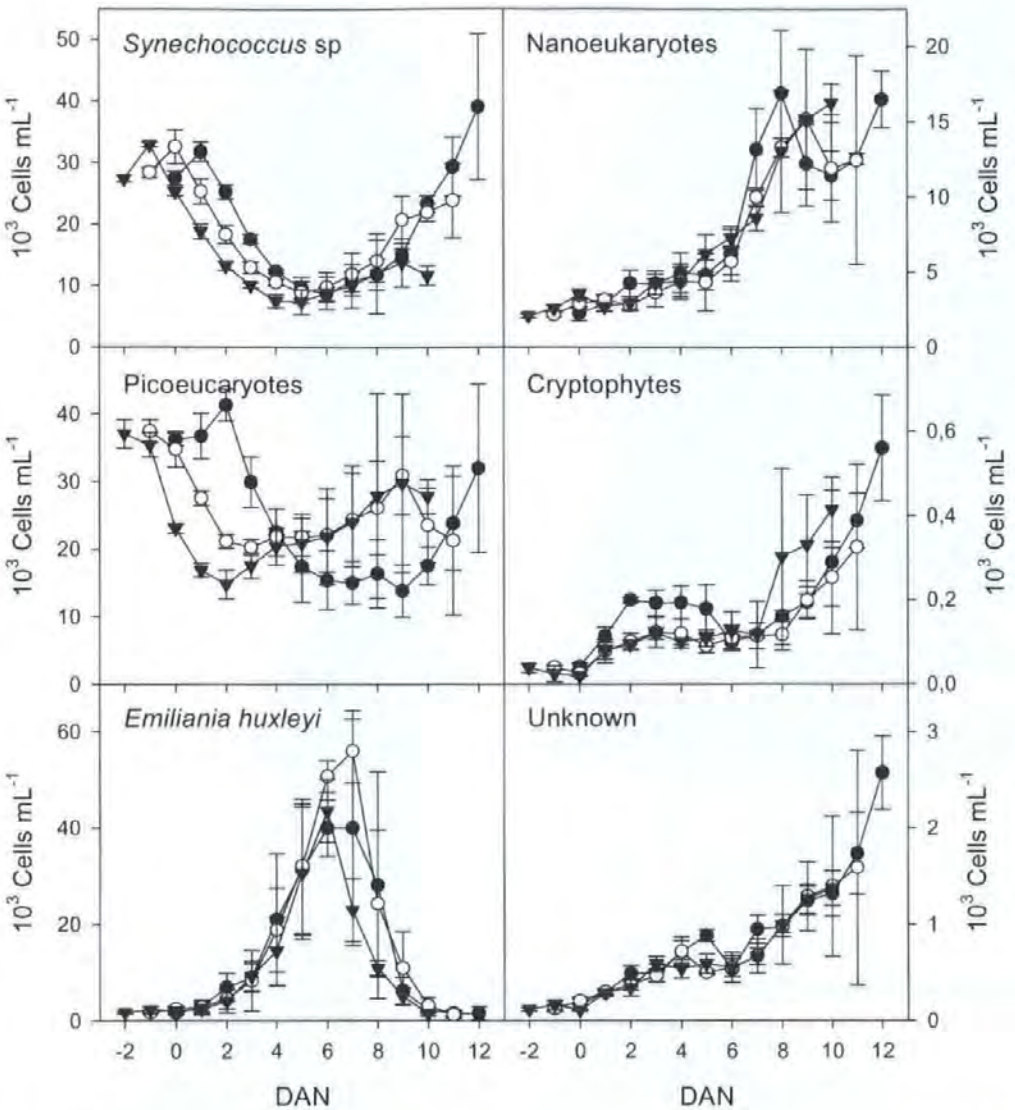

Fig. 4.6. Time series development of the 6 primary producers populations as determined by flow cytometry. The number on the x-axis corresponds to the number of days before or after the first nutrient addition (DAN), i.e. 0 is the day the first nutrient addition took place. Lines indicate mean values for the 3 enclosures in each Treatment Group. (●) TGA, (○) TGB, (▼) TGC. The error bars indicate standard deviation.

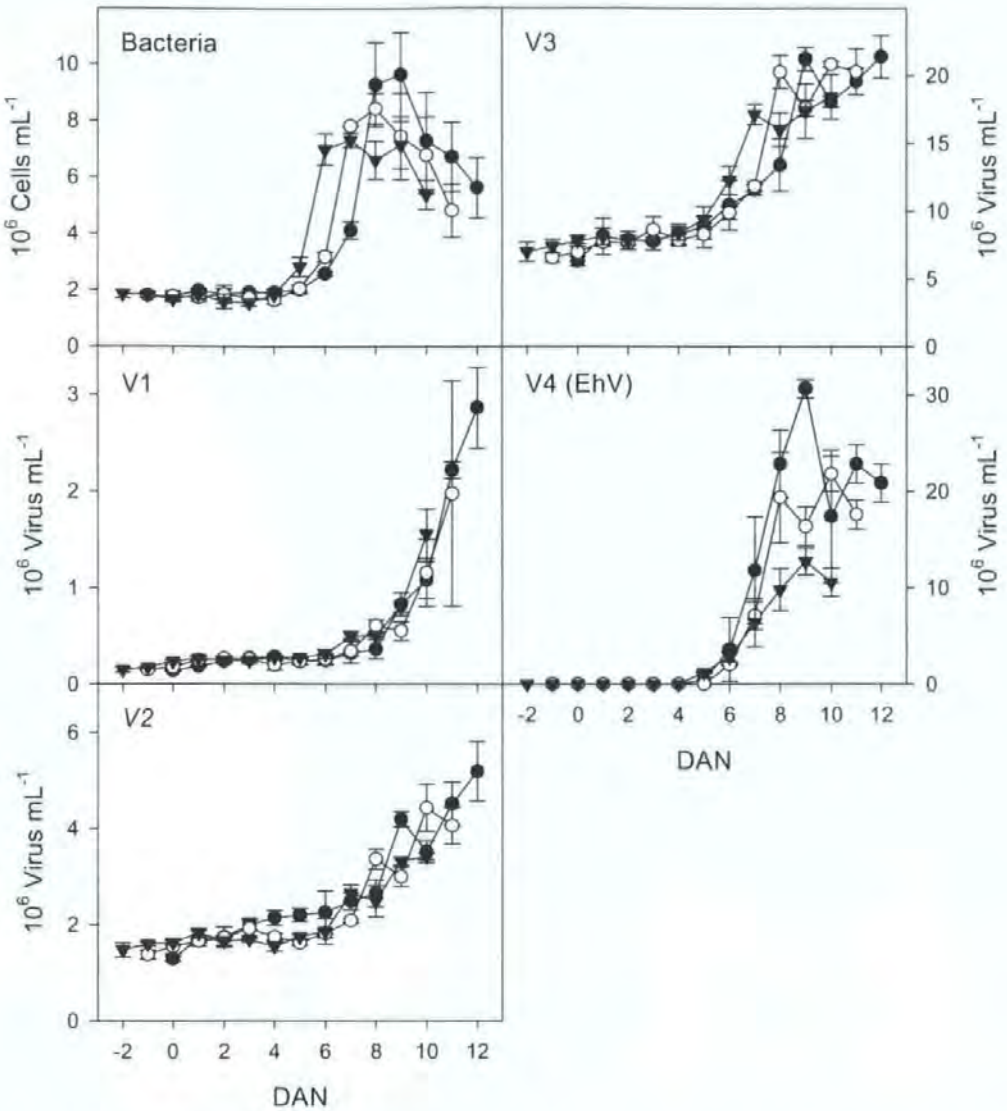

Fig. 4.7. Time series development of viruses and bacteria populations as determined by flow cytometry. The number on the horizontal axis corresponds to the number of days before or after the first nutrient addition (DAN), i.e. 0 is the day the first nutrient addition took place. Lines indicate mean values for the 3 enclosures in each Treatment Group. (●) TGA, (○) TGB, (▼) TGC. The error bars indicate standard deviation.

4.3.2. Statistical analysis: variability in microbial population dynamics between similarly perturbed mesocoms

Variance partitioning showed that the contribution to total variation of the time of start of the nutrient perturbation was small. The dominating fraction, 80 %, of the total variance could be attributed to among means variation of DAN (days after nutrient addition). Among means variation for TG accounted for not more than 3 %, and the among means variation of POS (position of the enclosure at the raft) for only 1 %.

Discriminant analyses showed that there was a significant difference (measured as Mahalanobis distances) between all mean vectors of DAN (time after initial nutrient addition) ($p<0.0035$), except for the following combinations: DAN -2 vs. DAN -1; DAN -2 vs. DAN 0; DAN -1 vs. DAN 0 and DAN 11 vs. DAN 12. The first linear discriminant axis (LD1) explained 62 % and the second (LD2) 32 % of the dispersion of means (Figure 4.8).

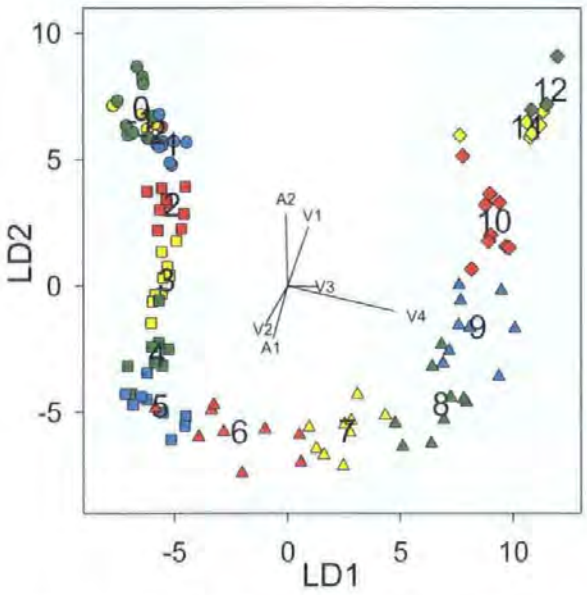

Fig. 4.8. Plot of the two first axes based on a discriminant analysis using DAN as grouping variable. The two axes account for 61 and 30 percent of the total dispersion, respectively. The projection of the 6 most important original axes is included. A1 represents *E. huxleyi*, A2 represents *Synechococcus* sp. and V4 represents EhV. Each symbol represents the canonical value for one dataset (i.e. data from one enclosure at a specific day): Circles, squares, triangles and diamonds represent DAN -2 – 1, 2 – 5, 6 – 9 and 10 – 12 respectively. Red, yellow, green and blue symbols represent DAN -2, 2, 6 and 10; -1, 3, 7 and 11; 0, 4, 8 and 12; and 1, 5, and 9 respectively. Numbers are DAN and are plotted at the mean position for each day.

There was also a significant difference between all three mean vectors of TG (delay before initial nutrient addition) ($p<0.00003$) while for the mean vectors of POS there was only a significant difference between POS=east and POS=west, the two on each end of the raft ($p<0.0002$).

Based on the canonical scores we computed the mean variance around each group mean vector for DAN. The mean within group variance increased throughout the entire experimental period (Figure 4.9).

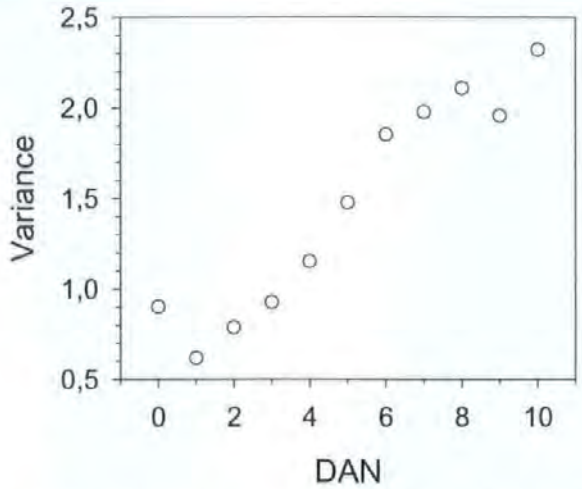

Fig. 4.9. The mean within-group variance (grouped by DAN) plotted versus DAN.

After the initial nutrient addition, all enclosures underwent a very similar development over time and most of this development could be attributed to DAN, which accounted for 80 % of the total variance. At the end of the experiment successions were slower and there was thus no significant difference between DAN 11 and 12.

There was a statistical significant difference between the bags when grouped by TG but in absolute terms the difference was small and accounted only for 3 % of the total variance. The enclosures placed furthest apart were statistically significantly different but again in absolute terms the difference was small and accounted only for 1 % of the total variance. Thus, by far the most important factor determining the development in the enclosures is the experimental manipulation (i.e. nutrient addition). The filling of the bags, the delay, and their position at the raft were of minor importance.

In the experimental period, there were fairly large day-to-day variations in natural light conditions (Figure 4.10). DAN 0 coincided with excellent light conditions for TG2 (4^{th} June), but very poor conditions for TG1 and TG3 (3^{rd} and 5^{th} June, respectively).

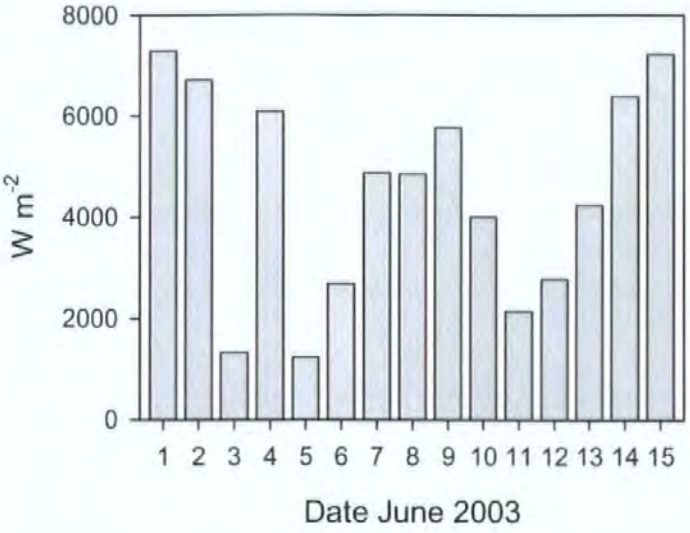

Fig. 4.10 Global radiation integrated for each day during the experiment. Data from Geophysical Institute, University of Bergen ca. 20 km from the experimental site.

4.3.3. Virus isolation

DGGE analysis of PCR products from the lysates produced by inoculation of the *E. huxleyi* strains with water samples from the enclosures showed the presence of two different EhV viruses (Fig. 4.11A). Both EhVs were successfully made clonal by plaque assay, as revealed by DGGE analysis (Figure 4.11B).

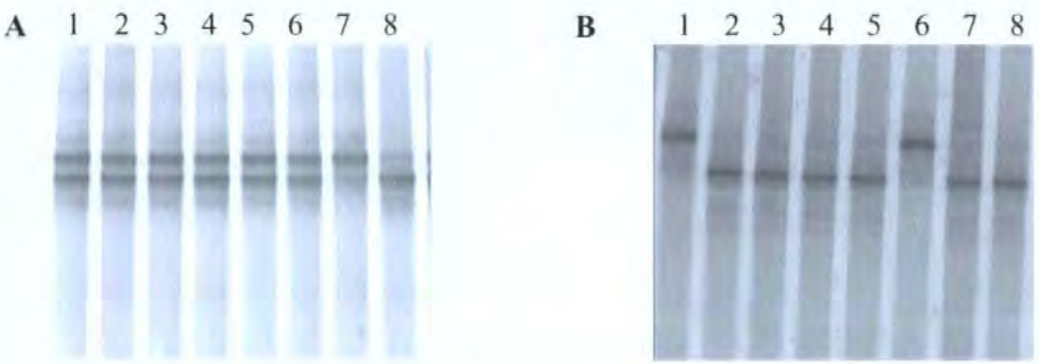

Fig. 4.11 Representative DGGE gels of PCR fragments amplified with MCP primers for analysis of EhV composition in the mesocosm samples. (**A**) Lanes 1-8 correspond to PCR products from lysates of Eh BOF92 inoculated with water samples collected from enclosure 1 on different dates. Bands with different migration rates indicate different EhVs. (**B**) Lanes 1-8 correspond to PCR products from single EhV plaques produced by plaque assay on one of the above Eh BOF92 lysates.

Only two of the phytoplankton species used for the 'enrichment cultures' experiment, *Micromonas pusilla* and *Chrysochromulina ericina*, lysed after approximately one week. AFC analysis of the lysates showed signatures with similar characteristics of those referred to previously as V1, V2 and V3 (Figure 4.12). The *C. ericina* population includes two different groups of viruses as revealed by AFC.

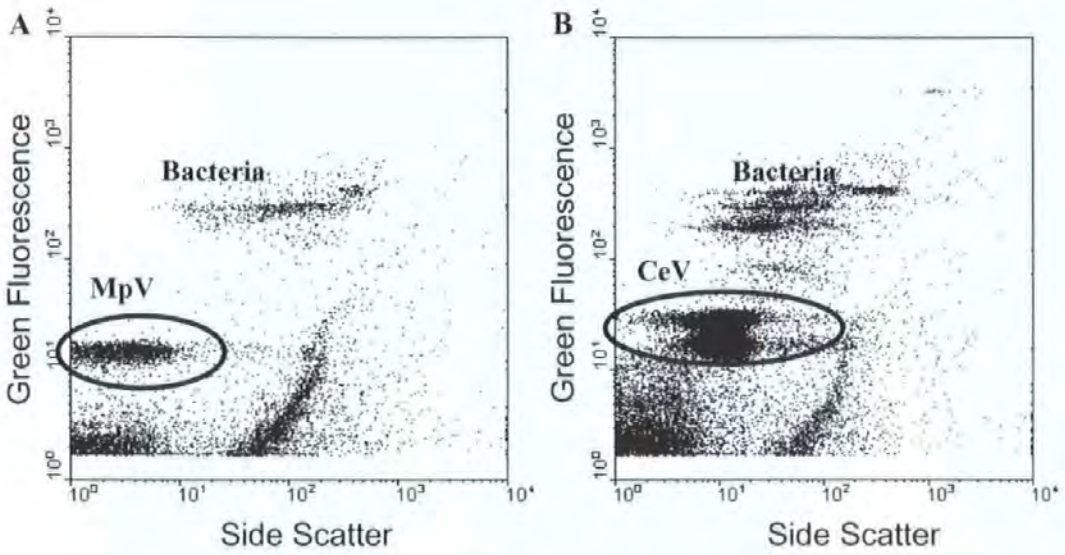

Fig. 4.12. Biparametric flow cytometry plots showing populations of *M. pusilla* viruses (MpV) (**A**) and *C. ericina* viruses (CeV) (**B**). Heterotrophic bacteria and different groups of viruses were discriminated on the basis of the green DNA dye complex fluorescence versus side scatter signal.

4.4. Discussion

4.4.1. Development of the *E. huxleyi* blooms. Effects of nutrient and zooplankton manipulation

Nutrient enrichment of the seawater enclosures resulted in induced phytoplankton blooms. Correlation of cell numbers and phytoplankton biomass (chl a) values show that *E. huxleyi* dominated the phytoplankton community and had a greater impact on the production than the other algal species present in the enclosures (data not shown). The same response to nutrient addition has been previously reported during a number of similar mesocosm studies (Bratbak et al. 1993, Egge & Heimdal 1994, Castberg et al. 2001, Jacquet et al. 2002). This is likely a consequence of the high competitive ability of *E. huxleyi* under high light irradiance and excess of nutrients, mainly phosphate, conditions. *E. huxleyi* has the highest affinity for inorganic phosphate ever measured among a wide range of phytoplankton species and therefore, it has the ability to out-compete other phytoplankton species such as *Synechococcus* sp. and picoeukaryotes; especially when P is at levels on the nM range (Riegman et al. 2000). The growth rate of *E. huxleyi* during this study was higher than previously observed during analogous induced blooms of *E. huxleyi* in the same area (Bratbak et al. 1993, Castberg et al. 2001, Jacquet et al. 2002). *E. huxleyi* grew at, possibly, its maximal rate, i.e. between 1.3 and 3 division d^{-1} (Paasche & Klaveness 1970, Brand 1981, Brand 1982, Paasche et al. 1996). First of all, the reproduction rates depend on the environmental regime and on genetic adaptations. It seems possible therefore that *E. huxleyi* could owe its success in Norwegian coastal waters to the presence of resident populations genetically adapted to local conditions. The optimal combination of salinity, temperature and light intensity during the period the mesocosm experiment was run might have led to this very high growth rate.

The concurrent rapid multiplication of EhV particles as the *E. huxleyi* bloom declined indicates lytic viral infection was the main cause of bloom termination (Figures 4.3 and

4.5). Viral-induced collapse of *E. huxleyi* populations has been inferred from a number of studies both in the open ocean (Brussaard et al. 1996b, Wilson et al. 2002a) and in mesocosms (Bratbak et al. 1993, Egge & Heimdal 1994, Castberg et al. 2001, Jacquet et al. 2002). Jacquet et al. (2002) monitored by AFC the development of *E. huxleyi* populations and their viruses during a similar mesocosm study. They observed how as viral particles accumulated, diel patterns of *E. huxleyi* physiological properties were lost, which is a characteristic of virally infected phytoplankton cells (Brussaard et al. 1999). During another mesocosm study of *E. huxleyi*, Castberg et al. (2001) isolated viruses that could be propagated on cultures of *E. huxleyi*. It was observed that they exhibited identical genome and particle size and AFC signature to the viruses that multiplied during the crash of the *E. huxleyi* bloom. We also isolated viruses during this mesocosm study infectious to several *E. huxleyi* strain cultures and with same AFC characteristics as the viruses referred to as EhV (V4).

During this mesocosm experiment Claire Evans measured *E. huxleyi* cell viability, using SYTOX staining, and detected high abundances of compromised cells during the decline of the bloom. Additionally, cell photosynthetic capacity (CPC) decreased concurrently with the decrease of the bloom (CPC was measured by Gill Malin). The appearance of compromised cells was concurrent with a rapid increase of the EhV group adding further support to the idea of viral termination of the bloom. Laboratory experiments show high numbers of nonviable *E. huxleyi* cells during viral infection (up to 60 % of the total population), whilst during apoptosis or programmed cell death, probably induced by nutrient limitation, only approximately 2 % of the total population is nonviable (Evans 2004). Although rates of grazing were not determined during this study, the lack of significant differences in bloom development and termination in TGD, subjected to zooplankton enrichment, suggests a low contribution of grazing on *E. huxleyi* as a factor in the decline of the bloom.

After maximum numbers of EhV particles were reached, this virus group experienced a sudden decrease followed by a second minor peak in abundance (Figure 4.5). The demise of the *E. huxleyi* bloom would result in higher rates of viral decay due to attachment to particles and host cells debris, consumption by protozoan grazers and digestion by bacterial enzymes (Kapuscinski & Mitchell 1980, Suttle & Chen 1992, Murray 1995, Noble & Fuhrman 1997). However, the second peak in EhV abundance for TGA, TGB and TGD might be explained by a new cycle of infection due to absorption of released EhVs to remaining *E. huxleyi* cells. The reason why this second increase in EhV numbers was not observed in TGC could just probably be a consequence of time limitation.

The low numbers of *E. huxleyi* cells in the fjord would explain that the EhV group was not distinguishable in the fjord samples throughout the period of study since infection has been shown to be density dependent (Murray & Jackson 1992).

EhV appeared as a clear group during AFC analysis first in the samples from TGA and TGD (8^{th}-9^{th} June), which were the first group to receive nutrient addition and the one subjected to copepod enhancement respectively, and one day after in TGB and TGC. Yet, the abundance of *E. huxleyi* in enclosures TGB and TGC on 9^{th} June was comparable to TGA and TGD. Additionally, the bloom crash occurred one day earlier in TGD than in any of the bags that received the same nutrient treatment, i.e. TGB. These observations suggest that the rate of progression of viral infection through the bloom was increased by an earlier nutrient addition as well as by enriching the copepods biomass.

Microzooplankton graze preferably on certain prey types (Hansen et al. 1996). For instance, it has been found that infected cells of *E. huxleyi* are preferentially grazed by microzooplankton (Claire Evans, unpublished data). This may be the case during this mesocosm study, that could explain how the reduction in microzooplankton abundance, by

copepods grazing, would lead to the earlier production of more viruses as a higher percentage of infected cells would complete the lytic cycle.

4.4.2. Influence of the *E. huxleyi* demise on the rest of the microbial community

The results in this study suggest a close link between the dynamics of the microbial populations and are comparable to other analogous experiments in the same area in terms of phytoplankton, bacteria and virus numbers and composition (Castberg et al. 2001, Jacquet et al. 2002).

Only after the collapse of the *E. huxleyi* population did other phytoplankton groups experience an increase in abundance. Yet, the groups referred to as unknown and cryptophytes did not seem to play a very important role in the total community production since both populations represented a very low percentage of cell numbers throughout the period of study (below 2 % for the unknown group and less than 1 % for cryptophytes).

Copepods enrichment in bag #10 (TGD) did not significantly alter the succession of micro-algae species and the progression of the bloom when compared with TGA, TGB and TGC. As observed in the other enclosures, *E. huxleyi* developed and crashed concurrently with an increase in EhV numbers. As a result of the *E. huxleyi* demise bacteria numbers increased along with the concentration of other phytoplankton groups.

Both the bloom of *E. huxleyi* and its viral termination also had a considerable impact on the bacterial community. At the time the coccolithophorid began its decrease the bacterial group experienced a sudden increment. During phytoplankton lysis a large proportion of the algal biomass is converted into dissolved organic carbon (DOC), which becomes available this way to the heterotrophic bacteria population (Bratbak et al. 1998a, Middelboe et al. 2002). Similar enhancements in bacterial numbers after a sharp decrease

of dominating algae have earlier been observed in mesocosm (Levasseur et al. 1996, Castberg et al. 2001) and field studies (Bratbak et al. 1990).

Also the virus groups V1, V2 and V3 increased more markedly in abundance towards the end of the study period subsequently to the termination of the *E. huxleyi* bloom. The increase in numbers of these virus groups coincides with an increase in some of the other microalgal groups. It should be noted that virus concentrations for V1 and V2 are an order of magnitude less than V3 and V4 (EhV); this is consistent with lower concentrations of some of the microalgal groups. Isolation of *M. pusilla* and *C. ericina*-specific viruses with similar flow cytometry characteristics of those viruses referred to as V1 and V2 in this study reveals that they were in the enclosures during the mesocosm experiment and were part of the V1 and V2 groups. V3 correlates very closely to bacteria increase both in the enclosures and in the fjord. However, the numbers of V3 are within the range of other algal virus abundances (Figure 4.5). If group V3 were bacteriophages one might expect higher numbers for this group since in marine heterotrophic bacteria, burst size can typically reach >500 viruses produced per lysed cell (Borsheim 1993). Analogous experiments (Larsen et al. 2001, Larsen et al. 2004) tend to interpret the viruses with the highest abundance, i.e. those with the lower green fluorescence values (GFL), as bacteriophages since among the potential host organisms, bacterioplankton was found in higher concentrations than phytoplankton. In this study, the virus group with the lowest GFL values has nevertheless been obviated since its signature could not be dissociated from the flow cytometer noise and the background signal caused by other small particles (impurities in solution) to form a discrete group. However, AFC data give a relatively coarse classification of the viral populations as they are based on only two parameters (SSC and GFL) what renders difficult to assure which virus types are exactly V1, V2 and V3.

4.4.3. Validity and reproducibility of mesocosm studies

The validity of mesocosm studies must be considered in order to discuss their accuracy as representations of the microbial community development under natural conditions. The water mass and the community inside the enclosures follow the natural fluctuations in irradiance and temperature (Egge 1993). A number of studies have previously shown that the development of the phytoplankton community inside the enclosures resembles that of the community in the surrounding water (Takahashi et al. 1975, Kuiper 1977, Davis 1982). The controlled water mass in a mesocosm is suitable for budget studies (Riemann et al. 1990) and for verification of simulation models (Andersen et al. 1987, Keller & Riebesell 1989).

AFC analysis in this study revealed the development of the same microbial community both inside the mesocosm bags and in the fjord. However, addition of nutrients to the seawater in the enclosures enhanced the conditions for phytoplankton growth. As a result, *E. huxleyi*, in this case the most successfully competitive component within the phytoplankton community, rapidly multiplied leading to what others have reported as an accelerated version of community succession commonly found in the environment (Davis 1982, Egge 1993). During this mesocosm experiment the concentration of *E. huxleyi* cells ($\sim 10^4$ cells ml^{-1}) was in the range of what has been typically observed before during similar studies (Bratbak et al. 1993, Castberg et al. 2001, Jacquet et al. 2002) and during natural blooms of this species in coastal water and Norwegian fjords (Holligan et al. 1983, Ackleson et al. 1988, Heimdal et al. 1994).

From this study we conclude that the mesocosm set up appears to be a very robust experimental system that gives a reproducible response in the microbial development and succession when subjected to the same nutrient manipulations. The *E. huxleyi* population progressed sequentially in line in the three enclosure groups with the staggered nutrient

additions. The differences in cell numbers and timing of peaks of abundance were probably due to slightly different airflow in the enclosures, differences in initial cell numbers and the different placing of the bags at the raft, so that light and water movements outside the bags might be different.

In the ideal situation discussed in the introduction, the dynamic patterns of abundance variations should not vary more between treatment groups than within treatment groups. Our analysis show that there is not statistically significant development in the bags before the first nutrient addition, which means that filling the enclosures and leaving them for 1-2 days before the initial nutrient addition did not affect the system significantly. The statistical differences between the bags when grouped by treatment group (TG) and by their position at the raft (POS) were also small in absolute terms (only 3 % and 1 % of the total variance respectively). Grouping the enclosures according to their east-west position at the raft (POS) potentially reveals whether the slight differences in light exposure had significant effects.

The magnitude of the *E. huxleyi* bloom was higher in the TGB enclosures in (Figure 4.3). This effect could be attributed to natural light conditions, which are a recognized important factor for the development of *E. huxleyi* blooms (Nanninga & Tyrrell 1996). In the experimental period, there were large day-to-day variations in natural light conditions (Figure 4.10). Notably, the first day of nutrient addition (DAN 0) coincided with excellent light conditions for TGB (4th June), but very poor conditions for TGA and TGC (3rd and 5th June, respectively). In principle, such day-to-day variations in light conditions may have interacted differently with food webs being in different phases of succession in the three treatment groups. With our design, these light effects could however not be separated from other among-group sources of variance. However, since among-group variance was minor; such effects of variable light conditions must have been small.

For the construction of dynamic models of this experiment, our results thus support the validity of a set of strongly simplifying and constraining assumptions. Assuming light to be available in excess and the filling manipulations have no perturbing effects will remove many assumptions concerning mechanisms and parameters. More important, however, are the strong constraints to model structure and parameter values implicit in the assumption of an initial system approximately in steady state. When this is true, the model should both have a steady state representing well the initial state, and a transient response reproducing the observed population dynamics. Earlier work has suggested that this approach may be valid, with the fast dynamics of the microbial part of the food web allowing this part to remain close to a steady state driven by the two variables: nutrient content of the system and predatory losses to mesozooplankton (Thingstad et al. 1999a, Thingstad et al. 1999b).

4.5. Conclusions

The reduction in cell photosynthetic capacity and the concomitant increase in EhV particles indicated that the collapse of the *E. huxleyi* bloom was caused by lytic viral infection. The significance of viral lysis in the bloom decline increased with the reduction in abundance of microzooplankton, which preferentially graze on infected *E. huxleyi* cells.

The *E. huxleyi* bloom and in particular its termination by viruses affected both diversity and dynamics of the rest of the microbial community, algae, bacteria and viruses. The results in this study can be added to a number of studies concluding the importance of viruses controlling the maintainable densities of algal and bacterial populations in the environment (Cottrell & Suttle 1991a, Suttle & Chan 1995, Tarutani et al. 2000, Castberg et al. 2001, Larsen et al. 2001, Jacquet et al. 2002).

The mesocosm setup appears to be a robust experimental system that gives a reproducible response when subjected to (nutrient) manipulations initiating a sizable succession. For the construction of dynamic models of this experiment, our results thus support the validity of a set of strongly simplifying and constraining assumptions (steady state).

CHAPTER FIVE

Molecular dynamics of *Emiliania huxleyi* and co-occurring viruses during two separate mesocosm studies

5. Molecular dynamics of *Emiliania huxleyi* and co-occurring viruses during two separate mesocosm studies

5.1. Introduction

There is a huge diversity of viruses in the ocean (Suttle 2005) and this fact alone makes them incredibly difficult to study as a single entity. Therefore it has become necessary to study specific groups of viruses to try and make sense of their propagation strategy and molecular dynamics.

Previous studies using mesocosm systems have investigated the effects of dissolved nutrient composition on the community dynamics of *E. huxleyi* dominated systems and the role viruses have in structuring different microbial components (Bratbak et al. 1993, Wilson et al. 1998, Jacquet et al. 2002). It is clear from these studies that viruses are instrumental in the demise of *E. huxleyi* blooms and allow succession of different micro algae following rapid bacterial remineralisation of organic matter (Castberg et al. 2001, Larsen et al. 2001). As the *E. huxleyi* bloom crashes there is a rapid increase in large virus particles, easily discriminated by analytical flow cytometry (AFC) (Jacquet et al. 2002, Wilson et al. 2002a).

These large virus particles can be isolated with relative ease by adding filtered seawater to cultures of *E. huxleyi* (Castberg et al. 2002, Wilson et al. 2002b). Characterization of these large *E. huxleyi*-specific viruses (EhVs) revealed that they belong to the family of algal viruses *Phycodnaviridae*, based on analysis of their DNA polymerase (pol) gene (Schroeder et al. 2002). The genome of one strain of EhV isolated from the English Channel was recently sequenced revealing a 407 kbp genome, the largest algal virus sequenced to date (Wilson et al. 2005a).

It is already recognized that there can be a broad genotypic variety within populations of *E. huxleyi* (Medlin et al. 1996, Iglesias-Rodriguez et al. 2002) and EhVs (Schroeder et al. 2003) during *E. huxleyi*-dominated blooms, although these tools have never been used together to assess the virus/host molecular dynamics. It is necessary to develop appropriate tools before such an assessment can be made. Thus, for the analysis of *E. huxleyi* Schroeder et al. (2005) showed that a gene encoding a protein with calcium-binding motifs (designated GPA), thought to be involved in regulating coccolith morphology (Corstjens et al. 1998), could be used as a genetic marker to definitively resolve differences that could be attributed to different *E. huxleyi* genotypes within the A and B morphotypes kept in culture. *E. huxleyi* is currently separated into five morphotypes based mainly on coccolith morphology, physiological properties and immunological properties of the polysaccharide associated with coccoliths. Morphotypes A and B are the best characterised.

For EhV analysis Schroeder et al. (2002) exploited variations in the Major Capsid Protein (MCP) gene to assess the genetic diversity of EhVs. Schroeder et al. (2003) used the MCP marker to reveal genetic richness of free-floating viruses during an *E. huxleyi* bloom in a mesocosm experiment in Norway in 2000. The DNA polymerase gene, more commonly used to resolve genetic variation among other algal viruses (Chen & Suttle 1995, Short & Suttle 2002) is not variable enough to differentiate EhVs.

In the current study we extend the research of Schroeder et al. (2003) by using a combination of GPA and MCP molecular markers to check the dynamics and genetic richness of *E. huxleyi* and their co-occurring viruses during the same mesocosm experiment (from June 2000). Additionally, we analyzed samples from a second mesocosm experiment at the same site 3 years later (June 2003). The aim of this study was two-fold; first to assess the molecular dynamics of the host/virus system *in situ*; and second, to determine the genetic stability/variability of *E. huxleyi* and their co-occurring viruses over

time (i.e. after a 3-year gap), particularly since *E. huxleyi* blooms occur annually in May through July in Norwegian coastal waters and fjords (Bratbak et al. 1993). In addition to the genotypic analysis, AFC was used to count the *E. huxleyi* and virus populations in mesocosm samples.

5.2. Materials and methods

5.2.1. Experimental design

Two mesocosm experiments designed to monitor the progression of a coccolithophore-induced bloom were carried out in Raunefjorden, western Norway, at the Marine Biological Field Station, Espeland 20 km south of Bergen, in June 2000 and June 2003. The experimental design and the AFC analysis of *E. huxleyi* and its natural viral communities for the 2000 mesocosm are as described by Jacquet et al. (2002). The setup, experimental design and AFC for the 2003 mesocosm are as described in Sections 2.2.20 and 4.2 in this thesis, respectively.

5.2.2. DNA isolation

For total genomic DNA preparations 1 L seawater samples from enclosure #1 for the 2000 mesocosm experiment and from enclosures #1, #4, #7 and #10 for the 2003 mesocosm experiment were filtered daily onto 0.45 μm pore size Supor-450 47 mm diameter filters (PALL Corp). Genomic DNA was isolated using an adapted phenol/chloroform method (Section 2.2.11.2).

5.2.3. Polymerase Chain Reaction (PCR) amplification and DGGE

E. huxleyi genotypic richness was studied using a nested PCR on the total genomic DNA preparations. Three oligomers were designed to the GPA gene of *E. huxleyi* strain L (Table 2.5). Two-stage PCR reactions (firstly with primers GPA-F1/GPA-R1 and secondly with GPA-F2/GPA-R1) were conducted to amplify the variable region within the GPA gene that separates the alleles into genotypes (Schroeder et al. 2005). The PCR reactions were performed as described in Section 2.2.12.

Viral diversity studies were also conducted by two stage PCR reactions (Section 2.2.12). Amplification of virus MCP gene was conducted using two pairs of MCP specific

oligomers coupled as MCP-F1/MCP-R1 and MCP-F2/MCP-R2 (Table 2.5). DGGE analysis of second-stage, host and viral, PCR products was conducted as described in Schroeder et al. (2003) with some minor adjustments (see Section 2.2.14).

5.2.4 DNA sequencing and sequence analysis

Single bands excised from the DGGE gels were re-amplified. PCR products were subsequently sequenced and the data for each fragment analysed (Section 2.2.15). The GPA sequences produced were aligned together with GPA sequences obtained from 15 *E. huxleyi* isolates kept in culture (Schroeder et al. 2005). The produced MCP sequence data was aligned with corresponding MCP sequences of 9 clonal EhVs isolated between 1999 and 2001 from the English Channel (Schroeder et al. 2002, Wilson et al. 2002b) and 1 clonal virus isolated during the 2000 mesocosm experiment in Raunefjorden (Schroeder et al. 2002) (see Tables 2.3 and 2.4 for GenBank accession numbers).

5.3. Results

For the 2003 mesocosm experiment only graphs and images obtained for samples from enclosure #7 will be presented since they are representative of the results obtained from four enclosures in the study. In fact, enclosures #1, #4 and #7 were replicates of each other since they were subjected to the same nutrient manipulation. Enclosure #10 received the same nutrient treatment as #1, but was additionally enriched with copepod biomass (see Section 4.2.2).

5.3.1. PCR amplification

E. huxleyi GPA gene fragments were amplified, yielding products of 500 bp in the first-stage PCRs (not revealed by agarose gel electrophoresis analysis) and ~ 285 bp in the second-stage PCRs (Figure 5.1A). PCR reactions using the specific MCP primers for EhV's amplified 284 bp fragments (not revealed by agarose gel electrophoresis analysis) in the first-stage reactions and 175 bp in the second-stage reactions (Figure 5.1B)

Fig. 5.1. Representative images of agarose gel electrophoresis of PCR fragments amplified in second-stage PCR from total genomic DNA extracted from a number of samples collected during the 2003 mesocosm. (**A**) Lanes 2-28, *E. huxleyi* GPA gene fragments. (**B**)Lanes 2-28, EhV MCP gene fragments. In both gels: lane 1, DNA molecular weight marker (100 bp ladder); lane 29, no DNA (negative control).

5.3.2. Flow cytometry analysis

AFC was used to monitor the total abundance of *E. huxleyi* and EhVs during the blooms in 2000 (Jacquet et al. 2002) (Figure 5.2) and 2003 (Figure 5.3). During the 2000 mesocosm *E. huxleyi* numbers increased by 2 orders of magnitude, from 10^3 to 10^5 cells ml^{-1}, between the beginning of the experiment and the peak of the bloom. *E. huxleyi* numbers returned to pre-bloom levels of 3×10^3 cells ml^{-1} at the end of the study (Figure 5.2A). An increase of ~ 2 orders of magnitude was also observed in EhV abundances, from 4.7×10^5 to 3.5×10^7 virus ml^{-1} during the collapse of the *E. huxleyi* bloom, revealing a classic lytic virus response to a susceptible host population (Figure 5.2B).

During the 2003 mesocosm a similar pattern in virus-host dynamics was observed compared to the 2000 mesocosm (Figure 5.3). *E. huxleyi* numbers increased by 1 order of magnitude, from ~ 1.5×10^3 to ~ 4×10^4 cells ml^{-1}, over the 7 days prior to the bloom crash. At this point, *E. huxleyi* numbers fell rapidly and returned to approximately the same cell numbers as before the initiation of the bloom, 1.5×10^3 cells ml^{-1} (Figure 5.3A). EhV numbers increased by ~ 2 orders of magnitude, from 4.3×10^5 to 3×10^7 virus ml^{-1} following the sudden demise of *E. huxleyi* (Figure 5.3B).

5.3.3. *E. huxleyi* DGGE gels

DGGE analysis of the PCR products using the GPA specific primers revealed a stable *E. huxleyi* community during the bloom progression in both mesocosm studies, 2000 (Figure 5.2A) and 2003 (Figure 5.3A). Since *E. huxleyi* strains can contain more than one allele (Schroeder et al. 2005), the number of bands revealed in this study is just an indication of the number of different alleles and does not show, quantitatively, diversity of *E. huxleyi* strains. The gels showed at least 6 distinguishable bands throughout both periods of study (Figure 5.3A). Not one of the alleles seemed to be dominant before, during or after the blooms (Figures 5.2A and 5.3A).

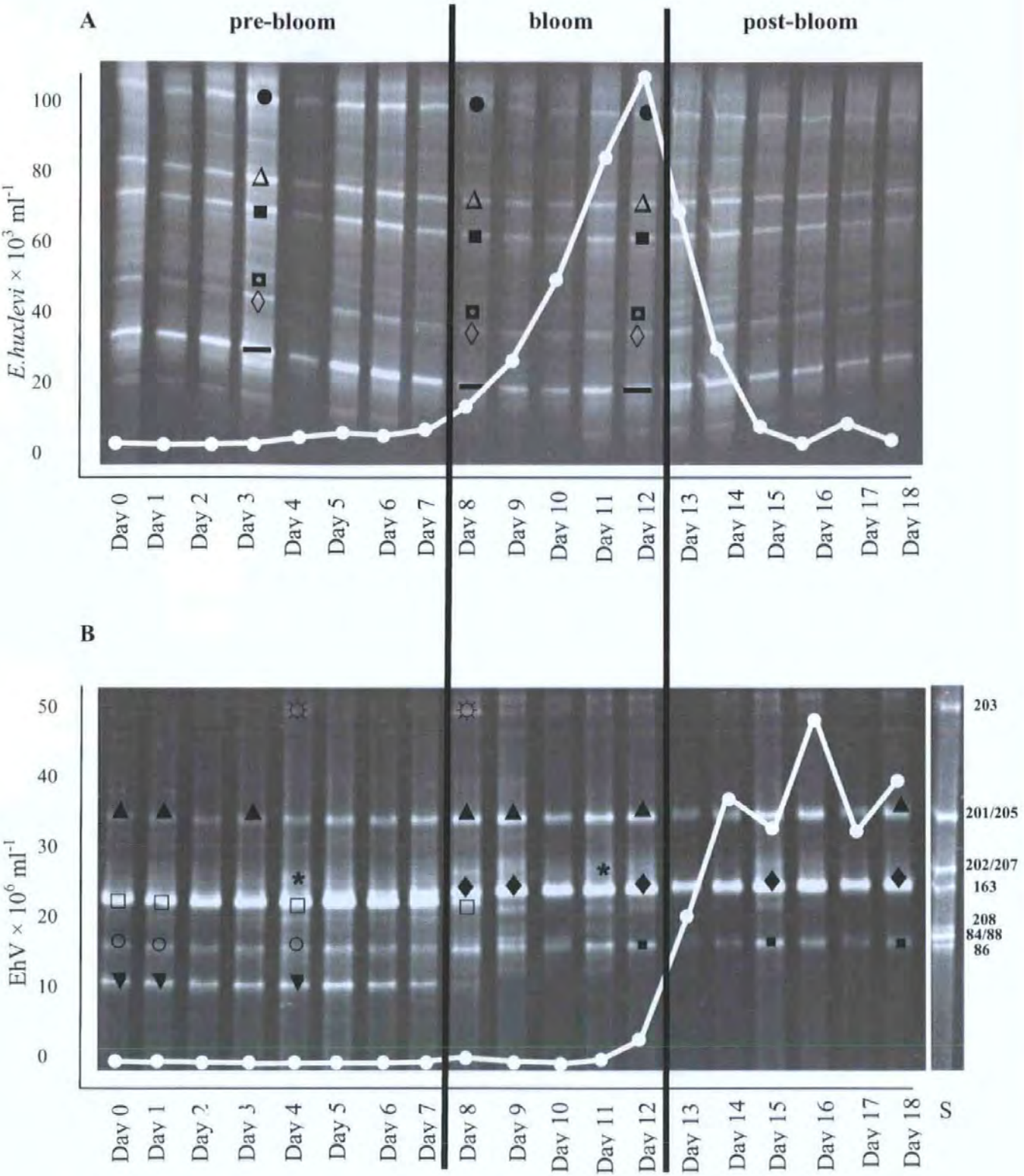

Fig. 5.2 DGGE gels of PCR fragments amplified from the mesocosm samples in 2000. The graphs depict the progression of *E. huxleyi* **(A)** and *E.huxleyi*-specific virus **(B)** populations during the bloom determined by flow cytometry. Symbols indicate the bands excised for sequencing, identical symbols indicating identical nucleotide sequence (see Table 5.1). Standards (S), MCP-PCR fragments amplified from known *E. huxleyi*-specific virus strains isolated from the English Channel and Raunefjorden (Norway) (Schroeder et al. 2002, Wilson et al. 2002b).

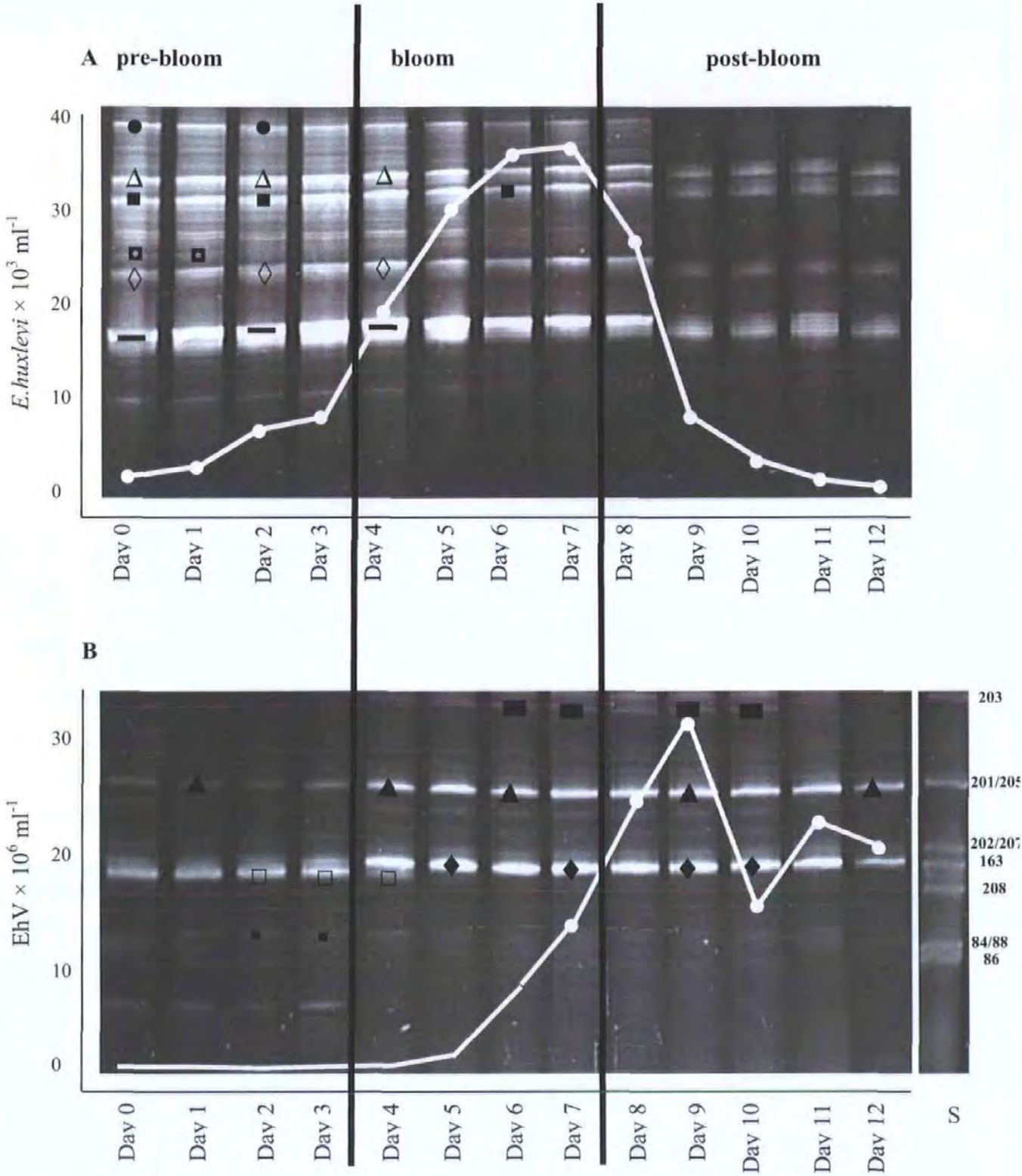

Fig. 5.3 DGGE gels of PCR fragments amplified from the mesocosm samples in 2003. The graphs depict the progression of *E. huxleyi* **(A)** and *E. huxleyi*-specific virus **(B)** populations during the bloom determined by flow cytometry. Symbols indicate the bands excised for sequencing, identical symbols indicating identical nucleotide sequence (see Table 5.1). Standards (S), same as Fig. 5.2.

All the alleles corresponded to *E. huxleyi* morphotype A, genotype CMM I (Schroeder et al. 2005) (Figure 5.4). The authenticity of the DGGE bands was confirmed by excising a total of 34 single bands (between both gels), verifying their purity by PCR and re-DGGE (data not shown) and sequencing. The migration rate on DGGE gels and sequence alignment revealed that multiple bands on an individual sampling day were different; whilst bands from different days that migrated at the same rate had identical nucleotide sequence (Figure 5.4). Table 5.1 summarizes the data and GenBank accession numbers of each fragment sequenced. The alleles present in 2000 were identical to the ones from the 2003 mesocosm study (Schroeder et al. 2005) (Table 5.1).

5.3.4. Virus DGGE gels

The 2000 mesocosm DGGE gel showed a diverse band pattern prior to the onset of *E. huxleyi* bloom (Figure 5.2B). At least 6 bands were distinguishable in the pre-bloom profile (ehvOTU9☼, ehvOTU3▲, ehvOTU10*, ehvOTU5□, ehvOTU7○ and ehvOTU2▼). A shift in bands present was observed during the bloom, where ehvOTU7○ and ehvOTU2▼ disappeared and two new bands (ehvOTU1♦ and ehvOTU4▪) became visible. During post-bloom ehvOTU3▲, ehvOTU1♦ and ehvOTU4▪ dominated; ehvOTU3▲ was detected before, during and after the *E. huxleyi* bloom.

The DGGE profile for the 2003 mesocosm (Figure 5.3B) also revealed a change in abundance of virus groups, with the appearance/disappearance of bands. In the 4 days prior to the onset of the bloom four bands were distinguishable (ehvOTU3▲, ehvOTU5□, ehvOTU4▪ and ehvOTU16◙). During the bloom and post-bloom periods a shift in the bands was observed where ehvOTU5□, ehvOTU4▪ and ehvOTU16◙ bands disappeared and they were replaced by ehvOTU11■ and ehvOTU1♦. Incredibly, the same two bands dominated during the bloom/post-bloom period in both 2000 and 2003 mesocosms

(ehvOTU3▲ and ehvOTU1♦); and the same band shift from ehvOTU5□ to ehvOTU1♦ was observed from the onset of the bloom between the 2 years.

E. huxleyi				
Year	DGGE band	GPA sequence[1]	Genotype CMM group	GenBank accession number
2000/2003	●	ehuxOTU1	I	DQ085072
2000/2003	Δ	ehuxOTU2	I	DQ085073
2000/2003	■	ehuxOTU3	I	DQ085074
2000/2003	◘	ehuxOTU6	I	DQ085075
2000/2003	◊	ehuxOTU4	I	DQ085076
2000/2003	—	ehuxOTU5	I	DQ085077

E. huxleyi-specific viruses (EhVs)				
Year	DGGE band	MCP sequence[2]	Genotype MCP group	GenBank accession number
2000	☼	ehvOTU9	I	DQ084392
2000/2003	▲	ehvOTU3	II	AY144376[3]
2000	*	ehvOTU10	III	DQ084393
2000/2003	♦	ehvOTU1	IV	AY144374[3]
2000/2003	□	ehvOTU5	V	AY144378[3]
2000	○	ehvOTU7	VI	AY144380[3]
2000/2003	▪	ehvOTU4	VII	AY144377[3]
2000	▼	ehvOTU2	VIII	AY144375[3]
2003	■	ehvOTU11	IX	DQ084394
2003	◙	ehvOTU16	X	DQ084399

Table 5.1. List of *E. huxleyi* and *E. huxleyi*-virus genotypes found in this study and GenBank references for their sequence data. [1]284-287 bp fragments from the GPA gene encoding a protein with calcium-binding motifs. [2]99 bp fragments from a gene encoding the putative major capsid protein. [3]GenBank accession numbers published previously to this study. The same DGGE bands and their corresponding sequences were also detected by Schroeder et al. (2003).

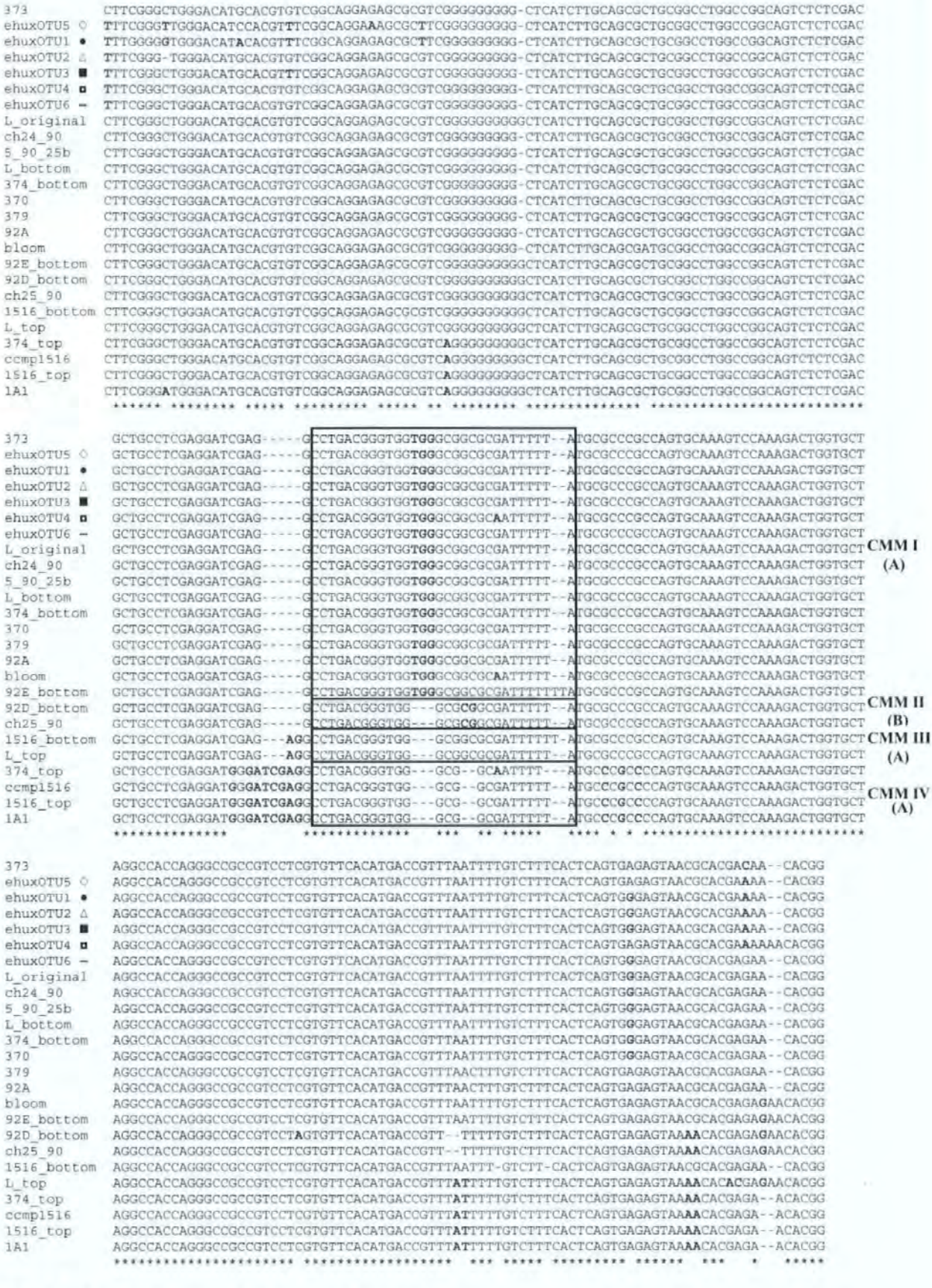

Fig. 5.4. Clustal alignment of *E. huxleyi* DGGE band sequences produced from the two mesocosm studies (designated 'ehuxOTUs') (Table 5.1) and from isolates in culture (Schroeder et al. 2005). The box indicates the region within the sequences that allows differentiating between genotypes (CMMs). A or B indicates CMM morphotype (Schroeder et al. 2005) Variations in sequence composition are highlighted in bold.

Excision, sequencing and alignment using ClustalW confirmed the diversity of bands (Figure 5.5) and revealed that single bands with different migration rates corresponded to different *E. huxleyi*-specific virus genotypes.

MCP sequence data and GenBank accession numbers of the EhV genotypes found in this study are summarized in Table 5.1. Four out of the 8 genotypes from the 2000 mesocosm, ehvOTU1♦, ehvOTU3▲, ehvOTU4▪ and ehvOTU5□, were also detected in the 2003 mesocosm studies. The rest of the genotypes were detected only during the 2000 (ehvOTU2▼, ehvOTU7○, ehvOTU9☼ and ehvOTU10*) or the 2003 (ehvOTU11■ and ehvOTU16◙) mesocosms (Table 5.1). Genotype ehvOTU1♦ was identical to the sequence obtained from the EhV-163 strain, which was isolated during the mesocosm experiment in 2000 (Schroeder et al. 2002). In addition, two of the genotypes detected only during the 2000 mesocosm, ehvOTU9☼ and ehvOTU10*, had the same MCP sequence as the EhV-203 and EhV-207 isolates from the English Channel (Schroeder et al. 2002) respectively (Figure 5.5).

DGGEs, conducted in triplicate, produced the same band pattern of *E. huxleyi* and *E. huxleyi*-specific viruses among the replicate enclosures (results not shown). The results presented here are representative of all the enclosures in the experiment.

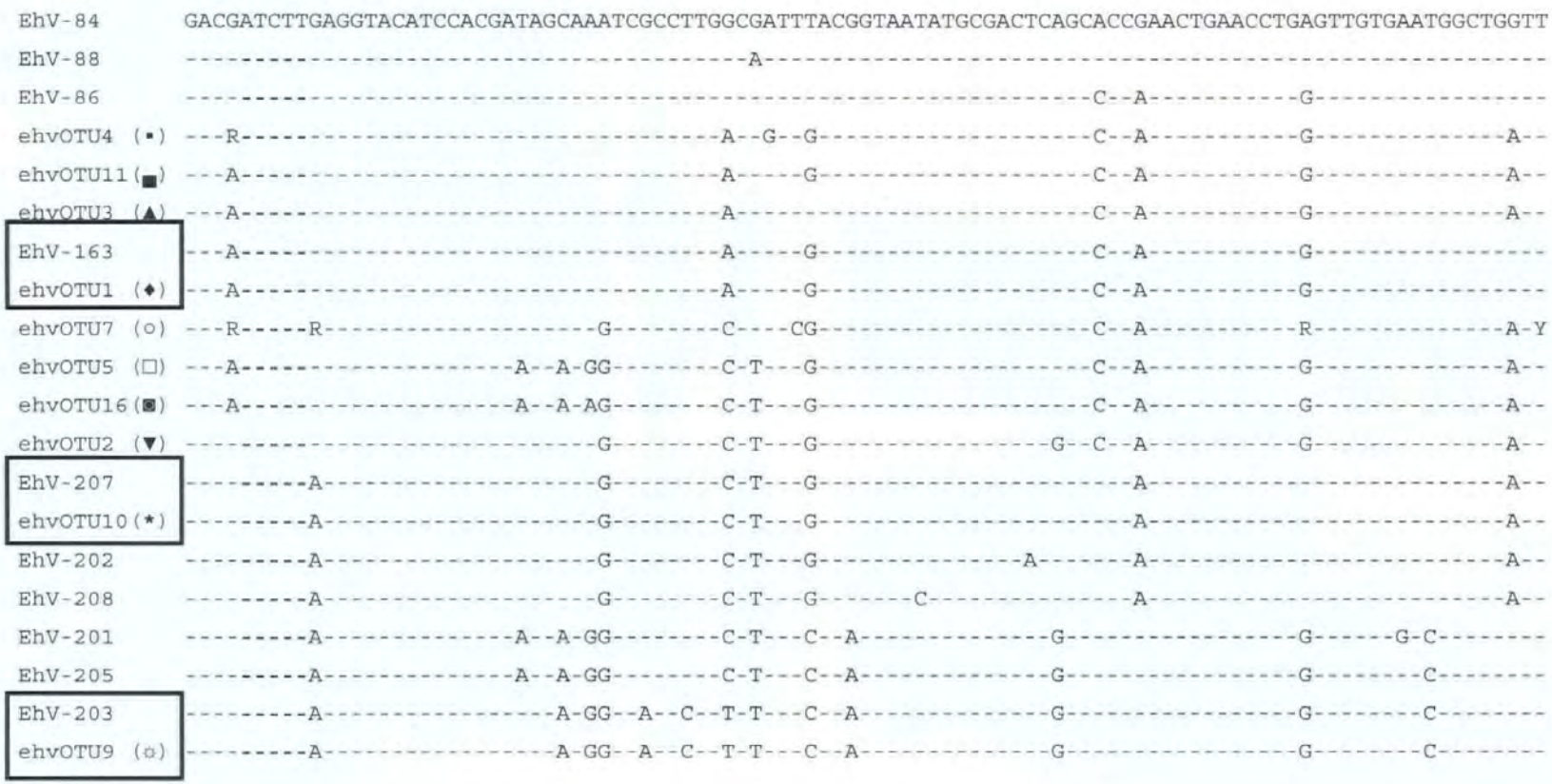

Fig. 5.5. Clustal alignment showing *E. huxleyi*-specific virus genotype richness ('ehvOTUs') during both mesocosm experiments based on the amplified MCP (see Table 5.1). Sequences from the known *E. huxleyi*-specific virus isolates used as DGGE standards are also included (Schroeder et al. 2002). Identical sequences are grouped together with boxes. Conserved bases are identified as a dash underneath the corresponding base from EhV84.

5.4. Discussion

This study examined and compared the succession and termination of two analogous induced blooms of *E. huxleyi* separated in time by 3 years. The use of the molecular markers GPA and MCP (Schroeder et al. 2002, Schroeder et al. 2003, Schroeder et al. 2005) allowed the resolution of genetic variation among *E. huxleyi* and EhVs respectively. The results from this investigation revealed not only a genetically rich *E. huxleyi* and EhV community, but also identical *E. huxleyi* genotypic composition and the same shift in EhV genotypes during the bloom and post-bloom periods in the 2000 and 2003 mesocosm studies. AFC data gave an overview of the progression in numbers of *E. huxleyi* and EhV populations (Figures 5.2 and 5.3). The increase in virus numbers as more hosts lysed revealed a typical lytic propagation strategy for this virus, and confirms what we already know from laboratory studies (Schroeder et al. 2002, Wilson et al. 2002b).

Only alleles correlated with *E. huxleyi* morphotype A were detected during both mesocosm experiments. This is in accordance with what previously reported by Båtvik et al. (1997) and Young (1994) who recorded only morphotype A coccoliths on samples collected from enclosures during similar mesocosm experiments in the same area between 1991 and 1994.

The development of the same *E. huxleyi* community and the same succession of the dominant virus genotypes in both years, despite some differences in bloom dynamics (i.e. cell numbers and duration of the lag, exponential and termination phases), is not likely to be a bias of the nutrient addition in the enclosures. Schroeder et al. (2003) observed that during the 2000 mesocosm the same viruses were responsible for the termination of the bloom also in enclosures that were either P- or N-depleted. Although they could not determine the genotypic composition of the *E. huxleyi* community in those enclosures, host-range specificity indicated the same viruses dominated despite the nutrient regime.

It is clear from the DGGE profiles produced prior to the onset of the bloom that a range of virus genotypes was present in the water column. It is likely that those viruses are remnants of previous bloom-lysis events. Detection of a diverse population of remnant viruses prior to the onset of the bloom indicates that they can remain in the water column long after their specific host(s) has 'disappeared'. However, our detection methods do not necessarily mean that they are still viable (Wommack et al. 1996). If a virus that is able to infect the dominant *E. huxleyi* genotype(s) is present during a bloom event, a very large part of the host assemblage could be infected and 'removed'. This would allow other *E. huxleyi* genotypes not susceptible to the, now, dominant viruses to occupy the niche, and therefore would determine the succession of different host genotypes and the subsequent production of new viral genotypes in the fjord, as described in the 'kill the winner' model (Thingstad 2000). Similar patterns in genetic succession were described in the Gulf of Aqaba, Red Sea. Changes in abundance and genetic diversity of the marine picophytoplankton *Synechococcus*, over an annual cycle, were determined by interactions with co-occurring cyanophages (Mühling et al. 2005) proving that virus infection can play an important role in determining the succession of *Synechococcus* genotypes.

The fact that we observed 'identical' events in 2000 and 2003 at the same time of the year indicates a periodical annual succession of identical *E. huxleyi* genotypes, which in turn would determine the viral genotypic succession. Our DGGE results did not show variation of dominant *E. huxleyi* genotypes throughout each mesocosm experiment. This suggests a genetically stable *E. huxleyi* population exists in this fjordic system and these dominant strains have an efficient survival strategy between blooms. The stability of *E. huxleyi* populations in 2000 and 2003 was reflected by the identical population shifts of the dominant virus genotypes between the two studies (Figures 5.2 and 5.3). This was despite two different genotypic virus profiles prior to the onset of the bloom.

Metaphorically, viruses seemed to be jostling for position until the appropriate host *E. huxleyi* strains started to increase in numbers. The fact that diverse populations of EhVs are present in the water column poses two questions: how do the same viruses persist and remain viable in the marine environment throughout the years even at times when the host numbers are low? And what *E. huxleyi* strains do they infect? For the first question, one hypothesis is that they sink out into deep water layers or sediments, where they can escape destruction by solar radiation (Suttle & Chen 1992, Weinbauer et al. 1999). Yet the ecological weight of algal virus reservoirs in sediments and deep waters and the importance of mixing in transferring viruses to surface water layers are currently subject to speculation. Another hypothesis could be that if *E. huxleyi* numbers do not completely disappear in the fjord, a low virus production could be maintained all year around. Mühling et al. (2005) observed that *Synechococcus* numbers always exceeded the density required for persistence of the phages that infect them (Suttle & Chan 1994, Mann 2003) in the Gulf of Aqaba. The second question could probably be answered after a much more comprehensive study comprising temporal and spatial sampling regimes to determine if more diverse *E. huxleyi* populations are indeed present. We know from culture studies that a broad genotypic diversity of *E. huxleyi* exists (Medlin et al. 1996, Iglesias-Rodriguez et al. 2002, Schroeder et al. 2005). In Chapter 6 the *E. huxleyi*/EhV dynamics in the North Sea were investigated and revealed a broad range of *E. huxleyi* genotypes and genotypic shifts were observed in that Lagrangian study.

Finally, it is noteworthy that ehvOTU9☼ and ehvOTU10* had identical MCP sequences to EhV strains EhV-203 and EhV-207 respectively (Figure 5.5), both of which were isolated in the English Channel in 2001 (Schroeder et al. 2002).

5.5. Conclusions

In summary, this study indicates, for the first time, the effectiveness of the GPA gene (Schroeder et al. 2005) as a molecular marker to differentiate *E. huxleyi* genotypes within the A and B morphotypes in natural communities.

Our findings also provide new insights of the progression and structuring, at a molecular level, of natural blooms of the key species *E. huxleyi*. Results suggest that *E. huxleyi* blooms may occur every year at the study site in a highly conserved manner with the same *E. huxleyi* and EhV genotypes probably re-occurring in annual cycles.

CHAPTER SIX

Dynamics and genotypic composition of *Emiliania huxleyi* and their co-occurring viruses during a phytoplankton bloom in the North Sea

6. Dynamics and genotypic composition of *Emiliania huxleyi* and their co-occurring viruses during a phytoplankton bloom in the North Sea

6.1. Introduction

Vast *E. huxleyi* blooms occur during spring and summer in offshore, coastal and oceanic waters at mid-latitudes (45 to 55 °N) (Ackleson et al. 1988). Indeed, coccolithophore blooms are seasonally predictable in certain areas including the North Sea (Holligan et al. 1983). The study of natural blooms is indispensable for determining biodiversity (Widdicombe et al. 2002), to clarify the importance of viruses as mortality agents (Brussaard et al. 1996b), to determine community dynamics through vertical profiles (Wilson et al. 2002b) and to quantify the processes that influence the biogeochemical cycling in surface waters (Turner et al. 1988, Holligan et al. 1993, Malin et al. 1993) during the progression of an *E. huxleyi* bloom.

An extraordinary opportunity to investigate all the aspects above, among others, was given during a multidisciplinary cruise that followed the progression of a developing *E. huxleyi*-rich phytoplankton bloom in a programme called 'DImethyl Sulphide biogeochemistry within a COccolithophore bloom (DISCO)', in the northern North Sea in June 1999. The study comprised analyses of the biological, optical and physical properties of the patch of water containing the bloom as well as studies of sulphur compounds, nutrients, and other chemical compounds cycling. In addition, the role of viruses, bacteria, phytoplankton and zooplankton, the dynamics of primary production, plankton respiration, grazing and sedimentation were investigated in relation to the biogeochemical cycling of dimethyl sulphide (DMS) (for an overview see Burkill et al. (2002)).

Between the 18th and 23rd June (lagrangian period of the study) the water column could be divided into 3 layers (surface, subsurface and bottom) based on the 10.5 °C and 8.5 °C

isotherms. A patch of warmer, lower salinity surface water entered the sampling area from the 23rd June, forming a new surface layer above the 11.5 °C isotherm (Figure 6.1) (Wilson et al. 2002a). The new patch of fresher water originated from the direction of the Norwegian coast. Further details of the physical structure of the study site were described by Burkill et al. (2002).

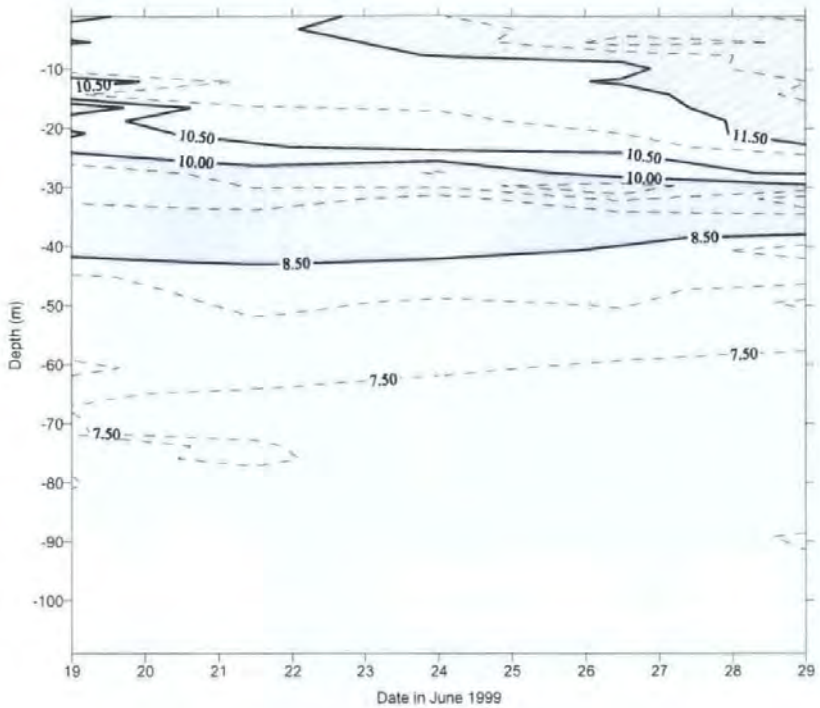

Fig. 6.1. Contour plot of temperature throughout the period of study. Warm surface, surface, subsurface and deep thermal layers are defined according to the 11.5 °C, 10 °C and 8.5 °C isotherms respectively. (Wilson et al. 2002a).

As part of the DISCO cruise Wilson et al. (2002a) investigated the *E. huxleyi* and *E. huxleyi*-specific virus (EhV) dynamics by examining their concentrations through vertical profiles by analytical flow cytometry (AFC) (Figure 6.2). Their aim was to obtain high-intensity sampling data of *E. huxleyi* and EhVs to gain information on the temporal and spatial dynamics in an open-water site. They could easily discriminate *E. huxleyi* and EhV populations from other phytoplankton and virus groups respectively due to their characteristic AFC signatures (Wilson et al. 2002a). Wilson et al. (2002a) found that *E. huxleyi* numbers were higher in surface water, becoming undetectable below

approximately 40-45 m depth, which corresponded to the 8.5 °C isotherm. Through out the lagrangian survey there was first an increase in *E. huxleyi* numbers (18th to 21st June), and then a decrease towards the end of this first part of the study (Figure 6.2A). The highest concentrations were observed in surface water immediately after the influx of the warmer patch of water on the 24th June then gradually decreased between the 27th and 29th June (Figure 6.2A). During those last 3 days *E. huxleyi* concentrations increased at depths of between 30-40 m. Concurrently with the increase of *E. huxleyi* during the lagrangian period there was a net decrease in EhV concentrations in the surface. Following the influx of warmer surface waters (23rd June) the virus group reached maximum concentrations (24-25th June) then decreased towards the end of the study (Figure 6.2B). There was no apparent change in EhV concentrations in the sub-surface (30-40 m) peak of *E. huxleyi* from 27-29 June.

In the current study we have gone a step further in the investigation of the *E. huxleyi* and their co-occurring virus dynamics by assessing changes in their genotypic composition during the bloom progression using specific primers. We have exploited the variations found in a gene encoding a protein with calcium-binding motifs (GPA) in *E. huxleyi* (Schroeder et al. 2005) and in the major capsid protein gene (MCP) of the *E. huxleyi*-specific viruses (Schroeder et al. 2002, Schroeder et al. 2003) to analyze samples taken during the cruise using denaturing gradient gel electrophoresis and sequencing analysis.

A

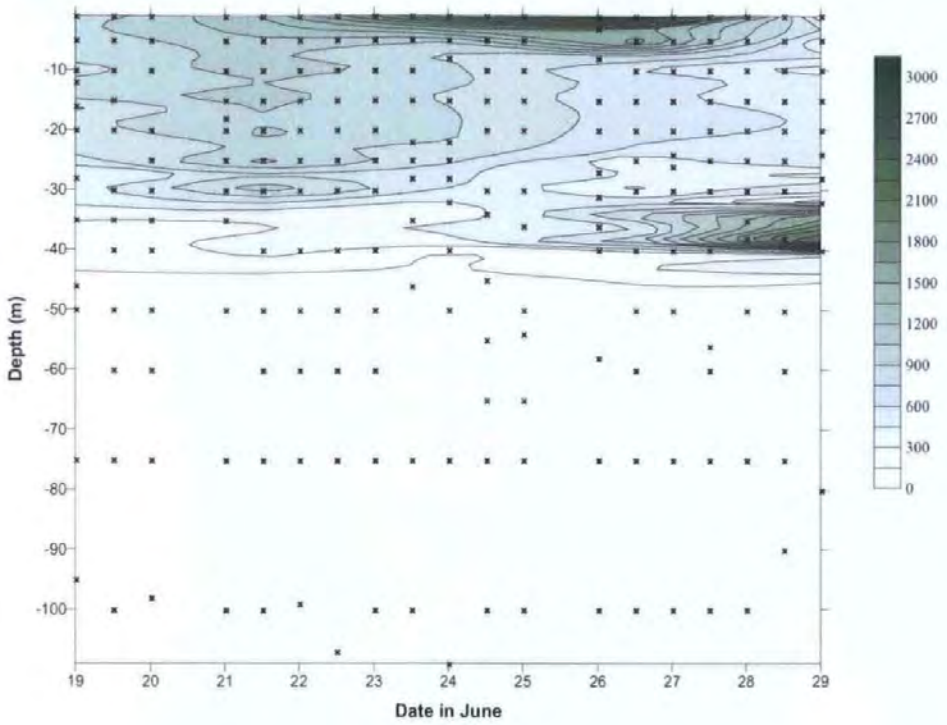

B

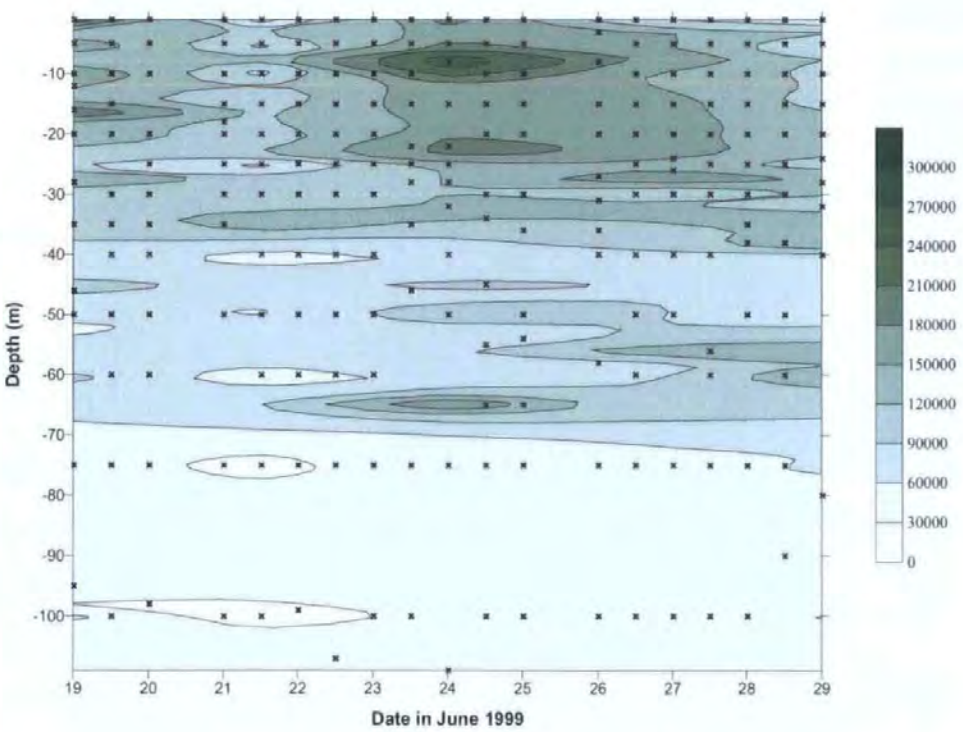

Fig. 6.2. Contour plot of *E. huxleyi* concentrations (cells ml^{-1}) **(A)** and EhV concentrations (virus particles ml^{-1}) **(B)**, as determined by AFC, throughout the course of the study. Crosses indicate the depth at which samples were collected. (Wilson et al. 2002a).

6.2. Material and methods

6.2.1. Study site

The samples were collected during a research cruise aboard the RRS-Discovery, between the 5th and 29th of June 1999, that followed a coccolithophore bloom originally located at 59 °N 01 °E in the North Sea. The experimental design and the AFC analysis are as described by Wilson et al. (2002a). Briefly, the cruise was split into three parts, an initial box survey to identify the bloom combining satellite imagery and measurements of *E. huxleyi* concentrations by AFC; a lagrangian time-series study was then conducted between the 18th and 23rd of June, when the selected patch of water was traced with sulphur hexafluoride (SF_6) using methods described previously (Law et al. 1998); and a final survey of the bloom between the 24th and 29th of June.

6.2.2. Sample collection

Seawater was collected daily from a depth profile, down to approximately 100 m, typically just after midnight and midday, using a stainless-steel CTD sampler system equipped with 12 Niskin bottles (30 L). Sampling for total genomic DNA preparations was conducted by William H. Wilson. One litre of seawater from each depth samples was filtered onto 0.45 μm pore size Supor-450 47 mm diameter filters (PALL Corp). The focus of the study was to look at viruses in infected cells which will be held on a 0.45 μm filter; however, the chances are that the filters would also retain some free-floating viruses upon clogging of the filter pores and viruses attached to other particles in the water column. The filters were transferred to 2 ml cryotubes, snap frozen in liquid nitrogen and stored at -20 °C until further processing (sampling was conducted by William H. Wilson). For virus and host enumeration using AFC, sub-samples were also collected from each depth sample as described by Wilson et al. (2002a).

6.2.3. DNA isolation

Genomic DNA was isolated from the particulate matter retained on the SUPOR filters using an adapted phenol/chloroform method (Section 2.2.11.2).

6.2.4. Polymerase Chain Reaction (PCR) amplification, DGGE and DNA sequencing

E. huxleyi and *E. huxleyi*-specific virus genotypic richness during this phytoplankton bloom were determined by nested PCR, DGGE and sequencing analysis as described in Chapter 5, Sections 5.2.3 and 5.2.4. GPA and MCP sequences from the North Sea were aligned together with the GPA and MCP sequences indicated in Chapter 5 (see Tables 2.3, 2.4 and 5.2 for GenBank accession numbers).

.

6.3. Results

6.3.1. EhV richness

DGGE analysis of virus MCP fragments revealed a diverse and dynamic EhV community throughout the period of study (Figure 6.3). Most of the DNA preparations from filtered seawater amplified good clean EhV-specific MCP products by PCR (results not shown) and bands on DGGE gels were easily defined. MCP bands represent different genotypes, each genotype represents a different virus (Schroeder et al. 2002, Schroeder et al. 2003). The symbols, abbreviations and GenBank accession numbers of the MCP bands and their sequences are summarised in Table 6.1.

DGGE gels showed a stable EhV community composition at all depths between the 18th - 23rd June (Figure 6.3). During this period 2 bands (ehvOTU3 (**a**) and ehvOTU1 (**b**)) were dominant in samples from all depths. The intensity of these 2 bands increased towards the 21st June in the upper 40 m and then decreased on following days. Low intensity bands during the same period had a more variable pattern and were not always easily visualised on the gels. An example of this is ehvOTU20 (**d**).

With the entrance of the new surface patch of water from midnight on the 23rd June, a clear change in the genotypic composition of the EhV community was observed, which developed into a broader range of higher intensity bands. The first obvious change after the influx of the warm water patch was the domination of new single band ehvOTU21 (**e**) in the upper 60 m of the water column (Figure 6.3; 23rd June - midnight) which prevailed almost to the end of the study (ehvOTU21 (**e**) was not detectable between 5 and 24 m on the last sampling day - 29th June). Notably, the bands that previously dominated, ehvOTU3 (**a**) and ehvOTU1 (**b**), no longer predominated in the surface 20 m from the midnight of the 23rd through to the 24th June; but reappeared back in the surface on the 25th June.

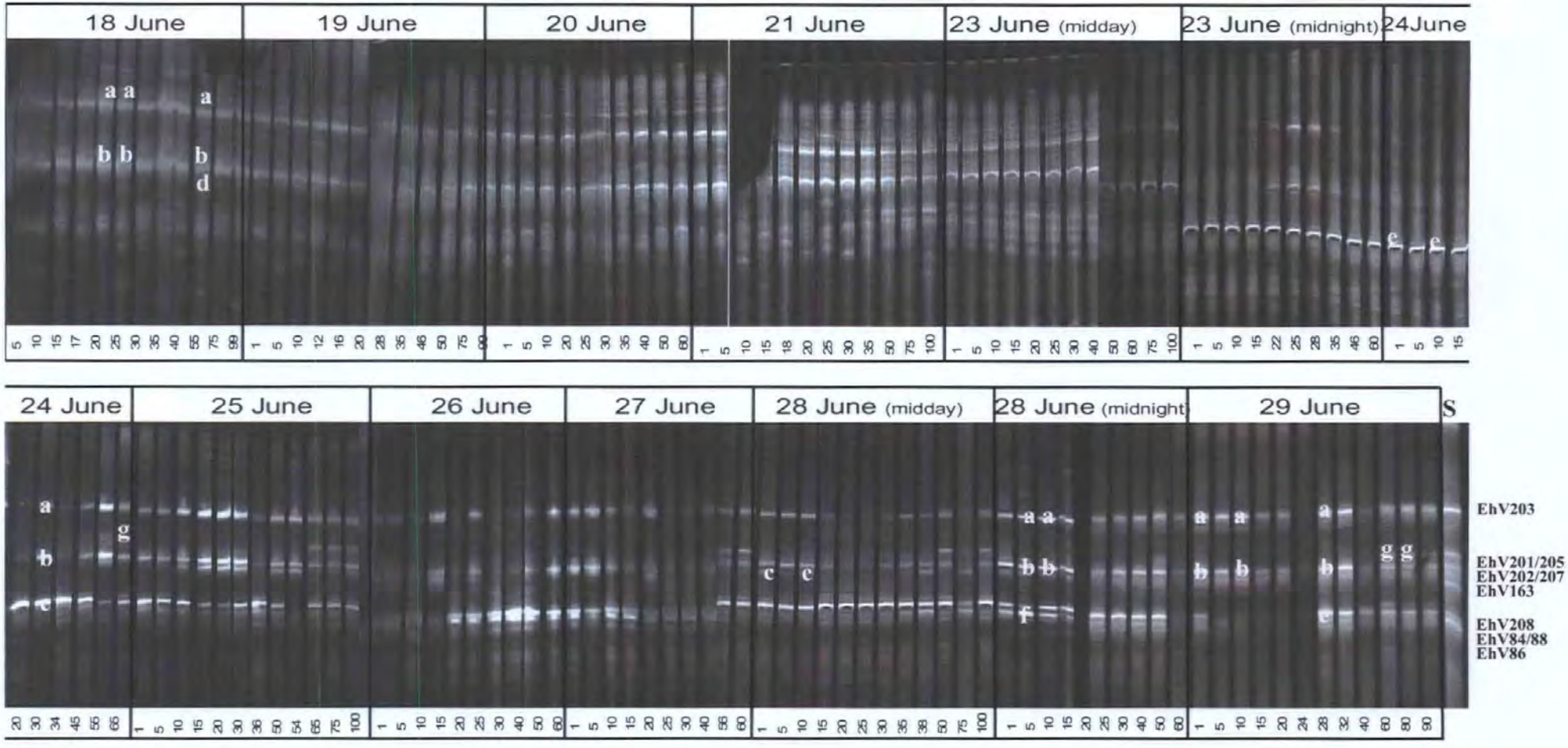

Fig. 6.3. DGGE gels of PCR fragments amplified with MCP primers for analysis of EhV richness. Different bands represent different genotypes. Date (in year 1999) and depth (in meters) of sample collection are indicated at the top and the bottom of the gel images respectively. Letters indicate the bands excised for sequencing, same letters indicate identical nucleotide sequence (see table 2). Standards (S), bands of known EhV isolates.

E. huxleyi-specific viruses			
DGGE band	MCP sequence[1]	Genotype MCP group	GenBank accession number
a	ehvOTU3	II	AY144376[2]
b	ehvOTU1	IV	AY144374[2]
c	ehvOTU5	V	AY144378[2]
d	ehvOTU20	XI	DQ084403
e	ehvOTU21	XII	DQ084404
f	ehvOTU22	XIII	DQ084406
g	Not available	undetermined	-
E. huxleyi			
DGGE band	GPA sequence[3]	Genotype CMM group	GenBank accession number
A	ehuxOTU7	III	DQ084407
B	ehuxOTU8	IV	DQ084408
C	ehuxOTU9	IV	DQ084409
D	ehuxOTU10	III	DQ084410
E	ehuxOTU11	IV	DQ084411
F	ehuxOTU12	IV	DQ084412
G	ehuxOTU13	II	DQ084413
H	ehuxOTU14	IV	DQ084414
I	ehuxOTU15	V	DQ084415
J	ehuxOTU17	I	DQ084417
K	ehuxOTU18	III	DQ084418
L	ehuxOTU16	I	DQ084416

Table 6.1. List of *E. huxleyi* and *E. huxleyi*-virus genotypes found in this study and GenBank references for their sequence data. [1]99 bp fragments from a gene encoding the putative major capsid protein. [2]GenBank accession numbers published previously to this study. The same DGGE bands and their corresponding sequences were also detected by Schroeder et al. (2003). [3]284-287 bp fragments from the GPA gene encoding a protein with calcium-binding motifs.

From the 25th June, at least 6 bands had higher intensity: ehvOTU3 (**a**) and ehvOTU1 (**b**) which were detected from surface to bottom layers; ehvOTU21 (**e**) which became dominant after the 23rd June; ehv (**g**) (MCP sequence not available), which was only

detected in samples collected below 50 m; ehvOTU5 (**c**), which was typically found in the surface 50 m; and ehvOTU22 (**f**), which followed a more irregular distribution pattern (Figure 6.3).

The alignment of virus sequences from DGGE bands (Figure 6.4) showed that 5 out of the 6 EhV genotypes detected during the bloom were identical in the amplified region to some of the viruses from English Channel isolates (Schroeder et al. 2002, Wilson et al. 2002b) and from a Norwegian mesocosm study (Schroeder et al. 2003): ehvOTU21 (**e**) was identical to EhV-84; ehvOTU22 (**f**) was identical to EhV-86; and ehvOTU1 (**b**), ehvOTU3 (**a**) and ehvOTU5 (**c**) were detected in this study and in the samples from the Norwegian mesocosm studies. The genotype ehvOTU1 (**b**) was the same as EhV-163. Genotype ehvOTU20 (**d**) had not match with any of the viruses from previous studies.

6.3.2. *E. huxleyi* richness

DGGE analysis of PCR products amplified with the specific primers for the GPA gene revealed a broad variety of *E. huxleyi* bands (Figure 6.5 and 6.6). Changes in presence/absence of bands were observed both in time and depth. Sequencing of those bands showed that they represent different alleles (Figure 6.7). Since *E. huxleyi* strains can contain more than one allele (Schroeder et al. 2005) the number of different bands or genotypes revealed in this study indicates the number of different alleles present instead of quantitative richness of *E. huxleyi* strains. Table 6.1 summarizes the symbols, abbreviations and GenBank accession numbers given to each of the GPA bands excised from the DGGE gels. The time/depth temporal profile for *E. huxleyi* allelic richness was partial since we were not able to amplify the GPA gene from all the depth samples.
To facilitate the interpretation of the DGGE gels we divided the samples into two layers, from surface to 35 m depth (Figure 6.6A 'surface') and from 38 m to 100 m depth (Figure 6.6B 'deep'). The 35 m depth threshold is just above the 8.5 °C isotherm (Figure 6.1) and

at this depth *E. huxleyi* is just starting to reach the limit of detection by AFC analysis, indicative of very low cell concentrations in the deep layer.

In general, a similar profile of *E. huxleyi* alleles were observed throughout the water column during the initial period of the study from 18th – 26th June, with a few alleles being more or less abundant in certain samples (Figures 6.5 and 6.6A). This level of variation is to be expected since only 2 out of the 17 samples analysed were taken at the same depth. Through out this period, in the deep layer, DGGE profiles were most similar to those observed in the surface layer on the 24th June (Figure 6.6), specifically the noticeable common encircled bands in Figure 6.6. The *E. huxleyi* community composition changed significantly from 27th June (Figure 6.5). In the surface layer, a more irregular band profile was observed during the 27th-28th June period (Figure 6.6A). The combination of DGGE (Figure 6.5) and sequencing analysis (Figure 6.7) of excised bands revealed the presence of at least 12 different *E. huxleyi* alleles between the 27th and 29th June. The alignment of GPA-DGGE bands (Figure 6.7) revealed that the *E. huxleyi* community during this bloom contained alleles that could be separated into five different genotypes of the A and B *E. huxleyi* morphotypes. Four of those genotypes (CMM I to IV) were previously characterised by Schroeder et al. (2005). We were not able to determine whether CMM V belonged to A or B *E. huxleyi* morphotype.

Fig. 6.4. Multiple sequence alignment of the EhV-MCP fragments produced in this study (**ehvOTUs**). The letters next to the **ehuxOTU** label correspond to the band letters in Fig. 6.3. Conserved bases are identified as a dash underneath the corresponding base from EhV84. Sequences from the mesocosm experiments (ehvOTUs) and known EhV isolates used as DGGE standards are also included. Identical sequences are grouped together with boxes. ehvOTU1, ehvOTU3 and ehvOTU5 were detected during both mesocosm experiments and this study.

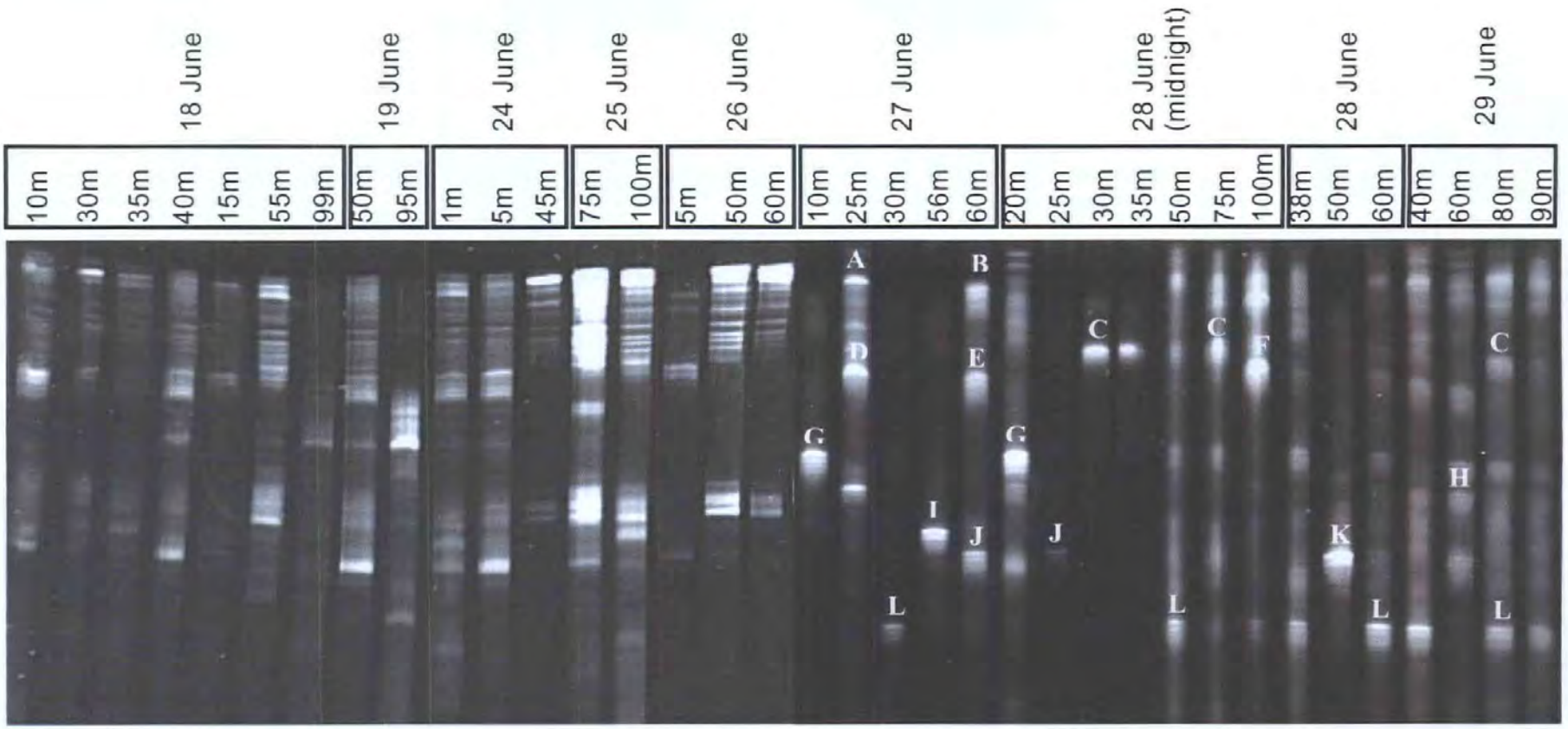

Fig. 6.5. DGGE gels of PCR fragments amplified with GPA primers for analysis of *E. huxleyi* diversity. Different bands represent different alleles. Date (in year 1999) and depth (in meters) of sample collection are indicated on top of the gels images. Letters indicate the bands excised for sequencing, same letters indicate identical nucleotide sequence (see table 6.2).

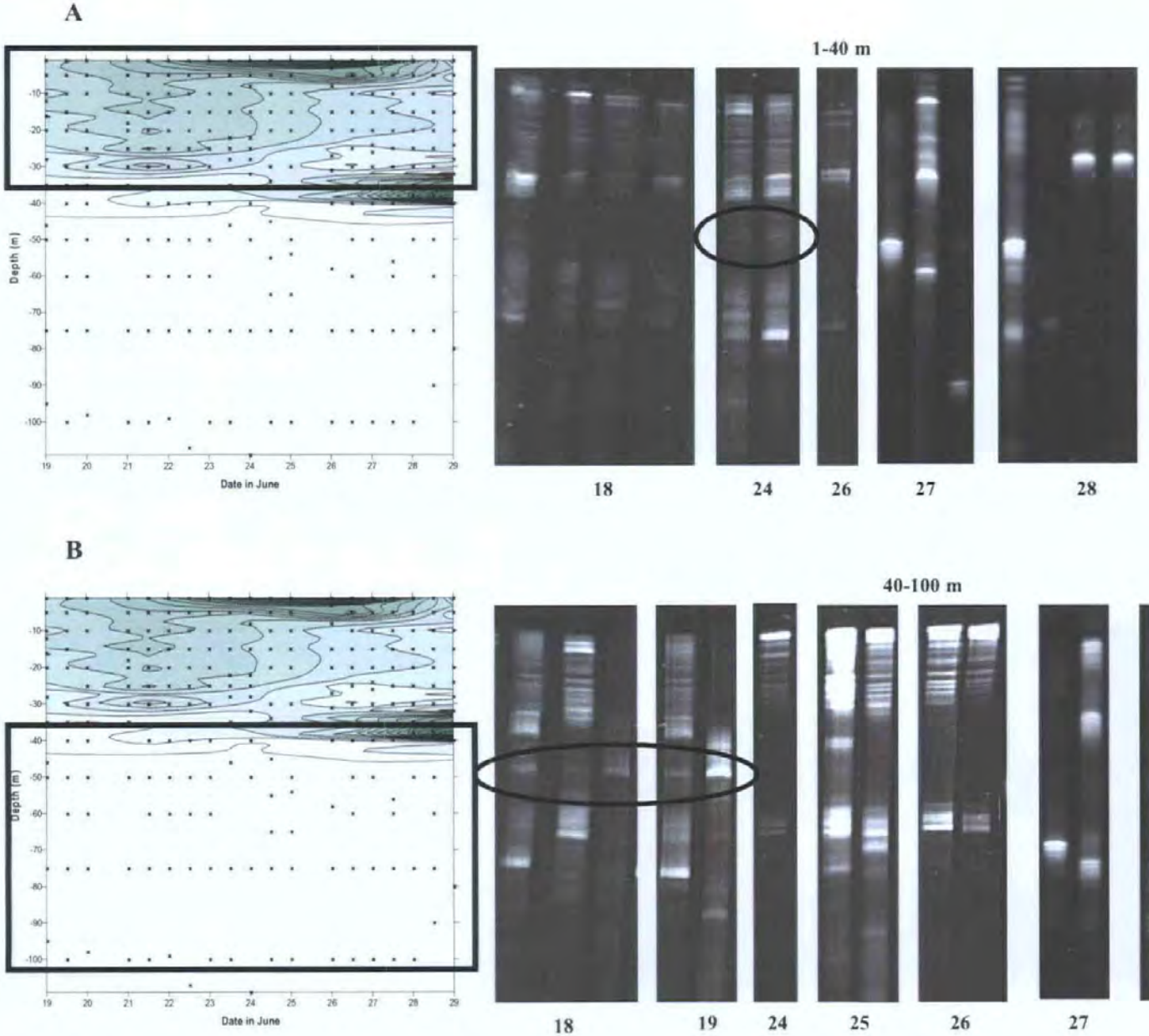

Fig. 6.6. Contour plot of *E. huxleyi* concentrations (cells ml^{-1}) and DGGE gels of GPA-PCR fragments from samples collected between 1-35 m depth (surface) **(A)** and 38-100 m depth (deep) **(B)**. Date (in June 1999) of sample collection is indicated below the gel images. The ovals mark a distinctive band only detectable below 40 m depth at the beginning of the study and at surface on 24th June.

Fig. 6.7. Clustal alignment of partial *E. huxleyi* sequences produced from excised DGGE bands from both mesocosms (**ehuxOTUs**) and from isolates in culture (Schroeder et al. 2005). Letters next to the **ehuxOTU** label indicate the band in Figure 6.3. The box indicates the region within the sequences that allows differentiating between genotypes (CMMs). A or B indicates CMM morphotype. Variations in sequence composition are highlighted in bold

6.4. Discussion

In their original report on virus-host dynamics of this study site in the North Sea, Wilson et al. (2002a) suggested that large viruses (EhVs) were actively infecting hosts. However, EhV concentrations were lower than expected, grazing rates were relatively high (Archer et al. 2002) and viruses showed no evidence of influencing DMS/DMSP production (Wilson et al. 2002a) hence, the implication was that viruses played a minor role in the dynamics of this coccolithophore-dominated phytoplankton bloom. Molecular data presented here, from samples collected during the same bloom, reveal extremely active virus-host dynamics concealed by what appears to be relatively uninteresting numerical population data. The sensitivity of PCR has allowed us to explore these dynamics in much greater detail, essentially revealing changing populations of viruses and their hosts beyond the limits of detection for AFC. This is the first time such a comprehensive temporal and spatial analysis of *E. huxleyi* and their corresponding viruses (or indeed any host-virus system) has been presented at the molecular level and during the progression of a natural coccolithophore bloom.

Seawater samples collected during this study provided an ideal opportunity to examine the host and virus dynamics during the progression of a natural *E. huxleyi*-rich phytoplankton bloom. AFC data (Figure 6.2) provided numerical population progression of *E. huxleyi* and their co-occurring viruses (EhVs), whilst the use of the molecular markers GPA and MCP revealed temporal and spatial variability of *E. huxleyi* and EhV genotypes respectively during the course of this naturally occurring bloom in the North Sea (Figures 6.3 and 6.5). We exploited heterogeneity in GPA and MCP using DGGE and sequencing analysis. While the flow cytometric analysis only detected *E. huxleyi* cells up to 45 m deep, DGGE revealed the presence of different *E. huxleyi* alleles as deep as 100m.

The results indicate that during the study period the dominating *E. huxleyi* genotypic profile changed significantly at least three times. The combination of DGGE and AFC (Wilson et al. 2002a) data showed the progression and termination of a diverse dominating genotypic *E. huxleyi* community in the surface layer between 18th and 23rd June (Figures 6.5 and 6.6A). The concurrent decrease followed by an increase in EhV concentrations in the surface during the same period suggests an active infection control process of *E. huxleyi* followed by the release of EhV progeny (Figure 6.2). Subsequent DGGE analysis of this EhV population showed that during this period the same two dominant EhV genotypes dominated until the entrance of the patch of warm surface water (23rd June) (Figures 6.3 and 6.4) indicating that those were the genotypes that controlled the initial dominating *E. huxleyi* community (Figure 6.5). It is, however, important to point out the qualitative nature of PCR amplification and limitations in DGGE resolution. Truly quantitative information using molecular methods can only be obtained if DNA extraction efficiency and biases in the PCR step are under experimental control. This is not feasible when analysing environmental samples containing an unknown amount of cells and virus particles as well as inhibitors. Yet, the variations in band intensity of a particular genotype compared to another from day to day or between depths may well suggest changes in relative abundance of certain genotypes in the water samples as the bloom developed rather than differences in DNA extraction efficiency or preferential amplification of some genotypes over anothers. Further investigations would benefit from the use of internal standards in the DNA extraction, PCR and DGGE steps to allow describing, at least more reliably, relative changes in abundance and diversity among samples, as described by Petersen and Dahllöf (2005).

Intriguingly, the remnants of the declining genotypic *E. huxleyi* community, i.e. similar *E. huxleyi* alleles, could be seen in the deep layer between the 24th and 26th June (Figure 6.6B) suggesting that *E. huxleyi* cells sink to deeper water as the bloom declines. In addition, we

hypothesize that the *E. huxleyi* allele revealed by DGGE on 18th-19th June at depths below 40 m (marked by an oval in Figure 6.6B) revealed the presence of remnant *E. huxleyi* genotypes from a previous bloom event. The presence of the same band at the surface on 24th June (Figure 6.6) can be explained by either the mixing caused by the warm surface water influx or entry of *E. huxleyi* strains with similar genotypes with the warm water. A combination of both scenarios is more plausible as the overall *E. huxleyi* genotypic profile remained static throughout this mixing period, while the entry of the warm surface water brought an additional dominant EhV genotype (ehvOTU21, Figure 6.3). Since the *E. huxleyi* genotypes were either senescent or actively being infected by a variety of dominating EhVs (24th – 26th June, Figure 6.3), this community disappeared quite rapidly (deep layer, 25th & 26th June, Figure 6.6).

Infection and 'removal' of a large part of the dominant *E. huxleyi* assemblage in the surface layers was followed by the development of a new *E. huxleyi* community (27th-28th midnight, June). If not entirely, we surmise that the now dominant *E. huxleyi* alleles will have been brought in by the patch of warmer surface water but were either resistant to or too few in number to be controlled by the EhV genotypes that killed the earlier two communities. However, as this *E. huxleyi* community was starting to develop it in turn was being controlled by a different EhV community (28th -29th June, Figure 6.3). This sinking out or removal of surface *E. huxleyi* genotypes is especially evident here due to the additional sequence data collected for this period. For example, alleles ehuxOTU9 (C) and ehuxOTU16 (L) were first detected in the 30 m surface layer on the 28th and 27th June, respectively, and again later in the 80 m deep layer on the 29th June.

The added insight given by this molecular analysis of DISCO samples revealed that the high concentrations of *E. huxleyi* found towards the end of the study between 30 to 40 m depth (Figure 6.2) were most probably the consequence of accumulation above the 8.5 °C

isotherm of already infected *E. huxleyi* cells pushed down by the warm surface water influx. The warm patch of water moved the 10.5 °C isotherm down to 30 m depth between 27th and 29th June. Additionally, the DGGE profile showed at these depths the same alleles found in surface before, supporting the idea of the concentration of the previous community above the 8.5 °C isotherm.

DGGE revealed 6 intense virus MCP bands during the warm surface water influx that probably controlled the *E. huxleyi* community in this patch. Virus ehvOTU21 (**e**) (Figure 6.3) came into the study site with the patch of warm surface water, probably among some other less dominant ones. However, the persistence in the water column of ehvOTU3 (**a**) and ehvOTU1 (**b**) until the last day of study (Figure 6.3) seems to indicate that the remaining viruses from previous lysis events also infected and controlled the incoming *E. huxleyi* community.

Low impact of *E. huxleyi* and EhVs on DMSP production was recorded during the DISCO study (Archer et al. 2002). However, Steinke et al. (2002) measured maximum DMSP lyase activity at approximately 50 m depth on 22nd June, 40 m on 23rd June and 35 m on 24th June, concurrently with the lowest cell numbers recorded for the *E. huxleyi* community that developed during the lagrangian study, suggesting the production of DMSP by dying *E. huxleyi* cells. Yet, the low impact of *E. huxleyi* and EhVs in DMSP production could be explained first by the fact that coccolithophores accounted for less than 30 % of the phytoplankton biomass (Widdicombe et al. 2002). Secondly, different *E. huxleyi* strains are known to have different DMS production rates (Steinke et al. 1998). It might be possible that the dominant strains during the main *E. huxleyi* bloom were not high DMS producers. It may be that the *E. huxleyi* contribution to the standing stocks of DMSP and the importance of EhVs as agents of DMS production were higher after the influx of warm surface water (24th-29th June) when new *E. huxleyi* and EhV communities developed.

However, DMSP and DMS measurements are lacking for this period. We hypothesized that further investigation might allow to establish links between the molecular results presented in this study and sulphur biogeochemical cycles in the sea.

Wilson et al. (2002a) suggested that, since no relationship between viruses and DMSP production was observed during this study in the North Sea, viruses did not play a major role in the developing bloom. However, the use of molecular tools has revealed the importance of viral infection for intraspecific succession of *E. huxleyi* in this environment. On three occasions during this study period, the changing dominating *E. huxleyi* community could be directly correlated with abundance and diversity of *E. huxleyi* specific viruses. Mühling et al. (2005) described similar patterns in genetic succession of the marine picophytoplankton *Synechococcus* in the Gulf of Aqaba, Red Sea. Changes in abundance and genetic diversity, over an annual cycle, were determined by interactions with co-occurring cyanophages (Mühling et al. 2005) proving that virus infection can play an important role in determining the succession of *Synechococcus* genotypes.

Finally, it is remarkable that 5 of the 6 different EhV bands sequenced had identical MCP sequence to some of the sequences from the English Channel isolates from 1999 and 2001 (Schroeder et al. 2002, Wilson et al. 2002b) or the Norwegian samples from 2000 and 2003 (Schroeder et al. 2003, Chapter 5) used as a reference. Viruses that have the same MCP sequence are likely to be the same strain (Schroeder et al. 2002), therefore the findings presented here support the idea of a wide geographical distribution of some EhV strains (Chapter 5). Indeed, host-range experiments showed that several virus isolates from the English Channel and a Norwegian fjord (Schroeder et al. 2002, Wilson et al. 2002b) could infect a range of cultured *E. huxleyi* strains from very distant areas (data not shown).

6.5. Conclusions

In summary, DGGE and sequencing analysis of *E. huxleyi* and EhV groups provided extra information about the dynamics of *E. huxleyi* blooms in open waters. Depth profiles showed 'past, present and future' of the progression and structuring within a natural coccolithophore-dominated bloom. The results from this study revealed a highly dynamic system with a broad *E. huxleyi* and co-occurring virus genotypic community closely linked; while blooms of the same species have been reported to occur every year in a highly conserved manner in a Norwegian fjord, where the same *E. huxleyi* and EhV genotypes re-occurred in annual cycles (Chapter 5). We can conclude that not all the *E. huxleyi* blooms are comprised of the same genotypic communities. Therefore, if separated blooms are different they might have different implications in local ecology, climate and biogeochemistry cycling and production of compounds such as DMS, calcite and carbon. The use of molecular tools, as the ones employed in this study, may be the key to answer unknown questions regarding the processes above.

CHAPTER SEVEN

Differential expression of a putative phosphate permease gene during the infection cycle of an *Emiliania huxleyi*-virus in response to phosphate availability

7. Differential expression of a putative phosphate permease gene during the infection cycle of an *Emiliania huxleyi*-virus in response to phosphate availability

7.1. Introduction

Phosphorus (P) is an essential mineral nutrient for phytoplankton growth and development. P serves a variety of functions that are fundamental to biology; it is a major component of nucleic acids, phospholipids and glycolytic intermediates, it is a constituent of energy transfer reactions and it is a regulator in many signal transduction cascades. Phytoplankton have evolved the ability to utilize P from diverse sources to cope with low nutrient availability in environments such as oligotrophic oceans (Cembella et al. 1984, Antia et al. 1991). Membrane transport proteins are used for nutrient uptake and waste export. Such transporters catalyse the translocation of solutes across the cell membrane, and are essential for the cell's growth and metabolism. However, some aspects regarding the mechanisms of P uptake, transport and utilization by phytoplankton are still uncertain and constitute and ongoing area of study for biological oceanographers.

In the case of the coccolithophorid *Emiliania huxleyi*, P availability can affect the formation and development of blooms (Lessard et al. 2005). Competition experiments in continuous cultures (Riegman et al. 2000) and mesocosm studies (Egge & Heimdal 1994) have shown *E. huxleyi* to become dominant exclusively in communities that were under P control. In fact, Riegman et al. (2000) reported that *E. huxleyi* has the highest affinity of the P-uptake system ever recorded for a phytoplankton species. Under P starvation in culture, *E. huxleyi* responds inducing several phosphate-regulated protein encoding genes involved in P metabolism (Dyhrman & Palenik 2003, Dyhrman et al. 2006) and increasing phosphate uptake rate and alkaline phosphatase activity (Riegman et al. 2000).

There are indications that an unbalanced nutrient regime, particularly low P concentrations, also has an effect on coccolith morphology and size in *E. huxleyi* morphotype A (Young & Westbroek 1991, Young 1994, Båtvik et al. 1997). A link between phosphorus limitation and calcification has been documented in mesocosm and laboratory culture experiments of calcifying *E. huxleyi* cells. For example, P starvation typically increases calcification rates relative to photosynthesis (Paasche 2002).

Previous studies have also investigated the role of nutrients and nutrient limitation in processes of viral infection and control over phytoplankton populations. Bratbak et al. (1993) demonstrated during a mesocosm study that the lack of P inhibited the development of viruses in *E. huxleyi* (EhVs). They suggested that viruses may be particularly sensitive to P limitation since viruses have a high nucleic acid to protein ratio. Wilson et al. (1996) demonstrated in laboratory experiments that only 9.3 % of virus-infected cells of *Synechococcus* sp. WH7803 grown under P-depleted conditions lysed, while 100 % of virus-infected cells lysed under P-replete growing conditions. During the study of a *Synechococcus* spp bloom in a mesocosm enclosure with simulated P-depleted conditions Wilson et al. (1998) found that virus numbers increased substantially following P addition shortly before the collapse of the *Synechococcus* bloom. Based on these observations it was suggested that lysogeny could be established in response to P-depleted growth of the host cells and that temperate viruses were induced after the P addition, supporting the hypothesis that nutrient availability may be responsible for the switch between lysogeny and lytic production.

Sequencing has revealed the presence of a putative phosphate-repressible phosphate permease in *E. huxleyi* strain CCMP 1516 (GenBank Accession Number AF334403) (Corstjens et al. 2003). In addition, a similar predicted gene (coding sequence; CDS) was found in the genome of *E. huxleyi*-specific virus EhV-86 (ehv117 gene, GenBank

Accession Number NC_007346) (Wilson et al. 2005a). EhV-86 is the type species of the genus *Coccolithovirus* within the family *Phycodnaviridae* (Schroeder et al. 2002). These findings raise the following questions: (1) what is the relationship between these two similar genes carried by the virus and the host? (2) do those genes have the same function? (3) is the ehv117 gene present in all EhVs? (4) what conditions determine the expression of this gene in the virus?

The scarcity of genome sequences and transcriptome analysis for members of the *Phycodnaviridae* family limits our knowledge of the biology and ecology of this important group of algal viruses. Gene expression analysis will provide crucial understanding of *Phycodnaviridae* genomes functioning in the ocean. In this study, ten different EhVs were screened for the presence of the putative phosphate permease by polymerase chain reaction (PCR) amplification using non-degenerate primers designed to the putative phosphate permease gene of EhV-86. Real-time reverse-transcription quantitative PCR was also performed to investigate differential expression of the EhV-86 phosphate permease gene during infection of axenic cultures of *E. huxleyi* strain CCMP 1516 grown in F/2 medium (phosphate-replete) and phosphate-depleted modified F/2 medium.

7.2. Materials and methods

7.2.1. Virus and host strains

Ten clonal EhV strains (Table 2.3) and two clonal strains of *E. huxleyi* (axenic CCMP 1516 and CCMP 374, Table 2.4) were employed in this study. EhV-84, EhV-86 and EhV-88 were isolated in 1999 (English Channel); EhV-201, EhV-202, EhV-203, EhV-205, EhV-207 and EhV-208 were isolated in 2001 (English Channel); and EhV- 163 was isolated in 2000 (Norwegian fjord).

7.2.2. Screening of EhV strains for presence/absence of the ehv117 gene

Genomic DNA (gDNA) was isolated from exponentially growing cultures of the *E. huxleyi* strains and from concentrated EhV lysates using the phenol/chloroform method described in Section 2.2.11.2. PCR reactions (Section 2.2.12) were performed on 100 ng gDNA template using a pair of oligomers designed to the ehv117 gene of EhV-86 (Phos-F1/Phos-R1, Table 2.5). PCR products were subsequently sequenced and the sequences aligned as described in Section 2.2.15.

7.2.3. Determination of culture conditions for induction of P-limitation

Batch cultures (250 ml) of *E. huxleyi* CCMP 1516 were grown in P-replete standard F/2 medium and in modified F/2 media containing 50 %, 10 % and 1 % final concentration PO_4^{3-} relative to standard F/2 medium. These culture medium conditions are referred to as P-replete, 50 % P, 10 % P and 1 % P respectively (see section 2.2.2, for details on culture conditions and media preparation). The 1 % P culture was done in duplicate.

Initial cell abundances were approximately 3×10^3 cells ml^{-1} for all the conditions. Cultures growth was monitored by AFC (Section 2.2.6) and by cell photosynthetic capacitiy (CPC) measurements (Section 2.2.5). EhV-86 was inoculated into the 50 %, 10 % and one of the two 1 % P cultures during stationary growth phase of the1 % P

cultures in a host:virus ratio of 1:3. Inoculations were done during cell division phase during the dark incubation period. The P-replete and the second 1 % P cultures served as virus-free controls. From this time point, in addition to the measurements above, EhV-86 abundances were determined by AFC (Section 2.2.6).

Fresh EhV-86 lysate stocks used for inoculations (see Section 2.2.4) were dialysed 3 times against 30 kD autoclaved oligotrophic seawater to reduce addition of extra PO_4^{3-} to the cultures (Section 2.2.9).

7.2.4. Differential expression of the ehv117 gene in EhV-86

7.2.4.1. Experimental design

To determine the expression profile of ehv117 in EhV-86, 8 L volume cultures of *E. huxleyi* CCMP 1516 were grown in P-replete F/2 medium and 6 L volume cultures were grown in 1 % P conditions (initial cell concentrations ~ 1.5×10^5 cells ml^{-1}). The growth of the cultures was monitored daily for 17 days by AFC counts (Section 2.2.6). At the onset of the stationary phase the cultures were divided in 3 × 2 L volume batches and they were inoculated with dialysed axenic EhV-86 (host:virus ratio of 1:3), allowing triplication of each nutrient treatment. The remaining 2 L P-replete culture were not inoculated to serve as a free-virus control. EhV-86 production was monitored by AFC (Section 2.2.6).

7.2.4.2. Isolation and quantification of total RNA

Total RNA was isolated from *E. huxleyi* CCMP 1516 cultures immediately prior to infection with EhV-86 (t_0) and 4 h, 12 h and 24 h post-inoculation (t_4, t_{12} and t_{24} respectively) (Section 2.2.11.3). RNA was then treated with DNase (Section 2.2.11.4), quantified (Section 2.2.11.5) and stored at -80 °C prior further use. One microlitre RNA sub-samples were used as template on a PCR reaction (Section 2.2.12) with Phos-F1/Phos-R1 (Table 2.5), to check for any potential DNA contamination after the DNase treatment.

7.2.4.3. Gene expression quantification by real-time reverse-transcription PCR

Real-time reverse-trancription PCR reactions with TaqMan primers and probe designed to the nucleotide sequence of the ehv117 gene of EhV-86 were performed as described in Sections 2.2.18 and 2.2.19. The reactions were done using 1000 pg total RNA template samples (Section 7.2.4.2) from the P-replete and 1 % P *E. huxleyi* cultures.

A calibration curve was constructed (Section 2.2.19.4) using EhV-86 Phos-F1/Phos-R1 PCR plasmid DNA fragments that were first transcribed into RNA (Section 2.2.18.1) and then into cDNA (Section 2.2.18.2). Gene expression was estimated as initial amount of target gene (ehv117) RNA contained in the 1000 pg total RNA template.

To determine if fluorescence contaminants or DNA contaminants were present in the reactions, three No Template Controls (NTC) and three No Amplification Controls (NAC) were included in the real-time reverse-transcription PCR (Section 2.2.19.1). Additionally, three of the culture RNA samples (1 % P r3-t_0, 1 % P r3-t_{12} and P-replete r1-t_{24}) were chosen randomly and included in the reaction without addition of reverse transcriptase in order to verify the lack of carry over DNA contamination that might have not been detected by standard PCR amplification using Phos-F1/Phos-R1 primers (Section 7.2.4.2).

7.3. Results

7.3.1. Comparison of ehv117 and putative phosphate-repressible phosphate permease in *E. huxleyi* strain CCMP 1516

The alignment of the nucleotide sequences (Figure 7.1) and the amino acid sequences (data not shown) of ehv117 from EhV-86 and the putative phosphate-repressible phosphate permease gene from CCMP 1516 reveals that both genes share conserved regions. In fact, blast searches at the nucleotide and amino acid levels (www.ncbi.nln.nlh.gov) with each of these gene sequences give top matches to the other gene. However, there are enough mismatches between both sequences to allow the design of primers specific to EhV-86, which theoretically would not amplify the phosphate permease in CCMP 1516.

```
ehv117    CAATTCTCATGTATGGTAATTTGTGCGTCATTGGGGCAGTTGGTATGTGGTTACTTGTGGCAACAAAGTTTGAAATGCCAGT
CCMP1516  CGATCCTGATGTACGGCAACCTCTGCGTCGTCGGCGCGGTCGGCATTTGGCTCCTCATCGCCACCAAGTTCGAGATGCCCGT
          * ** ** ***** ** **  * ****** * ** ** ** ** ** *** * **  * ** ** ***** ** ***** **

ehv117    TTCGACTACGCATTCTTGTGTTGGTGGTCTCGTTGGTATGACAATTGCAGCAAAAGGCGCTGATTGCGTTGTTTGGTACAAA
CCMP1516  CTCGACCACCCACTCCTGCGTCGGCGGCCTCGTCGGCATGGCCATCGCCTCCAAGGGCCCCGCCTGCGTCACGTGGTACAAG
           ***** ** ** ** ** ** ** ** ** ***** ** *** * ** **  * ** *** * *  *****    ********

ehv117    GAAATTGATATCGATAGCGGCAAATACCTACCAGGAGGCATTGTTGGTATTGTATTGTCATGGGTATTCTCACCATTACTAT
CCMP1516  GACCCCGACCCGGACAGCGCTAAGTACCTCCCGGGCGGCATCACCGGCATCGTGCTGTCGTGGATCTTCTCGCCCCTCCTCT
          **    **    ** **** ** ***** ** ** *****    ** ** **  **** *** * ***** **  * ** *

ehv117    CTGGGATAGTTGCAGTGCTTTTATTCTTGAGTATAAGAACATTTGTATTGCGCAGTGCTCAGCCATTTATTAGATCTATTCG
CCMP1516  CGGGCCTCTTCGCCGTCGCCCTCTTCGCCGTCGTCCGCTGCGTCGTCCTCCG-GTCGCAGAACTCCTTCATGCGTGCAATCA
          * **  *  * ** **     * ***       *  *     * **  * **    **  * *   **  *   *  * **

ehv117    CGCG-TATCCATTTCTTGTATGGGGGGCAGTTACAATCAACTCATTTTTCATTATATCCAAGGGGGTATCCAAAAAAATCTG
CCMP1516  AGTTCTACCCCGTCCTCATCTGGCTCGCCATCTGGATCAACACCTTCTTCATCATCTCCAAGGGCGTCAGCAAGAAGGTCTG
           *   ** **  * **  * ***   **  *    ****** * ** ***** ** ******** **   *** **  ****

ehv117    TCCATCGAAATACAACATCTGGATATGCCAAGGATGGGACGCTAGTTT----------ACCAAACGGAGCG------GAAGT
CCMP1516  CCCGAGCAAGACGAACATCTGGATCTGCTCCGGCTACGACTCCGACCTCAAGGAGGGCGCCGAGAAGGACGCCGCCGGCGGG
          **    **    ********** ***   ** *  *** *     *           ** *   *  **      *  *

ehv117    AA------CAAAAGCGATTGCACCAGGTAAAGTAAATGCAGGAATTGCATTTGGATTATCTGCTGGGTTTGGTGTTGTTGCT
CCMP1516  AAGCTCTCCAAGGACGACTAC-CCCGGCAAGGTCAACGGCTGGGTCGCCTTGGGCTTCTCGTGCGGCGTCGGCCTCTTCTTC
          **      ***   *** * * ** ** ** ** ** *   *  * ** ** ** ** **    **  * **  *  *

ehv117    GCTATTGCATTAATTCCACTTTATAAATATATTCACCGCACTACACTAGATACATTTTCAAAACCAAAACAAATAGA-----
CCMP1516  GCCGTCGCCCTCATCCCGCTCTACCT-CGCGATCAAGAAGCGCGTCGAGGCGGAGTTTGCGGACAAGGACACCGAGGCCGGC
          **  * **  * ** ** ** **        ***     *   * **    * ***    ** *  ***   **

ehv117    -----AAATAAAGCCGAAAATATAGAAAAACCA--------------AAAAATATATTA--GCAAAGAC--AGCAAGAA---
CCMP1516  GAGGCGGAGGAGGCCAAGGAGGAGGCCAAGCCGCCCCCGGAGCCGCCGACGACCTTCTGCGGCAAGGCCCTGGCGGCTATCT
            *  * *** *  *    *  ** **               *  *  *  *   **** * *   **    *

ehv117    --AATTGTTCGATAGAGATATTCATG----CAATAACT--GTTACAGACGAGAAAGTGTCGGTTATTCATAATAATGCAGAA
CCMP1516  CTACTCGATCAACCGCGACGTGCACGACGTCAAGAAGGAGGAGACGGACGGCGTCATCACGGCGATCCACGACAACGCCGAG
            * * * ** *  * **  * ** *    *** **    *  ** ****      *  ***  ** **  * ** ** **

ehv117    CAATTTGATGAAAAAGCAGAATATGTGTTCAAATATATTCAAATATTTTCAGCAATTTTCGATTCGTTTGCCCACGGGGCGA
CCMP1516  AAGTTCGACCCGAAGACGGAGGCCGTCTTCAAGTACATCCAGATCTTCACCGCCATCTGCGACTCGTTCGCGCACGGCGCCA
          * ** **    **  * **    ** ***** ** ** ** ** **  * ** ** * *** ***** ** ***** ** *

ehv117    ATGATGTCGCAAACGCAATGGGTCCATTTATGACAATATGGGTAATATG---GAAGGCGGAAGGAGAAGCAATTGGTGGGAG
CCMP1516  CGGACGTGGCCAATGCGATGGGCCCCTTCATGTCCATCTGGACAATCTACACGAACATCGACACCTTCGAGTTCGGCAAGGG
           ** ** ** ** ** ***** ** ** *** * ** ***  *** *   ***    **       *  * **   * *
```

Figure continues in next page

```
ehv117    T------AAAACAGATATTGGAGAT---GATTCATATTGGATACTTGCAATTGGAGGTATTGGTATTGGAATCGGTTTACTA
CCMP1516  CGCCCAGAAGACGGACCTCGAGAACAACGACCAGTACTGGATCCTCGCCCTCGGCGGCGTCGGCATCGGTCTCGGCCTCCTC
                ** ** **  * *   *    **    ** ***** ** **  * ** **  * ** ** **  ****  * **

ehv117    TTATATGGATACAAGATCATGCAGGAAATTGGTGTAAAACTTGCAGTAATTACACCAAGTCGTGGTGTTTGTATTGAGCTTG
CCMP1516  CTCTACGGCTACCAGATCATCCAGGCGATCGGCGTCAAGCTCGCCGTCATCACGCCGTCGCGCGGGTTCGCCATCGAGCTCG
           * ** ** *** ******* ****  ** ** ** ** ** ** ** ** ** **    ** **  *    ** ***** *

ehv117    GTTCCGCGGTTGTAATTATCACCGGAAGCTATATGGGGATTCCGTTATCAACGACTCATGCACAAGTTGGAGCAACAGTGGG
CCMP1516  GCGCCGCCATCGTCATCATCATCGGGTCGTACCTCGGCATCCCGCTCTCGACCACCCACTGCCAGGTCGGCGCCACCACCGG
          *  ****  * ** ** **** ***    **  * ** ** *** * ** ** ** **    ** ** ** ** **    **

ehv117    TGTTGCACTACTCGAAGGTAAAAAAGGAATCAATACAAAAGTGTTGAGTAAAGCAGGATTTGGTGGATAGTAACACTAATTG
CCMP1516  CGTCGCGCTCCTCGAGGGCGGCCGCGGCGTCAACAAGTGGGTCCTCGGCAAGACCGCCTTCGGTGGATCATCACCCTCATCA
           ** ** ** ***** **       **  **** *    **  *  * **  * *  ** *******  * ** ** **

ehv117    TGGCTGGGTTGTTAGCAGGATTGCTTACTTCCCAGGGGATATATTCTCCTATTAATGAA--TATGCATTTAATTCGGCAATC
CCMP1516  TCGCCGGCATCCTCGCCGGCATCCTCACCGGCCAGGGCATCCGCGCGCCCCTCGGCGGCGCCATCAACATCGCCGGCTGCTC
          * ** **  * * ** **  * ** **   ****** **     * **  *   *    ** * *    *   **

                <-------------------
ehv117    CGTGTTTAATGAAACATCTTAA
CCMP1516  CGCCCAAAGTGTGGACCGACGA
          **     * **          *
```

Fig. 7.1. Clustal alignment of ehv117 from EhV-86 and the putative phosphate-repressible phosphate permease in *E .huxleyi* strain CCMP 1516. Conserved bases are identified by an asterisk underneath the corresponding base. Highlighted nucleotide regions denote the sequence fragments to which the Phos-F1/Phos-R1 where designed. Arrows indicate the 5'-3' orientation of the primers. 5' 265 bp of ehv117 and 3' 352 bp of CCMP 1516 have been removed from this alignment.

7.3.2. Presence/absence of the ehv117 gene in EhV strains

EhV's ehv117 gene fragments were amplified using the pair of primers Phos-F1/Phos-R1. Products (~900 bp) were obtained for the English Channel EhV strains; however, these primers failed to amplify a product of the expected size for the Norwegian EhV strain (EhV-163). Phos-F1/Phos-R1 are specific to EhV's ehv117 and not to the putative phosphate permease in *E. huxleyi* strains CCMP 1516 and CCMP 374 since no amplification was produced from gDNA extracted from those host cultures (Figure 7.2).

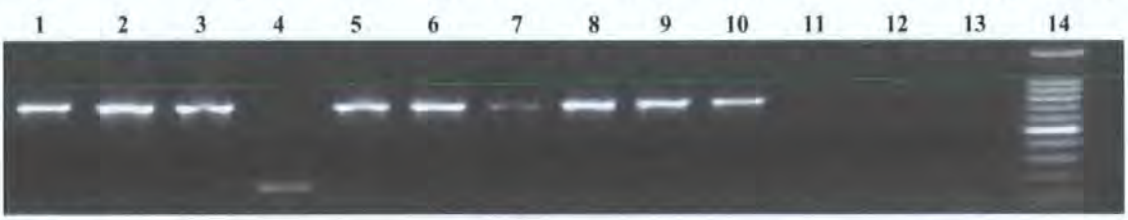

Fig. 7.2. Agarose gel electrophoresis of PCR products for the ehv117 gene from total gDNA extracted from EhVs and *E. huxleyi* strains. Lanes 1-10: EhV-84, EhV-86, EhV-88, EhV-163, EhV-201, EhV-202, EhV-203, EhV-205, EhV-207 and EhV-208 respectively. Lanes 11 and 12: *E. huxleyi* strains CCMP 1516 and CCMP 374 respectively. Lane 13: negative control PCR reaction (no DNA template). Lane 14: DNA molecular weight marker (100 bp ladder).

Direct sequencing of the purified PCR amplified fragments revealed that ehv117 is highly conserved, at the nucleotide level, among the EhVs originated from the English Channel. In fact, only 2 different types of ehv117 gene fragment sequences were obtained for these EhVs. One sequence common to all of the 1999 isolates (EhV-84, EhV-86, EhV-88) and another sequence shared by the 2001 isolates (EhV-201, EhV-203, EhV-205, EhV-207, EhV-208) (Figure 7.3).

The approximately 200 bp product from EhV-163 seemed to be the result of unspecific amplification; its nucleotide sequence did not show significant homology with any sequences from the GenBank (data not shown) and therefore was not included in the alignment.

```
EhV207    GGTAAAGTAAATGCAGGGATTGCATTTGGATTATCTGCTGGGTGTGGTGTCGTTGCTGCTATTGCATTGATTCCACTTTATAAATATATTCACCGCACTACACTAGATACATTTTCAAAA 120
EhV208    GGTAAAGTAAATGCAGGGATTGCATTTGGATTATCTGCTGGGTGTGGTGTCGTTGCTGCTATTGCATTGATTCCACTTTATAAATATATTCACCGCACTACACTAGATACATTTTCAAAA 120
EhV205    GGTAAAGTAAATGCAGGGATTGCATTTGGATTATCTGCTGGGTGTGGTGTCGTTGCTGCTATTGCATTGATTCCACTTTATAAATATATTCACCGCACTACACTAGATACATTTTCAAAA 120
EhV203    GGTAAAGTAAATGCAGGGATTGCATTTGGATTATCTGCTGGGTGTGGTGTCGTTGCTGCTATTGCATTGATTCCACTTTATAAATATATTCACCGCACTACACTAGATACATTTTCAAAA 120
EhV201    GGTAAAGTAAATGCAGGGATTGCATTTGGATTATCTGCTGGGTGTGGTGTCGTTGCTGCTATTGCATTGATTCCACTTTATAAATATATTCACCGCACTACACTAGATACATTTTCAAAA 120
EhV84     GGTAAAGTAAATGCAGGAATTGCATTTGGATTATCTGCTGGGTTTGGTGTTGTTGCTGCTATTGCATTAATTCCACTTTATAAATATATTCACCGCACTACACTAGATACATTTTCAAAA 120
EhV86     GGTAAAGTAAATGCAGGAATTGCATTTGGATTATCTGCTGGGTTTGGTGTTGTTGCTGCTATTGCATTAATTCCACTTTATAAATATATTCACCGCACTACACTAGATACATTTTCAAAA 120
EhV88     GGTAAAGTAAATGCAGGAATTGCATTTGGATTATCTGCTGGGTTTGGTGTTGTTGCTGCTATTGCATTAATTCCACTTTATAAATATATTCACCGCACTACACTAGATACATTTTCAAAA 120
          ********************* ************************** ****** ****************** ************************************************

EhV207    CCAAAACAAATAGAAAATAAAGCCGAAGATATAGAAAAACCAAAAAATATATTAGCAAAGACAGCAAGCAAATTGTTCGATATAGATATTCATGCAATAACTGTTACAGACGAGAAAGTG 240
EhV208    CCAAAACAAATAGAAAATAAAGCCGAAGATATAGAAAAACCAAAAAATATATTAGCAAAGACAGCAAGCAAATTGTTCGATATAGATATTCATGCAATAACTGTTACAGACGAGAAAGTG 240
EhV205    CCAAAACAAATAGAAAATAAAGCCGAAGATATAGAAAAACCAAAAAATATATTAGCAAAGACAGCAAGCAAATTGTTCGATATAGATATTCATGCAATAACTGTTACAGACGAGAAAGTG 240
EhV203    CCAAAACAAATAGAAAATAAAGCCGAAGATATAGAAAAACCAAAAAATATATTAGCAAAGACAGCAAGCAAATTGTTCGATATAGATATTCATGCAATAACTGTTACAGACGAGAAAGTG 240
EhV201    CCAAAACAAATAGAAAATAAAGCCGAAGATATAGAAAAACCAAAAAATATATTAGCAAAGACAGCAAGCAAATTGTTCGATATAGATATTCATGCAATAACTGTTACAGACGAGAAAGTG 240
EhV84     CCAAAACAAATAGAAAATAAAGCCGAAAATATAGAAAAACCAAAAAATATATTAGCAAAGACAGCAAGAAAATTGTTCGATAGAGATATTCATGCAATAACTGTTACAGACGAGAAAGTG 240
EhV86     CCAAAACAAATAGAAAATAAAGCCGAAAATATAGAAAAACCAAAAAATATATTAGCAAAGACAGCAAGAAAATTGTTCGATAGAGATATTCATGCAATAACTGTTACAGACGAGAAAGTG 240
EhV88     CCAAAACAAATAGAAAATAAAGCCGAAAATATAGAAAAACCAAAAAATATATTAGCAAAGACAGCAAGAAAATTGTTCGATAGAGATATTCATGCAATAACTGTTACAGACGAGAAAGTG 240
          **************************** ****************************************** ************* ************************************

EhV207    TCGGTTATTTATAATAATGCAGAACATTTTGATGAAAAAGCAGAATATGTGTTCAAATATATTCAAATATTTTCAGCAATTTTCGATTCGTTTGCCCACGGGGCGAATGATGTCGCAAAC 360
EhV208    TCGGTTATTTATAATAATGCAGAACATTTTGATGAAAAAGCAGAATATGTGTTCAAATATATTCAAATATTTTCAGCAATTTTCGATTCGTTTGCCCACGGGGCGAATGATGTCGCAAAC 360
EhV205    TCGGTTATTTATAATAATGCAGAACATTTTGATGAAAAAGCAGAATATGTGTTCAAATATATTCAAATATTTTCAGCAATTTTCGATTCGTTTGCCCACGGGGCGAATGATGTCGCAAAC 360
EhV203    TCGGTTATTTATAATAATGCAGAACATTTTGATGAAAAAGCAGAATATGTGTTCAAATATATTCAAATATTTTCAGCAATTTTCGATTCGTTTGCCCACGGGGCGAATGATGTCGCAAAC 360
EhV201    TCGGTTATTTATAATAATGCAGAACATTTTGATGAAAAAGCAGAATATGTGTTCAAATATATTCAAATATTTTCAGCAATTTTCGATTCGTTTGCCCACGGGGCGAATGATGTCGCAAAC 360
EhV84     TCGGTTATTCATAATAATGCAGAACAATTTGATGAAAAAGCAGAATATGTGTTCAAATATATTCAAATATTTTCAGCAATTTTCGATTCGTTTGCCCACGGGGCGAATGATGTCGCAAAC 360
EhV86     TCGGTTATTCATAATAATGCAGAACAATTTGATGAAAAAGCAGAATATGTGTTCAAATATATTCAAATATTTTCAGCAATTTTCGATTCGTTTGCCCACGGGGCGAATGATGTCGCAAAC 360
EhV88     TCGGTTATTCATAATAATGCAGAACAATTTGATGAAAAAGCAGAATATGTGTTCAAATATATTCAAATATTTTCAGCAATTTTCGATTCGTTTGCCCACGGGGCGAATGATGTCGCAAAC 360
          ********* ***************** ********************************************************************************************

EhV207    GCAATGGGTCCATTTATGACAATATGGGTAATATGGAAGGCGGAAGGAGGAGCAATTGGTGGGAGTAAAACAGATATTGGAGATGATTCATATTGGATACTTGCAATTGGAGGTATTGGC 480
EhV208    GCAATGGGTCCATTTATGACAATATGGGTAATATGGAAGGCGGAAGGAGGAGCAATTGGTGGGAGTAAAACAGATATTGGAGATGATTCATATTGGATACTTGCAATTGGAGGTATTGGC 480
EhV205    GCAATGGGTCCATTTATGACAATATGGGTAATATGGAAGGCGGAAGGAGGAGCAATTGGTGGGAGTAAAACAGATATTGGAGATGATTCATATTGGATACTTGCAATTGGAGGTATTGGC 480
EhV203    GCAATGGGTCCATTTATGACAATATGGGTAATATGGAAGGCGGAAGGAGGAGCAATTGGTGGGAGTAAAACAGATATTGGAGATGATTCATATTGGATACTTGCAATTGGAGGTATTGGC 480
EhV201    GCAATGGGTCCATTTATGACAATATGGGTAATATGGAAGGCGGAAGGAGGAGCAATTGGTGGGAGTAAAACAGATATTGGAGATGATTCATATTGGATACTTGCAATTGGAGGTATTGGC 480
EhV84     GCAATGGGTCCATTTATGACAATATGGGTAATATGGAAGGCGGAAGGAGAAGCAATTGGTGGGAGTAAAACAGATATTGGAGATGATTCATATTGGATACTTGCAATTGGAGGTATTGGT 480
EhV86     GCAATGGGTCCATTTATGACAATATGGGTAATATGGAAGGCGGAAGGAGAAGCAATTGGTGGGAGTAAAACAGATATTGGAGATGATTCATATTGGATACTTGCAATTGGAGGTATTGGT 480
EhV88     GCAATGGGTCCATTTATGACAATATGGGTAATATGGAAGGCGGAAGGAGAAGCAATTGGTGGGAGTAAAACAGATATTGGAGATGATTCATATTGGATACTTGCAATTGGAGGTATTGGT 480
          ********************************************** ********************************************************************************
```

Figure continues in next page

```
EhV207     ATTGGAATCGGTTTACTATTATATGGATACAATATCATGCAGGCAATTGGTGTAAAACTTGCAGTAATTACACCAAGTCGTGGTGTTTGTATTGAGCTTGGTTCCGCGGTTATAATTATT 600
EhV208     ATTGGAATCGGTTTACTATTATATGGATACAATATCATGCAGGCAATTGGTGTAAAACTTGCAGTAATTACACCAAGTCGTGGTGTTTGTATTGAGCTTGGTTCCGCGGTTATAATTATT 600
EhV205     ATTGGAATCGGTTTACTATTATATGGATACAATATCATGCAGGCAATTGGTGTAAAACTTGCAGTAATTACACCAAGTCGTGGTGTTTGTATTGAGCTTGGTTCCGCGGTTATAATTATT 600
EhV203     ATTGGAATCGGTTTACTATTATATGGATACAATATCATGCAGGCAATTGGTGTAAAACTTGCAGTAATTACACCAAGTCGTGGTGTTTGTATTGAGCTTGGTTCCGCGGTTATAATTATT 600
EhV201     ATTGGAATCGGTTTACTATTATATGGATACAATATCATGCAGGCAATTGGTGTAAAACTTGCAGTAATTACACCAAGTCGTGGTGTTTGTATTGAGCTTGGTTCCGCGGTTATAATTATT 600
EhV84      ATTGGAATCGGTTTACTATTATATGGATACAAGATCATGCAGGAAATTGGTGTAAAACTTGCAGTAATTACACCAAGTCGTGGTGTTTGTATTGAGCTTGGTTCCGCGGTTGTAATTATC 600
EhV86      ATTGGAATCGGTTTACTATTATATGGATACAAGATCATGCAGGAAATTGGTGTAAAACTTGCAGTAATTACACCAAGTCGTGGTGTTTGTATTGAGCTTGGTTCCGCGGTTGTAATTATC 600
EhV88      ATTGGAATCGGTTTACTATTATATGGATACAAGATCATGCAGGAAATTGGTGTAAAACTTGCAGTAATTACACCAAGTCGTGGTGTTTGTATTGAGCTTGGTTCCGCGGTTGTAATTATC 600
           ******************************** ********** ******************************************************************* *******

EhV207     GTCGGAAGTTATATGGGTATTCCATTATCGACGACCCATGCACAAGTTGGAGCAACAGTGGGTGTTGCACTACTCGAAGGTAAAAAAGGAATCAATACAAAAGTGTTGAGTAAAGCAGGA 720
EhV208     GTCGGAAGTTATATGGGTATTCCATTATCGACGACCCATGCACAAGTTGGAGCAACAGTGGGTGTTGCACTACTCGAAGGTAAAAAAGGAATCAATACAAAAGTGTTGAGTAAAGCAGGA 720
EhV205     GTCGGAAGTTATATGGGTATTCCATTATCGACGACCCATGCACAAGTTGGAGCAACAGTGGGTGTTGCACTACTCGAAGGTAAAAAAGGAATCAATACAAAAGTGTTGAGTAAAGCAGGA 720
EhV203     GTCGGAAGTTATATGGGTATTCCATTATCGACGACCCATGCACAAGTTGGAGCAACAGTGGGTGTTGCACTACTCGAAGGTAAAAAAGGAATCAATACAAAAGTGTTGAGTAAAGCAGGA 720
EhV201     GTCGGAAGTTATATGGGTATTCCATTATCGACGACCCATGCACAAGTTGGAGCAACAGTGGGTGTTGCACTACTCGAAGGTAAAAAAGGAATCAATACAAAAGTGTTGAGTAAAGCAGGA 720
EhV84      ACCGGAAGCTATATGGGGATTCCGTTATCAACGACTCATGCACAAGTTGGAGCAACAGTGGGTGTTGCACTACTCGAAGGTAAAAAAGGAATCAATACAAAAGTGTTGAGTAAAGCAGGA 720
EhV86      ACCGGAAGCTATATGGGGATTCCGTTATCAACGACTCATGCACAAGTTGGAGCAACAGTGGGTGTTGCACTACTCGAAGGTAAAAAAGGAATCAATACAAAAGTGTTGAGTAAAGCAGGA 720
EhV88      ACCGGAAGCTATATGGGGATTCCGTTATCAACGACTCATGCACAAGTTGGAGCAACAGTGGGTGTTGCACTACTCGAAGGTAAAAAAGGAATCAATACAAAAGTGTTGAGTAAAGCAGGA 720
             ****** ******** ***** ***** ***** ************************************************************************************

EhV207     TTTGGTTGGATAATAACACTAATTGTGGCTGGGTTGTTAGCAGGATTACTTACTGCCCAGGGTATTTATTCTCCTATTAAT 801
EhV208     TTTGGTTGGATAATAACACTAATTGTGGCTGGGTTGTTAGCAGGATTACTTACTGCCCAGGGTATTTATTCTCCTATTAAT 801
EhV205     TTTGGTTGGATAATAACACTAATTGTGGCTGGGTTGTTAGCAGGATTACTTACTGCCCAGGGTATTTATTCTCCTATTAAT 801
EhV203     TTTGGTTGGATAATAACACTAATTGTGGCTGGGTTGTTAGCAGGATTACTTACTGCCCAGGGTATTTATTCTCCTATTAAT 801
EhV201     TTTGGTTGGATAATAACACTAATTGTGGCTGGGTTGTTAGCAGGATTACTTACTGCCCAGGGTATTTATTCTCCTATTAAT 801
EhV84      TTTGGGTGGATAGTAACACTAATTGTGGCTGGGTTGTTAGCAGGATTGCTTACTTCCCAGGGGATATATTCTCCTATTAAT 801
EhV86      TTTGGGTGGATAGTAACACTAATTGTGGCTGGGTTGTTAGCAGGATTGCTTACTTCCCAGGGGATATATTCTCCTATTAAT 801
EhV88      TTTGGGTGGATAGTAACACTAATTGTGGCTGGGTTGTTAGCAGGATTGCTTACTTCCCAGGGGATATATTCTCCTATTAAT 801
           ***** ****** ********************************** ****** ******* ** ***************
```

Fig. 7.3. Clustal alignment of the English Channel EhV's ehv117 sequences (produced from the purified Phos_F1/Phos_R1 PCR amplified fragments). Conserved bases are identified by an asterisk underneath the corresponding base. Nucleotide differences between the 1999 and 2001 isolates are highlighted in blue and red respectively.

7.3.3. Effect of P limitation on *E. huxleyi* growth and EhV-86 production

The growth of *E. huxleyi* CCMP 1516 cultures that had received different dissolved inorganic phosphate additions was followed. Two of the cultures (P-replete and one 1 % P controls) were maintained virus-free, the rest were inoculated with EhV-86 (host:virus ratio approximately 1:3). The aim of this test was to detect which conditions may lead to P starvation based on the host growth and the effect on virus production.

Growth curves for each condition are presented in Figure 7.3. Under P-replete conditions the abundance of CCMP 1516 cells had logarithmic increase for 13 days before reaching the stationary phase (Figure 7.4 A). The growth rate of cells in the 1 % P control culture (Figure 7.4 B) decreased significantly after day 4 compared to the other of phosphate conditions. *E. huxleyi* cells in the 1 % P control culture were at stationary growth phase from day 9 until the end of the experimental period. Until day 11, the growth of CCMP 1516 cells in the culture with 50 % P addition did not deviate significantly from cells growth in the P-replete control culture (Figure 7.4 C). After this day, cell abundance decreased steadily concomitant with a high accumulation of EhV-86 particles in the culture medium. In the 10% P culture *E. huxleyi* cells (Figure 7.4 D) followed a similar progression and growth rate to the P-replete and 50 % P cultures until day 9. This day CCMP 1516 had reached the stationary phase in the 10 % P culture. The maximum *E. huxleyi* cell abundance was, in this case, approximately one third lower than in the 50 % P; although EhV particles production did not differ in numbers from the 50 % P culture. However, the collapse of the *E. huxleyi* culture and sudden increase of EhV numbers was delayed by 1 day in the 10 % P culture compared to the 50 % P condition. In both 1 % P cultures (with and without virus addition) the maximum CCMP 1516 cell abundances were approximately 4.6 and 3.2 times lower than in 50 % and 10 % P respectively.

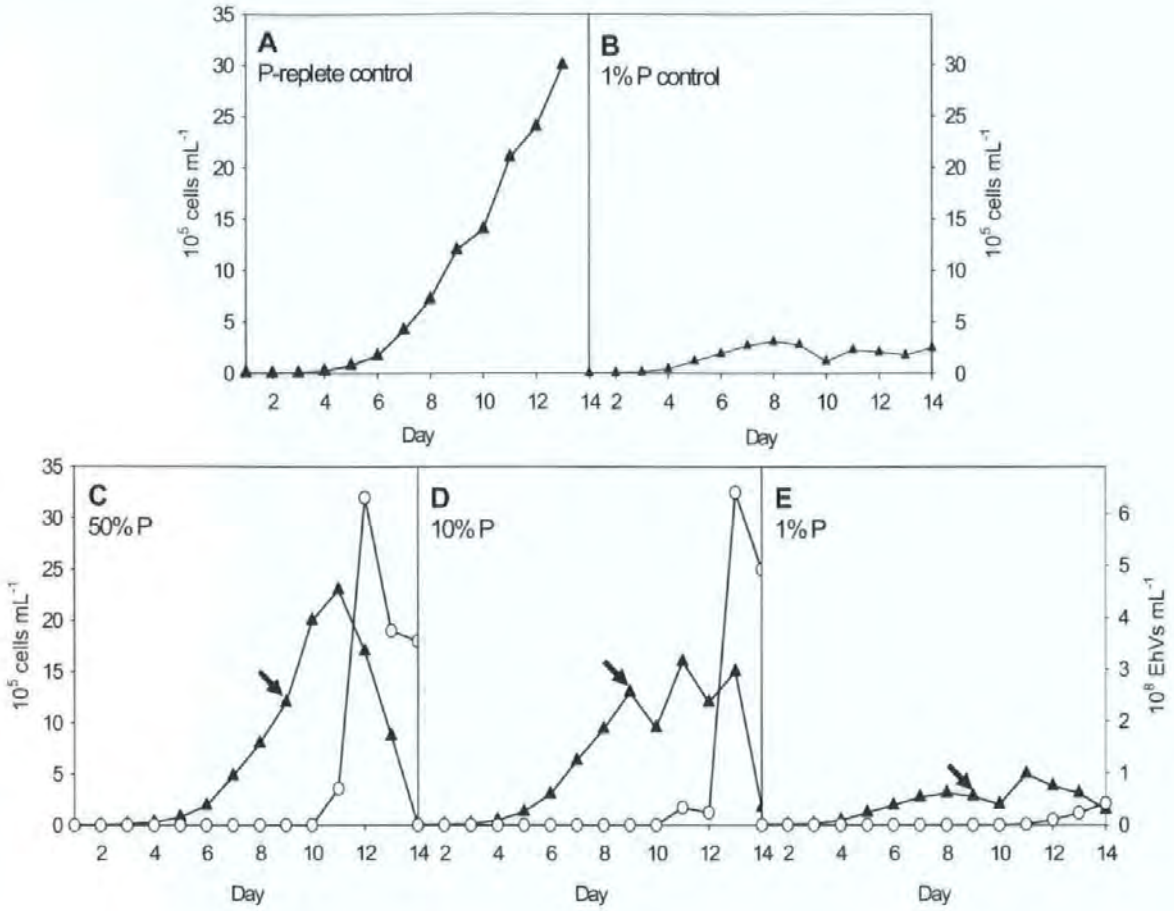

Fig. 7.4. Growth curves of *E. huxleyi* strain CCMP 1516 (filled triangles) and EhV-86 production (empty circles) as determined by flow cytometry counts. (**A**) Phosphate-replete control culture uninoculated; (**B**) 1 % added-phosphate control culture uninoculated; (**C**) 50 % added-phosphate culture inoculated with EhV-86; (**D**) 10 % added-phosphate culture inoculated with EhV-86; (**E**) 1 % added phosphate culture inoculated with EhV-86. Graphs are plotted as *E. huxleyi* cell and EhV abundances versus day in culture. Arrows denote inoculation of cultures with EhV-86.

The 1 % P culture inoculated with EhV-86 (Figure 7.4 E) only differed slightly from the 1 % P control culture after the virus addition. While the 1 % P control culture remained at stationary phase, a small decrease in cell numbers was observed in the former 1 % P culture during the last three days, concurrently with the accumulation of virus particles in the culture medium. However, EhV-86 abundances in the 1% P cultures were significantly lower than the abundances recorded in the 50 % and 10 % P cultures.

CPC of the different cultures, as estimated by relative fluorescence measurements, is shown in Figure 7.5. CPC in the P-replete control culture remained stable and above 0.5 units of relative fluorescence (R.U.) throughout the entire period of study. In the P-depleted cultures CPC decreased slightly on the first few days (days 1 to 4), then CPC increased to the same levels than those for the P-replete culture. However, despite the initial CPC decrease in the P-depleted cultures, the cells grown under such conditions maintained their photosynthetic capacity until day 10 (R.U.> 0.5). Then from day 11, CPC declined sharply in the 50 % P, 10 % P and 1 %P infected cultures as lysis occurred. After this day no sign of photosynthetic activity was detected in those cultures and measuring of relative fluorescence was not continued. In the P-replete control culture cell growth continued after day 11 (Figure 7.4) indicating that cells still had photosynthetic activity. No measurements are available for the 1 % P control culture.

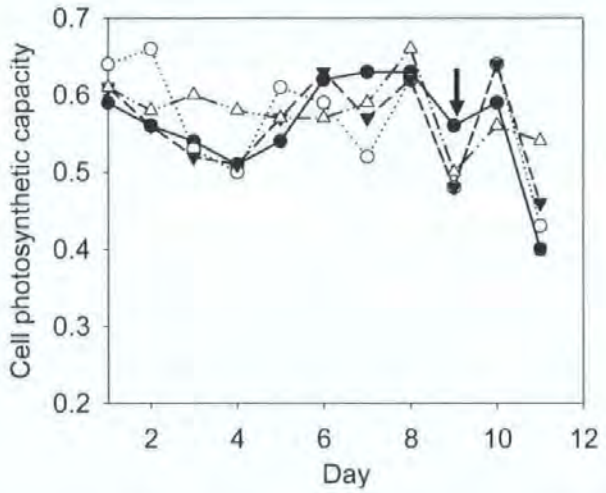

Fig. 7.5. *E. huxleyi* cell photosynthetic capacity as determined by the DCMU method, expressed as units of relative fluorescence. Δ P-replete control culture, • 50 % P culture, ○ 10 % P culture, ▼ 1 % P culture. The arrow denotes inoculation into the 50 %, 10 % and 1 % P cultures with EhV-86.

Based on these results a similar experiment was performed in triplicate to compare the development of 2 L batch cultures of *E. huxleyi* CCMP 1516 inoculated with EhV-86 during stationary growth phase (host:virus ratio approximately 1:3) and grown under P-replete and 1 % P conditions. These cultures were sampled at different time points for total RNA extraction (Section 2.2.11.3).

Additionally, one 2 L P-replete uninoculated culture was set up to serve as a negative control (Figure 7.6).

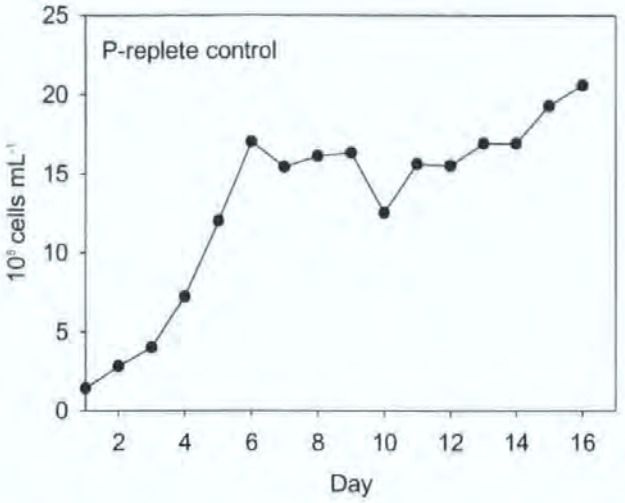

Fig. 7.6. Growth curve of *E. huxleyi* strain CCMP 1516 as determined by flow cytometry counts under P-replete phosphate culture conditions with no virus addition (control). Graph is plotted as *E. huxleyi* cell abundance versus day in culture.

Despite differences in numbers, the results obtained in this experiment under P-replete and 1 % P-modified F/2 medium culture conditions are comparable to what previously observed under 50 % and 1 % P-modified F/2 medium culture conditions respectively (Figure 7.7).

The P-replete cultures of *E. huxleyi* CCMP 1516 (Figure 7.7 A, B, C) had higher growth rate and reached cell abundances approximately 3.5 times higher than the cultures that grew with just 1 % P addition (Figure 7.7 D, E, F). Complete lysis of P-replete cultures occurred within 4 days post-inoculation and was accompanied by an intense EhV-86 production. On the other hand, *E. huxleyi* cell numbers in the 1 % P cultures decreased slowly after infection as EhV-86 particles accumulated in the culture medium.

Cultures that had received the same nutrient treatment were good replicates of each other. The only obvious difference was in treatment 1 % P replicate 3 (Figure 7.7 F), where the abundance of EhV-86 during the last 5 days of study was lower than in 1 % P replicates 1 and 2 (Figure 7.7 D, E). However, in terms of population development they did not differ significantly.

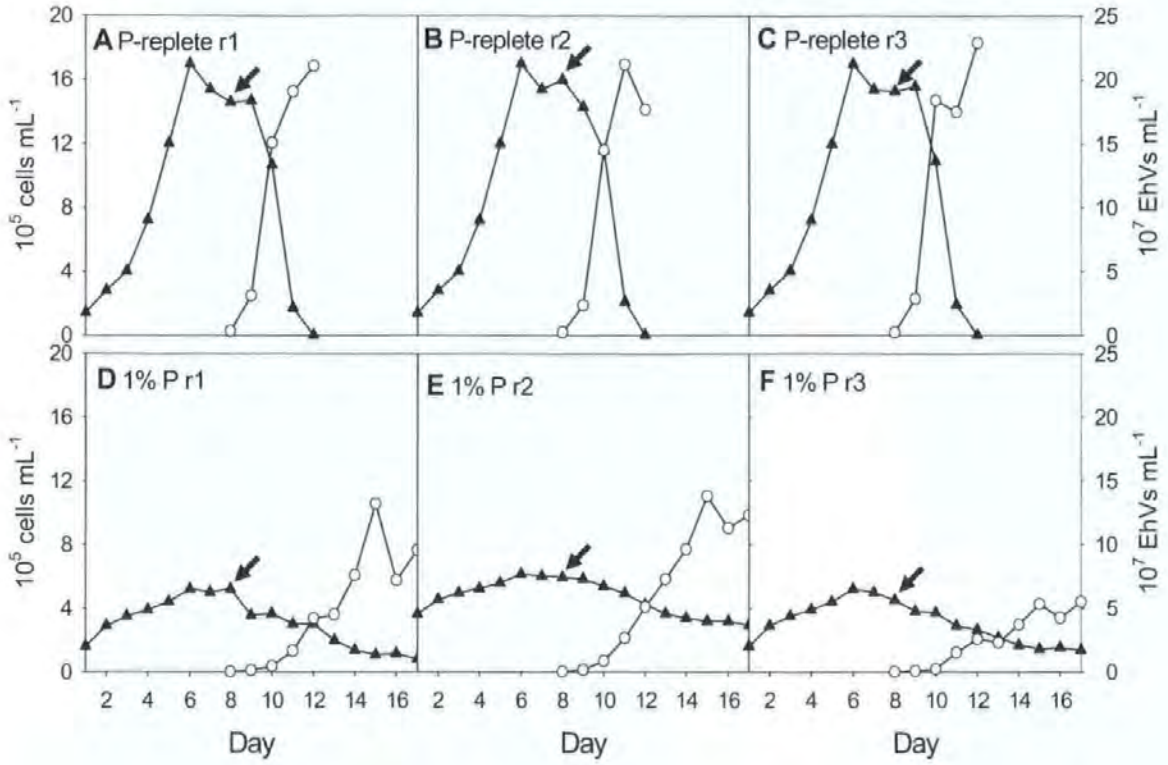

Fig. 7.7. Growth curves of *E. huxleyi* strain CCMP 1516 (filled triangles) and EhV-86 production (empty circles) as determined by flow cytometry counts. Graphs (**A**), (**B**) and (**C**) correspond to triplicate cultures under P-replete conditions. (**D**), (**E**) and (**F**) correspond to replicates grown in 1 % P-modified F/2 medium. Graphs are plotted as *E. huxleyi* cell and EhV abundances versus day in culture. r1, r2 and r3 denote replicates 1, 2 and 3 respectively. Arrows denote inoculation of cultures with EhV-86.

7.3.4. Isolation and quantification of total RNA from the infected cultures

Isolation and DNase methods yielded relatively low concentrations (250-8000 pg μl^{-1}) of total RNA. Low RNA yields may be a consequence of the DNase treatment, which may activate any RNases present in the sample, hence the loss of RNA. However, the RNA samples were of good quality and carried no DNA contamination as revealed by the lack of

product amplification by PCR using Phos-F1/Phos-R1 primers and by real-time PCR (without reverse transcriptase) reactions.

7.3.5. Differential expression of the ehv117 gene in EhV-86

The initial tests performed to establish the optimum conditions for the real-time PCR assay indicated that the suitable concentration of primers and probe were 300 nM and 125 nM respectively. Under the set PCR conditions, the calibration curve obtained from serial dilutions of known amount of ehv117 cDNA was log-linear and it had a correlation coefficient (R^2) of 0.98 (Figure 7.8). The efficiency (E) of the PCR reaction was 0.75.

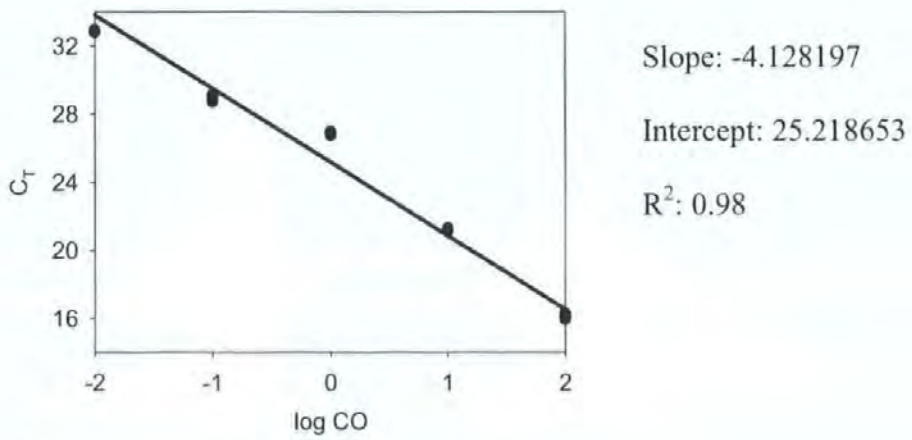

Fig. 7.8. Calibration curve for the real-time PCR amplification of known amounts of EhV-86 putative phosphate-repressible phosphate permease cDNA. Shown is a plot of cycle number (C_T) versus logarithm of known amounts of purified EhV-86 putative phosphate-repressible phosphate permease cDNA (log CO).

No product was amplified from the NTCs and the NACs indicating the absence of fluorescence or DNA contaminants in the instruments and/or the samples; although, one of the NAC produced some minor fluorescence signal after 38 cycles (data not shown). However, this late amplification should be interpreted as unspecific amplification rather than contamination (Contact Support, Applied Biosystems, UK, personal communication).

Real-time reverse-transcription PCRs were performed with 1000 pg sub-samples of total RNA isolated from the *E. huxleyi* CCMP1516 cultures and the fluorescence emitted was

monitored throughout the reaction as an indicator of amplicon production during each PCR cycle. The progression curves of relative fluorescence, for both nutrient treatments, are shown in Figure 7.9 (for simplicity, only one replicate for each treatment is shown). In the reactions with RNA samples from P-replete cultures the recorded fluorescence signal exceeded the fluorescence threshold (C_T) at 27 cycles for t_{24} samples, at 31 cycles for t_{12} samples, at 37 cycles for t_4 and at 39 cycles t_0 samples (Figure 7.9 A). With RNA isolated from the 1 % P cultures, C_T values of 33 and 34 were obtained for t_{24} and t_{12} samples respectively; no amplification was produced for the t_4 and t_0 samples indicating that ehv117 mRNA was not present in those samples (Figure 7.9 B). The initial amount of the ehv117 mRNA contained in the reactions was calculated, using those C_T values, as an indication of gene expression in EhV-86 at each sampling point. The estimated initial amounts of mRNA were averaged for each nutrient treatment and time (relative to EhV-86 inoculation) and the results are shown in Table 7.1.

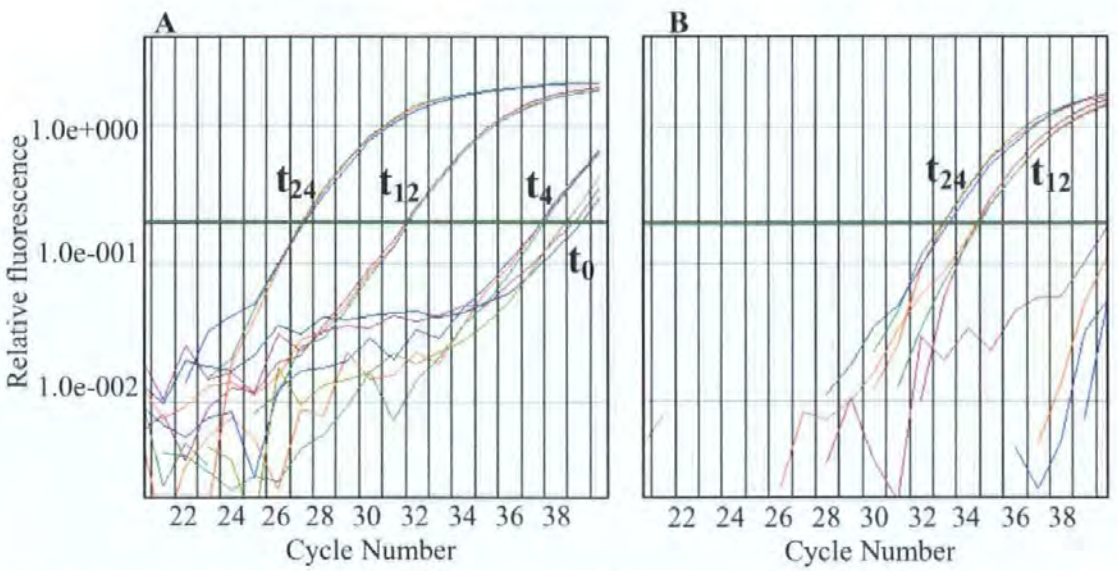

Fig. 7.9. Representative progress curves for the real-time reverse-transcriptase PCR amplification of EhV-86 putative phosphate-repressible phosphate permease cDNA during infection of *E. huxleyi* CCMP 1516 cultures grown in P-replete (**A**) and 1 % P (**B**) F/2 media. Shown are plots of increase in fluorescence signal versus PCR cycle number; t_{24}, t_{12}, t_4 and t_0 indicate the amplification curves (in triplicate) with total RNA samples extracted 24 h, 12 h, 4 h after inoculation and before inoculation of the cultures with EhV-86 respectively. The green bars indicate the fluorescence threshold that determines the C_T for each sample.

1 % P treatment	Initial amount of mRNA (pg per 1000 pg of total RNA)	P-replete treatment	Initial amount of mRNA (pg per 1000 pg of total RNA)
t_0	Not detected	t_0	5.35×10^{-4}
t_4	Not detected	t_4	1.12×10^{-3}
t_{12}	6.05×10^{-3}	t_{12}	3.30×10^{-2}
t_{24}	1.28×10^{-2}	t_{24}	4.02×10^{-1}

Table. 7.1. Initial amounts of EhV-86 ehv117 mRNA in the 1000 pg of total RNA template in the real-time reverse-transcriptase PCR reactions. The results indicate the average amount in samples isolated before and 4 h, 12 h and 24 h after (t_0, t_4, t_{12} and t_{24} respectively) inoculation with EhV-86 from cultures of *E. huxleyi* CCMP 1516 grown in 1 % P and P-replete F/2 media.

The amount of target ehv117 mRNA in the cultures increased in time after infection in both nutrient treatments. When comparing the two nutrient conditions at each sampling point, the amount of ehv117 mRNA was significantly higher in cultures that grew in P-replete conditions.

7.4. Discussion

The present study has mainly focussed on the role of phosphate availability over infection of the marine coccolithophore *E. huxleyi*. Previous studies have revealed the presence of a putative phosphate permease gene both in *E. huxleyi* strain CCMP 1516 and in EhV-86, which is the type species of the virus group specific to these phytoplankton species. Based on this knowledge the specific aims of the current experiments included first to determine whether or not the phosphate permease gene is commonly carried in the genome of all EhV strains and then to investigate the expression profile under P-replete and P-depleted conditions.

7.4.1. Presence/absence of the ehv117 gene in *E. huxleyi* viruses

PCR screening of ten EhV isolates available in culture indicated that nine of those EhVs, originally isolated from the English Channel, carry the ehv117 gene. Intriguingly, the sequences obtained allow differentiation among EhVs isolated in different years but do not differentiate isolates obtained in the same year. The ehv117 fragment was not amplified from EhV-163, the only isolate that originated from a geographically distant location (Raunefjorden, Norway), suggesting the absence of the gene in this virus strain. Since the primers employed in this study had been designed to the ehv117 sequence of one of the English Channel isolates (EhV-86) it would be possible that the PCR amplification was biased towards phylogenetically closely related EhVs and the failure to amplify the expected gene fragment from EhV-163 would mean that the sequence of a putative phosphate permease from EhV-163 differs significantly from that of the English Channel EhVs. However, all further attempts to amplify this gene from EhV-163 by PCR with several sets of primers have also failed (data not shown). In addition, two recent studies, a small scale sequencing project on EhV-163 (Allen et al. 2006b) and an EhV-86 based microarray assay (Allen et al. submitted) also failed to detect the ehv117 in EhV-163, and

have shown that a recombination event has occurred in EhV-163 causing a 5' partial deletion of ehv117 and the insertion of a putative nuclease (designated ehv117**a**)

7.4.2. Effect of phosphate availability on infected cultures of *E. huxleyi*

To investigate the effect of P limitation on the development of batch cultures of infected *E. huxleyi* and the subsequent release of viruses the model system formed by *E. huxleyi* CCMP 1516 and EhV-86 was used as a case study.

Manipulation of the dissolved inorganic P concentrations in batch cultures of *E. huxleyi* CCMP 1516 indicated that when P addition to the cultures was reduced down to 1 % (0.36 μM), relative to normal P addition for f/2 medium, a significant negative effect was induced on cell growth and virus production (Figure 7.4). A study by Shiraiwa (2003) also indicated the suppression of cell growth in coccolithophorids when availability of nutrients such as P is limited. The observations here presented are also in accordance with that previously reported for mesocosm experiments, where the lack of P inhibited virus production in *E. huxleyi* (Bratbak et al. 1993). However, despite the reduction in growth, the results in this experiment revealed that P limitation did not affect cell photosynthetic capacity. Cells grown at low P concentrations were equally healthy as those at P-replete conditions in terms of photosynthetic activity, which was shut down only as a consequence of viral lysis. Photosynthesis has also been found to continue until a late stage of viral infection in other phytoplankton species (Benson & Martin 1981, Suttle & Chan 1993, Brussaard et al. 1999).

7.4.3. Differential expression of the ehv117 gene induced by P regime

Genomic research with marine phytoplankton and their specific viruses is rapidly advancing our understanding of how they function and interact in the marine environment.

Many aspects of virus ecology such as survival, infectivity and specificity are most likely reflected in variations at the genomic level and altered patterns of gene expression.

Based on the observations on cell growth and virus production, P-replete and 1 % P culture conditions were selected as the optimum conditions to investigate potential differences in the level of expression of the ehv117 gene of EhV-86 during infection. EhV-86 were added into all the cultures during stationary growth phase. This was done in order to standardise the infection process and to eliminate possible differences in gene expression due to the growth phase of the host instead of P availability.

Dyhrman et al. (2006) reported that nutrient availability conditioned gene expression in *E. huxleyi* CCMP 1516; in particular they observed an increase in the expression of the host putative phosphate-repressible phosphate permease under P limitation. However, to my knowledge, these are the first transcriptome analyses of P starvation for a member of the *Phycodnaviridae* family.

So far, previous transcriptomic analysis using microarray assays had failed to detect the presence of any transcript for the ehv117 during the course of the EhV-86 infection cycle (Allen et al. 2006a). However, the findings from the present study employing real-time reverse-transcription PCR, a more sensitive and reliable approach to quantify gene expression (Bustin 2000, Walker 2002, Quinn et al. 2006), indicate the expression of the ehv117 gene of EhV-86 during the infection process of both, P-replete and P-depleted cultures. In the 1 % P cultures, mRNA was first detected 12 h after inoculation of the virus in the host culture. However, in P-replete cultures the fluorescence signal recorded was over the threshold after 37 and 39 cycles for t_4 and t_0 samples. This result should be interpreted as unspecific amplification and not as transcription of the ehv117 gene; first because this late amplification is comparable to the result from one of the NACs (data not

shown) and second because at t_0 there were no viruses in the samples, therefore viral mRNA could not be detected at this sampling point.

In contrast to what has been reported for *E. huxleyi* CCMP 1516, i.e. higher expression of the phosphate permease gene under P-limiting conditions, low concentrations of P induced a decrease in the level of ehv117 expression in EhV-86 as indicated by the lower amount of mRNA quantified from those cultures. A possible explanation for this observation could be that when excess of P is available in the culture medium, *E. huxleyi* CCMP 1516 does not need to transcribe (or does it at low levels) the phosphate permease gene (Dyhrman et al. 2006). Then during infection of *E. huxleyi* CCMP 1516, EhV-86 may start expressing its own putative phosphate permease (ehv117) to maintain the uptake of P, which is a major component of nucleic acids. As suggested by Bratbak et al. (1993), viral replication is highly dependant on P availability due to their high nucleic acid to protein ratio. On the other hand, as reported by Dyhrman et al. (2006), P starvation induces up-regulation of the phosphate permease in *E. huxleyi* CCMP 1516 over fourfold compared to P excess. Thus during the infection cycle of P-limited cultures, EhV-86 may not require the expression of its ehv117 gene if the host's phosphate permease is transcribed ensuring the acquisition of the required P.

7.4.4. Biological inferences

The results in this and in other studies (Allen et al. 2006b, Allen et al. submitted) reveal variation at the genomic level among several EhV isolates. Such variations imply most likely significant differences in the biology and ecology among the members of this algal virus group.

In chapter 3 in this thesis the results from an extensive host range experiment, under P-replete culture conditions, showed that all the EhV strains screened in the current

experiment for the presence of the putative phosphate permease (ehv117) were capable of infecting many of the same host strains. However, some remarkable differences in host range were also detected and it was suggested the need for further investigation focused on specific genes in order to find the genetic features that determine these phenotypic differences in this host/virus system. The most significant difference in terms of infectivity was observed in the case of EhV-163. This virus strain could infect *E. huxleyi* CCMP 1516 but failed to infect the closely related non-calcifying strain CCMP 1516b. Both of these strains originated from the same *E. huxleyi* isolate; however, CCMP 1516b changed its calcification state during culturing since the original isolation of the strain. Allen et al. (submitted) have recently found, using an EhV-86 based microarray, that all the EhV strains capable of infecting *E. huxleyi* CCMP 1516b (Table 3.1 in chapter 3) share 14 protein coding sequences (CDSs) that are absent or highly variable in EhV-163. Interestingly, one of those CDSs is the one encoding the putative phosphate permease, which in this chapter has been proven to be transcribed during the EhV-86 infection cycle. In place of ehv117 in EhV-163 there is a 600 bp region that contains a 75 bp 3' remnant of ehv117 and a 435 bp putative CDS that encodes a putative endonuclease (ehv117**a**), indicating a gene replacement (Allen et al. 2006b). The functional relevance of this gene replacement is yet to be determined, but it seems to indicate the existence of significant differences in the infection process among EhV strains. Quinn et al. (2006) have recently reported that the putative phosphate-repressible phosphate permease appear to be expressed in response to calcification rather than phosphate starvation. Therefore, if the phosphate-repressible phosphate permease gene is not expressed in the non-calcifying *E. huxleyi* CCMP 1516b, the lack of an orthologue in EhV-163 would prevent infection of this host strain. This suggestion is in accordance with the hypothesis that ehv117 in EhV-86 is expressed to compensate for low expression of the host putative phosphate permease gene and therefore to warrant a successful replication.

Finally, it is worth noting the role of viruses as vectors for the transfer of genetic material (transduction) between communities (Jiang & Paul 1998a). Phages, for instance, often carry in their genomes inserted genes that may come from other phages or hosts (Juhala et al. 2000). Phages may acquire ecologically important genes to adapt to new environments. For example, genes involved in phosphate metabolism have been found in many marine phages (Rohwer et al. 2000, Chen & Lu 2002). The similarity between the sequences of the putative phosphate-repressible phosphate permease gene in the host and ehv117 in the virus (Figure 7.1) indicates that both genes share a common ancestor. However, the degree of mismatches at the nucleotide level seems to suggest that these genes have been in their genomes long enough to allow differentiation. It is thus tempting to suggest that some EhVs may have acquired from *E. huxleyi* genes such as the phosphate permease, which make of this phytoplankton species a successful competitor in parts of the ocean where P is a major limiting nutrient.

7.5. Conclusions

To summarise, in the current investigation it was found that out of the ten EhV isolates included in the study, the nine that originated from the English Channel carry a putative phosphate permease gene (ehv117), while the only isolate obtained from a distant area (EhV-163) do not have this gene in its genome. Instead, EhV-163 has replaced ehv117 with a putative endonuclease.

The lack of P available in the culture medium reduces the growth rate of *E. huxleyi* CCMP 1516 and inhibits the production of EhV-86 particles. However, P availability does not have an effect on the cells photosynthetic capacity.

A novel finding from the present study is that, unlike other methods, the use of real-time reverse-transcription PCR has proven to be an accurate and sensitive technique that revealed the expression of the putative phosphate permease of EhV-86 during an infection cycle. Furthermore, to my knowledge this is the first study that investigates differences induced by different P regimes in transcriptomic levels of an algal virus during the course of an infection cycle. The results indicate an increase in gene expression levels under P-replete conditions compared to P-depleted culture conditions.

These results suggest that gene transfer may have provided some members of the algal virus genus *Coccolithovirus* with important ecological advantages that determine the existence of different propagation strategies among closely related EhV strains.

CHAPTER EIGHT

Phytoplankton community succession and role of viruses during *Phaeocystis pouchetii* blooms: a mesocosm study

8. Phytoplankton community succession and role of viruses during *Phaeocystis pouchetii* blooms: a mesocosm study

8.1. Introduction

The genus *Phaeocystis* play a significant role in global biogeochemistry (Smith Jr et al. 1991, Lancelot et al. 1994, 2005). Several species within the genus *Phaeocystis* have been documented to supply significant portions of the global DMS stocks (Gabric et al. 1999, Ayers & Gillett 2000) and play a key role in ecosystem structure (Verity & Smetacek 1996, Becquevort et al. 1998, Schoemann et al. 2005).

An interesting aspect of *Phaeocystis* is its ability to transform between the well-known colonial stage and the less studied flagellated solitary stage, which function as dual functional groups (Weisse et al. 1994, Hamm et al. 1999, Jacobsen 2000, Verity 2000, Tang 2003). *Phaeocystis* typically produces almost monospecific, vast blooms of gelatinous colonies (Stefansson & Olafsson 1991, Lancelot et al. 1994, Becquevort et al. 1998). However, in some cases the solitary cell stage can dominate (Wassmann et al. 2005). *Phaeocystis* colonies may be preferred when nitrogen is present as nitrate whereas solitary cells better assimilate ammonium (Riegman & van Boekel 1996, Hamm et al. 1999). Jacobsen (2000) also indicated that the colonial phase of *P. pouchetii* dominated when nutrients were in excess and incident irradiance was below 20 mol m^{-2} d^{-1}. (Peperzak et al. 2000) indicated that a low phosphate concentration and a reduction in daily irradiance triggered the transition of non-motile colony cells to flagellated cells in *P. globosa*.

The complex life cycle of *Phaeocystis* is a key to understanding its role in the surrounding ecosystem, but the transition mechanisms between both stages and their ecological benefits are poorly known. It has been proposed that the colonial stage confers protection against predation (Whipple et al. in press) or viral attack (Bratbak et al. 1998b, Jacobsen 2002,

Brussaard et al. 2004b) while the solitary life form enables higher growth efficiency (see review by Schoemann et al. (2005)). It has been hypothesised that since colony formation may defend the alga against predation, bacterial and viral attacks, this may result in trophic sequestration of nutrients and energy into forms not easily accessible to planktonic grazing and regenerating communities.

A mesocosm experiment with two fertilised and one unfertilised enclosures was conducted in spring 2003 (27th February-3rd April) in western Norway to follow the progression of a *Phaeocystis pouchetii* bloom. The main aim of the mesocosm study was to investigate the significance of the *P. pouchetii* bloom for the plankton community development and the trophic transfer (Nejstgaard et al. 2006). Several experiments were also conducted in order to fill perceived gaps in our understanding of *P. pouchetii* life cycle. Other colleagues working on this mesocosm study conducted a set of experiments that showed that while solitary flagellated cells were lysed within two to three days, colonies and detached colonial cells seemed to be non infectable (unpublished data). In addition, during the mesocosm study total *P. pouchetii* cells (solitary and non-motile single cells associated with colonies), *P. pouchetii* colony concentrations, other phytoplankton, microzooplankton and mesozooplankton in the enclosures were identified and enumerated by different means (Nejstgaard et al. 2006).

This chapter is a brief overview of collected data that shows evidence of the presence and potential implications in the plankton community of *P. pouchetii*-specific viruses during the development of the induced bloom. The majority of the data here presented has been used in the production of 3 different manuscripts (Nejstgaard et al. 2006, Whipple et al. in press, Jacobsen et al. submitted). This study was restricted by time limitation, however samples were collected that will allow future work to examine the molecular richness and dynamics of *P. pouchetii* and their co-occurring viruses.

8.2. Material and methods

8.2.1. Mesocosm initiation

Three polyethylene enclosures were filled *in situ* (in alternating thirds, such that filling was staggered, to minimize variability among them) with unfiltered fjord water (Section 2.2.20). From 27th February to 20th March 10 % of the water in each mesocosm was renewed daily with fjord water to allow the introduction of new species, avoid substantial pH changes, and replace sampled water over the course of the experiment (see discussions by Egge (1993) and Williams & Egge (1998)).

Two of the enclosures were amended with nitrate ($NaNO_3$) and phosphate (KH_2PO_4) (replicates NP (a) and NP (b)) corresponding to an initial enrichment of 16 µM nitrate and 1 µM phosphate by the addition of 100 ml each of stock solutions of $NaNO_3$ (1.76 M) and KH_2PO_4 (0.11 M). Nutrients removed by the 10 % water renewal were replaced daily. The third enclosure was left unamended and served as a control treatment (NP (c)). Further details about nutrient treatment and sampling procedures are as described by Nejstgaard et al. (2006).

8.2.2. Enumeration of phytoplankton and viral populations

Phytoplankton and viral abundances were estimated by analytical flow cytometry (AFC) as described in Section 2.2.6. In addition, flagellated cells, colonial cells and colonies of *P. pouchetii* were enumerated on a light microscope by Anita Jacobsen as described in Section 2.2.7. Colonies were heavily shaken in order to detach the cells from the mucus.

8.2.3. Virus isolation

P. pouchetii-specific viruses (PpVs) were isolated from seawater samples collected from the 3 enclosures as described in Sections 2.2.3.1 and 2.2.3.3.

8.2.4. Pulse field gel electrophoresis (PFGE)

PFGE was carried out on seawater samples collected from the NP (c) and the NP (b) enclosures according to the protocol described in section 2.2.10. Samples from two previously isolated PpVs (PpV AJ96 and PpV AL02) (Table 2.3) were run alongside the isolates obtained in this study for size comparison.

8.2.5. Transmission electron microscopy (TEM)

The PpV lysates produced in this study were inspected by TEM as described in Section 2.2.8. Briefly, lysate samples were harvested onto electron microscope nickel grids by ultracentrifugation. The grids were then stained with 2 % uranyl acetate and viewed in a JEOL 100S transmission electron microscope.

8.3. Results

8.3.1. Diversity and succession of the phytoplankton populations

Three major groups of primary producers (*Synechococcus* sp., picoeukaryotes and nanoeukaryotes) and one minor group (cryptophytes) were observed on all the samples analysed by AFC from the 3 different enclosures and the fjord daily (Figure 8.1).

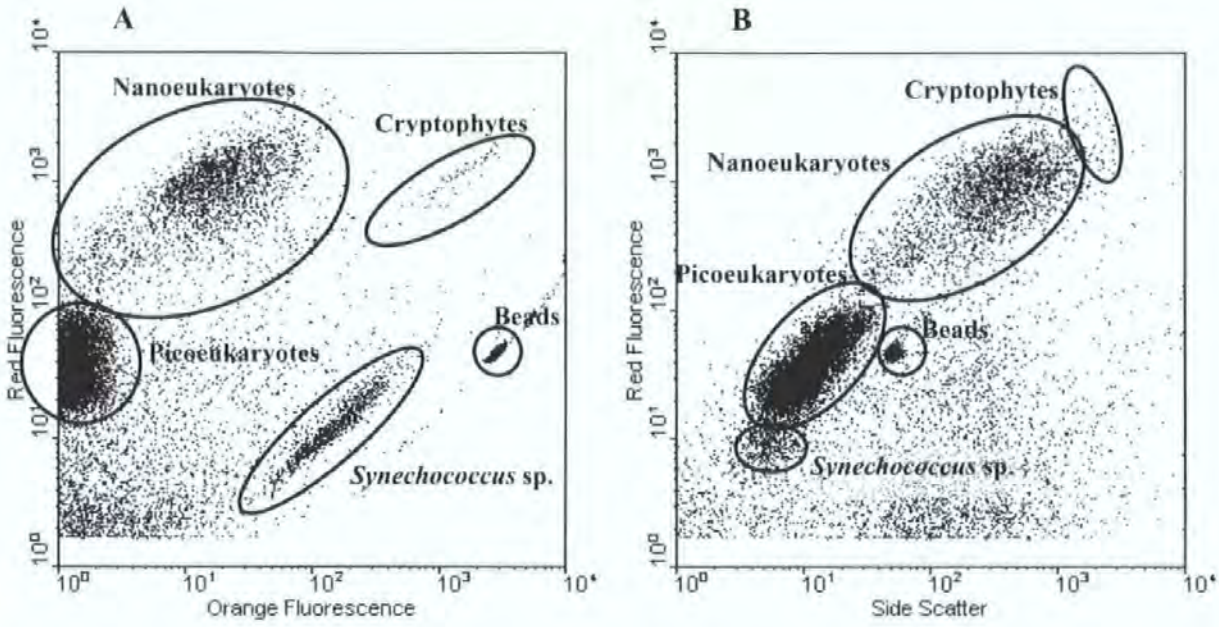

Fig. 8.1. Representative biparametric flow cytometry plots showing populations of algae. *Synechococcus* sp., picoeukaryotes, nanoeukaryotes, and cryptophytes were discriminated using both a combination of red and orange fluorescence signals (**A**), and a combination of red fluorescence and side scatter (**B**).

Description of each phytoplankton group:

***Synechococcus* sp.:** had the lowest red fluorescence (RFL) and side scatter (SSC) signals but the highest value for orange fluorescence (OFL) out of the three major algal groups. The high OFL signals and low SSC and RFL signals are properties consistent with that of *Synechococcus* sp. (Larsen et al. 2001, Li & Dickie 2001, Jacquet et al. 2002).

Picoeukaryotes: relatively low RFL and SSC compared to nanoeukaryotes but higher than those values for *Synechococcus* sp. The size and pigmentation of the algae in this population, as indicated by AFC scatter and fluorescence signals, resembled that of pure

cultures of *Micromonas pusilla*, which indicate that this group consisted of one or more species of picoeukaryotes with size and pigments similar to *M. pusilla* (Castberg et al. 2001, Larsen et al. 2001, Jacquet et al. 2002).

Nanoeukaryotes: similar RFL values as cryptophytes but lower OFL and SSC values. The comparison with the signals of pure cultures of *P. pouchetii* (personal observation) might lead to conclude that this cluster includes *P. pouchetii*. As the group seemed to consist of more than one population it is preferable to be less specific and according to its characteristics can be referred to as nanoeukaryotes (one or several species).

Cryptophytes: the high RFL, OFL and SSC values of this group indicate that the population was most likely consisting of cryptophytes (see section 4.3.1 in this thesis).

Temporal progression of phytoplankton groups:

AFC data showed different temporal progression in abundance of the phytoplankton groups present during the period of study. Fjord water samples were collected only from 17th March until the last sampling day (3rd April) (Figure 8.2).

Picoeukaryotes numerically dominated the microalgae community in all the enclosures at the start of the sampling period (3rd March) with abundances around 25×10^3 cells ml^{-1}. This group experienced a quick and steady decrease from the beginning and reached their lowest abundance on the 20th March, from this day onwards it remained relatively stable at low numbers until the end of the period of study. Abundance and temporal progression of picoeukaryotes was identical in the three enclosures and also in the fjord. Inversely, the nanoeukaryotes increased in abundance from the first day.

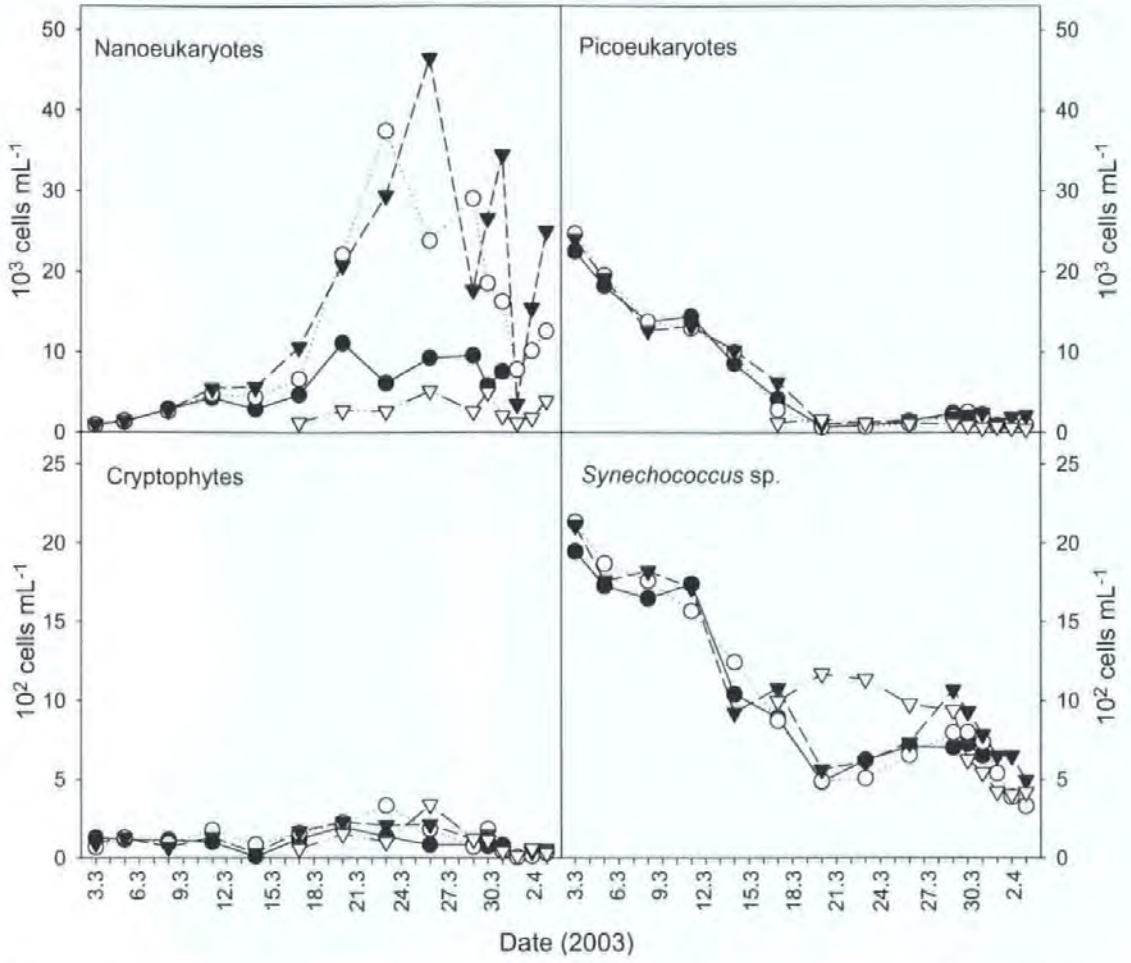

Fig. 8.2. Time series development of the 4 microalgal populations as determined by flow cytometry. (●) Control enclosure, (○) NP (a) enclosure, (▼) NP (b) enclosure, (▽) fjord.

Nanoeukaryotes abundances increased more markedly from the 17th March in the nutrient amended enclosures reaching approximately 36×10^3 and 47×10^3 cell ml^{-1} in NP (a) and NP (b) on 23rd and 26th March, respectively. In the control enclosure the maximum abundance for this group was significantly lower (~ 11×10^3 cell ml^{-1}). Nanoeukaryotes in the fjord followed similar progression to the one in the control enclosure, however, the maximum abundance was lower (~ 5.2×10^3 cell ml^{-1}). After peaking, the nanoeukaryotes decreased sharply towards the end of the study, but increased again on the last two sampling days both in the enclosures and the fjord. *Synechococcus* sp. followed similar progression to that of the picoeukaryotes in all three enclosures but the abundances were one order of magnitude lower. Between 17th and 26th March *Synechococcus* sp. concentrations were double in the fjord compared to the enclosures.

The other microalgal group, referred to as cryptophytes, remained stable at low numbers or had low growth rate throughout the entire period of study. Compared to the rest of the groups they did not seem to play an important role in terms of abundance in the community (maximum concentrations of 3×10^2 cells ml^{-1}).

In addition to AFC, light microscopy counts were performed to specifically determine the abundances of solitary flagellated and colonial *P. pouchetii* cells as well as the number of colonies per millilitre present in each of the enclosures. The abundances of each of the three forms of *P. pouchetii* are shown in Figure 8.3.

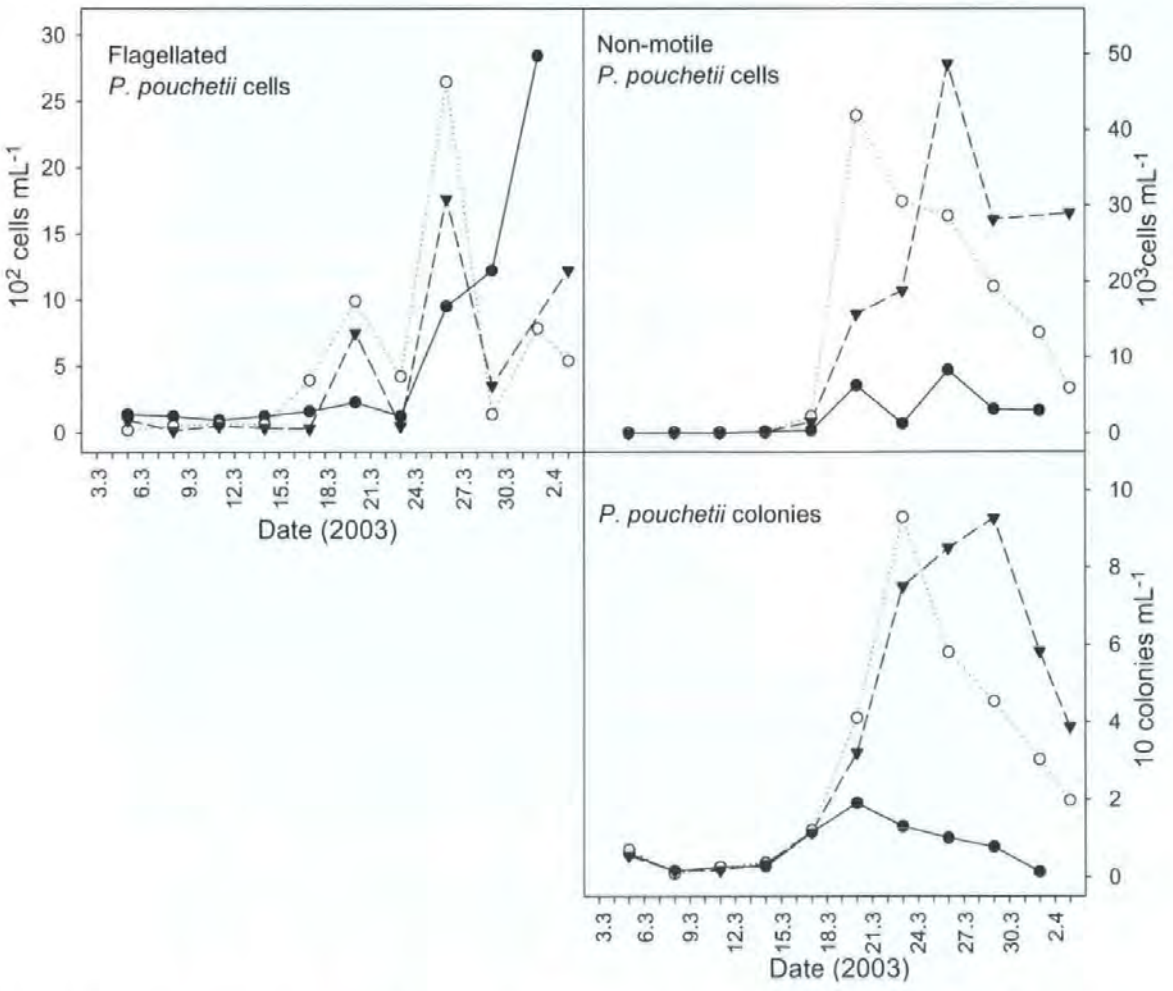

Fig. 8.3. Time series development of the 3 different forms of *P. pouchetii* as determined by light microscopy. (●) NP (c) enclosure, (○) NP (a) enclosure, and (▼) NP (b) enclosure.

The flagellated cells followed a similar progression profile in the two fertilised enclosures. After a lag period with low abundances (75 ± 60 ml^{-1}) flagellated cell showed small peaks in enclosures NP (a) and NP (b) on 20th March; then a decrease was followed by a second more intense increase in numbers that lead to maximum abundances of 26×10^2 and 18×10^2 cells ml^{-1}, respectively, on 26th March. After a subsequent decrease they increased one final time. In the control (unfertilised) enclosure the flagellated cells remained at low numbers until 24th March. From this date onwards *P. pouchetii* flagellated cells increased steadily until 1st April (last day counts were done for this enclosure) reaching the highest abundances (28×10^2 cells ml^{-1}) among the 3 enclosures.

Phaeocystis colonies were present in very low abundance (approximately 6 colonies ml^{-1}) at the start of the experiment. In all three enclosures they increased from 14th March. This increase was most pronounced in the two fertilized enclosures. On 23rd March Phaeocystis colony abundances peaked in NP (a) before a sharp decrease was observed. Colony numbers in enclosure NP (b) increased until the 29th March before decreasing. Both fertilised enclosures reached colony abundances of ~ 93 colonies ml^{-1} while the maximum colony concentration in the unfertilized enclosure was 19 colonies ml^{-1} (20th March).

The numbers of non-motile *P. pouchetii* colonial cells were lower than ~ 100 cells ml^{-1} between 5th and14th March, and then a sharp increase was observed in the fertilised enclosures. Maximum abundances of 42×10^3 and 49×10^3 cells ml^{-1} were recorded for the NP (a) and NP (b) enclosures, respectively, 3 days before the highest colony abundances for each of those enclosures. Therefore, the highest non-motile colonial cell numbers did not mean an increase in colony numbers but in number of cells per colony. The numbers of non-motile *P. pouchetii* colonial cells were significantly lower in the control enclosure ($< 9 \times 10^3$ cells ml^{-1}) than in the fertilized ones. This is in accordance with the (remarkably) low colony numbers reached in the absence of nutrient enrichment.

8.3.2. Diversity and succession of bacterial and viral populations

AFC analysis of samples diluted in TE buffer and stained with DNA dye SYBR Green I revealed the presence of heterotrophic bacteria, *P. pouchetii*-virus (PpV) like particles and other groups of viruses (Figure 8.4). These groups were easily discriminated based on their side scatter (SSC) and green fluorescence (GFL) characteristics.

The PpV-like group appeared to be composed of two subpopulations with slightly different GFL values. The PpV-like groups were identified by their GFL, which is substantially higher than for the other virus groups present, and by comparison to the AFC signature of PpV-AJ96 and PpV-AL02 lysates (see Section 8.3.3). The rest of virus populations are most probably specific to other algal species and bacteriophages (Larsen et al. 2001, Larsen et al. 2004). However, since this study is focused on *P. pouchetii* and their viruses, the counts for bacteria and other virus abundances are not included in this chapter.

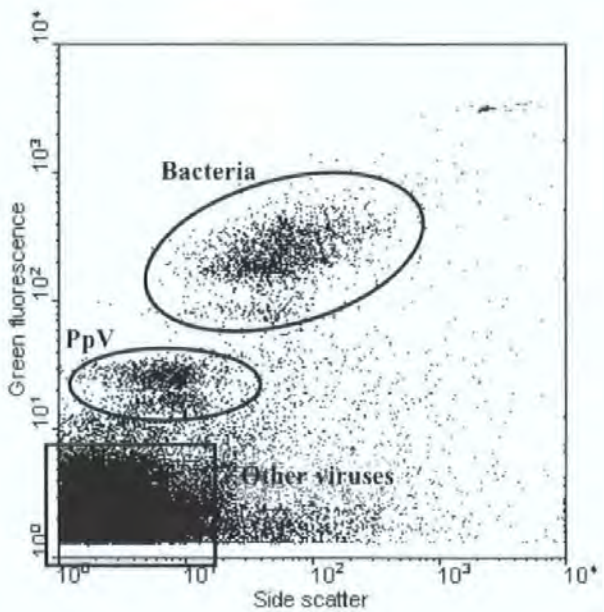

Fig. 8.4. Representative biparametric flow cytometry plot showing populations of *P. pouchetii*-specific viruses (PpVs), other viruses and bacteria detected in the seawater samples collected from the mesocosm enclosures.

PpV-like abundances (Figure 8.5) increased slightly in the 3 enclosures at the beginning of the experiment period until 17th March. Between 18th and 29th March they remained at relatively low concentrations, before a rapid increase took place in all three enclosures. In enclosure NP (a) PpV-like peaked on 1st April (~ 7.3×10^5 virus ml^{-1}) before decreasing again the last 2 days of the experiment. The increase in numbers in enclosure NP (b) continued until the last sampling day (3rd April) on which it reached abundances of approximately 13×10^5 virus ml^{-1}. In the control (NP (c)) enclosure PpV-like abundances also increased from 29th March, but the last sample for virus counts from this enclosure was (unfortunately) taken on 31st March. In the fjord PpV-like particles remained at low concentrations in during the whole experimental period.

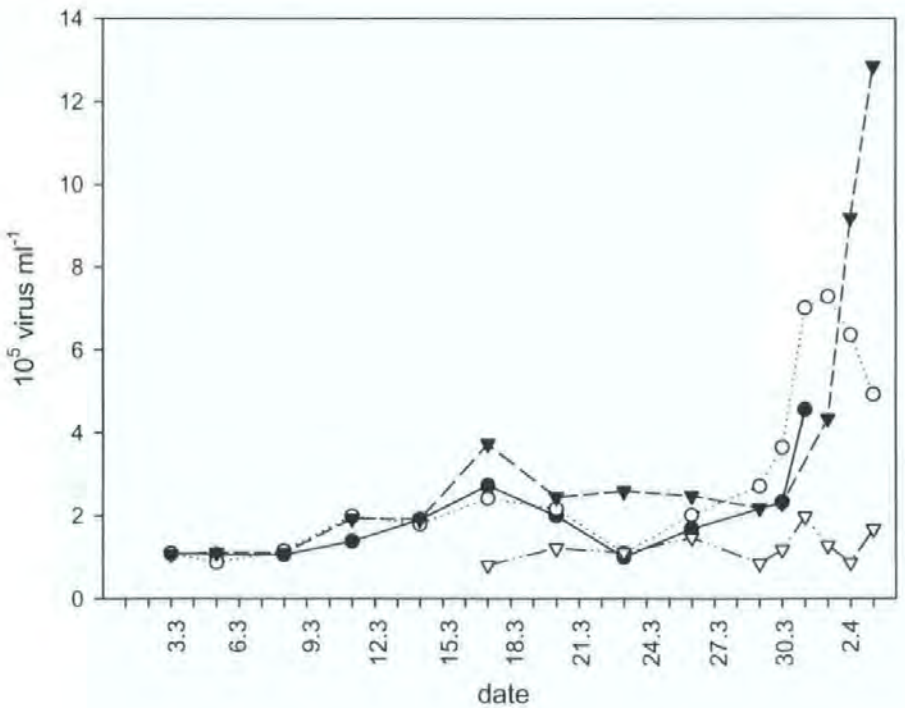

Fig. 8.5. Time series development of *P. pouchetii*-specific virus populations as determined by flow cytometry. (●) NP (c) enclosure, (○) NP (a) enclosure, (▼) NP (b) enclosure, (▽) fjord.

8.3.3. Virus isolation

Only inoculations with concentrated samples collected from the control enclosure (NP (c)) on 14th and 26th March, from the NP (a) enclosure on 26th March and from the NP (b) enclosure on 20th and 26th March resulted in lysis of *P. pouchetii* strain AJ01. AFC

analysis of those lysates showed signatures with similar characteristics to those of PpV strains AJ96 and AL02 (Figure 8.6). Therefore, PpV-like will be called PpV from now on. Clonal isolates were successfully obtained by 3 rounds of plaque assay purification of the PpV lysates. The clone viruses were stored at 4 °C in the dark. They were maintained infectious by periodically propagating an aliquot on cultures of *P. pouchetii* strain AJ01.

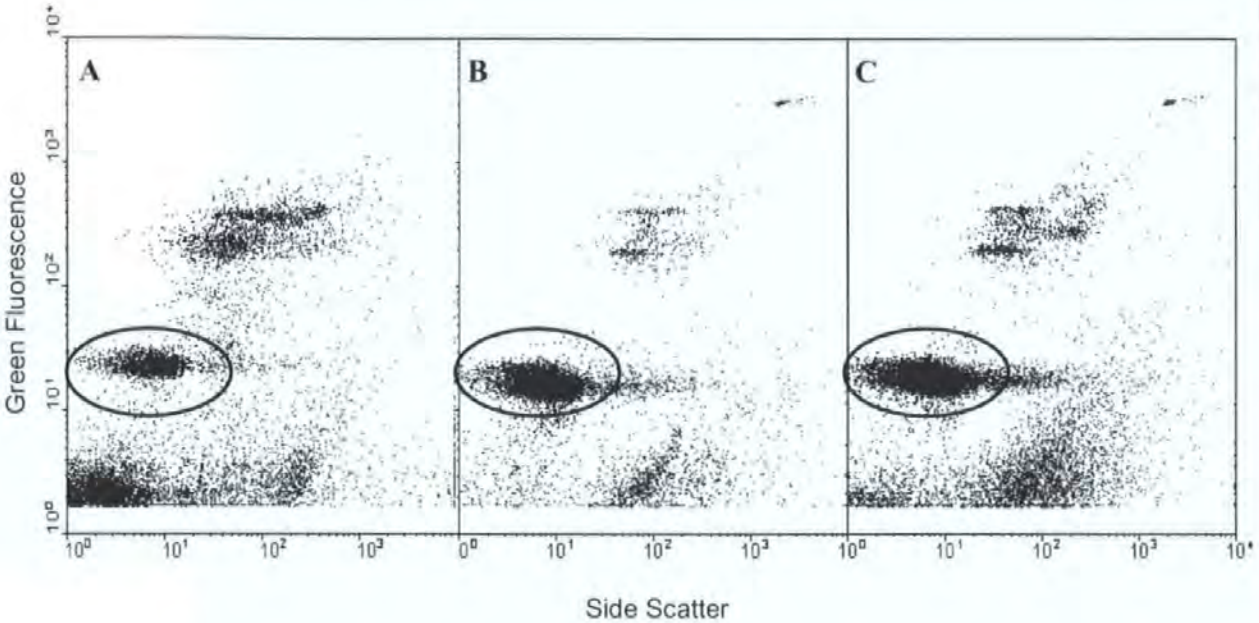

Fig. 8.6. Representative biparametric flow cytometry plots showing populations of PpV lysate originated in this study (**A**), PpV strain AJ96 (**B**) and PpV strain AL02 (**C**).

8.3.4. PFGE analysis

PFGE analysis of the new PpV isolates showed that they have identical genome size to the previously isolated PpVs from the same location (~ 460 kbp) (Figure 8.7) (Larsen et al. 2004). However, PFGE analysis of concentrate seawater samples from the enclosures (data not shown) did not reveal the presence of bands of the expected size for PpVs. For a typical seawater sample, at least 10^9 virus ml^{-1} or 50 ng of viral DNA are required to obtain a single fingerprint on PFGE (Steward 2001), but after the concentrating step by tangential flow filtration for the preparation of the plugs, estimated final concentrations were in the order of 10^7 PpV ml^{-1} (estimated by AFC, data not shown).

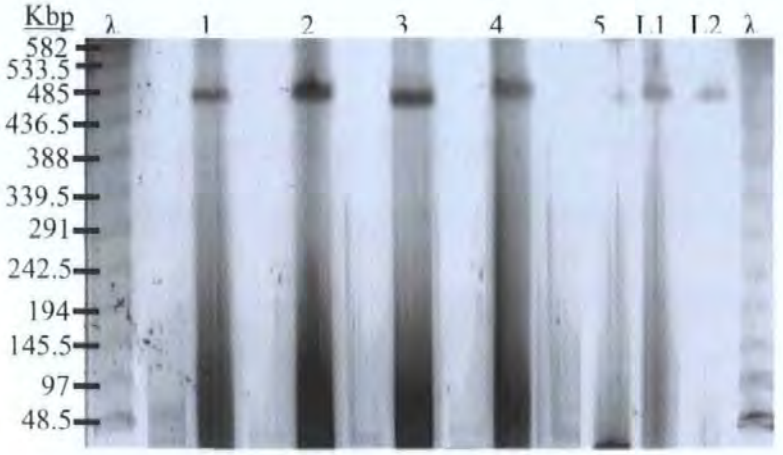

Fig.8.7. PFGE profiles from analysis of lysates obtained from *P. pouchetii* cultures inoculated with mesocosm seawater samples. The outermost lanes on each side of each image (**λ**) contain DNA size marker phage lambda concatamers from 48.5 kbp to approximately 600 kbp. Lane description (date and enclosure from where lysates were produced): **1**, 14th March control enclosure; **2**, 20th March NP (b) enclosure; **3**, 26th March control enclosure; **4**, 26th March NP (a) enclosure; **5**, 26th March NP (b) enclosure. **L1&L2**: isolates PpV AJ96 and PpV AL02, respectively.

8.3.5. TEM analysis

Electron micrographs of lysed *P. pouchetii*-cells (strain AJ01) inoculated with concentrated seawater samples from the mesocosm enclosures showed free viral particles of 140- 170 nm in diameter (Figure 8.8). These particles lack a tail structure or other distinctive appendages and have a hexagonal outline suggesting icosahedral symmetry. The PpV virions have a distinct capsid that surrounds a heavily stained internal region, which appear to be open and less stained in the centre. The observations in this study are in accordance with what previously described for PpV isolates by Jacobsen et al. (1996).

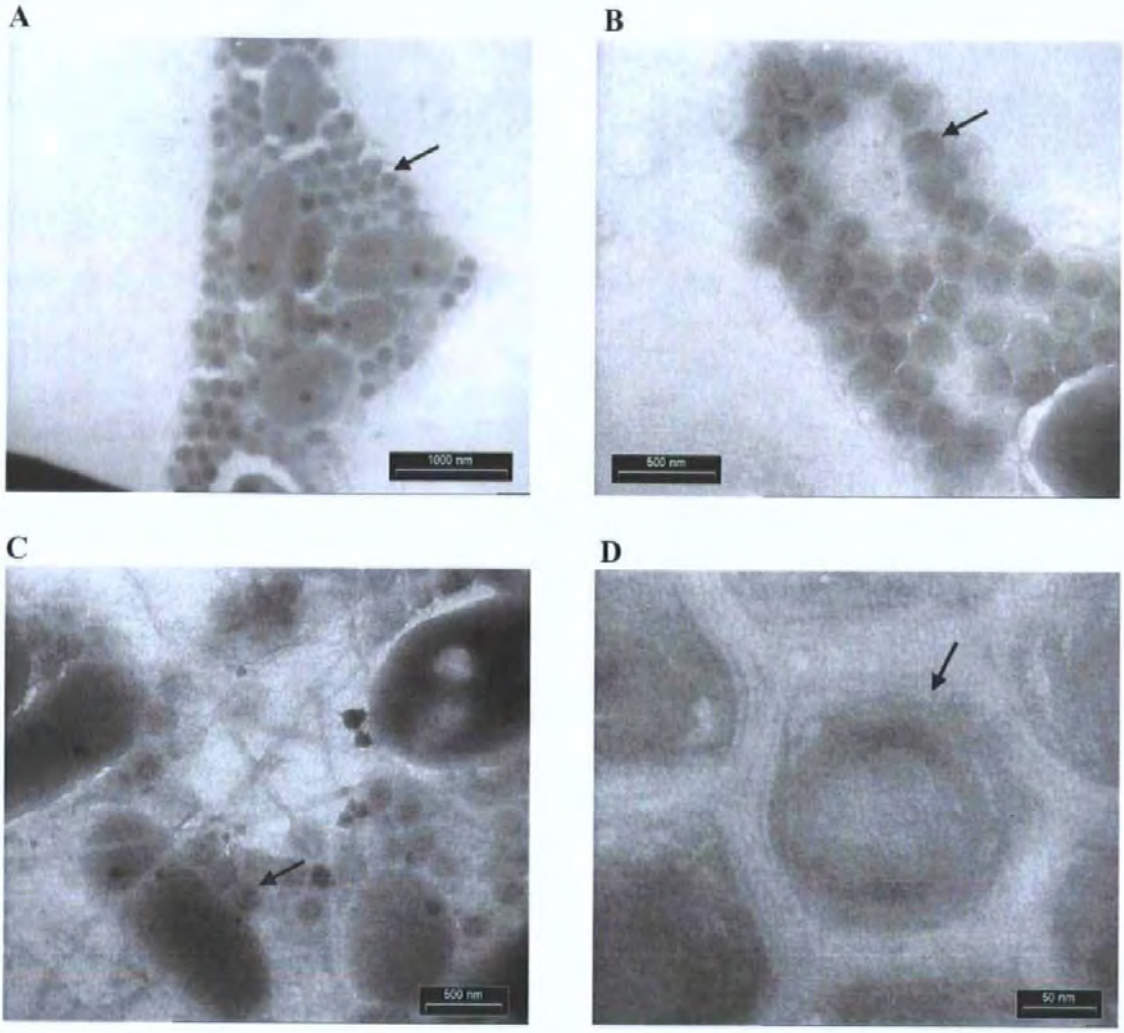

Fig.8.8. Transmission electron micrographs of free *P. pouchetii*-viral particles (examples marked by arrows) produced after inoculation of healthy *P. pouchetii* strain AJ01 cultures with filtered and concentrated water samples collected from the mesocosm enclosure NP (b) on 20th March. Micrograph **C** shows viral particles entrapped in mucilage (star-like shaped filaments) produced by *P. pouchetii*. Note the different scales in the images.

8.4. Discussion

8.4.1. *P. pouchetii* bloom and its effect on the rest of the microbial community

The comparison of the AFC results and microscopy counts of *P. pouchetii* cells allows one to suggest that the group identified as nanoeukaryotes by AFC is composed mainly of *P. pouchetii*. Fixation and freezing of the samples result in dissociation of colonial cells which makes it possible to count them in the flow cytometer. It is therefore reasonable to assume that the different sub-groups that formed the nanoeukaryotes population may be in fact *P. pouchetii* cells in their different life stages. The differences in abundance as determined by AFC and microscopy, slightly lower counts by AFC, could be explained by losses due to the fixation and storing of the samples prior analysis (Vaulot et al. 2005).

In the present mesocosm study, the majority of total *P. pouchetii* cells at the peak of the bloom were contained within colonies. Non-motile colonial cells were more than 20 times more abundant than flagellated cells. This was probably due the addition of nutrients to those enclosures as the presence of nitrogen as nitrate is known to favour the formation of colonies of *P. pouchetii* over single cells, which in turn are better at assimilating ammonium (Riegman & van Boekel 1996, Hamm et al. 1999). However, *Phaeocystis* blooms are not necessarily mainly formed of colonial cells. In north Norwegian fjords and elsewhere in the northeast North Atlantic, single flagellated cells may outnumber co-occurring non-motile cells within colonies (Wassmann et al. 2005). In the absence of nutrient addition (control enclosure) the number of colonies was very low, and the abundance of non-motile cells was only approximately 3 times higher that the abundance of flagellated cells. Yet, even in the unfertilised enclosure the estimated biomass of colonial cells was about 14 times higher than the average biomass of single cells in the same enclosure (Whipple et al. in press).

The development of the different groups in the phytoplankton community seemed to be linked to the development of the *P. pouchetii* bloom. As *P. pouchetii* abundances increased the other two major populations of phytoplankton detected by AFC, picoeukaryotes and *Synechococcus* sp., decreased steadily. The competitive ability of *P. pouchetii* cells depends on a number of factors like temperature, light conditions, nutrients, mixing and grazing. In Norwegian coastal waters blooms of *P. pouchetii* occur, mainly as colonies, either prior to, during, or just after the annual bloom of diatoms. *P. pouchetii* may take over the dominance during a spring bloom situation if the diatoms become silicate limited and there is surplus of nitrate and phosphate (Jacobsen 2000). Colonies of *P. pouchetii* are also adapted to low irradiance and temperature; under such conditions Weisse (1994) and Moisan & Mitchell (1999) measured photosynthetic parameters up to one order of magnitude higher than diatoms, indicating a potential for out-competing other phytoplankton species at low irradiance and temperature. In nature, *P. pouchetii* has an advantage over diatoms in turbulent environments (Lancelot et al. 1994), and also buoyancy of *P. pouchetii* may represent and advantage in relation to interspecific competition and dispersal strategies (Skreslet 1988). Resistance to grazing due to protection by the colony matrix (Weisse et al. 1994) and the role of infochemicals, which can act as a grazing repellent factor (Dutz et al. 2005), have also been reported to play and important role in controlling the abundance and competitive ability of *P. pouchetii* versus other phytoplankton species. However, the literature on *Phaeocystis* grazing rates is ample but reaches different conclusions (see review by Schoemann et al. (2005)).

In addition, during this study Nejstgaard et al. (2006) observed low biomass of ciliates and mesozooplankton despite the large production of *P. pouchetii* colonies. This suggests that *Phaeocystis* may be capable of limiting system complexity by sequestering nutrients and energy into forms not easily accessible to planktonic grazing. This observation supports the

fact that *Phaeocystis* may be a suboptimal food that does not support strong zooplankton production (Cotonnec et al. 2001, Tang et al. 2001).

8.4.2. Bloom termination

The senescence of *Phaeocystis* colonies has been observed under natural, mesocosm, and laboratory conditions (Veldhuis et al. 1986, Davidson & Marchant 1992, Lancelot et al. 1994, Rousseau et al. 1994). In this study, microscopy analysis, carried out by co-workers, confirmed that towards the bloom termination, cells within colonies had become motile and were released from senescent colonies as observed elsewhere (Verity et al. 1988, Rousseau et al. 1994). However, there is little detailed understanding of general colony-senescence and bloom termination processes in *Phaeocystis*.

Several studies point to a potentially important role of consumer organisms in controlling the *Phaeocystis* life cycle. Nejstgaard et al. (2006) showed that in the present mesocosm study the *P. pouchetii* bloom did not seem to be significantly grazed or support any significant production of mesozooplankton. Therefore, grazing by itself cannot be pointed out as the main cause for the bloom crash.

P. pouchetii blooms, both during mesocosm and environmental studies, in Norwegian fjords have been suspected to be terminated by specific virus infection (Jacobsen 2000, Larsen et al. 2004). In the current mesocosm study, the co-variation observed between bacteria and virus abundances led Nejstgaard et al. (2006) to suggest that the virus community was dominated by bacteriophages and that viral lysis did not contribute to re-proportioning biomass associated with *P. pouchetii* during the course of these experiments. Based on nutrient measurements, which revealed a decrease in nitrate and phosphate concentrations prior the crash of the bloom, these researchers suggested a relation between nutrient availability and the decrease in *P. pouchetii* cell abundances. However, evidence

for the presence of PpVs in the three enclosures and in the fjord is revealed in this chapter. Furthermore, the PpVs present in the enclosures during this mesocosm experiment were actively infectious and clearly linked to the demise of the *P. pouchetii* bloom as suggested by their rapid increase in abundance as the number of *P. pouchetii* cells suddenly decreased. In addition, another indicator of their infectivity was the fact that they were readily isolated and made clonal by inoculating exponentially growing cultures of the flagellated *P. pouchetii* strain AJ01 with seawater samples collected from the enclosures.

Nevertheless, given a burst size for *P. pouchetii* of 350-600 virus cell^{-1} (Jacobsen et al. 1996), one might expect PpV abundances in the order of 15-25 × 10^6 virus ml^{-1} if non-motile *P. pouchetii* cells within colonies would have been infected during this experiment. However, maximum PpV abundances in this study were within the range of 8-13 × 10^5 virus ml^{-1} making thus tempting to think that only infected flagellated *P. pouchetii* cells (18-28 × 10^2 cells ml^{-1}) were responsible for the production of new PpV particles. A speculated mechanism for lack of virus infection of *Phaeocystis* spp. colonies was a colony integument pore size too small to admit virus particles (Hamm et al. 1999, Jacobsen 2002). Other studies also indicated that only solitary flagellated cells of another *Phaeocystis* species, *P. globosa*, were susceptible to viral lysis (Hamm et al. 1999, Brussaard et al. 2004b, Brussaard et al. 2005). However, in one set of experiments, Baudoux & Brussaard (2005) showed that available cultures of non-flagellated *P. globosa* cells originated from colonies can be infected by viruses.

The results here presented seem to indicate the following progression: the decrease in *P. pouchetii* colony numbers in the enclosures was accompanied by a decrease in non-motile colonial cells. Microscopy analysis confirmed that cells within colonies had become motile and were released, possibly triggered by nutrient limitation, which explains the observed increase of free flagellated cells. Then free flagellated cells, susceptible to viral

infection, were lysed, making of PpVs, together with nutrient deprivation, the ultimate responsible for the bloom disappearance.

Yet, if it is generally true that only flagellated cells may be infected, it would imply several important ecological implications such as the formation of fewer colonies that could have been produced if viruses were not present and therefore not removing flagellated cells, which are potential colony formers. If *Phaeocystis* is prevented from producing colonies it could be more susceptible to viral mortality and grazing what in turn would influence the effect of *Phaeocystis* spp. on trophic transfer in the planktonic food web.

8.4.3. *P. pouchetii*- specific viruses

Viruses infecting cultures of *P. pouchetii* strain AJ01 were propagated during this study from water samples collected from the mesocosm enclosures. However, despite the presence of PpVs throughout the entire period of study, successful isolation only occur from samples collected from the enclosures between the 16th and 26th March when PpV abundances were relatively low but not from the last sampling days when PpV reached maximum abundances in the water. From the knowledge on other algae/virus systems such as *Emiliania huxleyi* and their specific viruses (see Chapters 5 and 6) it is likely that the *P. pouchetii* bloom in this study was possibly formed by more than one *P. pouchetii* and PpV strains. We also know that some phytoplankton viruses are strain specific (see Chapter 3). It might, therefore, be possible that the PpV population was initially formed by several strains, among which one or more were specific to *P. pouchetii* strain AJ96, used for virus isolation. However, different PpV(s) might have been responsible for the demise of the flagellated *P. pouchetii* strain(s) that dominated the community in the enclosures. AFC dotplots revealed that the PpV group are composed of at least two sub-groups with slightly different green fluorescence (GFL) (Figure 8.4). Baudoux and Brussaard (2005) also reported the co-existence of *P. globosa*-specific viruses that differed in their GFL

values and had different host ranges. However, there is not clear evidence in the current study to assess that both virus subpopulations are in fact different PpVs. A broader *P. pouchetii* strains culture collection might have increase the chances of isolating different PpVs towards the end of the bloom.

Based on phenotypic characteristics, all the PpV isolates in this study seem to belong to the virus family *Phycodnaviridae*: they are infectious to an eukaryotic microalgae, are polyhedral in shape, lack a tail structure, are large in diameter (140-170 nm) and contain large genomes (~ 460 Kbp). Additionally, Jacobsen et al. (1996) revealed that a similar PpV isolate (PpV AJ96) originated from the exact same area, several years before, had dsDNA genetic nature. However, phylogenetic information on their DNA polymerase genes is necessary in order to unequivocally assign this group of viruses as a separate genus or within one of the six defined genera in the family *Phycodnaviridae.*

Finally, it is worth mentioning that although this study indicates a clear effect of PpVs on the community dynamics of the ecologically important *P. pouchetii* species, there is little knowledge of their biology and ecological implications in the ocean. The study of these viruses' large genome sequence and transcriptomic analyses would certainly provide us with clues for a better understanding of the functioning of PpVs in the sea. In the past few years the genome of three members of the *Phycodnaviridae* family have been fully sequenced: a virus that infects the marine brown alga *Ectocarpus siliculosus* (EsV-1) (Delaroque et al. 2001), a virus that infects a chlorella-like algal symbiont of the freshwater protozoa, *Paramecium bursaria* (PBCV-1) (van Etten & Meints 1999a), and the *E. huxleyi*-specific virus EhV-86 (Wilson et al. 2005a). The analysis of those genome sequences has revealed the presence of components of a surprisingly complex signal transduction system as well as genes with functions more commonly observed in animal and plant cells (Wilson et al. 2005a).

8.5. Conclusions

P. pouchetii blooms composed of flagellated single cells and colonies were formed in nutrient-amended mesocosms. As the blooms occurred the rest of phytoplankton species that composed the community were out-competed.

This study reveals the presence of a group of large genome (~ 460 Kbp) viruses that actively infect *P. pouchetii*. In fact, AFC analysis suggests that the virus group may be formed by two distinctive sub-groups.

Phenotypic characteristics of PpVs isolated from the water in the mesocosm enclosures indicate that they are probably members of the *Phycodnaviridae* family.

Overall, the results show evidence that as previously suspected blooms of *P. pouchetii* can be terminated by specific virus infection. However, since *Phaeocystis* colonies appear to protect the cells against viral infection, the role of PpVs may be significant only for the flagellated stage.

CHAPTER NINE

Summary and future work

9. Summary and future work

Reports of marine viruses exist from long ago (Kriss & Rukina 1947); however, the concentration of viruses in natural waters was in general considered to be low and with no significant impact in marine ecology. Since viruses were first isolated against the marine phytoplankton species *Micromonas pusilla* (Mayer & Taylor 1979), a growing literature has reported the isolation and characterisation of other marine eukaryotic algae viruses (Table 1.1) revealing a broad genetic diversity . Other studies have shown the importance of viruses as mortality agents and controlling the structure and diversity of phytoplankton communities (e.g. Cottrell & Suttle 1991, Bratbak et al. 1993, Brussaard et al. 1996b, Wilson et al. 2001a). The biogeochemical and ecological effects of viruses in the sea are nowadays generally accepted. Yet, still many aspects of the biology of phytoplankton-virus systems remain unknown or uncertain. Understanding the factors that determine when and how a particular virus can and cannot infect an algal host under natural conditions is of great interest, due to potential differences in the ecological and biogeochemical implications.

The work carried out during this PhD project is mainly concerned with the study of the molecular ecology of marine phytoplankton viruses. In particular, this thesis focused on *E. huxleyi* and *P. pouchetii* host-virus systems. The use of new available microbiological and molecular approaches have granted several important findings that improve our understanding of the relationships between microalgae hosts and viruses, food web structure, biodiversity and biogeochemical cycles in the ocean.

9.1. Intraspecies host specificity of *E. huxleyi*-viruses

The host range experiment undertaken in this study (Chapter 3) suggests a link between host specificity and the phenotypic and/or genotypic variations within EhVs and *E. huxleyi*

strains, which do not depend on adaptations to the environment. Moreover, the highly variable host range shown in this study indicates complex interactions between *E. huxleyi* strains and their viruses in nature. The phenotypic and genotypic differences upon which host range specificity may depend could be important factors in sustaining the coexistence of *E. huxleyi* and EhVs in the sea. In addition, instraspecies host specificity of EhVs has important ecological implications as it determines which *E. huxleyi* strains may survive and form blooms, and therefore has and effect on local ecology, climate and biogeochemistry. For instance, different *E. huxleyi* strains are known to differ in: (1) their contribution to calcite reservoirs in the sea due to their variable production of coccoliths, which is also accompanied by outputs of CO_2 (Holligan et al. 1993), and (2) emissions of DMS to the atmosphere (Steinke et al. 1998).

In conclusion, determining the host range of *E. huxleyi* strains is not just needed as part of algal virus characterisation but it is also a necessary step towards a comprehensive understanding of their ecological role in the marine environment. In order to reach this understanding, further molecular investigations are required to find the genetic features that determine infectivity in this algal/virus system.

9.2. Validity of mesocosm experiments

Mesocosm experiments are important for studies of the pelagic ecosystem and render budget studies (Riemann et al. 1990) and model verifications possible (Andersen et al. 1987, Thingstad et al. 1999a, Thingstad et al. 1999b). Egge (1993) demonstrated that transparent enclosures situated in a natural body of water have higher repeatability and degree of realism than land constructions. However, constructing and operating marine mesocosm systems has a high cost in terms of money and manpower. Therefore, often a limited number of replicate enclosures are used in the experimental set up. One

consequence is that the reproducibility, and thereby the scientific value of the results may be questioned.

The design of the 2003 *E. huxleyi* mesocosm (Chapter 4) (triplication of 3 different nutrient treatments) provided a unique opportunity for comparing the reproducibility of these systems and for investigating the validity of the main assumptions associated to mesocosm experiments (i.e. the microbial part of the food web in the water filled into the bags is in steady state, the filling of the bags does not perturb the system, and light is in excess, making the cycling of nutrients the main responsible of the dynamics).

AFC was employed in this study to describe and compare the microbial community dynamics, in terms of changes in abundance. The results revealed the development of the same microbial community both inside the mesocosm enclosures and in the fjord, and therefore the validity of mesocosm studies as representations of the natural environment. However, addition of nutrients to the seawater in the enclosures enhanced the conditions for phytoplankton growth leading to an accelerated version of the community succession.

Variance partitioning and discriminant analysis of the AFC data set revealed that there is not statistically significant development in the bags before the first nutrient addition, which means that filling the enclosures and leaving them for 1-2 days before the initial nutrient addition did not have and important effect in the system. The statistical analysis showed that 80 % of the variance was ascribed to the population dynamics initiated by nutrient addition; only 3 % could be attributed to the difference in time of nutrient amendment and just 1 % to the position at the raft. It is possible to conclude that the mesocosm set up is a robust and well suited experimental system that allows investigating the response of the microbial community to manipulations of several parameters. In addition, the results

obtained from this study support the validity of a set of strongly simplifying and constraining assumptions for the construction of numerical models of microbial dynamics.

9.3. Influence of viruses on the microbial community dynamics

From the study of the microbial community development employing mesocosm enclosures is it also possible to draw important conclusions about the impact that viruses have on the community dynamics (Chapters 4 and 8).

Nutrient manipulations of enclosed water masses led to the development of *P. pouchetii* and *E. huxleyi*-dominated blooms in spring and summer 2003, respectively. As these two phytoplankton species increased in abundance, they out-competed other co-existent phytoplankton species. The results from these investigations suggested that the demise of blooms of both species, *P. pouchetii* and *E. huxleyi*, were ultimately the consequence of lytic viral infections. The significance of viral lysis in the decline of the *E. huxleyi* bloom was higher in the enclosure with lower abundance of microzooplankton, which preferentially graze on infected cells (Claire Evans, unpublished data). In the case of *P. pouchetii,* since viruses may infect only single flagellated cells, their effect in the bloom termination might be significant only after the cells within colonies had become motile and were released, possibly triggered by nutrient limitation. During the *E. huxleyi* experiment it was observed that only after the collapse of the dominant *E. huxleyi* populations did other phytoplankton groups experience an increase in abundance. Additionally, the conversion of algal biomass into DOC as the phytoplankton cells were lysed enhanced bacterial growth.

These findings revealed a close link among the dynamics of the microbial populations. Blooms of *E. huxleyi* and *P. pouchetii* and in particular their termination by viruses had a great influence in the diversity and dynamics of the rest of the microbial community, phytoplankton, bacteria and viruses.

However, the experiments conducted during the *P. pouchetii* mesocosm study (Chapter 8) were not designed to elucidate the specific viral infection mechanisms, and further investigation is needed to confirm our observations and to investigate possible mechanisms of lysis resistance. The findings reported might also indicate the existence of a genetically diverse PpV community and point out the need for developing specific molecular probes for the analysis of the *P. pouchetii* and PpV communities. The use of molecular probes can provide further insights of the progression and structuring of natural blooms of this key species as well as a more detailed knowledge of the ecological role of PpVs in the environment.

9.4. Molecular dynamics of *E. huxleyi* and EhVs during bloom events

Molecular techniques using the genetic markers GPA and MCP (Schroeder et al. 2002, Schroeder et al. 2003, Schroeder et al. 2005) allowed resolution of genetic variation among *E. huxleyi* and EhVs, respectively, during the progression of induced and natural phytoplankton blooms (Chapters 5 and 6). In fact, these studies proved for the first time the effectiveness of the GPA gene as a molecular marker to determine morphological and allelic richness of *E. huxleyi* in natural communities.

While AFC provided numerical population progression of *E. huxleyi* and their co-occurring EhVs, the sensitivity of techniques such as PCR, DGGE and sequencing (Chapter 2) have allowed exploration of population dynamics in much greater detail revealing temporal and spatial variability of both host and virus genotypes in the sea. A major outcome of these investigations is that different *E. huxleyi* blooms are comprised of different genotypic communities. The results showed that blooms of this species seems to occur every year in a conserved nature at the study site in a Norwegian fjord, where the same *E. huxleyi* and EhV genotypes re-occurred in annual cycles (Chapter 5). Conversely, the naturally occurring bloom in the North Sea (Chapter 6) was a highly dynamic system comprised of a

broad genotypic community of *E. huxleyi* and closely linked EhVs. Furthermore, depth profiles of the bloom in open waters revealed 'past, present and future' of the progression and structuring of the bloom.

If separate blooms differ in their genotypic composition they might have different ecological implications in terms of calcite production, outputs of CO_2, or DMS emissions. Further investigation using molecular tools, as those employed in this study, might allow establishing connections between specific phytoplankton and virus genotypes and the processes above, which may be the key to a better understanding of biogeochemical cycles in the sea.

9.5. Differences in the genome content and gene expression among EhVs

Variations in the genome and gene expression among virus and host strains are the most likely factors to explain many aspects related to virus ecology, such as survival and host specificity. Detailed transcriptomic analysis will surely provide crucial understanding of Phycodnaviridae genomes functioning in the ocean.

In the current investigation it was found that out of the ten EhV isolates tested, EhV-163 was the only coccolithovirus that did not carry a putative phosphate permease gene (ehv117). A recombination event seems to have occurred in EhV-163 causing a 5' partial deletion of ehv117 and its replacement with a putative endonuclease (designated ehv117a) (Allen et al. 2006c). Also remarkable is the fact that the presence of a putative phosphate permease gene has been reported for *E. huxleyi* CCMP 1516 (the main host strain used in this study). Both phosphate permease genes, in the virus and the host, have similar sequences (Chapter 7) indicating a shared common ancestor.

Real-time reverse-transcription PCR was then performed to investigate the expression of ehv117 in EhV-86 during the infection cycle of axenic cultures of *E. huxleyi* CCMP 1516 under different phosphate (P) regimes (Chapter 7). Other transcriptomic analysis using microarray assays had not detected the presence of transcripts for ehv117 during the course of the EhV-86 infection (Allen et al. 2006a). However, this study has proven real-time reverse-transcription PCR to be an accurate and sensitive technique that revealed that ehv117 is expressed during an infection cycle. Additionally, the results indicate differential gene expression depending on P availability. In contrast to what was reported for *E. huxleyi* CCMP 1516, i.e. higher expression of its phosphate permease gene under P-limiting conditions, ehv117 expression levels increased under P-replete conditions compared to P-depleted culture conditions. A possible explanation to this observation is that ehv117 is only expressed by the virus to compensate for low expression of the orthologue in *E. huxleyi* CCMP1516.

Furthermore, it is tempting to suggest that the presence or absence of ehv117 in the viral genome may determine the success or failure of different EhVs to infect some *E. huxleyi* strains. It could be that gene transfer may have provided some EhVs but not others with important ecological advantages that determine the existence of different propagation strategies among closely related strains. Of particular interest is the lack of infection by EhV-163 of CCMP 1516b, a non-calcifying strain closely related to the calcifying CCMP 1516. It is intriguing to postulate that this difference in host range could be an effect of the calcification state of the host. Expression of the putative phosphate permease gene in *E. huxleyi* has been reported to be related to calcification rather than to phosphate starvation (Quinn et al. 2006). Therefore, if the putative phosphate permease gene is not expressed in CCMP 1516b, the lack of an orthologue in EhV-163 would prevent infection of this host strain. This clearly warrants further investigation. The obvious following step would be first to determine whether or not *E. huxleyi* CCMP 1516b carries the putative phosphate

permease gene and the levels of expression under different culture conditions. Then perform an analogous experiment to the one described in Chapter 7 comparing the levels of expression of ehv117 in EhV-86 during infection of both *E. huxleyi* strains, CCMP 1516 and CCMP1516b. Additionally, the use of multiplex real-time PCR to amplify multiple specific targets simultaneously from the same sample (Bustin 2000) would provide extra information on other viral genes expressed during infection, which may possibly be the key to explain host specificity.

In order to investigate the functional relevance of the ehv117 replacement in EhV-163, it would also be of great interest to use real-time PCR to investigate the level of expression of ehv117**a** during infection cycles under different P conditions.

9.6. *P. pouchetii*-specific viruses

As revealed in this study (Chapter 8), PpVs have phenotypic characteristics suggesting that they belong to the family *Phycodnaviridae*. However, taxonomic assignment cannot be confirmed until phylogenetic information of their DNA polymerase genes becomes available. Further characterisation may assign them either as a separate genus or fall within one of the six genera already described in the family *Phycodnaviridae*. It is known and it has been shown in this thesis the fact that PpVs may play and ecological important role in the ocean through their control over the important phytoplankton species *P. pouchetii*; however, our knowledge is constrained by the scarce information of their genomes. It is likely that PpVs genome will reveal interesting aspects associated with their interesting ecology.

List of references

List of references

Aanesen RT, Eilertsen HC, Stabell OB (1998) Light-induced toxic properties of the marine alga *Phaeocystis pouchetii* towards cod larvae. Aquat Toxicol 40:109-121

Ackleson S, Balch WM, Holliga PM (1988) White waters of the Gulf of Maine. Oceanography 1:18-22

Agusti S, Duarte CM (2000) Strong seasonality in phytoplankton cell lysis in the NW Mediterranean Littoral. Limnology and Oceanography 45:940-947

Allen MJ, Foster T, Schroeder DC, Hall M, Roy D, Ghazal P, Wilson WH (2006a) Locus-specific gene expression suggest a unique propagation strategy for a giant algal virus. J Virol In press

Allen MJ, Martínez Martínez J, Schroeder DC, Somerfield PJ, Wilson WH (submitted) Use of microarrays to assess genomic variability in the *Coccolithoviridae*. Environ Microbiol

Allen MJ, Schroeder DC, Donkin A, Crawfurd KJ, Wilson WH (2006b) Genome comparison of two Coccolithoviruses. Virology Journal 3: 15

Allen MJ, Schroeder DC, Donkin A, Crawfurd KJ, Wilson WH (2006c) Genome comparison of two Coccolithoviruses. J Virol 3: 15

Andersen V, Nival P, Harris RP (1987) Modelling of a planktonic enclosed water column. J Mar Biol Assoc UK 67:407-430

Antia JJ, McAllister CD, T.R. P, Stephens K, Strickland JDH (1963) Further measurements of primary production using a large-volume plastic sphere. Oceanography 8:166-183

Antia NJ, Harrison PJ, Oliveira L (1991) The role of organic dissolved nitrogen in phytoplankton nutrition, cell biology and ecology. Phycologia 30:1-89

Archer SD, Smith GC, Nightingale PD, Widdicombe CE, Tarran GA, Rees AP, Burkill PH (2002) Dynamics of particulate dimethylsulphoniopropionate during a Lagrangian experiment in the northern North Sea. Deep-Sea Research II 49:2979-2999

Ask J (2004) Variation in hatching success and egg production of copepods from the northern Baltic Sea. Degree thesis in biology., Umeå University, Sweden

Ayers GP, Gillett RW (2000) DMS and its oxidation products in the remote marine atmosphere. Journal of Sea Research 43:275-286

Azam F, Fenchel T, Field JG, Gray JS, Meyel-Reil LA, Thingstad F (1983) The ecological role of water-column microbes in the sea. Mar Ecol-Prog Ser 10:257-263

Barker GLA, Green JC, Hayes PK, Medlin LK (1994) Preliminary results using the RAPD analysis to screen bloom populations of *Emiliania huxleyi* (Haptophyta). Sarsia 79:301-306

Batje M, Michaelis H (1986) *Phaeocystis pouchetii* blooms in the East Frisian coastal waters (German Bight. North Sea). Mar Biol 93:21-27

Båtvik H, Heimdal BR, Fagerbakke KM, Green JC (1997) Effects of unbalanced nutrient regime on coccolith morphology and size in *Emiliania huxleyi* (Prymnesiophyceae). European Journal of Phycology 332:155-165

Baudoux A-C, Brussaard C (2005) Characterisation of different viruses infecting the marine harmful algal bloom species *Phaeocystis globosa*. Virology 341:80-90

Beckman BR, Peterson WT (1986) Egg production by *Acartia tonsa* in Long Island Sound. Journal of Plankton Research 8:917-925

Becquevort S, Rousseau V, Lancelot C (1998) Major and comparable roles for free-living and attached bacteria in the degradation of Phaeocystis-derived organic matter in Belgian coastal waters of the North Sea. Aquat Microb Ecol 14:39-48

Belviso S, Kim SK, Rassoulzadegan F, Krajka B, Nguyen BC, Mihalopoulos N, Buatmenard P (1990) Production of dimethylsulfonium propionate (DMSP) and

dimethylsulfide (DMS) by a microbial food web. Limnology and Oceanography 35:1810-1821

Benson R, Martin E (1981) Effects of photosynthetic inhibitors and light-dark regimes on the replication of Cyanophage Sm-2. Arch Microbiol 129:165-167

Bergh O, Borsheim KY, Bratbak G, Heldal M (1989) High abundance of viruses found in aquatic environments. Nature 340:467-468

Beukema JJ (1991) Changes in composition of bottom fauna of a tidalfla; area during a period of eutrophication. Mar Biol 111:293-301

Biddle KD, Falkowski PG (2004) Cell death in planktonic, photosynthetic microorganisms. Nature Reviews 2:643-655

Bidle KD, Haramaty L, Corwonski C, Falkowski PGA (2005) A role for caspases during viral infection of the coccolithophorid *Emiliania huxleyi* 4th Algal Virus Workshop, Amsterdam

Billen G, Fontigny A (1987) Dynamics of *Phaeocystis*-dominated spring bloom in Belgian coastal waters.II. Bacteriplankton dynamics. Mar Ecol Prog Ser 37:249-257

Borsheim KY (1993) Native marine bacteriophages. FEMS Microbiol Ecol 102:141-159

Brand LE (1981) Genetic variability in reproduction rates in the marine phytoplankton populations. Evolution 35:1117-1127

Brand LE (1982) Genetic variability and spatial patterns of genetic differentiation in the reproductive rates of the marine coccolithophores *Emiliania huxleyi* and *Gephyrocapsa oceanica*. Limnology and Oceanography 27:236-245

Bratbak G, Egge JK, Heldal M (1993) Viral Mortality of the Marine Alga Emiliania-Huxleyi (Haptophyceae) and Termination of Algal Blooms. Mar Ecol-Prog Ser 93:39-48

Bratbak G, Heldal M (1993) Total counts of viruses in aquatic environments. In: Kemp PF, Sherr BF, Sherr EB, Cole JJ (eds) Current methods in aquatic microbial ecology. Lewis Publishers, Boca Raton, p 135-138

Bratbak G, Heldal M, Norland S, Thingstad TF (1990) Viruses As Partners in Spring Bloom Microbial Trophodynamics. Appl Environ Microbiol 56:1400-1405

Bratbak G, Heldal M, Thingstad TF, Riemann B, Haslund OH (1992) Incorporation of Viruses Into the Budget of Microbial C-Transfer - a 1st Approach. Mar Ecol-Prog Ser 83:273-280

Bratbak G, Heldal M, Thingstad TF, Tuomi P (1996a) Dynamics of virus abundance in coastal seawater. FEMS Microbiol Ecol 19:263-269

Bratbak G, Jacobsen A, Heldal M (1998a) Viral lysis of Phaeocystis pouchetii and bacterial secondary production. Aquat Microb Ecol 16:11-16

Bratbak G, Jacobsen A, Heldal M, Nagasaki K, Thingstad F (1998b) Virus production in Phaeocystis pouchetii and its relation to host cell growth and nutrition. Aquat Microb Ecol 16:1-9

Bratbak G, Levasseur M, Michaud S, Cantin G, Fernandez E, Heimdal BR, Heldal M (1995) Viral activity in relation to Emiliania huxleyi blooms: A mechanism of DMSP release? Mar Ecol-Prog Ser 128:133-142

Bratbak G, Thingstad F, Heldal M (1994) Viruses and the Microbial Loop. Microb Ecol 28:209-221

Bratbak G, Wilson W, Heldal M (1996b) Viral control of *Emiliania huxleyi* blooms? J Mar Syst 9:75-81

Breitbart M, Miyake JH, Rohwer F (2004) Global distribution of nearly identical phage-encoded DNA sequences. FEMS Microbiol Lett 236:249-256

Breitbart M, Rohwer F (2005) Here a virus, there a virus, everywhere the same virus? Trends Microbiol 13:278-284

Breitbart M, Salamon P, Andresen B, Mahaffy JM, Segall AM, Mead D, Azam F, Rohwer F (2002) Genomic analysis of uncultured marine viral communities. PNAS 99:14250-14255

Brussaard CPD (2004) Viral control of phytoplankton populations - a review. J Eukaryot Microbiol 51:125-138

Brussaard CPD, Gast GJ, vanDuyl FC, Riegman R (1996a) Impact of phytoplankton bloom magnitude on a pelagic microbial food web. Mar Ecol-Prog Ser 144:211-221

Brussaard CPD, Kempers RS, Kop AJ, Riegman R, Heldal M (1996b) Virus-like particles in a summer bloom of *Emiliania huxleyi* in the North Sea. Aquat Microb Ecol 10:105-113

Brussaard CPD, Kuipers B, Veldhuis MJW (2005) A mesocosm study of *Phaeocystis globosa* population dynamics I. Regulatory role of viruses in bloom control. Harmful Algae 4:859-874

Brussaard CPD, Noordeloos AAM, Sandaa RA, Heldal M, Bratbak G (2004a) Discovery of a dsRNA virus infecting the marine photosynthetic protist Micromonas pusilla. Virology 319:280-291

Brussaard CPD, Short SM, Frederickson CM, Suttle CA (2004b) Isolation and phylogenetic analysis of novel viruses infecting the phytoplankton Phaeocystis globosa (Prymnesiophyceae). Appl Environ Microbiol 70:3700-3705

Brussaard CPD, Thyrhaug R, Marie D, Bratbak G (1999) Flow cytometric analyses of viral infection in two marine phytoplankton species, Micromonas pusilla (Prasinophyceae) and Phaeocystis pouchetii (Prymnesiophyceae). J Phycol 35:941-948

Burkill PH, Archer SD, Robinson C, Nightingale PD, Groom SB, Tarran GA, Zubkov MV (2002) Dimethyl sulphide biogeochemistry within a coccolithophore bloom (DISCO): An overview. Deep-Sea Research II 49:2863-2885

Bustin SA (2000) Absolute quantification of mRNA suing real-time reverse transcription polymerase chain reaction assays. J Mol Endocrinol 25:169-193

Castberg T, Larsen A, Sandaa RA, Brussaard CPD, Egge JK, Heldal M, Thyrhaug R, van Hannen EJ, Bratbak G (2001) Microbial population dynamics and diversity during

a bloom of the marine coccolithophorid *Emiliania huxleyi* (Haptophyta). Marine Ecology Progress Series 221:39 - 46

Castberg T, Thyrhaug R, Larsen A, Sandaa RA, Heldal M, van Etten JL, Bratbak G (2002) Isolation and characterization of a virus that infects *Emiliania huxleyi* (Haptophyta). Journal of Phycology 38:767-774

Cembella AD, Antia NJ, Harrison PJ (1984) The utilization of organic and inorganic phosphorus compounds as nutrients by eukaryotic microalgae: a multidisciplinary perspective: part 1. Crit Rev Microbiol 10:317-391

Claustre H, Poulet SA, Williams R, Marty JC, Coombs S, Ben Mlih F, Hapette AM, Martin-Jezequel V (1990) A biochemical investigation of a *Phaeocystis* sp bloom in the Irish Sea. Journal of the Marine Biological Association of the United Kingdom 70:197-207

Cloern JE (1996) Phytoplankton bloom dynamics in coastal ecosystems: A review with some general lessons from sustained investigation of the San Francisco Bay, California. Rev Geophys 34:127-168

Cochlan WP, Wikner J, Steward GF, Smith DC, Azam F (1993) Spatial-distribution of viruses, bacteria and chlorophyll-a in neritic, oceanic and estuarine environments. Mar Ecol Prog Ser 92:77-87

Corstjens P, van der Kooij A, Linschooten C, Brouwers GJ, Westbroek P, de Vrind-de Jong EW (1998) GPA, a calcium-binding protein in the coccolithophorid *Emiliania huxleyi* (Prymnesiophyceae). Journal of Phycology 34:622-630

Corstjens PLAM, Zuiderwijk M, Nilsson M, Feindt H, Niedbala RS, Tanke HJ (2003) Lateral-flow and up-converting phosphor reporters to detect single-stranded nucleic acids in a sandwich-hybridization assay. Anal Biochem 312:191-200

Cotonnec G, Brunet C, Sautour B, Thoumelin G (2001) Nutritive value and selection of food particles by copepods during a spring bloom of *Phaeocystis* sp. in the English

Channel, as determined by pigment and fatty acid analysis. J Plankton Res 23:693-703

Cottrell MT, Suttle CA (1991a) Wide-Spread Occurrence and Clonal Variation in Viruses Which Cause Lysis of a Cosmopolitan, Eukaryotic Marine Phytoplankter, Micromonas- Pusilla. Mar Ecol-Prog Ser 78:1-9

Cottrell MT, Suttle CA (1991b) Wide-spread occurrence and clonal variation in viruses which cause lysis of a cosmopolitan, eukaryotic marine phytoplankter, *Micromonas pusilla*. Mar Ecol Prog Ser 78:1-9

Cottrell MT, Suttle CA (1995a) Dynamics of a Lytic Virus Infecting the Photosynthetic Marine Picoflagellate Micromonas-Pusilla. Limnol Oceanogr 40:730-739

Cottrell MT, Suttle CA (1995b) Genetic Diversity of Algal Viruses Which Lyse the Photosynthetic Picoflagellate Micromonas-Pusilla (Prasinophyceae). Appl Environ Microbiol 61:3088-3091

Chen F, Lu JR (2002) Genomic sequence and evolution of marine cyanophage P60: a new insight on lytic and lysogenic phages. Appl Environ Microbiol 68:2589-2594

Chen F, Suttle CA (1995) Amplification of DNA-Polymerase Gene Fragments From Viruses Infecting Microalgae. Appl Environ Microbiol 61:1274-1278

Chen F, Suttle CA (1996) Evolutionary relationships among large double-stranded DNA viruses that infect microalgae and other organisms as inferred from DNA polymerase genes. Virology 219:170-178

Chen F, Suttle CA, Short SM (1996) Genetic diversity in marine algal virus communities as revealed by sequence analysis of DNA polymerase genes. Appl Environ Microbiol 62:2869-2874

Chen MH, Icenogle JP (2004) Rubella virus capsin protein modulates viral genome replication and virus infectivity. J Virol 78:4314-4322

Dacey JWH, Wakeham SG (1986) Oceanic dimethylsulfide: Production during zooplankton grazing on phytoplankton. Science 233:1314-1316

Davidson AT, Marchant HJ (1992) The biology and ecology of *Phaeocystis* (Prymnesiophyceae). In: Round FE, Chapman DJ (eds) Progress in Phycological Research. Biopress Ltd., Bristol, UK, p 1-45

Davis CO (1982) The importance of understanding phytoplankton life strategies in the design of enclosures experiments. In: Grice GD, Reeve MR (eds) Marine mesocosms Biological and chemical research in experimental ecosystems. Springer-Verlag, New York, p 323-332

de Bruin A, Ibelings BW, van Donk E (2003) Molecular techniques in phytoplankton research: from allozyme electrophoresis to genomics. Hydrobiologia 491:47-63

Delaroque N, Maier I, Knippers R, Muller DG (1999) Persistent virus integration into the genome of its algal host, *Ectocarpus siliculosus* (Phaeophyceae). J Gen Virol 80:1367-1370

Delaroque N, Muller DG, Bothe G, Pohl T, Knippers R, Boland W (2001) The complete DNA sequence of the *Ectocarpus siliculosus* virus EsV-1 genome. Virology 287:112-132

Dodds JA (1979) Virus of marine algae. Experientia 35:440-442

Ducklow HW, Carlson CA (1992) Oceanic bacterial production. Adv Microb Ecol 12:113-181

Dutz J, Klein Breteler WCM, Kramer G (2005) Inhibition of copepod feeding by exudates and transparent exopolymer particles (TEP) derived from a Phaeocystis globosa dominated phytoplankton community. Harmful Algae 4:929-940

Dyhrman ST, Haley ST, Birkeland SR, Wurch LL, Cipriano MJ, McArthur AG (2006) Long serial analysis of gene expression for gene discovery and transcriptome profiling in the widespread marine coccolithophore *Emiliania huxleyi*. Appl Environ Microbiol 72:252-260

Dyhrman ST, Palenik B (2003) A characterization of ectoenzyme activity and phosphate-regulated proteins in the coccolithophorid *Emiliania huxleyi*. J Plankton Res 25:1-11

Egge JK (1993) Nutrient control of phytoplankton growth: Effects of macronutrient composition (N, P, Si) on species succession. PhD, University of Bergen. Norway

Egge JK, Aksnes DL (1992) Silicate as regulating nutrient in phytoplankton competition. Marine Ecology Progress Series 83:281-289

Egge JK, Heimdal BR (1994) Blooms of phytoplankton including *Emiliania huxleyi* (Haptophyta) - Effects of nutrient supply in different N-P ratios. Sarsia 79:333-348

Evans C (2004) The influence of marine viruses on the production of dimethyl sulphide (DMS) and related compounds from Emiliania huxleyi. Ph. D. Thesis, University of East Anglia

Evans C, Archer SD, Jacquet S, Wilson WH (2003) Direct estimates of the contribution of viral lysis and microzooplankton grazing to the decline of a *Micromonas* spp. population. Aquat Microb Ecol 30:207-219

Evans GT, Parslow JS (1985) A model of annual plankton cycles. Biolog Oceanogr 3:327--347

Fields BN, Knipe DM, Howley PM (1996) Fundamental virology, 3rd ed., Vol. Lippincott-Raven, Philadelphia, Pennsylvania

Flint SJ, Enquist LW, Krug RM, Racaniello VR, Skalka AM (2000) Principles of virology-molecular biology, pathogenesis, and control. In: Press A (ed), Washington, D.C

Foyn L, Magnussen M, Seglem K (1981) Automatic analysis of nutrients with on-line data processing: a representation of the construction and functioning of the system used at the Institute of Marine Research. Fisken Havet Serie B 4:1-39

Fuhrman JA (1999) Marine viruses and their biogeochemical and ecological effects. Nature 399:541-548

Fuller NJ, Wilson WH, Joint IR, Mann NH (1998) Occurrence of a sequence in marine cyanophages similar to that of T4 g20 and its application to PCR-based detection and quantification techniques. Appl Environ Microbiol 64:2051-2060

Gabric AJ, Matrai PA, Vernet M (1999) Modelling the production and cycling of dimethylsulphide during the vernal bloom in the Barents Sea. Tellus Ser B-Chem Phys Meteorol 51:919-937

Garrison DL, Buck KR, Silver MW (1983) Studies of ice-algal communities in the Weddel Sea. Antarct JUS 18:179-181

Gastrich MD, Anderson OR, Benmayor SS, Cosper EM (1998) Ultrastructural analysis of viral infection in the brown-tide alga, *Aureococcus anophagefferens* (Pelagophyceae). Phycologia 37:300-306

Girod A, Wobus CE, Zadori Z, Ried M, Leike K, Tijssen P, Kleinschmidt JA, Hallek M (2002) The VP1 capsid protein of adeno-associated virus type 2 is carrying a phospholipase A2 domain required for virus infectivity. J Gen Virol 83:973-978

Gobler CJ, Hutchins DA, Fisher NS, Cosper EM, Sanudo-Wilhelmy SA (1997) Release and bioavailability of C, N, P, Se, and Fe following viral lysis of a marine chrysophyte. Limnology and Oceanography 42:1492-1504

Green JC, Course PA, Tarran GA (1996) The life cycle of *Emiliania huxleyi*: a brief review and a study of relative ploidy levels analysed by flow cytometry. J Mar Syst 9:33-44

Guillard RRL (1975) Culture of phytoplankton for feeding marine invertebrates. In: Smith WL, Chanley MH (eds) Culture of marine invertebrate animals. Plenum Press, New York, p 29-60

Hallegraeff GM (1993) A review of harmful algal blooms and their apparent global increase. Phycologia 32:79-99

Hamm CE (2000) Architecture, ecology and biogeochemistry of *Phaeocystis* colonies. J Sea Res 43:307-315

Hamm CE, Simson DA, Merkel R, Smetacek V (1999) Colonies of *Phaeocystis globosa* are protected by a thin but tough skin. Mar Ecol Prog Ser 187:101-111

Hansen FC, Witte HJ, Passarge J (1996) Grazing in the heterotrophic dinoflagellate *Oxyrrhis marina*: size selectivity and preference for calcified *Emiliania huxleyi* cells. Aquat Microb Ecol 10:307-313

Hardy AC (1926) The herring in relation to its animate environment. Part 2. Report on trials with the plankton indicator. Fishery Investigations, Series 2 8:1-13

Heid CA, Stevens J, Livak KJ, Williams PM (1996) Real time quantitative PCR. Gen Res 6:986-994

Heimdal BR, Egge JK, Veldhuis MJW, Westbroek P (1994) The 1992 Norwegian Emiliania-Huxleyi Experiment - an Overview. Sarsia 79:285-290

Heldal M, Bratbak G (1991) Production and decay of viruses in aquatic environments. Mar Ecol Prog Ser 72:205-212

Hidaka Y (1971) Isolation of marine bacteriophages from sea water. Bull Jpn Soc Sci Fish 37:1199-1206

Hill RW, White BA, Cottrell MT, Dacey JWH (1998) Virus-mediated total release of dimethylsulfoniopropionate from marine phytoplankton: a potential climate process. Aquat Microb Ecol 14:1-6

Hoffmann E, Stech J, Guan Y, Webster RG, Perez DR (2001) Universal primer set for the full-length amplification of all influenza A viruses. Arch Virol 146:2275-2289

Holligan PM, Fernandez E, Aiken J, Balch WM, Boyd P, Burkill PH, Finch M, Groom SB, Malin G, Muller K, Purdie DA, Robinson C, Trees CC, Turner SM, Vanderwal P (1993) A Biogeochemical Study of the Coccolithophore, *Emiliania huxleyi*, in the North-Atlantic. Global Biogeochemical Cycles 7:879-900

Holligan PM, Viollier M, Harbour DS, Camus P, Champagnephilippe M (1983) Satellite and ship studies of coccolithophore production along a continental-shelf edge. Nature 304:339-342

Honjo T (1993) Overview on bloom dynamics and physiological ecology of Heterosigma akashiwo. In: Smayda TJ, Shimizu Y (eds) Toxic Phytoplankton Blooms in the Sea. Elsevier, New York., p 33–41

Horrigan SG, Montoya JP, Nevins JL, McCarthy JJ, Ducklow HW, Goericke R, Malone T (1990) Nitrogenous nutrient transformations in the spring and fall in the Chesapeake Bay. Estuarine, Coastal and Shelf Science 30:369-391

Iglesias-Rodriguez MD, Saez AG, Groben R, Edwards KJ, Batley J, Medlin LK, Hayes PK (2002) Polymorphic microsatellite loci in global populations of the marine coccolithophorid *Emiliania huxleyi*. Molecular Ecology notes 2:495-497

Jacobsen A (2000) New aspects of bloom dynamics of *Phaeocystis pouchetii* (Haptophyta) in Norwegian waters. PhD thesis, University of Bergen

Jacobsen A (2002) Morphology, relative DNA content and hypothetical life cycle of *Phaeocystis pouchetii* (Prymnesiophyceae); with special emphasis on the flagellated cell type. Sarsia 87:338-349

Jacobsen A, Bratbak G, Heldal M (1996) Isolation and characterization of a virus infecting *Phaeocystis pouchetii* (Prymnesiophyceae). Journal of Phycology 32:923-927

Jacobsen A, Egge J, Heimdal BR (1995) Effects of increased concentration of nitrate and phosphate during a springbloom experiment in mesocosm. J Exp Mar Biol Ecol 187:239-251

Jacobsen A, Larsen A, Martínez Martínez J, Frischer ME, Verity PG (submitted) Are colonies and colonial cells of *Phaeocystis pouchetii* (Haptophyta) susceptible to viral infection? Aquat Microb Ecol

Jacquet S, Heldal M, Iglesias-Rodriguez D, Larsen A, Wilson W, Bratbak G (2002) Flow cytometric analysis of an *Emiliana huxleyi* bloom terminated by viral infection. Aquat Microb Ecol 27:111-124

Jassby AD, Cloern JE, Powell TM (1993) Organic carbon sources and sinks in San Francisco Bay: variability induced by river flow. Mar Ecol Prog Ser 95:39-54

Jiang SC, Paul JH (1998a) Gene transfer by transduction in the marine environment. Appl Environ Microbiol 64:2780-2787

Jiang SC, Paul JH (1998b) Significance of lysogeny in the marine environment: Studies with isolates and a model of lysogenic phage production. Microb Ecol 35:235-243

Juhala RJ, Ford ME, Duda RL, Youlton A, Hatfull GF, Hendrix RW (2000) Genomic sequences of bacteriophages HK97 and HK022: Pervasive genetic mosaicism in the lambdoid bacteriophages. Journal of Molecular Biology 299:27-51

Juneau P, Lawrence JE, Suttle CA, Harrison PJ (2003) Effects of viral infection on photosynthetic processes in the bloom-forming alga *Heterosigma akashiwo*. Aquat Microb Ecol 31:9-17

Kapuscinski RB, Mitchell R (1980) Processes controlling virus inactivation in coastal waters. Water Res 14:363-371

Keller AA, Riebesell U (1989) Phytoplankton carbon dynamics during a winter-spring diatom bloom in an enclosed marine ecosystem: primary production, biomass and loss rates. Mar Biol 103:131-142

Keller MD, Bellows WK, Guillard RRL (1989) Dimethyl sulfide production in marine phytoplankton. In: Saltzman ES, Cooper WJ (eds) Biogenic Sulfur in the Environment. American Chemical Society., p pp 183 - 200

Kelly DP, Smith NA (1990) Organic sulfur compounds in the environment: biochemistry, microbiology and ecological aspects. Adv Microb Ecol 11:345-385

Kiene RP (1996) Production of methanethiol from dimethylsulfoniopropionate in marine surface waters. Mar Chem 54:69-83

Kiene RP, Bates TS (1990) Biological removal of dimethylsulfide from sea water. Nature Rev 345:702-705

Kleppel GS (1993) On the diet of calanoid copepods. Mar Ecol Prog Ser 99:183-195

Kriss AE, Rukina EA (1947) Bacteriophages in the sea. Doklady Akademii Nauk SSR 57:833-836

Kuiper J (1977) Development of North Sea coastal plankton communities in separate plastic bags under identical conditions. Mar Biol 44:97-107

Kwint RLJ, Kramer KJM (1995) Dimethylsulfide production by plankton communities. Mar Ecol Prog Ser 121:227-237

Kwint RLJ, Quist P, Hansen TA, Dijkhuizen L, Kramer KJM (1996) Turnover of dimethylsulfoniopropionate and dimethylsulfide in the marine environment: A mesocosm experiment. Mar Ecol-Prog Ser 145:223-232

Lancelot C, Wassman P, Barth H (1994) Ecology of *Phaeocystis*-dominated ecosystems. J Mar Syst 5:1-4

Lang AS, Culley AI, Suttle CA (2004) Genome sequence and characterization of a virus (HaRNAV) related to picoma-like viruses that infects the marine toxic bloom-forming alga *Heterosigma akashiwo*. Virology 320:206-217

Larsen A, Castberg T, Sandaa RA, Brussaard CPD, Egge J, Heldal M, Paulino A, Thyrhaug R, van Hannen EJ, Bratbak G (2001) Population dynamics and diversity of phytoplankton, bacteria and viruses in a seawater enclosure. Mar Ecol-Prog Ser 221:47-57

Larsen A, Fonnes Flaten GA, Sandaa RA, Castberg T, Thyrhaug R, Erga SR, Jacquet S, Bratbak G (2004) Spring phytoplankton bloom dynamics in Norwegian coastal waters: Microbial community succession and diversity. Limnology and Oceanography 49:180-190

Law CS, Watson AJ, Liddicoat MI, Stanton T (1998) Sulphur hexafluoride as a tracer of biogeochemical and physical processes in an open-ocean iron fertilisation experiment. Deep-Sea Research Part Ii-Topical Studies in Oceanography 45:977-994

Lawrence JE, Chan AM, Suttle CA (2001) A novel virus (HaNIV) causes lysis of the toxic bloom-forming alga Heterosigma akashiwo (Raphidophyceae). Journal of Phycology 37:216-222

Lawrence JE, Chan AM, Suttle CA (2002) Viruses causing lysis of the toxic bloom-forming alga Heterosigma akashiwo (Raphidophyceae) are widespread in coastal sediments of British Columbia, Canada. Limnology and Oceanography 47:545-550

Lawrence JE, Suttle C (2005) Simultaneous production of two distinct viral particles in *Heterosigma akashiwo*. 4th Algal Virus Workshop, Amsterdam

Lenski RE (1988) Dynamics of interactions between bacteria and virulent bacteriophage. Adv Microb Ecol 10:1-44

Lessard EJ, Merico A, Tyrrell T (2005) Nitrate:phosphate ratios and *Emiliania huxleyi* blooms. Limnology and Oceanography 50:1020-1024

Levasseur M, Michaud S, Egge J, Cantin G, Nejstgaard JC, Sanders R, Fernandez E, Solberg PT, Heimdal B, Gosselin M (1996) Production of DMSP and DMS during a mesocosm study of an Emiliania huxleyi bloom: Influence of bacteria and Calanus finmarchicus grazing. Marine Biology 126:609-618

Levin BR, Steward FM, Chao L (1977) Resource-limited growth, competition, and predation: a model and experimental studies with bacteria and bacteriophage. Am Nat 111:3

Li WKW, Dickie PM (2001) Monitoring phytoplankton, bacterioplankton and virioplankton in a coastal inlet (Bedford Basin) by flow cytomertry. Cytometry 44:236-246

Liss PS, Malin G, Turner SM, Holligan PM (1994) Dimethyl Sulfide and Phaeocystis - a Review. J Mar Syst 5:41-53

Lund JW, Kipling C, E.D. LC (1958) The inverted microscope method of estimating algal numbers by counting and the statistical basis of enumeration by counting. Hydrobiologia 11:143-170

Malin G, Kirst GO (1997) Algal production of dimethyl sulfide and its atmospheric role. Journal of Phycology 33:889-896

Malin G, Liss PS, Turner SM (1994) Dimethyl sulphide: production and atmospheric consequences. In: Green JC, Leadbeater BSC (eds) The Haptophyte Algae, Vol 51. Clarenden Press, Oxford, p 303 - 320

Malin G, Turner S, Liss P, Holligan P, Harbour D (1993) Dimethylsulfide and Dimethylsulphoniopropionate in the Northeast Atlantic During the Summer Coccolithophore Bloom. Deep-Sea Research Part I-Oceanographic Research Papers 40:1487-1508

Malin G, Turner SM, Liss PS, Aiken (1992) Sulfur - the plankton climate connection. Journal of Phycology 28:590-597

Malin G, Wilson WH, Bratbak G, Liss PS, Mann NH (1998) Elevated production of dimethylsulfide resulting from viral infection of cultures of Phaeocystis pouchetii. Limnology and Oceanography 43:1389-1393

Mann NH (2003) Phages of the marine cyanobacterial picophytoplankton. FEMS Microbiology Reviews 27:17-34

Mann NH, Cook A, Millard A, S. B, Clokie M (2003) Marine ecosystems: Bacterial photosynthesis genes in a virus. Nature 424:741

Manton I, Leadbeater BSC (1974) Fine structural observations on six species of *Chrysochromulina* from wild Danish marine nanoplankton, including a description of *C. campanulifera* sp. nov. and a preliminary summary of the nanoplankton as a whole. Biol Skr Dan Vid Selsk 20:1- 26

Margalef R (1978) Life-forms of phytoplankton as survival alternatives in an unstable environment. Oceanol Acta 1:493–509

Marie D, Brussaard CPD, Partensky F, Vaulot D (1999a) Enumeration of phytoplankton, bacteria and viruses in marine samples. . In: Robinson J.P. ZD, P.N. Dean, A. Orfao and 4 others (eds.) (ed) Current protocols in cytometry John Wiley & Sons, Chichester, p 11.11.11-11.11.15

Marie D, Brussaard CPD, Thyrhaug R, Bratbak G, Vaulot D (1999b) Enumeration of marine viruses in culture and natural samples by flow cytometry. Appl Environ Microbiol 65:45-52

Marie D, Partensky F, Jacquet S, Vaulot D (1997) Enumeration and cell cycle analysis of natural populations of marine picoplankton by flow cytometry using the nucleic acid stain SYBR Green I. Appl Environ Microbiol 63:186-193

Mayer JA, Taylor FJR (1979) A virus which lyses the marine nanoflagellate *Micromonas pusilla*. Nature 281

McAllister CD, Parsons KS, Strickland JDH (1961) Measuments of primary production in coastal seawater using a large-volume plastic sphere. Limnology and Oceanography 6:237-258

McLachlan GJ (1992) Discriminant analysis and statistical pattern recognition In: Wiley series in probability and mathematical statistics. John Wiley and Sons, New York

Medlin LK, Barker GLA, Campbell L, Green JC, Hayes PK, Marie D, Wrieden S, Vaulot D (1996) Genetic characterisation of *Emiliania huxleyi* (Haptophyta). J Mar Syst 9:13-31

Medlin LK, Lange M, Nothig EM (2000) Genetic diversity in the marine phytoplankton: a review and a consideration of Antarctic phytoplankton. Antarct Sci 12:325-333

Meints RH, Lee K, Burbank DE, Vanetten JL (1984) Infection of a Chlorella-Like Alga With the Virus, Pbcv-1 - Ultrastructural Studies. Virology 138:341-346

Meints RH, Lee K, Vanetten JL (1986) Assembly Site of the Virus Pbcv-1 in a Chlorella-Like Green- Alga - Ultrastructural Studies. Virology 154:240-245

Middelboe M, Jorgensen NOG, Kroer N (1996) Effects of viruses on nutrient turnover and growth efficiency of noninfected marine bacterioplankton. Appl Environ Microbiol 62:1991-1997

Middelboe M, Lyck PG (2002) Regeneration of dissolved organic matter by viral lysis in marine microbial communities. Aquat Microb Ecol 27:187-194

Middelboe M, Nielsen TG, Bjørnsen PK (2002) Viral and bacterial production in the North water: in situ measurements, batch-culture experiments and characterisation and distribution of a virus-host system. Deep-Sea Research II 49:5063-5079

Moisan TA, Mitchell BG (1999) Photophysiological acclimation of *Phaeocystis antarctica* Karsten under light limitation. Limnology and Oceanography 44:247-258

Mühling M, Fuller NJ, Millard A, Somerfield PJ, Marie D, Wilson WH, Scanlan DJ, Post AF, Joint I, Mann NH (2005) Genetic diversity of marine *Synechococcus* and co-occurring cyanophage communities: evidence for viral control of phytoplankton. Environ Microbiol 7:499-508

Muller DG (1991) Marine Virioplankton Produced By Infected Ectocarpus- Siliculosus (Phaeophyceae). Mar Ecol-Prog Ser 76:101-102

Muller DG, Westermeier R, Morales J, Reina GG, del Campo E, Correa JA, Rometsch E (2000) Massive prevalence of viral DNA in Ectocarpus (Phaeophyceae, Ectocarpales) from two habitats in the North Atlantic and South Pacific. Bot Marina 43:157-159

Murray AG (1995) Phytoplankton Exudation - Exploitation of the Microbial Loop As a Defense Against Algal Viruses. J Plankton Res 17:1079-1094

Murray AG, Jackson GA (1992) Viral Dynamics - a model of the effects of size, shape, motion and abundance of single-celled planktonic organisms and other particles. Mar Ecol Prog Ser 89:103-116

Nagasaki K (2001) Domestication of eucaryotic microalgal viruses from marine environments. Microbes Environ 16:3-8

Nagasaki K, Ando M, Imai I, Itakura S, Ishida Y (1994) Virus-Like Particles in Heterosigma-Akashiwo (Raphidophyceae) - a Possible Red Tide Disintegration Mechanism. Marine Biology 119:307-312

Nagasaki K, Shirai Y, Takao Y, Mizumoto H, Nishida K, Tomaru Y (2005) Comparison of genome sequences of single-stranded RNA viruses infecting the bivalve-killing

Dinoflagellate *Heterocapsa circularisquama*. Appl Environ Microbiol 71:8888-8894

Nagasaki K, Tarutani K, Yamaguchi M (1999) Growth characteristics of Heterosigma akashiwo virus and its possible use as a microbiological agent for red tide control. Appl Environ Microbiol 65:898-902

Nagasaki K, Tomaru Y, Tarutani K, Katanozaka N, Yamanaka S, Tanabe H, Yamaguchi M (2003) Growth characteristics and intraspecies host specificity of a large virus infecting the dinoflagellate *Heterocapsa circulatisquama*. Appl Environ Microbiol 69:2580-2586

Nagasaki K, Yamaguchi M (1997) Isolation of a virus infectious to the harmful bloom causing microalga *Heterosigma akashiwo* (Raphidophyceae). Aquat Microb Ecol 13:135-140

Nagasaki K, Yamaguchi M (1998) Intra-species host specificity of HaV (Heterosigma akashiwo virus) clones. Aquat Microb Ecol 14:109-112

Nanninga HJ, Tyrrell T (1996) Importance of light for the formation of algal blooms by *Emiliania huxleyi*. Marine Ecology Progress Series 136:195-203

Nazarenko IA, Bhatnagar SK, Hohman RJ (1997) A closed tube format for amplification and detection of DNA based on energy transfer. Nucl Acids Res 25:2516-2521

Nejstgaard JC, Frischer ME, Verity P, Anderson JT, Jacobsen A, Zirbel MJ, Larsen A, Martínez Martínez J, Sazhin AF, Walters T, Bronk DA, Whipple SJ, Borrett SR, Patten BC, Long JD (2006) Plankton development and trophic transfer in seawater enclosures with nutrients and *Phaeocystis pouchetii* added. Mar Ecol Prog Ser 321:99-121

Noble RT, Fuhrman JA (1997) Virus decay and its causes in coastal waters. Appl Environ Microbiol 63:77-83

Noble RT, Fuhrman JA (1998) Use of SYBR Green I for rapid epifluorescence counts of marine viruses and bacteria. Aquat Microb Ecol 14:113-118

Norrman B, Zweifel UL, Hopkinson CS, Fry B (1995) Production and utilization of dissolved organic carbon during an experimental diatom bloom. Limnology and Oceanography 40:898-907

Ortmann AC, Suttle C (2005) High abundances of viruses in a deep-sea hydrothermal vent system indicates viral mediated microbial mortality. Deep-Sea Research I 52:1515-1527

Paasche E (1964) A tracer study of the inorganic carbon uptake during coccolith formation and photosynthesis in the coccolithophorid *Coccolithus huxleyi*. Physiologia Plantarum 3:1-82

Paasche E (2002) A review of the coccolithophorid *Emiliania huxleyi* (Prymnesiphyceae), with particular refenrence to growth, coccolith formation and calcification-photosynthesis interactions. Phycologia 40:503-529

Paasche E, Brubak S, Skattebøl S, Young JR, Green JC (1996) Growth and calcification in the coccolithophorid *Emiliania huxleyi* (Haptophyceae) at low salinities. Phycologia 35:394-403

Paasche E, Klaveness D (1970) A physiological comparison of coccolith-forming and naked cells of *Coccolithus huxleyi*. Arch Microbiol 73:143-152

Paerl HW (1988) Nuisance phytoplankton blooms in coastal, estuarine, and inland waters. Limnology and Oceanography 33:823-847

Parsons TR MY, Lalli CM. (1984) Plant pigments. In: Parsons TR MY, Lalli CM (ed) A manual of chemical and biological methods for seawater analysis. Pergamon, Oxford, p 99- 112

Paul JH, Rose JB, Jiang SC, Kellogg CA, Dickson L (1993) Distribution of Viral Abundance in the Reef Environment of Key Largo, Florida. Appl Environ Microbiol 59:718-724

Peduzzi P, Weinbauer MG (1993) Effect of Concentrating the Virus-Rich 2-200-Nm Size Fraction of Seawater On the Formation of Algal Flocs (Marine Snow). Limnology and Oceanography 38:1562-1565

Peperzak L, Colijn F, Vrieling EG, Gieskes W, Peeters JCH (2000) Observations of flagellates in colonies of *Phaeocystis globosa* (Prymnesiophyceae); a hypothesis for their position in the life cycle. J Plankton Res 22:2181-2203

Petersen DG, Dahllöf I (2005) Improvements for comparative analysis of changes in diversity of microbial communities using internal standards in PCR-DGGE. FEMS Microbiol Ecol 53:339-348

Petterson H, Gross F, Koczy F (1939) Large-scale plankton culture. Nature 144:332-333

Pienaar RN (1976) Virus-like particles in three species of phytoplankton from San Juan Island, Washington. Phycologia 15:185-190

Pieters H, Kluytmans JH, Zandee DI (1980) Tissue composition and reproduction of *Mytilus edulis* in relation to food availability. Netherlands Journal of Sea Research 14:349-361

Powell EN, Klinck JM, Hofmann EE, Wilson-Ormond EA, Ellis MS (1995) Modeling oyster populations, V, Declining phytoplankton stocks and the population dynamics of American oyster (*Crassostrea virgznica*) populations. Fish Res 24:199 -222

Proctor LM, Fuhrman JA (1990) Viral mortality of marine-bacteria and cyanobacteria. Nature 343:60-62

Proctor LM, Fuhrman JA (1991) Roles of viral infection in organic particle flux. Mar Ecol Prog Ser 69:133-142

Quinn P, Bowers RM, Zhang X, Wahlund TM, Fanelli M, Olszova D, Read BA (2006) cDNA microarrays as a tool for identification of biomineralization proteins in the coccolithophorid *Emiliania huxleyi* (Haptophyta). Appl Environ Microbiol 72:5512-5526

Riegman R, Stolte W, Noordeloos AM, Slezak D (2000) Nutrient uptake and alkaline phosphatase (EC 3:1:3:1) activity of *Emiliania huxleyii* (Prymnesiophyceae) during growth under P and N limitation in continuous cultures. J Phycol 36:87-96

Riegman R, Van Bleijswijk JDL, Brussaard C (2002) The use of dissolved esterase activity as a tracer of phytoplankton lysis. Limnology and Oceanography 47:916-920

Riegman R, van Boekel W (1996) The ecophysiology of *Phaeocystis globosa*: a review. Journal of Sea Research 35:235-242

Riemann B, Sørensen HM, Bjørnsen PK, Horsted SJ, Jensen LM, Nielsen TG, Søndergaard M (1990) Carbon budgets of the microbial food web in estuarine enclosures. Mar Ecol Prog Ser 65:159-170

Rohwer F, Edwards R (2002) The Phage Proteomic Tree: a Genome-Based Taxonomy for Phage. J Bacteriol 184:4529-4535

Rohwer F, Segall A, Steward G, Seguritan V, Breitbart M, Wolven F, Azam F (2000) The complete genomic sequence of the marine phage Roseophage SIO1 shares homology with nonmarine phages. Limnology and Oceanography 45:408-418

Rondon MR, August PR, Bettermann AD, Brady SF, Grossman TH, Liles MR, Loiacono KA, Lynch BA, MacNeil IA, Minor C, al. e (2000) Cloning the soil metagenome: a strategy for accessing the genetic and functional diversity of uncultured microorganisms. Appl Environ Microbiol 66:2541-2547

Rosenberg R, Elmgren R, Fleischer S, Jonsson P, Persson G, Dahlin H (1990) Marine eutrophication case studies in Sweden. Ambio 19:102-108

Rousseau V, Mathot S, Lancelot C (1990) Calculating carbon biomass of *Phaeocystis* sp. from microscopic observations. Mar Biol 107:305-314

Rousseau V, Vaulot D, Casotti R, Cariou V, Lenz J, Gunkel J, Baumann M (1994) The life lycle of *Phaeocystis* (Prymnesiophyceae) - Evidence and hypotheses. J Mar Syst 5:23-39

Ruiz C, Martinez D, Mosquera G, Abad M, Sanchez JL (1992) Seasonal variations in condition, reproductive activity and biochemical composition of the flat oyster, Ostrea edulis, from San Cibran (Galicia, Spain). Marine Biology 112:67-74

Rynearson TA, Ambrust EV (2000) DNA fingerprinting reveals extensive diversity in a field population of the centric diatom *Ditylum brightwellii*. Limnology and Oceanography 45:1329-1340

Sandaa RA, Heldal M, Castberg T, Thyrhaug R, Bratbak G (2001) Isolation and characterization of two viruses with large genome size infecting Chrysochromulina ericina (Prymnesiophyceae) and Pyramimonas orientalis (Prasinophyceae). Virology 290:272-280

Sanders JG, Riedel GF (1993) Trace element transformation during the development of an estuarine algal bloom. Estuaries 16:521–532

Sargent JR, Eilertsen HC, Falk-Pettersen S, Taasen JP (1985) Carbon assimilation and lipid production in phytoplankton in northern Norwegian fjords. Mar Biol 85:106-116

Schoemann V, Becquevort S, Stefels J, Rousseau V, Lancelot C (2005) *Phaeocystis* blooms in the global ocean and their controlling mechanisms: a review. J Sea Res 53:43

Schroeder DC, Biggi GF, Hall M, Davy J, Martínez Martínez J, Richardson AJ, Malin G, Wilson WH (2005) A genetic marker to separate Emiliania huxleyi (Prymnesiophyceae) morphotypes. J Phycol 41:874-879

Schroeder DC, Oke J, Hall M, Malin G, Wilson WH (2003) Virus succession observed during an *Emiliania huxleyi* bloom. Appl Environ Microbiol 69:2484-2490

Schroeder DC, Oke J, Malin G, Wilson WH (2002) Coccolithovirus (Phycodnaviridae): Characterisation of a new large dsDNA algal virus that infects Emiliania huxleyi. Archives of Virology 147:1685-1698

Shin K, Jang M, Jang P, Ju S, Lee T, Chang M (2003) Influence of food quality on egg production and viability of the marine planktonic copepod *Acartia omorii*. Prog Oceanogr 57:265-277

Shiraiwa Y (2003) Physiological regulation of carbon fixation in the photosynthesis and calcification of coccolithophorids. Comp Biochem Physiol B-Biochem Mol Biol 136:775-783

Short S, Suttle C (2005) Nearly identical bacteriophage structural gene sequences are widely distributed in marine and freshwater environments. Appl Environ Microbiol 71:480-486

Short SM, Suttle CA (1999) Use of the polymerase chain reaction and denaturing gradient gel electrophoresis to study diversity in natural virus communities. Hydrobiologia 401:19-32

Short SM, Suttle CA (2002) Sequence analysis of marine virus communities reveals that groups of related algal viruses are widely distributed in nature. Appl Environ Microbiol 68:1290-1296

Sieburth JM (1960) Acrylic acid, an 'antibiotic' principle in *Phaeocystis* blooms in Antarctic waters. Science 132:676-677

Sieburth JM, Johnson PW, Hargraves PE (1988) Ultrastructure and ecology of *Aureococcus anophagefferens* gen. et sp. nov. (Chrysophyceae): The dominant picoplankter during a bloom in Narraganset Bay, Rhode Island, Summer 1985. Journal of Phycology 24:416-425

Simó R (2001) Production of atmospheric sulfur by oceanic plankton: biogeochemical, ecological and evolutionary links. Trends in Ecology & Evolution 16:287-294

Skreslet S (1988) Buoyancy in *Phaeocystis pouchetii* (Hariot) Lagerheim. J Exp Mar Biol Ecol 119:157-166

Smith Jr WO, Codispoti LA, Nelson DM, Manley T, Buskey EJ, Nieubauer HJ, Cota GF (1991) Importance of *Phaeocystis* blooms in the high-latitute ocean carbon cycle. Nature 352:514-516

Sode K, Oonari R, Oozeki M (1997) Induction of a temperate marine cyanophage by heavy metal. Journal of Marine Biotechnology 5:178-180

Spencer (1960) Indigenous marine bacteriophages. Journal of Bacteriology 79:614

Starr M, Himmelman JH, Therriault J-C (1991) Coupling of nauplii release in barnacles with phytoplankton blooms: A parallel strategy to that of spawning in urchins and mussels. J Plankton Res 13:561-571

Stefansson U, Olafsson J (1991) Nutrients and fertility of Icelandic waters. Rit Fiskideildar 12

Steinke M, Malin G, Liss PS (2002) Trophic interactions in the sea: An ecological role for climate relevant volatiles? Journal of Phycology 38:630-638

Steinke M, Wolfe GV, Kirst GO (1998) Partial characterisation of dimethylsulfoniopropionate (DMSP) lyase isozymes in 6 strains of *Emiliania huxleyi*. Mar Ecol Prog Ser 175:215-225

Steward FM, Levin BR (1984) The population biology of bacterial viruses: why be temperate? Theor Popul Biol 26:93-117

Steward GF (2001) Fingerprinting viral assemblages by pulsed field gel electrophoresis (PFGE). In: Paul JH (ed) Methods in Microbiology, Marine Microbiology, Vol 30. Academic Press, London, San Diego, p 85-103

Stramska M, Dickey TD (1993) Phytoplankton bloom and the vertical thermal structure of the upper ocean. Journal of Marine Research 51:819-842

Strickland JDH, Parsons TR (1972) A practical handbook of seawater analysis, Vol 1. Bull Fish Res Board Can

Suttle C (2005) Viruses in the sea. Nature 437:356-361

Suttle CA (1992) Inhibition of Photosynthesis in Phytoplankton By the Submicron Size Fraction Concentrated From Seawater. Mar Ecol-Prog Ser 87:105-112

Suttle CA (2000a) Cyanophages and their role in the ecology of cyanobacteria. In: Whitton BA, Potts M (eds) The ecology of cyanobacteria: Their diversity in time and space. Kluwer Academic Publishers, Boston., Boston, p 563-589

Suttle CA (2000b) Ecological, evolutionary and geochemical consequences of viral infection of cyanobacteria and eukaryotic algae. In: Hurst CJ (ed) Viral Ecology. Academic Press, p 247-296

Suttle CA, Chan AM (1993) Marine Cyanophages Infecting Oceanic and Coastal Strains of *Synechococcus* - Abundance, Morphology, Cross-Infectivity and Growth-Characteristics. Mar Ecol-Prog Ser 92:99-109

Suttle CA, Chan AM (1994) Dynamics and Distribution of Cyanophages and Their Effect On Marine *Synechococcus* spp. Appl Environ Microbiol 60:3167-3174

Suttle CA, Chan AM (1995) Viruses Infecting the Marine Prymnesiophyte Chrysochromulina Spp - Isolation, Preliminary Characterization and Natural-Abundance. Mar Ecol-Prog Ser 118:275-282

Suttle CA, Chan AM, Cottrell MT (1990) Infection of phytoplankton by viruses and reduction of primary productivity. Nature 347:467-469

Suttle CA, Chen F (1992) Mechanisms and Rates of Decay of Marine Viruses in Seawater. Appl Environ Microbiol 58:3721-3729

Tai V, Lawrence JE, Lang AS, Chan AM, Culley AI, Suttle CA (2003) Characterization of HaRNAV, a single-stranded RNA virus causing lysis of *Heterosigma akashiwo* (Raphidophyceae). Journal of Phycology 39:343-352

Takahashi M, Thomas WH, Seibert DLR, Beers J, Koeller P, Parson TR (1975) The replication of biological events in enclosed water columns. Arch Hydrobiol 76:5-23

Tang KW (2003) Grazing and colony size development in *Phaeocystis globosa* (Prymnesiophyceae): the role of a chemical signal. J Plankton Res 25:831-842

Tang KW, Visscher PT, Dam HG (2001) DMSP-consuming bacteria associated with the calanoid copepod Acartia tonsa (Dana). J Exp Mar Biol Ecol 256:185-198

Tarutani K, Nagasaki K, Itakura S, Yamaguchi M (2001) Isolation of a virus infecting the novel shellfish-killing dinoflagellate *Heterocapsa circularisquama*. Aquat Microb Ecol 23:103-111

Tarutani K, Nagasaki K, Yamaguchi M (2000) Viral impacts on total abundance and clonal composition of the harmful bloom-forming phytoplankton Heterosigma akashiwo. Appl Environ Microbiol 66:4916-4920

Teira E, Pazo MJ, Quevedo M, Fuentes MV, Niell FX, Fernandez E (2003) Rates of dissolved organic carbon production and bacterial activity in the eastern North Atlantic subtropical gyre during summer. Mar Ecol Prog Ser 249:53-67

Thierstein HR, Geitzenauer KR, Molfino B, Shackleton NJ (1977) Global synchroneity of late quaternary coccolith datum levels: validation by oxygen isotopes. Geology 5:400-404

Thingstad F, Billen G (1994) Microbial degradation of *Phaeocystis* material in the water column. J Mar Syst 5:55-65

Thingstad TF (2000) Elements of a theory for the mechanisms controlling abundance, diversity, and biogeochemical role of lytic bacterial viruses in aquatic systems. Limnology and Oceanography 45:1320-1328

Thingstad TF, Havskum H, Kaas H, Nielsen TG, Riemann B, Lefevre D, Williams PJLB (1999a) Bacteria-protist interactions and organic matter degradation under P-limited conditions: Analysis of an enclosure experiment using a simple model. Limnology and Oceanography 44:62-79

Thingstad TF, Havskum H, Zweifel UL, Berdalet E, Sala MM, Peters F, Alcaraz M, Scharek R, Perez M, Jacquet S, Fonnes GA, Dolan JR, Marrasé C, Rassoulzadegan F, Hagstrøm A, Vaulot D (in press) Ability of a minimum microbial food web

model to reproduce response to patterns observed in mesocosms manipulated with N and P, glucose, and Si. J Mar Syst

Thingstad TF, Heldal M, Bratbak G, Dundas I (1993) Are Viruses Important Partners in Pelagic Food Webs. Trends in Ecology & Evolution 8:209-213

Thingstad TF, Lignell R (1997) Theoretical models for the control of bacterial growth rate, abundance, diversity and carbon demand. Aquat Microb Ecol 13:19-27

Thingstad TF, Perez M, Pelegri S, Dolan J, Rassoulzadegan F (1999b) Trophic control of bacterial growth in microcosms containing a natural community from northwest Mediterranean surface waters. Aquat Microb Ecol 18:145-156

Thyrhaug R, Larsen A, Brussaard CPD, Bratbak G (2002) Cell cycle dependent virus production in marine phytoplankton. Journal of Phycology 38:338-343

Thyrhaug R, Larsen A, Thingstad TF, Bratbak G (2003) Stable coexistence in marine algae-virus systems. Mar Ecol Prog Ser 254:27-35

Townsend DW (1984) Comparison of inshore zooplankton and ichthyoplankton populations of the Gulf of Maine. Mar Ecol Prog Ser 15:79-90

Turner SM, Malin G, Liss PS, Harbour DS, Holligan PM (1988) The seasonal variation of dimethyl sulfide and dimethylsulfoniopropionate concentrations in nearshore waters. Limnology and Oceanography 33:364-375

van Bleijswijk J, van der Wal P, Kempers R, Veldhuis M, Young JR, Muyzer G, Devrinddejong E, Westbroek P (1991) Distribution of two Types of *Emiliania huxleyi* (Prymnesiophyceae) in the northeast Atlantic region as determined by immunofluorescence and coccolith morphology. Journal of Phycology 27:566-570

van Bleijswijk JDL (1996) Ecophysiology of the calcifying marine alga *Emiliania huxleyi*. PhD thesis, Rijksuniversitet, Groningen, The Netherlands

van Bleijswijk JDL, Kempers RS, Veldhuis MJ, Westbroek P (1994) Cell and growth characteristics of types A and B of *Emiliania huxleyi* (Prymnesiophyceae) as

determined by flow cytometry and chemical analyses. Journal of Phycology 30:230-241

van der Wal P, Kempers RS, Veldhuis MJW (1995) Production and downward flux of organic mattera and calcite in a North Sea bloom of the coccolithophore *Emiliania huxleyi*. Mar Ecol Prog Ser 126:247-265

van Duyl FC, Gieskes WWC, Kop AJ, Lewis WE (1998) Biological control of short-term variations in the concentration of DMSP and DMS during a *Phaeocystis* spring bloom. J Sea Res 40:221-231

van Etten JL (1995) Giant *Chlorella* viruses. Mol Cells 5:99-106

van Etten JL, Burbank DE, Xia Y, Meints RH (1983) Growth-Cycle of a Virus, Pbcv-1, That Infects Chlorella-Like Algae. Virology 126:117-125

van Etten JL, Graves MV, Muller DG, Boland W, Delaroque N (2002) Phycodnaviridae - large DNA algal viruses. Archives of Virology 147:1479-1516

van Etten JL, Lane LC, Meints RH (1991) Viruses and virus-like particles of eukaryotic algae. Microb Rev 55:586-620

van Etten JL, Meints RH (1999a) Giant viruses infecting algae. Annu Rev Microbiol 53:447-494

van Etten JL, Meints RH (1999b) Giant viruses infecting algae. Annu Rev Microbiol 53:447-494

Vaulot D (2001) Phytoplankton. In: Encyclopedia of Life Sciences. Macmillan Publishers Ltd., p 1-7

Vaulot D, Courties C, Partensky F (2005) Heterogeneity in fragility and other biogeochemical and biophysical properties a simple method to preserve oceanic phytoplankton for flow cytometric analyses. Cytometry 10:629-635

Veldhuis MJW, Colijn F, Venekamp LAH (1986) The spring bloom of *Phaeocystis pouchetii* (Haptophyceae) in Dutch coastal waters. Netherlands Journal of Sea Research 20:37-48

Veldhuis MJW, Wassman P (2005) Blooms dynamics and biological control of a high biomass HAB species in European coastal waters: A *Phaeocystis* case study. Harmful Algae 4:805-809

Verity P (2000) Grazing experiments and model simulations of the role of zooplankton in *Phaeocystis* food webs. J Sea Res 43:317-343

Verity P, Villareal TA, Smayda TJ (1988) Ecological investigations of blooms of colonial *Phaeocystis pouchetii*. II. The role of life-cycle phenomena in bloom termination. J Plankton Res 10:749-766

Verity PG, Smetacek V (1996) Organism life cycles, predation and the structure of marine pelagic ecosystems. Mar Ecol Prog Ser 130:277-293

Visscher PT, Vangemerden H (1991) Production and consumption of dimethylsulfoniopropionate in marine microbial mats. Appl Environ Microbiol 57:3237-3242

Vives-Rego J, Lebaron P, Nebe-von Caron G (2000) Current and future applications of flow cytometry in aquatic microbiology. FEMS Microbiology Reviews 24:429-448

Walker NJ (2002) A technique whose time has come. Science 296:557-559

Wassman P, Vernet M, Mitchell BG (1990) Mass sedimentation of *Phaeocystis pouchetii* in the Barents Sea. Mar Ecol Prog Ser 66:183-195

Wassmann P, Ratkova T, Reigstad M (2005) The contribution of single and colonial cells of *Phaecystis pouchetii* to spring and summer blooms in the north-eastern North Atlantic. Harmful Algae 4:823-840

Waters RE, Chan AT (1982) *Micromonas pusilla* virus: the virus growth cycle and associated physiological events within the host cells; host range mutation. J Gen Virol 63:199-206

Weinbauer MG, Rassoulzadegan F (2004) Are viruses driving microbial diversification and diversity? Environ Microbiol 6:1-11

Weinbauer MG, Wilhelm SW, Suttle CA, Garza DR (1997) Photoreactivation compensates for UV damage and restores infectivity to natural marine virus communities. Appl Environ Microbiol 63:2200-2205

Weinbauer MG, Wilhelm SW, Suttle CA, Pledger RJ, Mitchell DL (1999) Sunlight-induced DNA damage and resistance in natural viral communities. Aquat Microb Ecol 17:111-120

Weisse T, Tande K, Verity P, Hansen F, Gieskes W (1994) The trophic significance of *Phaeocystis* blooms. J Mar Syst 5:67-79

Westbroek P, Brown CW, Vanbleijswijk J, Brownlee C, Brummer GJ, Conte M, Egge J, Fernandez E, Jordan R, Knappertsbusch M, Stefels J, Veldhuis M, Vanderwal P, Young J (1993) A Model System Approach to Biological Climate Forcing - the Example of *Emiliania huxleyi*. Glob Planet Change 8:27-46

Whipple SJ, Patten BC, Verity P (2005) Life cycle of the marine alga *Phaeocystis*: A conceptual model to summarize literature and guide research. J Mar Syst 57:83-110

Whipple SJ, Patten BC, Verity P, Nejstgaard JC, Long JD, Anderson JT, Hay ME, Jacobsen A, Larsen A, Martínez Martínez J, Borret SR (in press) Gaining integrated understanding of *Phaeocystis* spp. (Prymnesiophyceae) through model-driven laboratory and mesocosm studies Biogeochemistry

Widdicombe CE, Archer SD, Burkill PH, Widdicombe S (2002) Diversity and structure of microplankton community during a coccolithophore bloom in the stratified northern North Sea. Deep-Sea Research II 49:2887-2903

Wilcox RM, Fuhrman JA (1994) Bacterial-Viruses in Coastal Seawater - Lytic Rather Than Lysogenic Production. Mar Ecol-Prog Ser 114:35-45

Wilhelm SW, Suttle CA (1999) Viruses and Nutrient Cycles in the Sea - Viruses play critical roles in the structure and function of aquatic food webs. Bioscience 49:781-788

Wilhelm SW, Weinbauer MG, Suttle CA, Pledger RJ, Mitchell DL (1998) Measurements of DNA damage and photoreactivation imply that most viruses in marine surface waters are infective. Aquat Microb Ecol 14:215-222

Wilson WH, Carr NG, Mann NH (1996) The effect of phosphate status on the kinetics of cyanophage infection in the oceanic cyanobacterium *Synechococcus* sp WH7803. Journal of Phycology 32:506-516

Wilson WH, Mann NH (1997) Lysogenic and lytic viral production in marine microbial communities. Aquat Microb Ecol 13:95-100

Wilson WH, Schroeder DC, Allen MJ, Holden M, Parkhill J, Barrell BG, Churcher C, Hamlin N, Mungall K, Norbertczak H, Quail MA, Price CC, Rabbinowitsch E, Walker D, Craigon M, Roy D, Ghazal P (2005a) Complete genome sequence and lytic phase transcription profile of a *Coccolithovirus*. Science 309:1090-1092

Wilson WH, Tarran G, Zubkov MV (2002a) Virus dynamics in a coccolithophore-dominated bloom in the North Sea. Deep-Sea Research Part Ii-Topical Studies in Oceanography 49:2951-2963

Wilson WH, Tarran GA, Schroeder D, Cox M, Oke J, Malin G (2002b) Isolation of viruses responsible for the demise of an *Emiliania huxleyi* bloom in the English Channel. J Mar Biol Ass UK 82:369-377

Wilson WH, Turner S, Mann NH (1998) Population dynamics of phytoplankton and viruses in a phosphate- limited mesocosm and their effect on DMSP and DMS production. Estuar Coast Shelf Sci 46:49-59

Wilson WH, Van Etten JL, Schroeder DS, Nagasaki K, Brussaard C, Delaroque N, Bratbak G, Suttle C (2005b) Family: Phycodnaviridae. In: Fauquet CM, Mayo MA, Maniloff J, Dusselberger U, Ball LA (eds) Virus Taxonomy, VIIIth ICTV Report. Elsevier/Academic Press, London, p 163-175

Williams PJLB, Egge JK (1998) The management and behaviour of the mesocosms. Estuar Coast Shelf Sci 46:3-14

Wolfe GV, Steinke M (1996) Grazing-activated production of dimethyl sulfide (DMS) by two clones of *Emiliania huxleyi*. Limnology and Oceanography 41:1151-1160

Wommack KE, Colwell RR (2000) Virioplankton: Viruses in aquatic ecosystems. Microbiol Mol Biol Rev 64:69-114

Wommack KE, Hill RT, Kessel M, Russekcohen E, Colwell RR (1992) Distribution of viruses in the Chesapeake Bay. Appl Environ Microbiol 58:2965-2970

Wommack KE, Hill RT, Muller TA, Colwell RR (1996) Effects of sunlight on bacteriophage viability and structure. Appl Environ Microbiol 62:1336-1341

Wommack KE, Ravel J, Hill RT, Chun JS, Colwell RR (1999) Population dynamics of Chesapeake bay virioplankton: Total-community analysis by pulsed-field gel electrophoresis. Appl Environ Microbiol 65:231-240

Young JR (1994) Variation in *Emiliania huxleyi* coccolith morphology in samples from the Norwegian EHUX experiment, 1992. Sarsia 79:417-425

Young JR, Westbroek P (1991) Genotypic Variation in the Coccolithophorid Species Emiliania- Huxleyi. Mar Micropaleontol 18:5-23

Zachary A (1976) Physiology and ecology of bacteriophages of the marine bacterium *Beneckea natriegens*: salinity. Appl Environ Microbiol 31:415-422

Zeidner G, Bielawski JP, Shmoish M, Scanlan DJ, Sabehi G, Béjà O (2005) Potential photosynthesis gene recombination between Prochlorococcus and Synechococcus via viral intermediates. Environ Microbiol 7:1505

Zhong Y, Chen F, Wilhelm SW, Poorvin L, Hodson RE (2002) Phylogenetic diversity of marine cyanophage isolates and natural virus communities as revealed by sequences of viral capsid assembly protein gene g20. Appl Environ Microbiol 68:1576-1584

Zingone A, Sarno D, Forlani G (1999) Seasonal dynamics in the abundance of *Micromonas pusilla* (Prasinophyceae) and its viruses in the Gulf of Naples (Mediterranean Sea). J Plankton Res 21:2143-2159